Rheology and morphology of polyolefin / functional oligomer blends : application to the formulation of polymer materials

Michael Robert

N°d'ordre NNT : **2019LYSE1033**

THESE de DOCTORAT DE L'UNIVERSITE DE LYON
opérée au sein de
l'Université Claude Bernard Lyon 1

Ecole Doctorale N° 34
Matériaux

Spécialité de doctorat : Matériaux polymères

Soutenue le 21/03/2019, par :

Michaël ROBERT

Rheology and morphology of polyolefin/functional oligomer blends: application to the formulation of polymer materials

Devant le jury composé de :

Mme	BOUNOR-LEGARE Véronique	Directrice de recherche CNRS	Université Lyon 1	Examinatrice
M.	BOUQUEY Michel	Maître de conférences	Université de Strasbourg	Rapporteur
Mme	CARO-BRETELLE Anne-Sophie	Maître-assistante	IMT Mines Alès	Rapporteure
M.	CASSAGNAU Philippe	Professeur	Université Lyon 1	Directeur de thèse
M.	FULCHIRON René	Professeur	Université Lyon 1	Président
M.	GAROIS Nicolas	Directeur R&I	Hutchinson	Examinateur

UNIVERSITÉ CLAUDE BERNARD - LYON 1

Président de l'Université	**M. le Professeur Frédéric FLEURY**
Président du Conseil Académique	M. le Professeur Hamda BEN HADID
Vice-président du Conseil d'Administration	M. le Professeur Didier REVEL
Vice-président du Conseil Formation et Vie Universitaire	M. le Professeur Philippe CHEVALIER
Vice-président de la Commission Recherche	M. Fabrice VALLÉE
Directrice Générale des Services	Mme Dominique MARCHAND

COMPOSANTES SANTÉ

Faculté de Médecine Lyon Est – Claude Bernard	Directeur : M. le Professeur G.RODE
Faculté de Médecine et de Maïeutique Lyon Sud - Charles Mérieux	Directeur : Mme la Professeure C. BURILLON
Faculté d'Odontologie	Directeur : M. le Professeur D. BOURGEOIS
Institut des Sciences Pharmaceutiques et Biologiques	Directeur : Mme la Professeure C. VINCIGUERRA
Institut des Sciences et Techniques de la Réadaptation	Directeur : M. X. PERROT
Département de formation et Centre de Recherche en Biologie Humaine	Directeur : Mme la Professeure A-M. SCHOTT

COMPOSANTES ET DÉPARTEMENTS DE SCIENCES ET TECHNOLOGIE

Faculté des Sciences et Technologies	Directeur : M. F. DE MARCHI
Département Biologie	Directeur : M. le Professeur F. THEVENARD
Département Chimie Biochimie	Directeur : Mme C. FELIX
Département GEP	Directeur : M. Hassan HAMMOURI
Département Informatique	Directeur : M. le Professeur S. AKKOUCHE
Département Mathématiques	Directeur : M. le Professeur G. TOMANOV
Département Mécanique	Directeur : M. le Professeur H. BEN HADID
Département Physique	Directeur : M. le Professeur J-C PLENET
UFR Sciences et Techniques des Activités Physiques et Sportives	Directeur : M. Y.VANPOULLE
Observatoire des Sciences de l'Univers de Lyon	Directeur : M. B. GUIDERDONI
Polytech Lyon	Directeur : M. le Professeur E.PERRIN
Ecole Supérieure de Chimie Physique Electronique	Directeur : M. G. PIGNAULT
Institut Universitaire de Technologie de Lyon 1	Directeur : M. le Professeur C. VITON
Ecole Supérieure du Professorat et de l'Education	Directeur : M. le Professeur A. MOUGNIOTTE
Institut de Science Financière et d'Assurances	Directeur : M. N. LEBOISNE

Présentation du laboratoire

Le laboratoire IMP (Ingénierie des Matériaux Polymères) est une unité mixte de recherche du CNRS (UMR CNRS 5223), localisée sur trois sites de l'Université de Lyon : l'INSA de Lyon, l'Université Lyon 1 et l'Université Jean Monnet de St Etienne.

Le laboratoire associe près de 250 personnes, dont 86 permanents et plus de 150 doctorants et post-doctorants, autour de la thématique des matériaux polymères. L'originalité de ses recherches est de mener des études sur les aspects fondamentaux et de compréhension, liés aux propriétés applicatives, de la synthèse de nouvelles macromolécules ou d'architectures macromoléculaires à la formulation des polymères, à leur élaboration et à leur caractérisation, à travers une forte collaboration avec le monde socio-économique autour de grands enjeux sociétaux.

L'IMP est un acteur majeur de la recherche française et européenne dans le domaine des matériaux polymères.

www.imp.cnrs.fr

Remerciements

Je tiens tout d'abord à remercier mon directeur de thèse Philippe Cassagnau pour son encadrement au cours de ces trois années de thèse. Sa pédagogie, son humour et ses encouragements ont contribué à me faire grandir tant d'un point de vue personnel que professionnel. Je salue aussi chaleureusement Aurélie Bergeron-Vanhille et Matthieu Fumagalli pour leur accompagnement et leurs conseils qui m'ont permis d'aller plus loin dans mon travail.

Ces quelques paragraphes sont aussi l'occasion de remercier Michel Bouquey et Anne-Sophie Caro-Bretelle pour avoir accepté d'évaluer ce travail écrit en tant que rapporteurs.

Je souhaite ensuite remercier le personnel Hutchinson impliqué dans le laboratoire commun, Nicolas Garois et Grégory Martin, pour leur intérêt et leur suivi, ainsi que toutes les personnes investies dans le projet REPEAT, Emmanuelle Carabeuf, Christophe Boisson, Franck d'Agosto, Sébastien Norsic, Winnie Nzahou Ottou, Vivien Henryon, Jérôme Monbrun, Jean-Laurent Pradel et Stéphane Danièle, pour leurs précieuses remarques. J'en profite pour remercier au passage Alexandre Bernard pour la persévérance dont il a fait preuve au cours de son stage.

Je remercie également Adrien Tauleigne, Guillaume Sudre, Olivier Gain, Pierre Alcouffe, René Fulchiron et Véronique Bounor-Legaré du laboratoire IMP pour leur expertise technique et leurs conseils, sans oublier Christine Lucas, David Gajan et Olivier Boyron du laboratoire C2P2 ainsi que Xavier Jaurand du CTμ pour leur aide.

Un grand merci à tout le personnel administratif et technique du laboratoire, Agnès, Ali, Flavien, Florian, Irina, Laurent, Marine, Nadia, Noëllie, Sabine, Sylvie, Thierry et Valentin, sans qui il nous serait impossible de travailler dans de bonnes conditions.

Merci mille fois à la joyeuse bande des « anciens » qui ont su nous accueillir et nous intégrer au laboratoire, et qui ont chacun contribué à leur façon à faire de ces années de thèse une expérience inoubliable : Abdel, Alice, Amira, Anaïs, Antho, Antoine, Asma, Baptiste, Bastien, Christophe, Cyrille, Fabien, Gautier, Guillaume, Hend, Imed (mon fils !), Jiji, Jimmy, Jingping, Mamoudou, Manue, Marga, Marie-Camille, Marjo, Marwa, Mélanie, Mona, Nico, Pierre, Pierre, Quanyi, Thibaud, Walid et Yann.

J'en profite pour adresser une pensée particulière aux doctorants qui ont également rejoint le laboratoire à la rentrée 2015 : Amani, Bryan (aka Brigand Posay), Laurent, Mathilde, Soline et Thomas. Je suis heureux d'avoir pu partager ces années avec vous.

Pour en finir avec les doctorants du labo, merci à tous les jeunes (et aussi aux moins jeunes) avec qui j'ai passé de super moments : Aileen, Anatole, Antoine, Benjamin, Chloé, Claire, Clémence, Clément,

Dimitri, Florian, Laura, Luisa, Manon, Mathieu, Maxime, Mohammad, Noémie, Orianne, Renaud, Sara et Thibaut. Gardez la pêche !

Un petit coucou aux copainx d'abord, Antho, Aurélie, Caro, Doudou, Gaëtan, Gaugau, John, Julien, Kéo, Louis-Do et Stan, ainsi qu'à la « Châtenoy Family », Alun, Aurèl, Beub, Bouz, Dobby, Dust, Guit, Léa, Lolo, Momi, Quentin, Romi et Titilde. Merci pour votre amitié toutes ces années.

Pour terminer, je tiens à remercier mes parents, mon frère, ma sœur et surtout Camille pour m'avoir soutenu toutes ces années.

This is Ground Control to Major Tom

You've really made the grade

And the papers want to know whose shirt you wear

Now it's time to leave the capsule if you dare

This is Major Tom to Ground Control

I'm stepping through the door

And I'm floating in a most peculiar way

And the stars look very different today

For here am I sitting in a tin can

Far above the world

Planet Earth is blue

And there's nothing I can do

David Bowie, "Space Oddity" (1969)

Abstract

Rheology and morphology of polyolefin/functional oligomer blends: application to the formulation of polymer materials

The objective of this work was to use end-functionalized polyethylene oligomers as interface agents in glass fibre-reinforced thermoplastics and as compatibilizer precursors in immiscible polymer blends. The first part of this work was focused on the understanding of the morphology developments occurring during the melt processing and crystallization of binary systems where a low molar mass polyethylene oligomer was blended with polypropylene and high-density polyethylene resins. It was found that the polyethylene oligomer was easily incorporated into the selected polyolefins thanks to rapid molecular diffusion and good miscibility in the molten state. However, it appeared that the blends underwent solid-liquid phase separation upon crystallization, leading to biphasic materials in the solid state. In a second part, a reactive system consisting of two functional oligomers was studied as a new strategy for the compatibilization of immiscible high-density polyethylene/polyamide 6 blends. Despite the interesting morphologies and properties observed, it was concluded that the use of such a reactive system did not result in efficient compatibilization compared to commonly used compatibilizer precursors. Lastly, polyethylene oligomers with various functional groups were investigated as interface agents in glass fibre-reinforced high-density polyethylene, with the aim of improving both processability and mechanical properties. It was demonstrated that polyethylene oligomers with adequate functional groups could be successfully used as dispersants by reducing interparticle interactions during melt processing as well as as coupling agents improving matrix-filler interfacial adhesion in the solid state.

Keywords: functional oligomers, polyolefins, polymer blends, reinforced polymers, rheology, crystallization, miscibility

Résumé

Rhéologie et morphologie de mélanges polyoléfine/oligomère fonctionnel : application à la formulation de matériaux polymères

L'objectif de ces travaux était l'utilisation d'oligomères de polyéthylène fonctionnels comme agents d'interface dans des thermoplastiques renforcés par des fibres de verre ainsi que comme agents compatibilisants dans des mélanges de polymères non-miscibles. Une première partie s'est portée sur la compréhension de l'évolution de la morphologie de mélanges binaires composés d'une résine polypropylène ou polyéthylène haute densité et d'un oligomère de polyéthylène de faible masse molaire au cours de leur mise en œuvre et de leur cristallisation. Il a été constaté qu'un tel oligomère pouvait être incorporé sans difficulté aux résines polyoléfines sélectionnées, et ce grâce à une diffusion rapide ainsi qu'à une bonne miscibilité à l'état fondu. Cependant, il est apparu que ces mélanges étaient sujets à une séparation de phase solide-liquide lors de leur cristallisation, entraînant la formation de matériaux biphasiques à l'état solide. Dans une deuxième partie, un système réactif composé de deux oligomères fonctionnels a été étudié comme une potentielle stratégie de compatibilisation pour des mélanges polyéthylène haute densité/polyamide 6 non-miscibles. Malgré les morphologies et propriétés intéressantes observées, il a été conclu que l'utilisation d'un tel système réactif n'était pas efficace comparé aux agents compatibilisants usuels. Enfin, des oligomères de polyéthylène avec différentes fonctionnalités ont été étudiés en tant qu'agents d'interface dans du polyéthylène haute densité renforcé par des fibres de verre dans l'optique d'améliorer à la fois la facilité de mise en œuvre et les propriétés mécaniques de ces matériaux. Il a ainsi été démontré que des oligomères avec les fonctionnalités appropriées pouvaient être utilisés comme agents dispersants en réduisant les interactions interparticulaires au cours de la mise en œuvre, ainsi que comme agents de couplage en améliorant l'adhésion interfacial matrice-fibre à l'état solide.

Mots-clés : oligomères fonctionnels, polyoléfines, mélanges de polymères, polymères renforcés, rhéologie, cristallisation, miscibilité

Présentation synthétique des travaux

La formulation de matériaux polymères nécessite l'incorporation de nombreux additifs et charges dans le but de faciliter leur mise en œuvre et d'améliorer leurs propriétés d'usage. De plus, il y a une demande croissante pour l'élaboration de matériaux innovants avec des propriétés spécifiques afin de satisfaire des critères de plus en plus stricts et des besoins de plus en plus diversifiés. Par conséquent, le développement de nouvelles molécules pour améliorer la dispersion de charges dans des matrices polymères ou pour la compatibilisation de mélanges de polymères non-miscibles est le sujet de nombreuses études dans la littérature scientifique. Dans ce contexte, l'ambition du projet FUI REPEAT est donc de valoriser l'utilisation de nouveaux oligomères de polyéthylène fonctionnalisés en bout de chaîne – développés par le laboratoire C2P2 – comme agents d'interface dans divers matériaux polymères. Dans le cadre de ce projet, l'objectif de cette thèse a donc été l'étude du comportement rhéologique et de la morphologie de mélanges de polyoléfines et d'oligomères de polyéthylène, ainsi que de leur utilisation comme agents compatibilisants dans des mélanges polyéthylène-polyamide non-miscibles et comme agents d'interface dans du polyéthylène renforcé par des fibres de verre discontinues. Ce mémoire est donc découpé en cinq parties, dont les chapitres 1 et 2 sont respectivement dédiés à une recherche bibliographique sur les différents sujets mentionnés et à la présentation des matériels et méthodes utilisés.

Les travaux présentés dans le Chapitre 3 se sont portés sur la compréhension de l'évolution de la morphologie de mélanges binaires composés d'une résine polypropylène (PP) ou polyéthylène haute densité (HDPE) et d'un oligomère de polyéthylène (PE) de faible masse molaire au cours de leur mise en œuvre et de leur cristallisation. Leur comportement rhéologique en fondu, leur structure cristalline à l'état solide, ainsi que leur évolution morphologique au cours de la cristallisation ont ainsi été étudiés.

Une des difficultés liées à la mise en œuvre de tels systèmes est le faible rapport de viscosité entre le composé de faible masse molaire et la résine polymère. Les aspects de mélange et de diffusion ont ainsi été étudiés grâce à l'utilisation d'un mélangeur batch ainsi que par le biais d'expériences rhéologiques modèles. Il a ainsi été constaté qu'un tel oligomère pouvait être incorporé sans difficulté aux résines polyoléfines sélectionnées, et ce grâce à une diffusion rapide ainsi qu'à une bonne miscibilité à l'état fondu. Cependant, l'utilisation du modèle rhéologique de Carreau-Yasuda a permis de montrer que cette miscibilité pouvait être limitée à de hautes concentrations en oligomère, en particulier dans le cas de la résine polypropylène qui présente en fait des inhomogénéités à partir de 5%m d'oligomère de polyéthylène.

Les aspects de cristallisation et de miscibilité à l'état solide ont quant à eux été étudiés par calorimétrie différentielle à balayage avec en parallèle de la microscopie optique en lumière polarisée. De plus, la structure cristalline de ces mélanges a été observée par microscopie électronique à balayage. Il est ainsi

apparu que de tels mélanges étaient sujets à une séparation de phase solide-liquide au cours de leur solidification, entraînant la formation de milieux biphasiques à l'état solide. Cependant, certains résultats laissent penser que de petites portions de chaînes d'oligomère de PE sont capables de co-cristalliser avec le HDPE, amenant ainsi une meilleure compatibilité à l'état solide. En comparaison, le mélange d'un oligomère de PE avec du PP aboutit plutôt à la rétention d'une faible quantité de chaînes d'oligomère dans la phase amorphe du PP en raison du phénomène de dilution observé à l'état fondu.

Etant donné ces résultats, il serait intéressant d'étudier d'autres systèmes similaires avec les mêmes outils, en portant une attention particulière à la masse molaire des oligomères ainsi qu'à la nature chimique de leur groupe fonctionnel porté en bout de chaîne.

Dans le chapitre suivant (Chapitre 4), une nouvelle stratégie de compatibilisation de mélanges non-miscibles polyéthylène haute densité/polyamide 6 (HDPE/PA6) a été étudiée. Cette étude était ainsi tournée vers l'utilisation d'un système réactif composé de deux oligomères : (i) un polyéthylène portant des fonctions anhydride maléique (Ceramer 1608) ainsi que (ii) une polyétheramine trifonctionnelle (Jeffamine T-403), tous deux disponibles commercialement.

Les résultats ont montré que l'utilisation d'un tel système réactif ne permettait pas de compatibiliser le mélange, alors que l'utilisation d'un polyéthylène greffé anhydride maléique (PE-g-MA) de haute masse molaire – qui fait partie des agents compatibilisants couramment utilisés – a permis d'obtenir des mélanges homogènes avec de très bonnes propriétés mécaniques. Cela suggère que la faible efficacité des oligomères de PE fonctionnels est liée à un manque d'interaction avec la phase polyéthylène du mélange. Cependant, l'association de ces oligomères fonctionnels soit avec le HDPE, soit avec le PA6, a permis l'observation de propriétés intéressantes qui sont détaillées dans les paragraphes suivants.

Premièrement, il a été constaté que le simple mélange de ces deux oligomères fonctionnels produisait un composé dont les caractéristiques sont similaires à celles d'un réseau réticulé. Il est intéressant de noter que les propriétés rhéologiques et mécaniques d'un tel mélange dépendent des caractéristiques physiques et chimiques des oligomères fonctionnels, en particulier leur masse molaire et le nombre de leurs groupes fonctionnels. Des produits similaires sont disponibles sur le marché et il serait donc possible d'ajuster assez facilement les propriétés d'un tel matériau.

Ensuite, il a été démontré que ces deux oligomères fonctionnels présentaient de fortes interactions avec le PA6 au travers de différents mécanismes réactionnels. Les résultats présentés dans cette partie de l'étude indiquent également que les propriétés rhéologiques et mécaniques des mélanges PA6/Ceramer 1608/Jeffamine T-403 pourraient être optimisées en ajustant plus finement leur composition. De plus, il serait intéressant de mener une étude plus approfondie sur les propriétés mécaniques de ce type de mélanges, en particulier leur résistance au choc.

Enfin, il a été observé qu'un tel mélange d'oligomères fonctionnels n'était pas miscible avec une résine HDPE, produisant ainsi une phase dispersée. Cependant l'adhésion interfaciale entre le HDPE et ces

domaines dispersés a pu être améliorée par l'addition d'un PE-g-MA de haute masse molaire (ici l'Exxelor PE 1040). En dépit de la complexité de ce type de mélanges, il serait intéressant de déterminer la quantité minimum de PE-g-MA à introduire pour obtenir une bonne interface entre le HDPE et le système réactif Ceramer 1608/Jeffamine T-403.

Au vu de ces résultats, des travaux supplémentaires seront nécessaires pour étudier l'utilisation d'oligomères fonctionnels similaires avec différentes masses molaires dans le but de compatibiliser des mélanges HDPE/PA6. Dans cette perspective, l'utilisation de PE-g-MA de haute masse molaire en plus des deux oligomères fonctionnels constitue une piste intéressante, d'autant que la question de l'optimisation de la composition de tels mélanges quaternaires n'a pas été abordée dans le cadre de cette étude.

Les essais rapportés dans le Chapitre 5 se sont focalisés sur l'étude d'oligomères de PE fonctionnels en tant qu'agents d'interface dans du HDPE par des fibres de verre (FV) dans le but d'améliorer à la fois la facilité de mise en œuvre et les propriétés mécaniques de ces matériaux.

Dans une première partie, l'effet dispersant de ces oligomères dans des systèmes HDPE/FV a été évaluée par le biais d'un procédé batch à l'échelle laboratoire ainsi que par des mesures rhéologiques. Il a ainsi été démontré qu'un tel oligomère de PE avec un groupe fonctionnel approprié (ici un acide carboxylique) pouvait être utilisé comme agent dispersant, permettant ainsi d'augmenter le volume maximum de fibres de verre pouvant être incorporé dans la matrice HDPE, tout en maintenant la cohésion du matériau. Ces résultats ont été attribués à l'amélioration de l'interface matrice-fibre ainsi qu'à une réduction des interactions interparticulaires grâce à la stabilisation stérique apportée par l'oligomère, tout particulièrement aux hauts taux de fibres.

La deuxième partie de ce chapitre s'est portée sur l'amélioration du renforcement de composites HDPE/FV. Au travers d'essais préliminaires et d'un screening de différentes fonctionnalités, il a pu être constaté que des oligomères de PE avec les groupes fonctionnels adéquats (acide carboxylique, anhydride maléique et amine dans ce cas) pouvaient être utilisés comme agents de couplage en améliorant l'adhésion interfaciale entre les fibres de verre et la matrice HDPE. Au contraire, l'utilisation d'oligomères portant des fonctionnalités de type alkoxysilane – qui sont pourtant communément utilisés comme agents de couplage dans l'ensimage des fibres de verre – n'a pas eu d'impact significatif sur les propriétés mécaniques des composites HDPE/FV.

Ces résultats permettent de conclure que des oligomères de PE fonctionnels peuvent être utilisés comme agents d'interface dans du polyéthylène renforcé par des fibres de verre sans qu'il y ait besoin de modifier chimiquement la surface des fibres au préalable (mis à part l'ensimage appliqué par le fabriquant). Cependant, considérant les conclusions des précédents chapitres ainsi que les propriétés mécaniques supérieures obtenues avec des additives usuels tels que des PE-g-MA de haute masse molaire, il apparaît que le principal inconvénient de ces oligomères réside dans leur manque d'interaction avec la matrice polymère du fait de leur faible masse molaire, bien que leur faible viscosité soit un avantage pour la mise

en œuvre en fondu de tels systèmes chargés. Il serait donc judicieux de s'intéresser à des oligomères avec des masses molaires un peu plus élevées (5000-10000 g/mol) pour ces applications. De plus, l'utilisation d'oligomères téléchéliques – également développés par le laboratoire C2P2 dans le cadre du projet REPEAT – constitue une piste intéressante dans des systèmes où la réactivité de la matrice polymère peut être exploitée, comme par exemple les polyamides renforcés par des fibres de verre.

Nomenclature

$\dot{\gamma}$	Shear rate
ε	Strain
ε_b	Strain at break
ε_y	Yield strain
δ	Chemical shift
δ_i	Solubility parameter of i
ΔG_m	Free energy of mixing
$\Delta H_f(i)$	Heat of fusion of i
$\Delta H_f°$	Heat of fusion of a purely crystalline polymer
ΔH_m	Enthalpy of mixing
ΔH_u	Heat of fusion of the repeat unit of a polymeric compound
Δx	Difference between two values x_1 and x_2
η	Viscosity
$[\eta]$	Intrinsic viscosity
η_0	Zero-shear viscosity
η^*	Complex viscosity
η'	Real viscosity
η''	Imaginary viscosity
λ_d	Characteristic time of diffusion
λ_i	Characteristic elastic time of i
ξ	Molar volume ratio
ρ	Density
σ	Stress
σ_b	Stress at break
σ_y	Yield stress
τ	Relaxation time
φ_m	Maximum packing fraction
φ_i	Volume fraction of i
φ_c	Critical volume fraction
χ	Flory-Huggins interaction parameter
ω	Angular frequency
ω_{co}	Crossover angular frequency
ω_i	Mass fraction of i
a_φ	Free volume correction parameter
ATD	Analytical thermal desorption
BSE	Back-scattered electron
C67	Ceramer 67
C1608	Ceramer 1608
CP	Compatibilizer precursor
D	Diffusion coefficient
D_1	Self-diffusion coefficient
D_b	Deborah number

DMA	Dynamic mechanical analysis
DSC	Differential scanning calorimetry
E	Young's modulus
E_a	Activation energy
E_i	Activation energy of i
E1040	Exxelor PE 1040
EPDM	Ethylene-propylene-diene monomer
f	Frequency
FTIR	Fourier-transform infrared spectroscopy
G*	Complex shear modulus
G'	Shear storage modulus
G"	Shear loss modulus
G_c	Free energy of the crystalline phase
G_e	Elastic modulus
G_m	Free energy of the melt phase
$G_m°$	Free energy of the melt phase of a pure compound
GC	Gas chromatography
GF	Glass fibre
GPC	Gel permeation chromatography
HDPE	High-density polyethylene
HDPE-g-MA	Maleic anhydride-grafted high-density polyethylene
HSOM	Hot stage optical microscopy
iPP	Isotactic polypropylene
IR	Infrared spectroscopy
L_0	Thickness of the polymer layer
LDPE	Low-density polyethylene
LDPE-g-MA	Maleic anhydride-grafted low-density polyethylene
LLDPE	Linear low-density polyethylene
LLDPE-g-MA	Maleic anhydride-grafted linear low-density polyethylene
M_c	Critical molar mass
$\overline{M_c}$	Number-average molar mass in between cross-links
$\overline{M_i}$	Number-average molar mass of i
M_n	Number-average molar mass
M_p	Peak molar mass
M_w	Weight-average molar mass
M_z	Centrifugation-average molar mass
MA	Maleic anhydride
MS	Mass spectroscopy
NMR	Nuclear magnetic resonance
p	Aspect ratio of a particle
PA	Polyamide
PA6	Polyamide 6
PA11	Polyamide 11
PB	Polybutylene
PB-g-MA	Maleic anhydride-grafted polybutylene
PBAE	Poly-beta-amino-ester
PE	Polyethylene

PE-COOH	Carboxylic acid end-functionalized polyethylene
PE-g-MA	Maleic anhydride-grafted polyethylene
$PE\text{-}NH_2$	Amine end-functionalized polyethylene
$PE\text{-}Si(OMe)_3$	Trimethoxy silane end-functionalized polyethylene
$PE\text{-}Si(OMe)(Me)_2$	Dimethyl methoxy silane end-functionalized polyethylene
PEO	Polyethylene oxide (i.e. polyethylene glycol, PEG)
PET	Polyethylene terephtalate
PIB	Polyisobutylene
PP	Polypropylene
PP-g-MA	Maleic anhydride-grafted polypropylene
R	Ideal gas constant
R_v	Viscosity ratio
SE	Secondary electron
SEBS	Styrene-ethylene-butylene-styrene copolymer
SEBS-g-MA	Maleic anhydride-grafted styrene-ethylene-butylene-styrene copolymer
SEC	Size-exclusion chromatography
SEM	Scanning electron microscopy
t	Time
t_D	Diffusion time
T	Temperature
T_α	Main transition temperature
T_b	Boiling temperature
T_c	Crystallization temperature
T_g	Glass transition temperature
T_m	Melting temperature
$T_m°$	Melting temperature of a pure component
T403	Jeffamine T-403
tan δ	Loss factor
TGA	Thermogravimetric analysis
TIPS	Thermally-induced phase separation
ToF-SIMS	Time-of-flight secondary-ion mass spectroscopy
U700	Unicid 700
UHMWPE	Ultra-high molecular weight polyethylene
V	Volume
V*	Minimum free volume into which a solvent molecule can jump
V_i*	Specific volume of i at 0K
V_{FH}	Average free volume
VOC	Volatile organic compound
W725	Polywax 725
X_m	Degree of crystallinity

Table of contents

General introduction

The formulation of thermoplastic materials involves the blending of numerous additives and fillers in order to improve their technical features as well as their processability.[1] Nowadays these formulations are becoming more complex because of the growing demand to produce new materials with specific properties designed to meet more restricting and more diversified requirements.[2]

A good example is the use of short fibre-reinforced thermoplastics that are now common engineering materials used in a wide range of applications.[3] These materials are often used to replace metal parts in order to produce lightweight structures in several sectors such as the automotive and aerospace industry or the field of energy and environment. In addition to excellent mechanical properties, the use of reinforced thermoplastics also requires reasonable costs in terms of processing energy, despite de high viscosity that is usually inherent to filled polymers, as well as other features including for instance recyclability or the ability to be associated with other types of materials such as metals or thermosets. On the one hand, the reinforcement of polymers mainly relies on the interfacial adhesion between the reinforcing filler and the polymer matrix to ensure proper load transfer under mechanical solicitation[4]; a careful design of the matrix-filler interphase is therefore required to ensure the good mechanical behaviour of such materials from the nano-scale to the macro-scale. On the other hand, one of the major issues with short fibre-reinforced thermoplastics is certainly their processing, which requires the incorporation of high amounts of rigid, non-spherical particles, thus resulting in very high viscosity suspensions.[5] A good understanding of the interparticle as well as polymer-particle interactions governing the rheological behaviour of such systems is therefore necessary in order to achieve a good control of the filler dispersion in thermoplastic matrices.

Another example is the increasing use of polymer blends and alloys in diverse applications ranging from impact-resistant materials in the automotive sector to multi-layered films for the food packaging industry.[6] In that perspective, the issue of polymer-polymer miscibility and compatibility is of prime importance as incompatible blends usually result in properties inferior to that of the original constituents. Most polymers are actually immiscible with each other, even those with very close chemical structures such as polyethylene and polypropylene.[7] For this reason, a lot of effort has been put into the research of efficient ways to compatibilize blends of immiscible polymers[8], with the objective of preventing uncontrolled morphology developments, usually by incorporating a compatibilizer which acts as an interface agent between the two constituents of the blend.[9]

In the light of these considerations, the need for the development of new molecules to promote the dispersion of fillers such as short fibres or to ensure the compatibilization of incompatible polymer blends is indisputable. The aim of the REPEAT II project[(A)] was therefore to meet such scientific and technical challenges by using end-functionalized polyethylene oligomers as interface agents in fibre-reinforced thermoplastics and in immiscible thermoplastic blends.

While some functional additives are already commercially available, they remain rather limited in terms of accessible functionalities and are usually either (i) very small molecules (such as amine hardeners for

epoxy resins or silane coupling agents used in the sizing of glass fibres) or (ii) high molar mass functional polymers obtained via copolymerization or grafting of the desired moiety onto a polymer backbone (such as ethylene-acrylate copolymers or maleated polyolefins). In this latter category, the most commonly encountered additives are certainly maleated polyolefins such as those in the Lotader[(B)], Orevac[(C)], Fusabond[(D)] or Exxelor[(E)] commercial product ranges.

On the contrary, the flexible synthesis strategy developed by the C2P2[(F)] laboratory, which involves catalysed chain growth (CCG) on a main-group metal[10,11], allows the synthesis of mono-functional or telechelic polyethylene oligomers with controlled molar masses between 500 and 5000 g/mol, as well as a wide range of end-functions and high degrees of functionality.[12,13] The main advantages of such functional polyethylene oligomers are:

- A wide range of accessible functional groups;
- Compatibility with polyolefin resins due to the polyethylene chain;
- Intermediate molar masses.

Regarding this last point, the intermediate molar masses achievable with this synthesis strategy places these functional oligomers between small molecules, which may migrate undesirably thus causing exudation or be classified as volatile organic compounds (VOC), and high molar mass additives, whose molecular architecture and diffusion into polymer resins are often difficult to control.

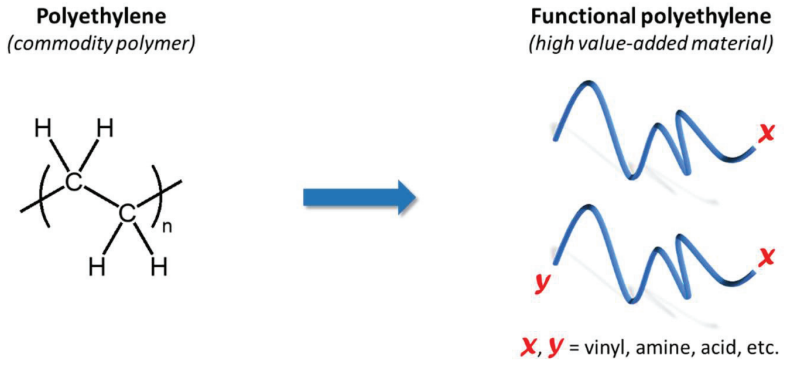

In the course of this thesis, which took place within the framework of the REPEAT II project, several aspects of the incorporation of such functional polyethylene oligomers into polymer blends and composites were tackled. This document is thus divided into five chapters.

In the first chapter, a literature review is proposed in order to provide a theoretical basis for the experimental work reported in the following chapters, as well as a concise review of the existing studies on the subjects of (i) polymer-polymer blending, especially in the case of blends involving polyolefin resins with low molar mass hydrocarbon compounds, and (ii) the compatibilization of immiscible polymers, particularly polyethylene-polyamide blends compatibilized by the addition of a reactive compatibilizer precursor.

A detailed account of the various materials, mixing processes and characterization methods used throughout the work reported in Chapters 3–5 is given in Chapter 2.

The objective of the experimental work presented in Chapter 3 is to get a better understanding of the morphology developments taking place during the blending and crystallization of binary systems where a low molar mass polyethylene oligomer is incorporated into polypropylene or high-density polyethylene. The rheological behaviour of such systems in the molten state as well as their crystalline microstructure in the solid state are thus investigated along with the crystallization behaviour during the transition between those states.

In Chapter 4, new strategies for the compatibilization of immiscible high-density polyethylene/polyamide-6 blends are investigated. This study focuses on the use of a reactive system involving two types of functional oligomers as compatibilizer precursors, which are (i) a maleic anhydride-grafted polyethylene oligomer as well as (ii) a tri-functional polyetheramine oligomer, both of which are commercially available products.

In the last chapter, the use of functional polyethylene oligomers as dispersing and coupling agents in high-density polyethylene reinforced with discontinuous glass fibres is investigated, with the underlying objectives of improving both the processability and the mechanical properties of such systems.

(A) REPEAT II is a collaborative R&D project funded with the help of the Fond Unique Interministériel (FUI). This project involved four companies (Hutchinson, Activation, Addiplast and Lotus Synthesis) as well as two public research laboratories (Ingénierie des Matériaux Polymères UMR CNRS 5223 and Chimie Catalyse Polymères et Procédés UMR CNRS 5265) and was certified by three competitiveness clusters (Axelera, Plastipolis and Elastopôle). Public financers include: BPI France, Fonds Européen de Développement Régional (FEDER), Région Auvergne-Rhône-Alpes, Métropole de Lyon, Conseil Général du Loiret and Direction Générale des Entreprises. Additional information can be found at www.repeat2.fr (in French).

(B) Lotader® terpolymers (Arkema) are reactive polyolefins which contain chemical functions such as maleic anhydride and/or glycidyl methacrylate.

(C) Orevac® resins (Arkema) are polyolefins modified with maleic anhydride.

(D) Fusabond® (DuPont) is a family of functional polymers typically modified with maleic anhydride.

(E) Exxelor® (ExxonMobil) resins are maleic anhydride-functionalized elastomers or polyolefins copolymers.

(F) The C2P2 (laboratory of Chemistry, Catalysis, Polymers and Processes) is a public research laboratory and a CNRS joint research unit (UMR 5265) based in Villeurbanne (France).

References

[1] B. Bitsch, Amélioration des thermoplastiques : Rôle du compoundeur, Techniques de l'ingénieur. Plastiques et composites. 2 (2003) AM3238.1-AM3238.14.

[2] I. Manas-Zloczower, Z. Tadmor, 1. Basic concepts, in: Mixing and Compounding of Polymers; Theory and Practice, 2nd edition, Carl Hanser Verlag GmbH & Co. KG, 2009: pp. 3–5.

[3] L. Tong, A.P. Mouritz, M. Bannister, 3D Fibre Reinforced Polymer Composites, Elsevier, 2002.

[4] W.T.Y. Tze, D.J. Gardner, C.P. Tripp, S.C. O'Neill, Cellulose fiber/polymer adhesion: effects of fiber/matrix interfacial chemistry on the micromechanics of the interphase, Journal of Adhesion Science and Technology. 20 (2006) 1649–1668. doi:10.1163/156856106779024427.

[5] M.M. Rueda, M.-C. Auscher, R. Fulchiron, T. Périé, G. Martin, P. Sonntag, P. Cassagnau, Rheology and applications of highly filled polymers: A review of current understanding, Progress in Polymer Science. 66 (2017) 22–53. doi:10.1016/j.progpolymsci.2016.12.007.

[6] L.A. Utracki, ed., 1. Introduction to polymer blends, in: Polymer Blends Handbook, Kluwer Academic Publishers, Dordrecht; Boston, 2002: pp. 1–122.

[7] J.W. Teh, A. Rudin, J.C. Keung, A review of polyethylene–polypropylene blends and their compatibilization, Adv. Polym. Technol. 13 (1994) 1–23. doi:10.1002/adv.1994.060130101.

[8] C. Koning, M. Van Duin, C. Pagnoulle, R. Jerome, Strategies for compatibilization of polymer blends, Progress in Polymer Science. 23 (1998) 707–757. doi:10.1016/S0079-6700(97)00054-3.

[9] D.R. Paul, Chapter 12 - Interfacial Agents ("Compatibilizers") for Polymer Blends, in: D.R. Paul, S. Newman (Eds.), Polymer Blends, Academic Press, 1978: pp. 35–62. doi:10.1016/B978-0-12-546802-2.50008-7.

[10] J. Mazzolini, E. Espinosa, F. D'Agosto, C. Boisson, Catalyzed chain growth (CCG) on a main group metal: an efficient tool to functionalize polyethylene, Polymer Chemistry. 1 (2010) 793–800. doi:10.1039/B9PY00353C.

[11] I. German, W. Kelhifi, S. Norsic, C. Boisson, F. D'Agosto, Telechelic Polyethylene from Catalyzed Chain-Growth Polymerization, Angewandte Chemie International Edition. 52 (2013) 3438–3441. doi:10.1002/anie.201208756.

[12] S. Norsic, C. Thomas, F. D'Agosto, C. Boisson, Divinyl-End-Functionalized Polyethylenes: Ready Access to a Range of Telechelic Polyethylenes through Thiol–Ene Reactions, Angewandte Chemie International Edition. 54 (2015) 4631–4635. doi:10.1002/anie.201411223.

[13] W. Nzahou Ottou, S. Norsic, I. Belaid, C. Boisson, F. D'Agosto, Amino End-Functionalized Polyethylenes and Corresponding Telechelics by Coordinative Chain Transfer Polymerization, Macromolecules. 50 (2017) 8372–8377. doi:10.1021/acs.macromol.7b01396.

Chapter 1 – Literature review

Table of contents

1. Introduction

A large number of commercial polymer materials produced nowadays consists of polymer blends, alloys and compounds. While the association of two or more polymer components is generally the best way to achieve optimal properties, polymer compounding also involves various types of additives and fillers. This results in very complex mixtures that have been studied extensively in the literature. Several aspects of polymer blending are investigated in this chapter with the aim of providing a theoretical basis as well as a review of existing studies on those subjects in order to contribute to the discussions on the results reported in Chapters 3 and 4.

The general aspects associated with the importance of miscibility in polymer blends are presented in the first part (Section 2) of this chapter, including the consequences on the morphology of polymer blends. The following sections deal with the impact of low molar mass additives on polyolefins and are focused respectively on (i) the morphology developments in polymer blends with low viscosity ratios in Section 3 and (ii) the crystallization behaviour of polyolefins in the presence of low molar mass hydrocarbon compounds in Section 4. Finally, the compatibilization of immiscible polyethylene/polyamide blends is tackled in the last part (Section 5), with particular attention given to maleic anhydride-grafted compatibilizer precursors as well as reactive compatibilization strategies involving low molar mass functional additives.

The issues relating to the reinforcement of thermoplastics and to the rheology of glass fibre suspensions are not tackled in this chapter. In order to provide a scientific and technical context to the experimental work on glass fibre-reinforced HDPE, a synthetic review of the literature is proposed at the beginning of Chapter 5 instead.

2. Importance of miscibility in polymer-polymer blending

2.1. Definition of miscibility in polymer blends and polymer solutions

The issue of polymer-polymer miscibility is of great importance, as incompatible blends usually result in properties inferior to that of the original constituents, and most polymers are actually immiscible with each other, even those with very close chemical structures such as polyethylene and polypropylene.[1] Many studies have focused on the morphology and crystallization kinetics of immiscible blends where both constituents are high molar mass polymers, especially in the case of polyolefins[2–6], although some instances of partial miscibility resulting in macroscopically homogeneous blends have been reported.[7,8]

In chemical terms, miscibility is achieved when favourable interactions occur between the different constituents of a blend. This chemical affinity can be defined by the Hansen solubility parameters[9], which were first introduced by Hildebrand and Scott[10,11] and have since been studied extensively for applications in the field of polymer materials.[12–15] However, while miscibility can be defined easily for small molecules such as solvents (based on polar forces and hydrogen bonding), it is much more complex in the case of polymers because of their higher molar masses.[16]

Polymer miscibility is more commonly studied from a thermodynamic point of view. According to Gedde[17], a polymer mixture is considered thermodynamically miscible when it is composed of a single phase which is homogeneous on a molecular level. In the case of miscible polymer blends, this means that the domain size is comparable to the macromolecular dimension. The definition given by Utracki[18] states that miscibility is associated with the values of free energy of mixing ΔG_m and enthalpy of mixing ΔH_m, such as:

$$\Delta G_m \approx \Delta H_m \leq 0$$

This criterion is illustrated in Figure 1, where the free energy of mixing is plotted as a function of the volume fraction of polymer at a given temperature.

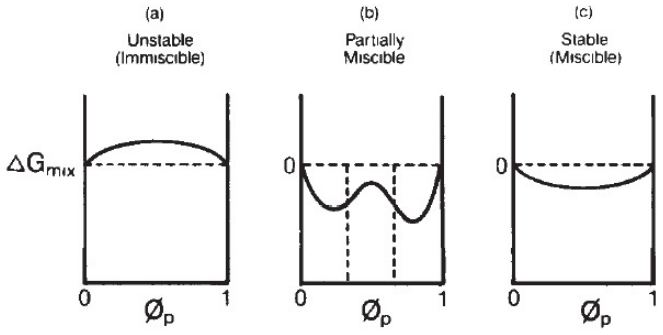

Figure 1. Free energy of mixing (ΔG_{mix}) as a function of the volume fraction of polymer ($\emptyset_P$)[19]

According to this representation, partially miscible systems can form single phase at certain blend compositions. It is also worth noting that the free energy of mixing is also highly dependent on the temperature, which is a critical point in the field of polymer processing as some binary blends may be miscible in the melt and immiscible in the solid state.

This definition of miscibility is based on the mean-field theory developed by Flory[20] and Huggins[21] to describe polymer-solvent interactions in polymer solutions, which have been investigated extensively over the past century. It can therefore be applied to binary systems involving a semi-crystalline polymer with a much lower molar mass component such as an oligomer, which will be further discussed in Sections 3 and 4 of this chapter.

2.2. Morphology of immiscible polymer blends

Most polymer materials that are produced nowadays consist of polymer blends and alloys, as the blending of two or more polymer components is generally the best way to achieve optimal properties, compared to single homopolymers. However, most polymers are actually incompatible with each other, meaning that the simple association of two polymers is very likely to result in highly heterogeneous materials with properties that are poorer than that of the initial components.

Blends involving two immiscible polymers can result in various morphology, some of which can be useful to attain the desired material properties (e.g. tensile strength, impact strength, electrical conductivity, etc.).[22] Some examples of useful immiscible blends morphologies are illustrated in Figure 2.

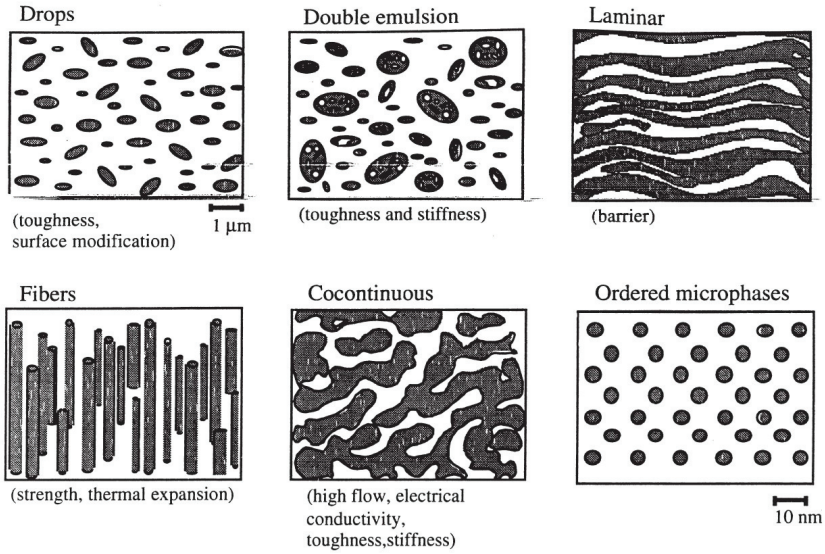

Figure 2. Schematic representations of useful morphologies that can be produced by polymer-polymer melt blending[23]

The type of morphology that is spontaneously created is highly dependent on the chemical nature of the constituents, blend composition, viscosity ratio and processing conditions.[24,25] During the

blending of two immiscible polymers, unfavourable thermodynamics as well as high interfacial tension lead to the formation of separate phases, which generally results in the minor phase being dispersed in the form of droplets in the major continuous phase.[26] The number and dimensions of the dispersed domains is largely controlled by droplet break-up and coalescence mechanisms that are extensively described in the literature[23,27,28] and may lead to the gross segregation of the two phases on a macroscopic scale.

3. Processing of low viscosity additives in polymer resins

3.1. Morphology developments during the initial stages of blending

It is well known that the final morphology of a blend has a controlling influence on its final properties. Therefore, the morphology developments during the processing of polymer-polymer blends have been studied extensively. Controlling parameters include the processing technique and conditions, the composition of the blend and the chemical nature of the constituents as well as their physical properties such as their viscoelastic behaviour in the molten state.

The fundamental objective of mixing is to achieve an even distribution of both fluids by decreasing heterogeneities of concentration throughout the mixing equipment. While distributive mixing essentially relies on the mixing ability of the equipment, dispersive mixing is essentially dependent on the shear flow and viscoelastic behaviour of the constituents.[29] It is generally admitted that the deformation of the dispersed domains is the elementary step towards the increase of the interfacial surface area. The deformation of the dispersed phase is promoted by shear stress and counteracted by interfacial stress. The latter tends to minimize the surface to volume ratio, favouring spherical domain shapes.[27] The stretching of the initial phases by the flow leads to an increase of the interface between the two constituents in a process called striation. In the case of thermodynamically miscible polymers there is no surface tension at the interface, which implies that interdiffusion eventually plays a role in the homogenization of the blend at the molecular scale.[30] However, most polymer combinations result in thermodynamically immiscible blends, meaning that the homogenization process relies exclusively on mechanical mixing mechanisms.

Scott and Macosko[31,32] proposed a mechanism to describe the morphology developments during the early mixing process. In their work, an internal batch mixer was used to blend small amounts of a low viscosity polymer additive in a high viscosity polymer resin. The mixing torque was monitored and the aspect of the content of the mixer was observed after different times of mixing. Those observations showed that in the initial stages of mixing, the dispersed phase formed complex sheets, ribbons and laces shapes due to the dragging of the polymer pellets against the hot surface of the mixer. Shearing and interfacial instability seemed to subsequently break those structures into spherical domains. The mechanism proposed by Scott and Macosko to explain those morphology developments is depicted in Figure 3.

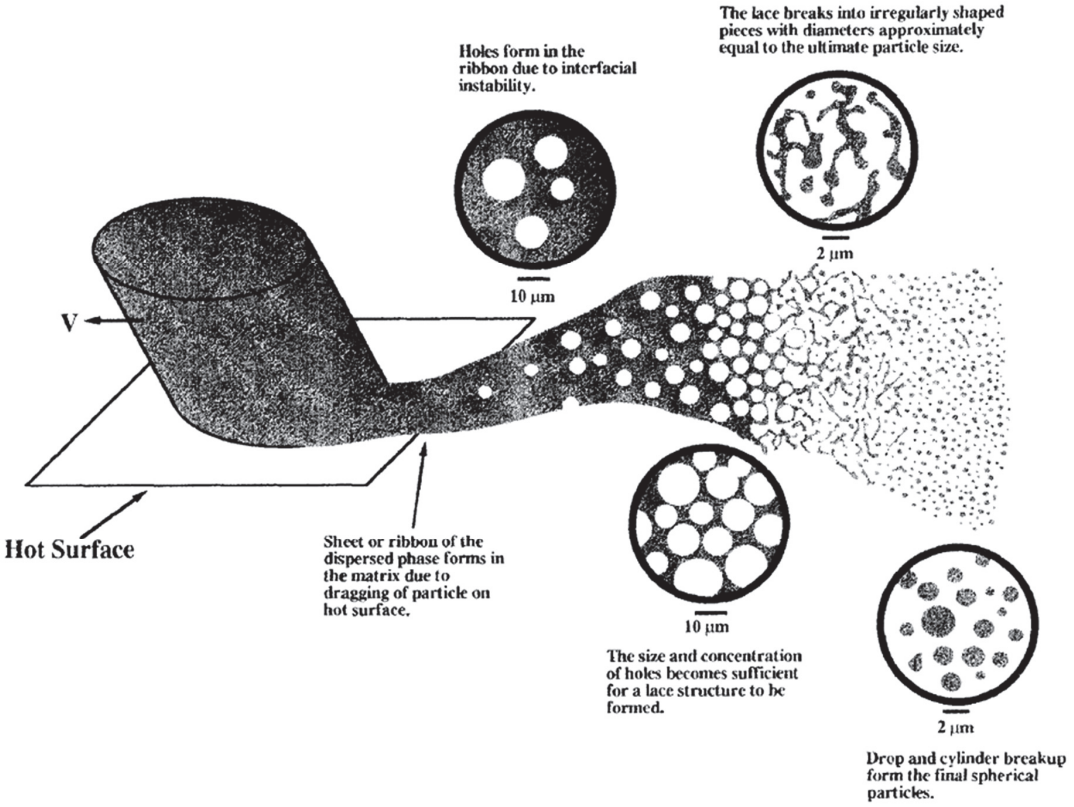

Figure 3. Mechanism proposed by Scott and Macosko to describe the morphology developments occurring during the initial stages of polymer-polymer blending.[31,32]

It is worth noting that the morphology developments during initial stages of the mixing process appeared to be independent from miscibility or reactivity between the resin and the dispersed phase, since these effects only become significant once a sufficiently large interfacial area has been created between the two components.[31]

3.2. Impact of the viscosity ratio on morphology developments

While polymers with similar viscosities blended in equal volume fractions generally lead to a co-continuous morphology, it has been observed that phase continuity is highly dependent on the viscosity ratio[33], which is defined as the ratio between the viscosity of the minor constituent (η_{minor}) and that of the major constituent (η_{major}), and is written $R_v = \eta_{minor}/\eta_{major}$. As explained in Section 3.1, under flow, drops of the dispersed phase are extended to threads and breakup into smaller drops. The breakup mechanism is quite complex and essentially depends on flow and viscosity ratio. In simple shear flow, four types of deformation and breakup mechanisms have been described, depending on the viscosity ratio. The influence of composition and viscosity ratio on the final morphology of uncompatibilized PE/PA blends has been correlated to the drop breakup mechanisms proposed in the literature[27] in the recent work of Epinat et al.[34] and is summarized in Figure 4.

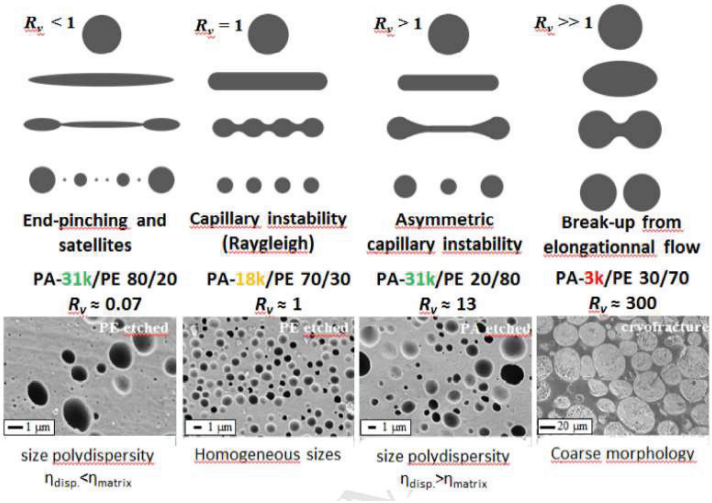

Figure 4. Proposed schematics of the various drop break-up mechanisms under flow for polyamide/polyethylene blends, depending on the viscosity ratio R_v. Indicated viscosity ratios are those estimated at 100 rad/s. The observed representative examples of morphologies (SEM pictures) are well described by the proposed mechanisms.[34]

It was demonstrated that when the constituents of the blend do not have the same viscosities, the low viscosity constituent encapsulates the high viscosity constituent and becomes the continuous phase, even when the low viscosity constituent is the minor phase. The point of phase inversion, expressed in terms of blend composition, was therefore found to be highly dependent on the viscosity ratio.

From an industrial point of view, the viscosity ratio has a dramatic impact on the blending process, as many formulations involve the incorporation of low viscosity additives, such as plasticizers, in high viscosity polymers. In their work, Scott and Joung[35] and Burch and Scott[36] have investigated the blending of miscible and immiscible low viscosity additives into polymer resins, the viscosity ratio considered in these studies being in the range of 1 to 10^{-4}. Those studies essentially relied on the analysis of mixing torque variations in a batch internal mixer as well as on the observation of the content of the mixer after different mixing times (in the same way as in [31,32]). The authors found that several parameters seemed to have an influence on the mixing time of such blends, whether the additive was miscible in the polymer resin or not, including:

- Processing temperature: a higher mixing temperature resulted in shorter mixing times;
- Filling level: faster and better homogenization was achieved when the mixing equipment was optimally filled;
- Viscosity ratio: longer mixing times were required at low viscosity ratios;
- Blend composition: higher volume fractions of the low viscosity component resulted in longer times to achieve homogenization.

Furthermore, similarities were found in the dynamic mixing behaviour of miscible and immiscible systems, for which the introduction of a very low viscosity additive in a high viscosity polymer resin (viscosity ratios of 10^{-2} to 10^{-4}) resulted in a lubricating effect, characterized by a strong and persistent

decrease of the mixing torque. Considering the mechanism proposed by Scott and Macosko[31,32], this was attributed to the segregation of the low viscosity component to the high shear rate zones of the mixing equipment.

The observation of the mixer content after short mixing times revealed that the low viscosity additive had molten and coated the polymer pellets, therefore appearing to be the continuous phase (despite being the minor constituent in terms of volume fraction) and confirming previous findings.[33] The introduction of a low viscosity additive therefore reduced the viscous dissipation and stress transfer by acting as a lubricant, consequently decreasing the energy available to soften and melt the polymer. Additionally, in both cases (miscible or immiscible systems) lubrication was followed by a rapid increase of the mixing torque before reaching a steady torque value, which is typical of a phase inversion behaviour.

Further work on this matter by Cassagnau and Fenouillot[37] demonstrated that during the blending of a miscible low viscosity additive with a high viscosity polymer, the homogenization of the system proceeds through two mechanisms: mixing and diffusion. It was actually found that the simple striation model described by Tadmor and Gogos[29] could not be applied and that the behaviour of the system was more sensitive to diffusion than to mixing in the case of viscosity ratios below 10^{-3}. Lubrication therefore occurs in the case where the characteristic time of diffusion is shorter than the mixing time, causing the low viscosity component to segregate to the high shear rate zones of the mixing equipment. The apparent phase inversion phenomenon should accordingly be considered as the result of the homogenization on a molecular level through interdiffusion.

In the case of immiscible systems, no diffusion takes place and the homogenization on a macroscopic scale relies solely on the mixing ability of the mixing equipment. Therefore, lubrication occurs because of the absence of diffusion of the low viscosity component into the high viscosity component and phase inversion ensues, following the mechanism proposed by Scott and Macosko.[31,32]

3.3. Diffusion behaviour of small molecules into polymer resins

3.3.1. Theoretical aspects of molecular transport in polymers

The formulation of thermoplastic and thermoset materials generally involves the incorporation of small molecules such as plasticizers or reactive polymer modifiers. In reactive blending for example, the chemical transformation of the polymer relies on the ability of the reactants to diffuse to the reactive sites.[38–40] The study of the diffusion mechanisms during the blending of low viscosity additives into polymer resins is therefore an important issue to be considered as it directly affects the blending process and the design of the mixing equipment.

The diffusion of a solvent into a polymer is characterized by the Deborah number D_b, which is defined as the ratio of the characteristic time of the fluid λ_m to the characteristic time of the diffusion process

λ_d, thus comparing the rate of conformational rearrangement of the polymer chains with the rate of diffusion.

$$D_b = \frac{\lambda_m}{\lambda_d}$$

When the Deborah number is large, the molecular transport is called elastic diffusion. Values close to 1 denote comparable rates of diffusion and molecular relaxation, thus the molecular transport is considered viscoelastic. If the Deborah number is small, the polymer and the solvent are considered to behave like purely viscous fluids and the diffusion can be described by a Fickian law. The diffusion of small molecules (e.g. a solvent or a low molar mass additive) in a polymer at a temperature significantly higher than their glass transition temperature is generally considered to correspond to the third situation where the Deborah number is small.

The diffusion of small molecules into polymer resins can be described by the free volume theory, which was first introduced by Cohen and Turnbull[41] and extensively developed by Vrentas and Duda[42–46]. According to this theory, if V* is the minimum free volume (or hole) into which a solvent molecule can jump and V_{FH} is the average free volume, then the self-diffusion coefficient D_1 can be considered to be proportional to the probability of finding a hole V* or larger:

$$D_1 = A.\exp\left(-\frac{\gamma V^*}{V_{FH}}\right)$$

where γ is a numerical factor introduced to account for the overlap between free volume elements and A is a constant of proportionality relating to the gas kinetic theory. This expression is usually developed as follows:

$$D_1 = D_0.\exp\left(-\frac{E}{RT}\right).exp\left(-\frac{\omega_1 V_1^* + \xi\omega_2 V_2^*}{V_{FH}/\gamma}\right)$$

Here, D_0 is a constant, E is the critical energy necessary for a molecule to overcome attractive forces, ω_1 and ω_2 are the weight fractions of solvent and polymer in the system, respectively, V_1* and V_2* are the specific volumes of the solvent and the polymer at 0 K, respectively, and ξ is the molar volume ratio for the solvent and polymer jumping units.

The mutual diffusion coefficient D_{12} can then be deduced using the Flory-Huggins theory for polymers above their glass transition temperature:

$$D_{12} = D_1(1-\varphi_1)^2(1-2\chi\varphi_1)$$

with φ_1 the volume fraction of solvent in the system and χ the Flory-Huggins interaction parameter. The parameters in these equations are difficult to determine and several studies have proposed methods to predict them.[47,48]

3.3.2. Rheological measurement and modelling of the diffusion phenomenon

More recent studies[49–51] have demonstrated that such parameters (used to determine diffusion coefficients) can be derived from viscoelastic measurements and used to model the diffusion behaviour of small molecules into polymers. The goal of these investigations was to get a better understanding of the dependence of molecular transport kinetics on process parameters, such as temperature, as well as formulation parameters, such as miscibility of the diffusing molecule with the polymer resin or molar mass of the polymer.

These studies used rheological measurements based on a bi-layer setup well described in the work of Joubert et al.[49], where a layer of the penetrant molecule was placed on top of a polymer layer so that the diffusion would occur in a single direction normal to the surface of the sample. Rheology was found to be a sensitive tool which allowed to directly link the evolution of viscosity to the transport behaviour in miscible and partially miscible systems, as illustrated on Figure 5:

1. During the initial stages of the experiment the viscosity of the system is dominated by the lower viscosity fluid;
2. In the intermediate stages of the diffusion process, a concentration gradient is created, which induces viscosity variations;
3. Eventually, the system reaches a steady value of viscosity with no further diffusion, indicating that the homogenization of the sample is achieved.

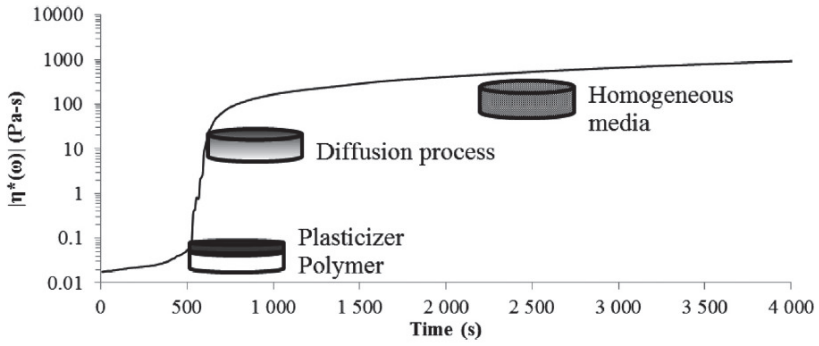

Figure 5. Illustration of the absolute complex viscosity variations during the diffusion of a mineral oil (Torilis® 7200) into EPDM (Vistalon® 8800) at T = 160 °C and ω = 10 rad/s[12]

While all studies agreed that an increase in temperature resulted in an increased rate of diffusion, the impact of other parameters such as the molar mass of the polymer resin on the mutual diffusion coefficient seemed to vary depending on the chemical nature of the system studied. These investigations on the rheological modelling of the diffusion process were mainly focused on the diffusion of plasticizers in elastomers, and so far not much research has been done on thermoplastic systems. In the work of Ponsard-Fillette et al.[50], the subject of diffusion in thermoplastics is addressed and it is shown that the previously mentioned model based on the free volume theory can be

used to predict the rheological properties of polypropylene/paraffinic oil blends. The validity of this model relies on the homogeneous nature of the relaxation mechanisms and the fact that the reduction of entanglement arising from the dilution is the dominating mechanism.

In fact, the use of a model based on the free volume theory to describe polymer-plasticizer interactions during the diffusion process relies on the groundwork laid by Marin et al.[52] and Raju et al.[53] on the dilution aspects in concentrated and semi-dilute polymer solutions. They extensively discussed the modelling of intramolecular and intermolecular forces which govern the relaxation mechanisms of entangled macromolecules, according to the reptation theory proposed by de Gennes[54] as well as the theoretical approach to the thermodynamics of polymer solutions developed by Flory[55]. The conclusions of these early investigations are that the dilution of a polymer by a solvent leads to a reduction of macromolecular entanglements (and therefore to a shift in the relaxation spectrum). The viscoelastic properties of the polymer solution thus depend on the one hand on the chemical nature of the solvent (due to a shift in the glass transition temperature) and on the other hand on the concentration of the polymer in solution (dilute, semi-dilute or concentrated regime).

More recent studies by Gimenez et al.[56] and Ponsard-Fillette et al.[50] have demonstrated that the introduction of small molecules such as monomers and oligomers (paraffinic oils) resulted in the modification of the viscoelastic properties of polymer resins due to a dilution effect similar to that caused by a solvent. It is therefore not unreasonable to assume that the diffusion process in miscible polyolefin systems (involving a high molar mass polymer resin and a low molar mass additive) can be described using a similar model.

However, it should be noted that the modelling of the diffusion of small molecules into polymer resins heavily relies on the miscibility of the system. For instance, it has been shown that in immiscible systems, the absence of diffusion resulted in the absence of viscosity variations throughout the bi-layer rheological experiments presented above.[12] Moreover, while the mechanisms of molecular transport in miscible systems are rather straightforward, they are quite complex and still not well understood in systems that are only partially miscible, as diffusion kinetics have been shown to rely on the chemical affinity between the diffusing species and the polymer resin.[12,51,57]

4. Miscibility and crystallization behaviour of polyolefins in the presence low molar mass hydrocarbon additives

4.1. Physical properties of low molar mass hydrocarbon additives and miscibility in polyolefin resins

The compounding of polyolefins involves several types of additives, including stabilizers, flame retardants, anti-static agents, colorants and processing aids, as well as many types of fillers.[58] Processing aids are usually classified as external and internal lubricants[59], depending on whether they provide slip between the polymer and the surface of the processing equipment or decrease the frictional forces between the polymer chains, respectively.

A large number of processing aids that are used in the formulation of polyolefins consists of hydrocarbon derivatives such as paraffinic, naphthenic and aromatic oils, paraffinic and microcrystalline waxes or saturated fatty acids.[60,61] More recently, blends of polyolefins with low molar mass hydrocarbon compounds have generated new interest for their use in the field of energy storage. For instance, mineral oils have been studied extensively for their use in polyethylene-based battery separators[19,62–66], and other investigation have focused on blends of polyolefins (especially polyethylene or polypropylene) with paraffin waxes for potential applications in phase change materials.[67–75]

Paraffinic compounds are short linear hydrocarbon chains (or alkanes) whose physical properties depend on the number of -CH_2- repeating units.[76] At room temperature, alkanes containing 1 to 4 carbon atoms are gases and alkanes containing roughly 5 to 15 carbon atoms are liquids. Heavier compounds with 20 carbon atoms or more are usually found in the form of waxy solids at room temperature. While hydrocarbon oils generally comprise a mixture of paraffinic, naphthenic and aromatics compounds, hydrocarbon waxes on the other hand usually consist of linear paraffins, which provides them with a high degree of crystallinity in the solid state. The crystallization behaviour of paraffin mixtures can be quite complex, usually showing several melting endotherms and crystallization exotherms as a result of solid-solid transition[77] from one crystalline structure to another or fractionated crystallization[78] due to the molar mass distribution of the n-alkane chains.

The low molar masses of linear hydrocarbon compounds (such as paraffin waxes, which are solid at room temperature) lead to lower melting temperatures compared to that of polyolefin resins as well as very low viscosities at typical polymer processing temperatures. It can therefore be assumed that hydrocarbon oils and waxes have similar viscoelastic behaviours at the high temperatures considered for the blending of polyolefins. However, the difference in their degree of crystallinity in the solid state implies very different behaviours upon the cooling and subsequent crystallization of binary blends also involving high molar mass semi-crystalline polymers.

As explained previously (see Section 2.1), the definition of miscibility developed by Flory[20] and Huggins[21] to describe polymer-solvent interactions can be applied to binary systems involving a semi-crystalline polymer with a much lower molar mass component, such as hydrocarbon oils and waxes in this case. Nevertheless, the study of such systems can be quite complex due to the singular behaviour of those low molar mass additives, which usually exhibit very good diffusion and solvation abilities in polymer melts, but can also be characterized by a high degree of crystallinity in the solid state (in the case of waxes) or remain in the liquid state at room temperature (in the case of oils). For this reason, very different phase separation mechanisms may apply upon solidification of such mixtures. From this point of view, polymer-oligomer systems can be considered as polymer solutions and binary polymer blends at the same time. Understanding the morphology developments during the solidification of such systems is a critical issue, as the formulation of polymers involves a wide range of additives with intermediate molar masses.

The aforementioned studies on battery separators and phase change materials found that paraffin oils and waxes were mostly miscible in polyethylene and polypropylene in the melt, but induced liquid-liquid phase separation when added in large amounts[79,80], which is usually typical of immiscible systems. Solid-liquid (in the case of oils or crystallizable waxes) phase separation was also observed upon crystallization of the polyolefin resins. The conclusion of those studies are that those compounds were totally or partially miscible in polyethylene[62,19,70,71,75] and partially miscible or immiscible in polypropylene.[63,81] The good compatibility between low molar mass linear hydrocarbon compounds and polyethylene arises from their similar chemical structure and close solubility parameters (e.g. δ_{HDPE} = 8.0 and $\delta_{liquid\ paraffin}$ = 7.8).[64] Furthermore, most investigations found that short alkanes (such as mineral oil or liquid paraffin) were miscible in polyethylene and polypropylene in the melt, and some waxes were found to be miscible in polypropylene when added in small amounts. However, while co-crystallization is has been reported in the case of PE/wax blends[82–84], crystalline waxes are always found to crystallize separately from polypropylene because of their different crystalline structures.[71,72]

Observations on the miscibility and crystallization behaviour of blends of polyolefins with low molar mass hydrocarbon additives are summarized in Table 1.

Table 1. Miscibility and phase separation behaviour in polyolefin/low molar mass hydrocarbon additive blends, as reported in the literature

Polymer	Hydrocarbon additive					Observations	Reference
	Type	Chain length (№ of C atoms)	Molar mass (g/mol)	Melting point (°C)	Contents investigated (%)		
LLDPE	Hard paraffin wax	C18-C120	785	77-101	2-40	Miscibility in the melt, no conclusion in solid state	Krupa et Luyt[85]
LLDPE	Hard paraffin wax	C33-C128	785	90	5-40	Miscible in the melt with possible co-crystallization	Hlangothi et al.[82]
LDPE	Oxidized paraffin wax	n/a	750	50-100	5-50	Miscible in the melt, co-crystallization <20 wt% wax, phase separation >30 wt%	Djoković et al.[84]
HDPE, LLDPE & LDPE	Hard paraffin wax	n/a	813	90	10-30	Miscible in HDPE up to 20 wt%, partially miscible in LDPE or LLDPE	Hato et Luyt[86]
	Oxidized paraffin wax	n/a	669	96		Miscible with LLDPE, partially miscible with HDPE or LDPE	
HDPE, LLDPE & LDPE	Soft paraffin wax	C15-C78	440	40-60	30-50	Immiscible at those contents	Molefi et al.[73,74]
iPP	Hard paraffin wax	C18-C120	785	77-101	5-30	Miscible in the melt at low wax contents, phase separation in solid state	Krupa et Luyt[70]
iPP	Hard, oxidized paraffin wax	n/a	785	72-95	10-40	Both waxes immiscible with iPP, the hard wax being slightly more compatible	Krupa et al.[71]
	Soft paraffin wax	C18-C40	374	41-57			
PP	Paraffin wax	n/a	n/a	37	40-80	Immiscible	Alkan et al.[72]
iPP	Soft paraffin wax	C15-C78	440	40-60	5-20	Wax may act as a diluent for PP	Molaba et al.[87]
HDPE	Liquid paraffin	n/a	n/a	n/a	20-85	Miscible in the melt, solid-liquid phase separation	Sun et al.[79], Matsuyama et al.[80], Akbari et Yegani[65]
UHMWPE	Liquid paraffin	n/a	n/a	n/a	20-95	Miscible in the melt, solid-liquid phase separation	Zhang et al.[88], Liu et al.[64], Park et al.[89]
iPP	n-alkanes	C14, C20, C32	n/a	n/a	10-90	Miscible in the melt, solid-liquid phase separation	Li et al.[63], Kim et al.[81]
iPP	n-fatty acids	C14-C19	n/a	n/a	10-90	Miscible in the melt, solid-liquid phase separation	Kim et Lloyd[81]
iPP	Polyethoxylated tallow amine	n/a	350	n/a	30-75	Miscible under 40 wt% in the melt, solid-liquid phase separation	Lloyd et al.[19]
HDPE & PP	Mineral oil	n/a	n/a	n/a	50-80	Miscible in both PE and PP	Lloyd et al.[62]
HDPE, LLDPE & LDPE	n-alkane	C18	n/a	28	30	Partial miscibility	Chen et Wolcott[75]
UHMWPE	Naphthenic oil	n/a	n/a	n/a	5-90	Miscible	Toquet et al.[66]

n/a = information is not available

The miscibility of linear hydrocarbon oils and waxes with polyolefins in the molten state implies that those low molar mass additives can be considered as diluents and that the Flory-Huggins theory on polymer-solvent interactions can therefore be used to describe such binary systems in the molten state.[79] In their paper, Lloyd et al.[62] explain the effect of miscibility on the melting temperature of the semi-crystalline polymer resin in polymer-diluent systems, based on the Flory-Huggins theory. The melting temperature T_m of the polymer in solution is given by the following expression:

$$T_m = \left(\frac{R}{\Delta H_u}\frac{V_u}{V_d}\left(\phi_d - \chi\phi_d^2\right) + \frac{1}{T_m^\circ}\right)^{-1}$$

where $T_m°$ is the melting temperature of the pure polymer, ΔH_u is the heat of fusion of the repeat unit of the polymer, V_u is the molar volume of the repeat unit of the polymer, V_d is the molar volume of the diluent, φ_d is the volume fraction of the diluent, R is the ideal gas constant and χ is the Flory-Huggins interaction parameter. T_m is then plotted against the volume fraction of polymer in solution $\varphi_p = 1 - \varphi_d$ in the case of blends of polypropylene with three different diluents, which are characterized by their interaction with the polymer resin. The resulting temperature-composition phase diagram is represented in Figure 6, where each plotted line corresponds to a different diluent.

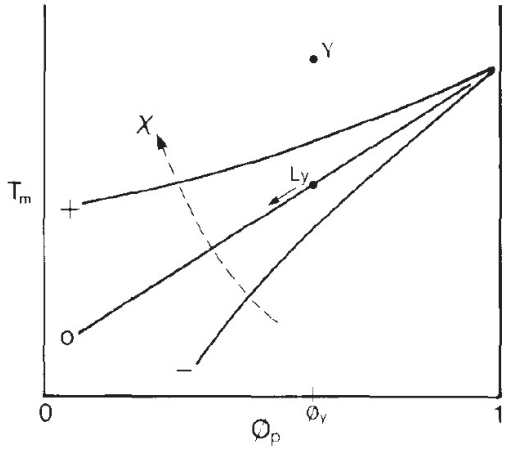

Figure 6. Temperature-composition phase diagram for a polymer-diluent system in which the polymer is semi-crystalline[62]

In this diagram, the lines referred to as melting point depression curves give the melting temperature of the polymer depending on the composition of the system. They separate the homogeneous one-phase region (above the line) from the heterogeneous two-phase solid-liquid region (below the line). Here, the effect of the Flory-Huggins interaction parameter expressing the strength of interaction (i.e. degree of miscibility) between the polymer and the diluent is put forward, and it can be observed that a good polymer-diluent miscibility ($\chi \leq 0$) results in a decrease in the melting temperature of the polymer due to the dilution effect. It should also be noted that in non-equilibrium processes, the cooling rate has a severe impact on the phase diagram. In the same study, Lloyd et al.[62] show that increasing the

cooling rate leads to the supercooling of the blend, thus resulting in a lowering of the melting point depression curve as the system cools below its equilibrium crystallization temperature.

The effect of low viscosity hydrocarbon additives, either liquid (e.g. oils or liquid paraffins) or solid (such as crystalline paraffin waxes), on the crystallization behaviour of polyolefins, especially polyethylene and polypropylene, will be discussed in the next sections.

4.2. Crystallization behaviour of polyolefins in the presence of a low molar mass amorphous additive

As explained in the previous section, a large number of additives used in the formulation of polyolefins consists of low molar mass hydrocarbons, such as mineral oil or liquid paraffin, which are in the liquid state at rooms temperature. As a consequence, they remain amorphous liquids within the processing, melting and crystallization temperature ranges usually considered for the study of polyolefins. Solid-solid interactions can therefore not be considered for this type of systems, and the cooling of such blends eventually leads to a separation between the solidified semi-crystalline polymer and the liquid additive.

The segregation of the two constituents can occur through solid-liquid or liquid-liquid phase separation, depending on the miscibility of the system.[19] If the additive is miscible with the polymer, it acts as a diluent and the system remains homogeneous in the molten state, eventually undergoing solid-liquid phase separation upon crystallization of the polymer. On the contrary, liquid-liquid phase separation occurs if the interaction between the polymer and the additive is weak (i.e. the system is immiscible).[79] Some methods such as thermally induced phase separation (TIPS) rely on the limited miscibility of the low molar mass compounds in polymer resins to control the morphology of the dispersed phase via solid-liquid or liquid-liquid phase separation.[19,62]

4.2.1. Immiscible systems

In the case of immiscible systems, separate phases are formed in the molten state and the crystallization behaviour of the polymer is hardly affected by the presence of the dispersed phase and usually crystallizes like the bulk homopolymer[90], although dispersed domains may act as additional nucleation sites depending on the interfacial tension and on the potential migration of impurities from the additive to the polymer.[91] However, the presence of an amorphous dispersed phase may impact the ultimate morphology of the crystalline phase of the polymer, which has a controlling influence on the mechanical properties of the blend. For instance, Martuscelli et al.[92] demonstrated that several factors influence the morphology of a binary blend of immiscible polymers, such as the chemical nature, molar mass and crystallization temperature of the constituents, as well as the blend composition and the spherulite growth rate of the semi-crystalline constituent. These parameters may lead to the amorphous phase being either rejected from the crystalline front or engulfed within the

spherulites, such as illustrated in Figure 7, where the effect of the blend composition on the final morphology of isothermally crystallized iPP/PIB films is shown.

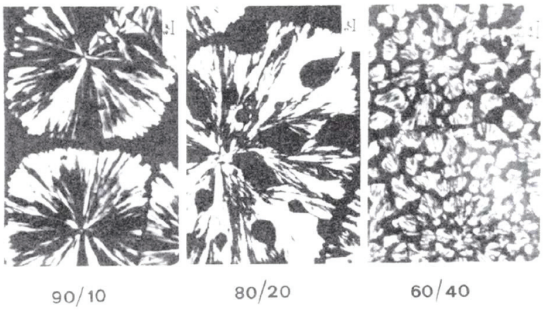

Figure 7. Optical micrographs of iPP/PIB blends (T_c = 135 °C) with different compositions[90,92]

Moreover, the authors emphasized the fact that such variations in the structure, shape and dimensions of the crystalline phase have a controlling influence on the fracture behaviour of polypropylene.[93] Other authors also observed the final morphology of the blend to be dependent on variations of the viscosity ratio, which was induced by changing the molar mass of the polymer resin[79] or that of the linear hydrocarbon additive.[81] However, the effect of the chain length of the low molar mass component was only studied in the range of roughly C15 to C30, thus no data was found as to the impact of longer alkane derivatives.

4.2.2. Miscible systems

If the amorphous constituent is miscible with the polymer resin, the blend is considered homogeneous in the molten state and no liquid-liquid phase separation occurs. The final morphology of the blend is therefore controlled by the solid-liquid phase separation occurring during the solidification of the semi-crystalline polymer.[79] Phase separation in polyolefin/diluent systems resulting from a solid-liquid segregation process has been reported several times in the literature, especially in the case of polyethylene[65,80,88] and polypropylene[63,81] resins. These investigations mainly involved low molar mass hydrocarbon additives such as naphthenic oil and linear alkanes in the range of C10-C30 (i.e. liquid paraffin) which were found totally of partially miscible with the polyolefin resins considered.

Groeninckx et al.[90] described the crystallization process of such miscible systems as involving two types of molecular transport occurring simultaneously: the diffusion of the semi-crystalline polymer to the crystalline front and the rejection of the amorphous component from the crystalline phase. This segregation can be characterized as inter-spherulitic or intra-spherulitic, as illustrated in Figure 8, where the amorphous component is shown to be located between the crystal lamellae, between stacks of lamellae (fibrils) or between the spherulites.

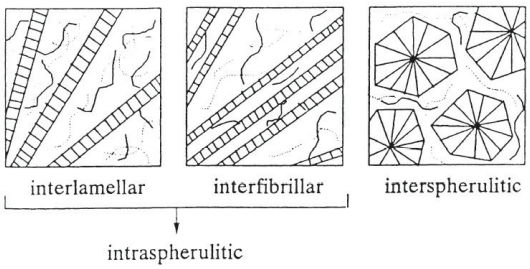

Figure 8. Schematic representation of the different types of segregation of the amorphous component from the crystallizable component in miscible polymer blends[90]

For instance, several authors have commented on the morphology in polypropylene-based systems involving low molar mass hydrocarbon additives.[19,62,63,79] In their study, Lloyd et al.[62] explain that the observed fracture patterns can be qualitatively explained by a solid-liquid phase separation process, resulting in inter-spherulitic segregation of the diluent.

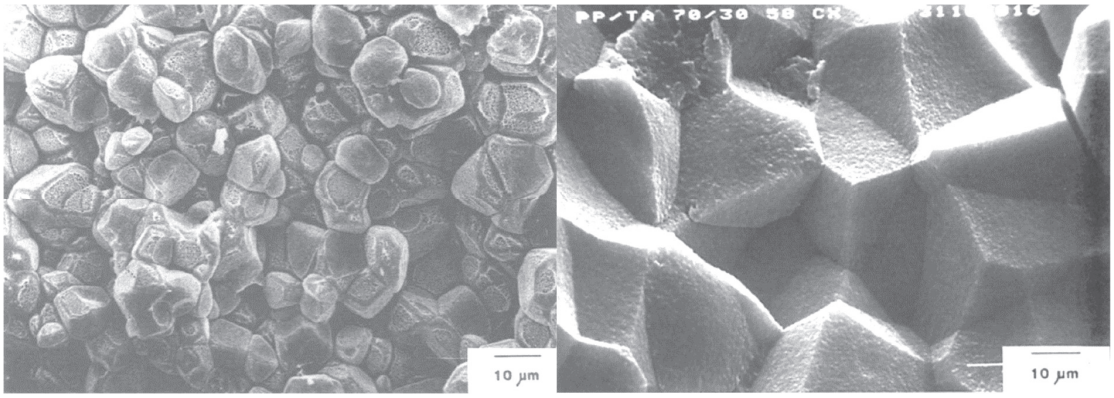

Figure 9. Scanning electron micrographs of the spherulitic structure resulting from the solid-liquid phase separation of a PP/mineral oil (70/30) solution (left)[62] and a PP/polyethoxylated amine (70/30) solution (right)[19]

Variations in shape and dimensions of the observed microstructures were found to be dependent on the polymer/diluent combination, blend composition, nucleation density of the polymer and cooling rate. Polypropylene appeared to be a particularly adequate polymer to investigate inter-spherulitic segregation because of the neat spherulitic morphology of its crystalline phase in the solid state. Other studies have focused on other polymer resins, and for instance several examples of microporous membranes prepared with polyethylene (which typically exhibit "leafy" fracture patterns as a result of solid-liquid phase separation) can be found in the literature.[62,64,65]

Besides the impact on the crystalline morphology of the blends in the solid state, the presence of miscible low molar mass components implies that they act as diluents in the molten state, therefore influencing the crystallization and melting behaviour of semi-crystalline polymers. Although mineral oil or liquid paraffin appeared to have no effect on the ultimate crystallinity of polyethylene or polypropylene[66,75], the incorporation of such additives was reported to result in a decrease of the crystallization and melting temperatures due to the reduction of chain entanglements arising from the

dilution of the semi-crystalline polymer.[88,89] While the decrease in crystallization temperature is linked to the lower nucleation density in the melt, the shift in melting temperature due to the addition of a miscible amorphous component can be explained by the higher mobility of the polymer chains. According to Groeninckx et al.[90], the melting point depression results from kinetic, morphological and thermodynamical factors. Kinetic effects arise from the cooling conditions and morphological effects are associated with changes in the morphology of the nascent crystals. Thermodynamical effects consist in the decrease of the free energy of the semi-crystalline polymer as a result of dilution by a miscible amorphous component in the molten state[55,94], which leads to a shift in the equilibrium melting point, as schematized in Figure 10.

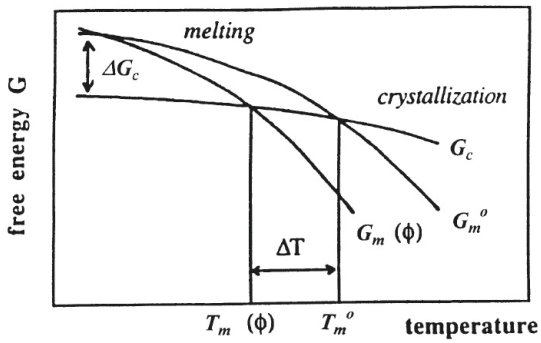

Figure 10. Schematic diagram of the free energy of the crystalline phase (G_c) and free energy of the melt phase of a homopolymer ($G_m°$), as well as the free energy of a miscible blend ($G_m(\Phi)$), as a function of temperature[90]

4.3. Crystallization behaviour of polyolefins in the presence of a low molar mass semi-crystalline additive

As mentioned earlier, hydrocarbon additives with a higher molar mass (C20 and above) are usually found in the form of waxy solids at room temperature. Additives such as paraffin waxes and polyolefin oligomers exhibit a particular behaviour as they are characterized by a very low viscosity in the molten state as well as a high degree of crystallinity in the solid state due to their linear structure. This implies that the crystallization behaviour of blends involving semi-crystalline polymers with such additives can be quite complex.

It is important to note that due to their low molar mass (compared to that of polymers), these additives present relatively low melting and crystallization temperatures. This means that the melting and crystallization of the semi-crystalline polymer can be considered to always occur in the presence of a liquid (or molten) phase, whether the system is miscible or immiscible. Consequently, the solid-liquid separation mechanisms described in the previous section are still valid, provided that there is a significant difference between the melting temperatures as well as between the crystallization temperatures of the two components. However, if the melting and/or crystallization temperatures of the two components are close, they can undergo concurrent melting and/or crystallization. In that

regard, it should also be noted that the melting and crystallization temperatures of the semi-crystalline polymer may be shifted as a result of dilution and plasticizing in the case of miscible systems (as mentioned in the previous section).[71,74]

4.3.1. Miscible systems

In the case of miscible systems involving two crystallizable components, several modes of crystallization have been described: separate, concurrent and co-crystallization. Co-crystallization only occurs in rare cases where the blend constituents have similar crystalline structures and are completely miscible in the crystalline phase[90], which requires chemical compatibility as well as close matching of the chain conformation and crystal lattice. Most of the time, the miscibility is limited to the molten state and the components crystallize separately due to the segregation of the component with the lower crystallization temperature (segregation mechanism described in Figure 8). Concurrent crystallization on the other hand is mostly the result of overlapping crystallization temperature ranges, which should be taken in account in the analysis of DSC thermograms, where a single melting endotherm and crystallization exotherm may not necessarily be the result of co-crystallization. Some examples of co-crystallization are mentioned in the literature, where linear paraffin chains of low molar mass polyethylene were reported to co-crystallize with the linear sequences of LLDPE or LDPE.[8,95,96] One hypothesis to support those observations is that the short paraffin chains are unable to fold (see Figure 11) but may be assimilated to straight polyethylene sections, and can therefore be incorporated in polyethylene lamellae.[86]

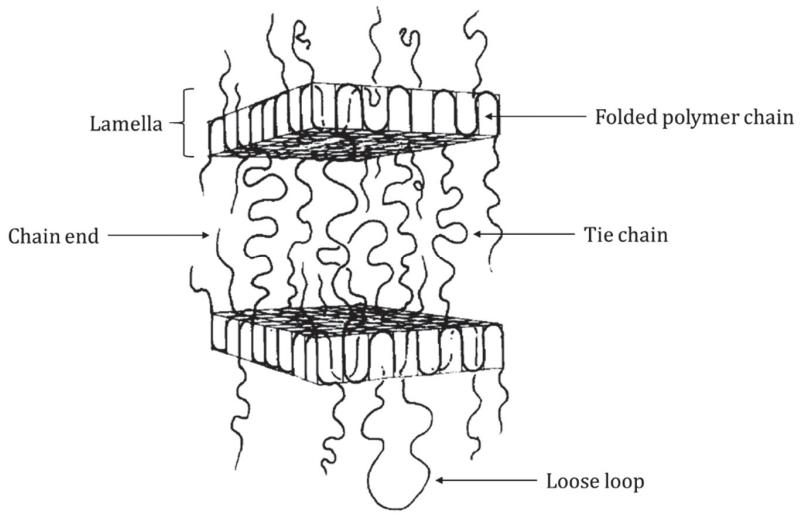

Figure 11. Model illustrating the arrangement of polyethylene chains into lamellar structures upon crystallization[97,98]

Additionally, the incorporation of crystalline paraffin wax in polyethylene was reported to significantly increase the overall degree of crystallinity, which is mainly due to the high degree of crystallinity of those compounds and therefore not necessarily showing evidence of co-crystallization. The result is the improvement of some mechanical features of the blends, such as higher Young's modulus, but also

the degradation of the ultimate mechanical properties, such as stress and strain at break.[82,84,86] The ultimate mechanical properties of semi-crystalline polymers are known to be closely related to the number of tie chains between lamellae[97,99], which is reduced because of the dilution of the polymer by a short hydrocarbon compound. However, in systems where the miscibility is limited by blend composition[84,86], the presence of defects arising from phase separation may be a more straightforward explanation to the lower stress and strain at break observed at high wax concentrations.

4.3.2. Immiscible systems

Immiscible systems are characterized by a lack of compatibility inducing liquid-liquid phase separation in the molten state. Blends with two immiscible components with different crystallization temperatures would thus be expected to crystallize sequentially and independently in the same manner as isolated homopolymers. However, the crystallization behaviour of a semi-crystalline polymer may be affected by the presence of a dispersed component despite the physical separation in the melt.

Coincident crystallization of both components has been reported in cases where the dispersed phase has a higher crystallization temperature than the continuous phase, therefore acting as a nucleation site.[100] However, low molar mass hydrocarbon additives exhibit relatively low melting and crystallization temperatures compared to that of polyolefins, which can be considered to crystallize in the presence of a liquid phase, hence the case of coincident crystallization will not be further discussed.

In investigations on immiscible systems, such as PP/paraffin wax blends, it was found that the crystallization of the polymer resin is mostly unhindered by the presence of the low molar mass additive (despite a slight decrease in the melting temperature of polypropylene due to plasticizing), showing separate melting endotherms and crystallization exotherms in DSC analyses as a result of the phase separation in the solid state as well as in the molten state.[71,72] In fact, blending seemed to have a much greater effect on the dispersed wax, decreasing its degree of crystallinity and wearing off its complex melting and crystallization behaviour (see Section 4.1), due to the lack of mobility in an already solidified resin.[90] Other studies on immiscible PP/PE systems showed that the spherulite growth rate of the polypropylene continuous phase remains unaffected by the presence of polyethylene. They also pointed out that the nucleation density of propylene may be affected by the presence of molten polyethylene, either decreasing because of the migration of nucleation sites to the dispersed phase[101] or increasing as a result of additional nucleation at the interface between the two polymers.[102]

Nevertheless, the main consequence of blending immiscible compounds is surely the impact on the ultimate crystalline morphology of the blend, which has been thoroughly investigated by several authors over the past fifty years.[1] According to Bartczak and Gałeski[91], variations of the spherulitic

morphology of polypropylene in the presence of polyethylene are the result of changes in the interface shape during the crystallization of the blend.

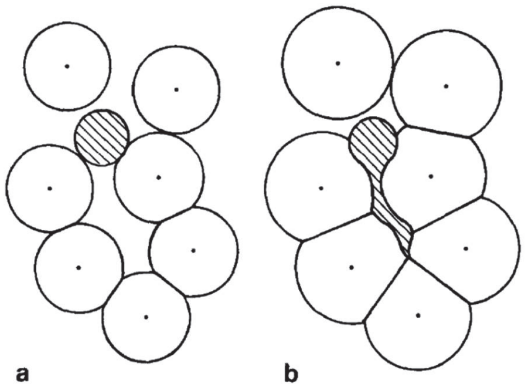

Figure 12. Schematic representation of the deformation of a dispersed PE phase during the crystallization of the PP resin[91]

Figure 12 indeed illustrates the deformation of the dispersed phase upon crystallization of the resin, leading to an alteration of the crystalline morphology in the solid state, which directly impacts the mechanical properties of the blend. The magnitude of this deformation is dependent on the ability of the dispersed phase to flow between the spherulites of the crystallizing dispersed phase. This implies that low molar mass (i.e. low viscosity) hydrocarbon compounds are very likely to be deformed during the crystallization of the polyolefins resins, which may also apply to miscible systems undergoing an inter-spherulitic segregation process.

5. Compatibilization of polyethylene-polyamide blends

5.1. General aspects of polymer-polymer compatibilization

As mentioned in Section 2.2, blends involving two immiscible polymers may result in various morphologies which can be useful to achieve certain properties.[22] However, these morphologies can be quite difficult to achieve and may be thermodynamically unstable.[23] For this reason, a lot of effort has been put into the research of efficient ways to compatibilize and/or control the morphology of immiscible polymer blends.[103] The objective of compatibilization in immiscible systems is therefore to prevent uncontrolled morphology developments[104,105], usually by incorporating a compatibilizer which acts as an interface agent between the two constituents of the blend.[106]

There are three aspects to the compatibilization of immiscible systems, which are (i) the reduction of interfacial tension in order improve dispersion, (ii) the stabilization of blend morphology against shear stress during the processing and forming steps, and (iii) the enhancement of adhesion between the two phases in the solid state in order to ensure an efficient stress transfer within the final material. These requirements can be fulfilled either by the addition of a third component to the blend, usually a block or graft copolymer, or by forming such copolymer in situ via reactive compatibilization of the blend.[107]

Compatibilization by addition consists in the incorporation of a small amount of a third component to the blend. While a co-solvent (miscible with both phases) can be used, such compatibilizers are usually block or graft copolymers with segments that are miscible (or at least have sufficient interactions) with one or both polymers in the blend.[108] Their role is to reduce the interfacial tension between the two immiscible phases in order to stabilize the dispersed domains (i.e. prevent droplet coalescence) and promote interfacial adhesion. In that regard, copolymer compatibilizers can be considered as interphase agents that are similar to the surfactants used to stabilize emulsions.[26] The molar mass and sequential distribution of blocks or grafts are key factors influencing the efficiency of such copolymers, and their molecular structure should therefore be carefully optimized in order to ensure proper diffusion of the copolymer to the polymer-polymer interface as well as to avoid the formation of micelles.[107] Besides, the incorporation of a third component to a polymer blend usually results in modified viscoelastic properties and crystallization behaviour, and may therefore impact the processability or final properties of the blend. As a consequence, reactive compatibilization of the blends is usually preferred over compatibilization by addition.

In the case of reactive compatibilization, the compatibilizer is produced by a chemical reaction directly at the interface between the two immiscible phases, thus forming a copolymer based on segments of the initial homopolymers in the blend. As a consequence, this type of compatibilization has several advantages compared to compatibilization by addition, including the fact that the copolymer does not need to diffuse to the polymer-polymer interface, while the molar mass of the copolymer segments is

comparable to that of the homopolymer in each phase.[109] However, reactive compatibilization must be carried out under adequate processing conditions (i.e. sufficiently distributive and dispersive mixing) in order to be efficient. Moreover, the reactivity and reaction rate must be sufficiently high to promote the formation of a significant amount of compatibilizer across the phase boundary in the molten state.[107,110]

According to Brown[109], reactive compatibilization strategies can be classified into five main categories depending on which parts of the polymer chains are involved in the formation of the copolymer. For each strategy in this classification, there are actually two types of processes leading to the formation of the copolymer, that are (i) the direct reaction between the polymer chains of the immiscible phases or (ii) the introduction of a third component to the blend. The latter is fairly similar to compatibilization by addition, except that the added component is a reactive species involved in the formation of the copolymer. This reactive component can simply act as a catalyst activating the reaction between the two polymers, although coupling agents reacting with one or both polymers are more frequently used. In this case, the reactive component incorporated in the blend may be designated as a "compatibilizer precursor".

5.2. Introduction to polyethylene/polyamide blends

Polyethylene and polyamide are some of the most widely spread thermoplastic polymers, with a large variety of industrial applications.[111–113] The blending of these polymers is primarily motivated by combination of the good technical features of polyamide with the cost-effectiveness and moisture resistance of polyethylene.[114] However, polyethylene and polyamide have significantly different crystalline structures and polarities due to their very different molecular structures, resulting in highly incompatible blends with coarse biphasic morphologies.[115,116] The compatibilization of such immiscible systems has therefore been the subject of a considerable number of investigations, with the aim of achieving various controlled morphologies depending on the targeted applications.

For instance, the use of polyethylene is limited in technical applications, such as in the automotive industry, because of its poor heat resistance. The improvement of thermal and mechanical properties can be achieved with polyamide as the continuous phase, while the demand for cost-effective materials requires to keep polyethylene as the major component. These requirements can be met by producing co-continuous morphologies.[117] On the other hand, lamellar, fibrillar or finely dispersed morphologies may be interesting for other applications as they can also result in outstanding properties, provided that the interfacial adhesion between the two immiscible components is sufficiently improved through compatibilization.[118,119]

As explained in the previous section, adequate compatibilization should promote the reduction of interfacial tension between the two phases and avoid coalescence, resulting in the formation of a stable morphology as well as a narrow domain size distribution. The addition of various functional polymers

or oligomers as coupling agents in immiscible polymer blends has therefore been studied extensively as an effective way to achieve reactive compatibilization.[120,121] However, this strategy poses problems that are similar to the ones described in the case of compatibilization by addition, the main issues being the migration of the compatibilizer precursor to the interface between the immiscible phases, as well as good compatibility with at least one of the polymer resins. The compatibility issue is commonly overcome by using a chemically modified version of one of the two polymers as the compatibilizer.[121] A good example of this strategy is the use of maleic-anhydride-grafted polyolefins as compatibilizers in polyolefin/polyamide blends, where the compatibilizer is miscible in the polyolefin and reacts with the amine end-groups of the polyamide.[118,122–124]

Compatibilization strategies for immiscible blends of polyethylene and polyamide are detailed in the following sections.

5.3. Compatibilization strategies for polyethylene/polyamide blends

In immiscible polymer systems such as polyethylene/polyamide blends, reactive compatibilization is usually preferred over compatibilization by addition because of difficulties associated with the synthesis of linear PE-PA block copolymers to be used as compatibilizers.[117] Reactive compatibilization of polyethylene/polyamide blends is usually ensured by using a functional copolymer such as a polyethylene grafted with an acidic group (carboxylic acid, acrylic acid, maleic anhydride, etc). The acidic groups undergo an acid-base reaction with the terminal amines of polyamide to form covalent bonds while the apolar backbone of the copolymer interacts with the polyethylene phase, consequently reducing the interfacial tension between the two immiscible polymers. Reactive compatibilization with a grafted polyethylene copolymer can be implemented either by directly adding the compatibilizer precursor to the immiscible blend, or by promoting the in-situ functionalization of polyethylene along with compatibilization in a single-step reactive process.[120,125]

Various strategies for the morphology control and/or compatibilization of immiscible polyethylene/polyamide blends are described in the literature. With few exceptions where organoclay is used to control the blend morphology[126–129], most investigations are focused on the use of grafted polyolefin copolymers as compatibilizer precursors. Hence, a review of the compatibilizer precursors studied in the literature is summarized in Table 2, where such polyolefin copolymers are divided into four groups depending on the nature of their functional groups: maleic anhydrides, acids, ionized acids or other functionalities. In most of the papers reviewed the compatibilizing component was either used as received from the supplier, or in some cases synthesized prior to blending. Two synthesis routes are described for the preparation of such functional polyolefins, namely (i) the copolymerization of ethylene with another monomer bearing functional groups or (ii) the direct modification of a polyolefin by free radical grafting.

Table 2. Summary of the morphology control and reactive compatibilization strategies investigated in the literature for polyethylene/polyamide blends

Polymer blend	Blend compositions investigated	Compatibilizer precursor (CP)	CP contents investigated	Reference
Polyolefins grafted with maleic anhydride				
PE/PA	30/70 & 50/50	PP-g-MA	5 %	Chen et al.[130]
PE/PA	90/10 to 10/90	PE-g-MA	1-10 %	Serpe et al.[131]
HDPEPA6	70/30	PE-g-MA	5 %	Kyu Kim et al.[132]
LDPE/PA6	75/25	SEBS-g-MA	1-5 %	Lim et White[123]
LDPE/PA6	60/40 to 90/10	LDPE-g-MA	5 %	Jurkowski et al.[133]
HDPE/PA6	80/20 to 20/80	PP-g-MA	5 %	Palabiyik et Bahadur[134]
LDPE/PA6	75/25	SEBS-g-MA	0.5-2 %	Minkova et al.[135]
LDPE/PA6	75/25	PE-g-MA	1-10 %	Jiang et al.[136]
LDPE/PA6	75/25 & 25/75	SEP-g-MA	5 %	Filippi et al.[137]
LDPE/PA12	70/30	PE-g-MA	0.2-2 %	Huitric et al.[105]
HDPE/PA6	80/20 & 20/80	HDPE-g-MA	1-10 %	Chetreenuwat et al.[138]
HDPE/PA6	75/25 to 25/75	PE-g-MA	2 %	Araújo et al.[125]
HDPE/PA6	30/70	HDPE-g-MA	2-8 %	Hamid et al.[139]
HDPE/PA6	57/43 to 19/81	HDPE-g-MA	16-27 %	Argoud et al.[118]
Polyolefins grafted with acidic functionalities				
LDPE/PA6	75/25 & 25/75	Ethylene/acrylic acid copolymer	5 %	Filippi et al.[140]
LDPE/PA6	75/25	Ethylene/acrylic acid copolymer	0.5-2 %	Minkova et al.[135]
HDPE/PA6	75/25 & 25/75	Ethylene/acrylic acid copolymer	5 %	Scaffaro et al.[119]
HDPE/PA6	75/25	Ethylene/acrylic acid copolymer	5 %	Filippone et al.[128]
Polyolefins grafted with acidic functionalities, neutralized with metal cations (ionomers)				
HDPE/PA6	90/10 to 10/90	Ethylene/methacrylic acid/isobutyl acrylate terpolymer, zinc-neutralized	0.5 %	Willis et Favis[141]
HDPE/PA6	90/10 to 10/90	Ethylene/methacrylic acid/isobutyl acrylate terpolymer, zinc-neutralized	5 %	Willis et al.[142]
HDPE/PA6	80/20	Ethylene/methacrylic acid/isobutyl acrylate terpolymer, zinc-neutralized	2.5 %	González-Núnez et al.[143]
LDPE/PA6	75/25 & 25/75	Ethylene/acrylic acid copolymer, zinc-neutralized	2 %	Filippi et al.[140]
LDPE/PA6	75/25	Ethylene/acrylic acid copolymer, zinc-neutralized	0.5-2 %	Minkova et al.[135]
LDPE/PA6	80/20 to 20/80	Ethylene/methacrylic acid/isobutyl acrylate terpolymer, zinc-neutralized	0.1-35 %	Leewajanakul et al.[144]
LDPE/PA6	80/20 to 20/80	Ethylene/methacrylic acid copolymer, sodium-neutralized	0.5 %	Lahor et al.[145]
HDPE/PA66	75/25 & 25/75	Ethylene/methacrylic acid/isobutyl acrylate terpolymer, zinc-neutralized	2.5-10 %	Baouz et Fellahi[146]
HDPE/PA6	80/20 & 20/80	HDPE-g-MA, zinc-neutralized	1-10 %	Charoenpongpool et al.[147]
Polyolefins grafted with other functionalities				
LDPE/PA6	25/75 to 5/95	LDPE-g-butyl acrylate	2.5 %	Raval et al.[148]
LLDPE/PA6	20/80	Ethylene/(ethyl-, isobutyl- or hydroxylethyl-)methacrylate copolymer	20 %	Valenza et al.[149]
LDPE/PA6	80/20 to 20/80	SEBS-g-ricinoloxazoline maleinate	10 %	Vocke et al.[150]
LDPE/PA6	90/10 to 10/90	Ethylene/glycidyl methacrylate copolymer	1-5 %	Chiono et al.[151]
HDPE/PA6	75/25 & 25/75	Ethylene/acrylic acid copolymer + cyclophosphazene-epoxy	5 %	Scaffaro et al.[119]
HDPE/PA6	75/25 & 25/75	Ethylene/acrylic acid copolymer + cyclophosphazene-oxazoline	5 %	Scaffaro et al.[119]
Organoclays				
HDPE/PA6	30/70	Alkyl ammonium-modified montmorillonite	1.2-2.4 %	Fang et al.[127]
HDPE/PA6	75/25	Alkyl ammonium-modified montmorillonite	5 %	Filippone et al.[128]
HDPE/PA6	75/25 & 25/75	Alkyl ammonium-modified montmorillonite	1-20 %	Filippone et al.[129]

All studies presented in Table 2 reported that the addition a compatibilizer precursor induced the enhancement of interfacial adhesion between polyethylene and polyamide as well as the inhibition of coalescence (to various extents), resulting in a reduction of the size of the dispersed domains and a narrower size distribution. Some studies also reported an improvement of the mechanical properties of the blends, especially tensile strength and impact resistance. While some authors investigated large amounts of compatibilizer precursors, in most cases sufficient compatibilization and optimal properties were achieved with only a few percent, typically 0.5-5 wt% of the blend.

It appears that compatibilizer precursors for polyethylene/polyamide systems mostly consist in functional polyethylenes. Ethylene/acrylic acid copolymers provide good compatibilization via acidolysis reactions between the carboxyl groups and the terminal amines of polyamide[140], and neutralization of the acidic units by a bivalent metal cation (usually zinc or sodium) to form ionomers is reported to further enhance the compatibilizing ability of such copolymers because of the additional ion-dipole interactions with polyamide.[145] However, comparative studies show that maleic-anhydride-grafted polyethylenes are the most efficient compatibilizer precursors for polyethylene/polyamide systems, which is attributed to their faster reaction rate and higher reactivity of maleic anhydride functional groups compared to acids.[135,136] This was confirmed by Orr et al.[152] in a study on melt coupling reactions to form block and graft copolymers, in which functional group pairs are ranked in terms of reactivity. The conclusion of this study is that the rate of conversion for a reaction between an amine and a cyclic anhydride is much faster than that of other reactions which could potentially be involved in the grafting of polyamide chains onto a functional polyethylene compatibilizer precursor according to Table 2 (acid/amine, epoxy/amine, epoxy/acid and oxazoline/acid).

Nowadays, maleic anhydride grafted polyethylenes (PE-g-MA) are the most widely spread compatibilizers for polyethylene/polyamide blends. The maleic anhydride content these commercial additives is usually around 1 wt% (typically in the range of 0.5-2 wt%). While the graft copolymer must remain apolar to be compatible with the polyethylene phase, the maleic anhydride content must be sufficiently high to ensure a good compatibilization. The reaction between the maleic anhydride groups of the compatibilizer precursor and the amine end-groups of polyamide is illustrated in Figure 13. This reaction results in the grafting of polyamide onto polyethylene chains to form a PE-g-PA copolymer, which is characterized by a cyclic imide moiety.

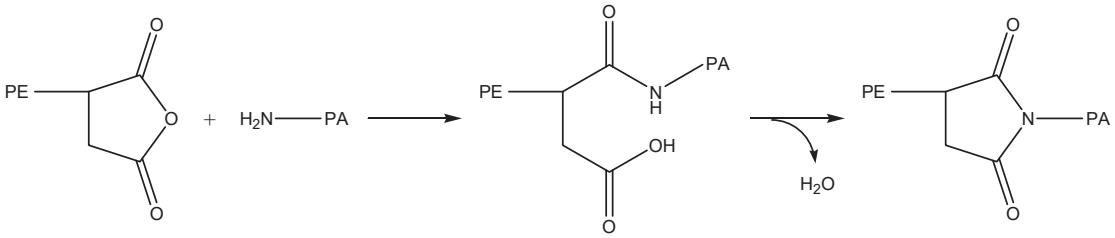

Figure 13. Reaction between PE-g-MA and an amine-terminated polyamide[152]

This reaction also generates water as a bi-product, which may cause the degradation of polyamide[113] or impact reactive compatibilization by shifting the reaction equilibrium. However, Argoud et al.[118] noted that water does not react with maleic anhydride at the melt processing temperatures considered and that it can be easily eliminated through venting zones during the extrusion process.

5.4. Impact of molar mass on the morphology control and compatibilization of polyethylene/polyamide blends

5.4.1. Molar mass of the homopolymers

As explained in Section 3.2 of this chapter, the morphology of immiscible systems is greatly influenced by the viscosity of its homopolymer constituents, which is related to their respective molar masses. The relationship between viscosity ratio and blend morphology can be easily described by a simple diagram, as shown in Figure 14.

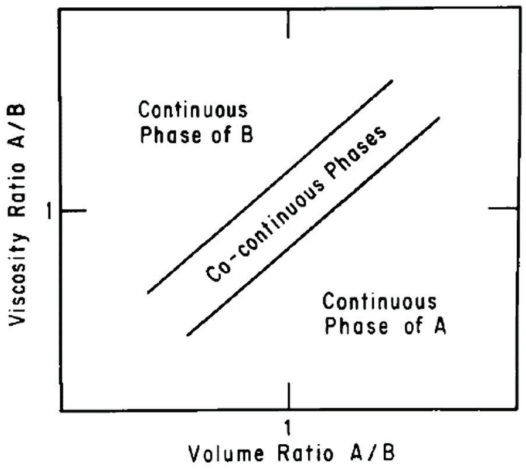

Figure 14. Effect of the blend composition and viscosity ratio on the blend morphology[26]

This is particularly well illustrated in the work of Epinat et al.[34] where compatibilized and uncompatibilized blends of polyethylene and polyamide exhibit a wide variety of morphologies depending on the blend composition and molar mass of the polyamide (see Figure 4). Typically, this study shows that in uncompatibilized polyethylene/polyamide blends the point of phase inversion is between 10 and 20 vol% polyamide when the viscosity ratio is 0.003 (M_n(PA) ≈ 3000 g/mol) and between 50 and 60 vol% polyamide when the viscosity ratio is 1.7 (M_n(PA) ≈ 18 000 g/mol).

In other recent investigations by Pernot et al.[117] and Córdova et al.[153] on compatibilized polyethylene/polyamide systems, the fine tuning of the molar mass of the constituents as well as the degree of functionalization of the compatibilizer precursor allowed to successfully control the morphology of the blends on a sub-micrometric scale. An example of morphology control using these parameters is illustrated in Figure 15.

Blend	PE copolymer		PA homopolymer		MA/NH_2 ratio
	M_n (g/mol)	Monomers	M_n (g/mol)	Terminal groups	
MB	16 000	9 wt% acrylate, 0.8 wt% MA	15 000	35 % NH_2, 65 % COOH	7:1
MC	16 000	17 wt% acrylate, 2.9 wt% MA	2 500	50 % NH_2, 50 % CH_3	3:1

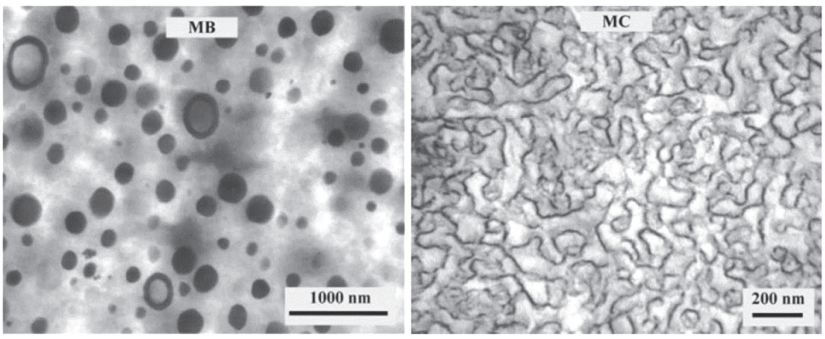

Figure 15. TEM micrographs of PE/PA (80/20) blends prepared by reactive extrusion[153]

In these studies, the authors highlight the influence of the particular morphologies obtained on the crystallization behaviour of the polymers as the confinement of the polyamide phase influences its nucleation. More generally, in the case of dispersed morphologies, the size and nature (polyethylene dispersed in polyamide or polyamide dispersed in polyethylene) of the dispersed domains has a significant impact on the crystallization behaviour of the blends. For instance, polyamide dispersed domains may act as nucleation sites for polyethylene upon cooling of the blend as a result of the difference in crystallization temperatures between the two polymers.

5.4.2. Molar mass of the compatibilizer precursor

The efficiency of the compatibilization and morphology control of immiscible blend is also highly dependent on the molar mass of the copolymer compatibilizer. In reactive processes where the reaction rate is a key factor to achieve efficient compatibilization, the high molar mass of the compatibilizing agent may have a significant influence.[110,154] Theoretically, the compatibilization ability of copolymer compatibilizers can be improved by increasing their molar mass (to produce more entanglement, thus allowing deeper anchoring into the homopolymer phases) and number of blocks/grafts (to allow multiple interlocking).[155] However, the use of high molar mass compatibilizer precursors may result in poor compatibilization as a result of their low chain mobility and potential inability to migrate to the interface.

As a consequence, lower molar mass compatibilizers have generated interest thanks to their greater diffusion ability and lower viscosity during melt processing. For instance, Todd et al.[156] successfully introduced a low molar mass amino-telechelic polyethylene (3-17 kg/mol) to compatibilize an immiscible PET/HDPE system via aminolysis of the PET chains. The use of a functional PE oligomer resulted in the improvement of the interfacial adhesion between PET and HDPE and the consequent reduction of the volume of the dispersed phase. Another example is the interface optimization of an

immiscible PBAE/PEO system by O'Brien et al.[157] via the in-situ formation of a multiblock copolymer, which was generated from a reaction involving the end-groups of two telechelic oligomers (diepoxy terminated PBAE and diamine terminated PEO, both 4000 g/mol), each one miscible in one of the homopolymers (as illustrated in Figure 16). However, no such example has been reported in the case of polyethylene/polyamide compatibilization.

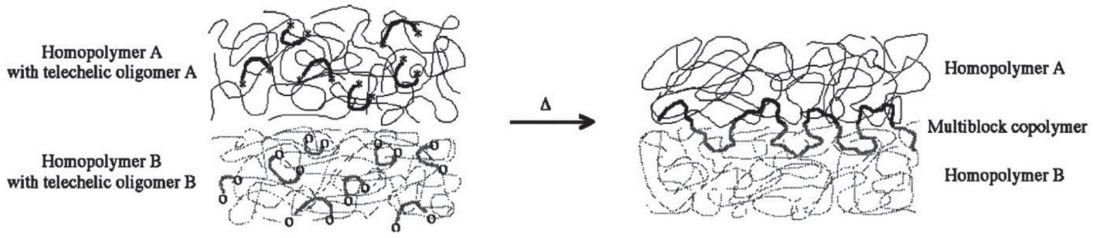

Figure 16. Illustration of the reactive processing scheme proposed by O'Brien et al.[157] using telechelic oligomers to form a multiblock copolymer at the interface between two homopolymers

In their study, Shi et al.[158] achieved stable co-continuous morphologies by forming polyamide-grafted copolymers with both high and low molar mass polyolefin backbones from LLDPE-g-MA (M_n = 20 000 g/mol) and PB-g-MA (M_n = 3000 g/mol) compatibilizer precursors. While high molar mass copolymers strengthened the interface and induced finer dispersion, low molar mass copolymers were found to promote the formation of a flat interface between the polyethylene and polyamide phases. These observations are attributed to the poorer ability of low molar mass copolymers to hinder coalescence. In less complex polypropylene/polyamide systems, Duvall et al.[122] observed that despite a higher maleic anhydride content, the PP-g-MA compatibilizer precursor with lower molar mass did not provide a strong enough interaction with the polypropylene phase. On the other hand, other investigations by Padwa et al.[159] and Jiang et al.[136] demonstrated that the compatibilization efficiency of PE-g-MA precursors was increased with decreasing the molar mass of the polyethylene backbone, thus producing finer and more uniform dispersions of the polyamide phase. Although these observations may seem to contradict the conclusions of the studies cited in the previous paragraph, the higher compatibilization efficiency of those low molar mass compatibilizer precursors was attributed to a higher reactivity towards polyamide chains and to the decrease of the viscosity of the polyethylene phase.

The observations made in those studies clearly indicate that the molar mass of copolymer compatibilizers has a controlling influence of the final morphology of polyethylene/polyamide blends. However, the number of adjustable parameters and the variety of morphologies obtained show that this relationship is complex and that it is difficult to precisely predict the impact of using lower molar mass compatibilizer precursors such as PE-g-MA oligomers on the ultimate morphology of polyethylene/polyamide blends.

6. Conclusion

Several aspects of polymer blending were tackled in this chapter, with a focus on the incorporation of low molar mass compounds in polyolefins and polyethylene/polyamide blends.

In Section 3, it was shown that the low viscosity and good diffusion ability of low molar mass additives have a controlling influence on the morphology developments of binary blends in the molten state. The main issue described in the literature is the lubricating effect caused by those additives, which results in a delayed homogenization during the processing of the blends. Nevertheless, these morphology developments are strongly correlated with modifications in the viscoelastic behaviour of polymers. Consequently, the behaviour of polyethylene oligomers in polyolefin resins in the molten state may be easily studied by means of rheological measurements (Chapter 3).

The influence of low molar mass hydrocarbon additives on the melting and crystallization behaviour of polyolefins was discussed in Section 4. While immiscible systems lead to liquid-liquid phase separation in the molten state, blends involving a miscible additive are characterized by a dilution of the polymer, which results in solid-liquid phase separation upon solidification. In both cases, the degree of crystallinity and final morphology of the system may be impacted, with potential consequences on the final properties of the polymer materials. The miscibility of polyethylene oligomers in polyolefin resins in the solid state can therefore be investigated by studying the crystallization behaviour of the blends (Chapter 3).

Lastly, several strategies for the compatibilization of immiscible polyethylene/polyamide blends were reviewed in Section 5. It appeared that the most common compatibilizer precursors are high molar mass polyethylenes grafted with maleic anhydride. This compatibilization strategy is based on the reaction of the maleic anhydride groups with the terminal amines of polyamide, as well as miscibility with the polyethylene phase. However, some studies suggest that similar compatibilizer precursors with lower molar masses could be of interest, thanks to their greater diffusion ability and lower viscosity during melt processing. Maleic anhydride-grafted polyethylene oligomers could therefore be used in the compatibilization of polyethylene/polyamide blends (Chapter 4). Additionally, the use of a reactive pair of oligomers appears to be a promising strategy to promote the in-situ formation of a multiblock copolymer compatibilizer.

7. Bibliography

[1] J.W. Teh, A. Rudin, J.C. Keung, A review of polyethylene–polypropylene blends and their compatibilization, Adv. Polym. Technol. 13 (1994) 1–23. doi:10.1002/adv.1994.060130101.

[2] E. Martuscelli, M. Pracella, M. Avella, R. Greco, G. Ragosta, Properties of polyethylene-polypropylene blends: Crystallization behavior, Makromol. Chem. 181 (1980) 957–967. doi:10.1002/macp.1980.021810417.

[3] R. Greco, G. Mucciariello, G. Ragosta, E. Martuscelli, Properties of polyethylene-polypropylene blends, J Mater Sci. 15 (1980) 845–853. doi:10.1007/BF00552093.

[4] J. Li, R.A. Shanks, R.H. Olley, G.R. Greenway, Miscibility and isothermal crystallisation of polypropylene in polyethylene melts, Polymer. 42 (2001) 7685–7694. doi:10.1016/S0032-3861(01)00248-8.

[5] P. Vadhar, T. Kyu, Effects of mixing on morphology, rheology, and mechanical properties of blends of ultra-high molecular weight polyethylene with linear low-density polyethylene, Polymer Engineering & Science. 27 (1987) 202–210. doi:10.1002/pen.760270305.

[6] R.A. Shanks, J. Li, L. Yu, Polypropylene–polyethylene blend morphology controlled by time–temperature–miscibility, Polymer. 41 (2000) 2133–2139. doi:10.1016/S0032-3861(99)00399-7.

[7] T. Kyu, P. Vadhar, Cocrystallization and miscibility studies of blends of ultrahigh molecular weight polyethylene with conventional polyethylenes, Journal of Applied Polymer Science. 32 (1986) 5575–5584. doi:10.1002/app.1986.070320625.

[8] M.T. Conde Braña, U.W. Gedde, Morphology of binary blends of linear and branched polyethylene: composition and crystallization-temperature dependence, Polymer. 33 (1992) 3123–3136. doi:10.1016/0032-3861(92)90224-K.

[9] C.M. Hansen, Hansen solubility parameters, a user's handbook, 2nd Edition, CRC Press, 2007.

[10] J.H. Hildebrand, R.L. Scott, The Solubility of Nonelectrolytes, Reinhold Pub, New York. (1950).

[11] J.H. Hildebrand, R.L. Scott, Regular Solutions, Prentice Hall. (1962).

[12] C. Bétron, V. Bounor-Legaré, C. Pinel, G. Scalabrino, L. Djakovitch, P. Cassagnau, Diffusion of modified vegetables oils in thermoplastic polymers, Materials Chemistry and Physics. 200 (2017) 107–120. doi:10.1016/j.matchemphys.2017.07.059.

[13] M. Bocqué, C. Voirin, V. Lapinte, S. Caillol, J.-J. Robin, Petro-based and bio-based plasticizers: Chemical structures to plasticizing properties, Journal of Polymer Science Part A: Polymer Chemistry. 54 (2016) 11–33. doi:10.1002/pola.27917.

[14] A.N. Ghebremeskel, C. Vemavarapu, M. Lodaya, Use of surfactants as plasticizers in preparing solid dispersions of poorly soluble API: Selection of polymer–surfactant combinations using solubility parameters and testing the processability, International Journal of Pharmaceutics. 328 (2007) 119–129. doi:10.1016/j.ijpharm.2006.08.010.

[15] L.G. Krauskopf, Prediction of plasticizer solvency using hansen solubility parameters, Journal of Vinyl and Additive Technology. 5 (1999) 101–106. doi:10.1002/vnl.10316.

[16] C.M. Hansen, Polymer additives and solubility parameters, Progress in Organic Coatings. 51 (2004) 109–112. doi:10.1016/j.porgcoat.2004.05.003.

[17] U. Gedde, 4. Polymer Solutions, in: Polymer Physics, Springer Netherlands, 1999: pp. 55–76. //www.springer.com/us/book/9780412590207 (accessed June 8, 2018).

[18] L.A. Utracki, ed., 2. Thermodynamics of polymer blends, in: Polymer Blends Handbook, Kluwer Academic Publishers, Dordrecht ; Boston, 2002: pp. 123–202.

[19] D.R. Lloyd, S.S. Kim, K.E. Kinzer, Microporous membrane formation via thermally-induced phase separation. II. Liquid—liquid phase separation, Journal of Membrane Science. 64 (1991) 1–11. doi:10.1016/0376-7388(91)80073-F.

[20] P.J. Flory, Thermodynamics of High Polymer Solutions, The Journal of Chemical Physics. 10 (1942) 51–61. doi:10.1063/1.1723621.

[21] M.L. Huggins, Thermodynamic Properties of Solutions of Long-Chain Compounds, Annals of the New York Academy of Sciences. 43 (1942) 1–32. doi:10.1111/j.1749-6632.1942.tb47940.x.

[22] R.C. Willemse, A.P. de Boer, J. van Dam, A.D. Gotsis, Co-continuous morphologies in polymer blends: a new model, Polymer. 39 (1998) 5879–5887. doi:10.1016/S0032-3861(97)10200-2.

[23] C.W. Macosko, Morphology development and control in immiscible polymer blends, Macromol. Symp. 149 (2000) 171–184. doi:10.1002/1521-3900(200001)149:1<171::AID-MASY171>3.0.CO;2-8.

[24] D. Bourry, B.D. Favis, Cocontinuity and phase inversion in HDPE/PS blends: Influence of interfacial modification and elasticity, Journal of Polymer Science Part B: Polymer Physics. 36 (1998) 1889–1899. doi:10.1002/(SICI)1099-0488(199808)36:11<1889::AID-POLB10>3.0.CO;2-3.

[25] H. Veenstra, P.C.J. Verkooijen, B.J.J. van Lent, J. van Dam, A.P. de Boer, A.P.H.J. Nijhof, On the mechanical properties of co-continuous polymer blends: experimental and modelling, Polymer. 41 (2000) 1817–1826. doi:10.1016/S0032-3861(99)00337-7.

[26] D.R. Paul, J.W. Barlow, Polymer Blends, Journal of Macromolecular Science, Part C. 18 (1980) 109–168. doi:10.1080/00222358008080917.

[27] H.E.H. Meijer, J.M.H. Janssen, P.D. Anderson, 3. Mixing of immiscible liquids, in: Mixing and Compounding of Polymers; Theory and Practice, 2nd edition, Carl Hanser Verlag GmbH & Co. KG, 2009: pp. 41–182.

[28] W. Yu, C. Zhou, T. Inoue, A coalescence mechanism for the coarsening behavior of polymer blends during a quiescent annealing process. I. Monodispersed particle system, Journal of Polymer Science Part B: Polymer Physics. 38 (2000) 2378–2389. doi:10.1002/1099-0488(20000915)38:18<2378::AID-POLB50>3.0.CO;2-I.

[29] Z. Tadmor, C. Gogos, 7. Mixing, in: Principles of Polymer Processing, 2nd edition, Wiley, 2006: pp. 322–408.

[30] C. Tucker, 2. Mixing of miscible liquids, in: Mixing and Compounding of Polymers; Theory and Practice, 2nd edition, Carl Hanser Verlag GmbH & Co. KG, 2009: pp. 5–40.

[31] C.E. Scott, C.W. Macosko, Morphology development during the initial stages of polymer-polymer blending, Polymer. 36 (1994) 461–470. doi:10.1016/0032-3861(95)91554-K.

[32] C.E. Scott, C.W. Macosko, Model experiments concerning morphology development during the initial stages of polymer blending, Polymer Bulletin. 26 (1991) 341–348. doi:10.1007/BF00587979.

[33] G.N. Avgeropoulos, F.C. Weissert, P.H. Biddison, G.G.A. Böhm, Heterogeneous Blends of Polymers. Rheology and Morphology, Rubber Chemistry and Technology. 49 (1976) 93–104. doi:10.5254/1.3534954.

[34] C. Épinat, L. Trouillet-Fonti, P. Sotta, Predicting phase inversion based on the rheological behavior in Polyamide 6/Polyethylene blends, Polymer. 137 (2018) 132–144. doi:10.1016/j.polymer.2018.01.019.

[35] C.E. Scott, S.K. Joung, Viscosity ratio effects in the compounding of low viscosity, immiscible fluids into polymeric matrices, Polymer Engineering & Science. 36 (1996) 1666–1674. doi:10.1002/pen.10563.

[36] H.E. Burch, C.E. Scott, Effect of viscosity ratio on structure evolution in miscible polymer blends, Polymer. 42 (2001) 7313–7325. doi:10.1016/S0032-3861(01)00240-3.

[37] P. Cassagnau, F. Fenouillot, Rheological study of mixing in molten polymers: 1-mixing of low viscous additives, Polymer. 45 (2004) 8019–8030. doi:10.1016/j.polymer.2004.09.027.

[38] P. Cassagnau, T. Nietsch, M. Bert, A. Michel, Reactive blending by in situ polymerization of the dispersed phase, Polymer. 40 (1999) 131–138. doi:10.1016/S0032-3861(98)00210-9.

[39] P. Cassagnau, F. Fenouillot, Rheological study of mixing in molten polymers: 2-mixing of reactive systems, Polymer. 45 (2004) 8031–8040. doi:10.1016/j.polymer.2004.09.028.

[40] R. Bella, F. Fenouillot, P. Cassagnau, L. Falk, Characterization and modelling of diffusion and reaction of low molecular weight reactants in molten polymer, Polymer. 48 (2007) 6902–6912. doi:10.1016/j.polymer.2007.09.019.

[41] M.H. Cohen, D. Turnbull, Molecular Transport in Liquids and Glasses, The Journal of Chemical Physics. 31 (1959) 1164–1169. doi:10.1063/1.1730566.

[42] J.S. Vrentas, J.L. Duda, Diffusion in polymer-solvent systems. I. Reexamination of the free-volume theory, Journal of Polymer Science: Polymer Physics Edition. 15 (1977) 403–416. doi:10.1002/pol.1977.180150302.

[43] J.S. Vrentas, J.L. Duda, Diffusion in polymer-solvent systems. II. A predictive theory for the dependence of diffusion coefficients on temperature, concentration, and molecular weight, Journal of Polymer Science: Polymer Physics Edition. 15 (1977) 417–439. doi:10.1002/pol.1977.180150303.

[44] J.S. Vrentas, J.L. Duda, Diffusion in polymer-solvent systems. III. Construction of Deborah number diagrams, Journal of Polymer Science: Polymer Physics Edition. 15 (1977) 441–453. doi:10.1002/pol.1977.180150304.

[45] J.S. Vrentas, J.L. Duda, Molecular diffusion in polymer solutions, AIChE Journal. 25 (1979) 1–24. doi:10.1002/aic.690250102.

[46] J.L. Duda, J.S. Vrentas, S.T. Ju, H.T. Liu, Prediction of diffusion coefficients for polymer-solvent systems, AIChE Journal. 28 (1982) 279–285. doi:10.1002/aic.690280217.

[47] J.S. Vrentas, C.M. Vrentas, Predictive methods for self-diffusion and mutual diffusion coefficients in polymer–solvent systems, European Polymer Journal. 34 (1998) 797–803. doi:10.1016/S0014-3057(97)00205-X.

[48] M.P. Tonge, R.G. Gilbert, Testing free volume theory for penetrant diffusion in rubbery polymers, Polymer. 42 (2001) 1393–1405. doi:10.1016/S0032-3861(00)00518-8.

[49] C. Joubert, P. Cassagnau, L. Choplin, A. Michel, Diffusion of plasticizer in elastomer probed by rheological analysis, Journal of Rheology. 46 (2002) 629–650. doi:10.1122/1.1470521.

[50] M. Ponsard-Fillette, C. Barrès, P. Cassagnau, Viscoelastic study of oil diffusion in molten PP and EPDM copolymer, Polymer. 46 (2005) 10256–10268. doi:10.1016/j.polymer.2005.08.015.

[51] R. Bella, P. Cassagnau, F. Fenouillot, L. Falk, C. Lacoste, Diffusion of liquids in molten polymers: Mutual diffusion coefficient dependence on liquid miscibility and polymer molar mass, Polymer. 47 (2006) 5080–5089. doi:10.1016/j.polymer.2006.05.024.

[52] G. Marin, E. Menezes, V.R. Raju, W.W. Graessley, Propriétés viscoélastiques linéaires de solutions de polybutadiène en régime semi-dilué et concentré, Rheol Acta. 19 (1980) 462–476. doi:10.1007/BF01524019.

[53] V.R. Raju, E.V. Menezes, G. Marin, W.W. Graessley, L.J. Fetters, Concentration and molecular weight dependence of viscoelastic properties in linear and star polymers, Macromolecules. 14 (1981) 1668–1676. doi:10.1021/ma50007a011.

[54] P.G. de Gennes, Reptation of a Polymer Chain in the Presence of Fixed Obstacles, The Journal of Chemical Physics. 55 (1971) 572–579. doi:10.1063/1.1675789.

[55] P.J. Flory, Principles of Polymer Chemistry, Cornell University Press, 1953.
[56] J. Gimenez, P. Cassagnau, A. Michel, Bulk polymerization of ε-caprolactone: Rheological predictive laws, Journal of Rheology. 44 (2000) 527.
[57] C. Bétron, P. Cassagnau, V. Bounor-Legaré, Control of diffusion and exudation of vegetable oils in EPDM copolymers, European Polymer Journal. 82 (2016) 102–113. doi:10.1016/j.eurpolymj.2016.06.027.
[58] B. Bitsch, Amélioration des thermoplastiques : Rôle du compoundeur, Techniques de l'ingénieur. Plastiques et composites. 2 (2003) AM3238.1-AM3238.14.
[59] C.A. Harper, E.M. Petrie, Plastics Materials and Processes: A Concise Encyclopedia, John Wiley & Sons, 2003.
[60] G. Wypych, Handbook of Plasticizers, ChemTec Publishing, 2004.
[61] D.F. Cadogan, C.J. Howick, Plasticizers, in: Ullmann's Encyclopedia of Industrial Chemistry, American Cancer Society, 2000. doi:10.1002/14356007.a20_439.
[62] D.R. Lloyd, K.E. Kinzer, H.S. Tseng, Microporous membrane formation via thermally induced phase separation. I. Solid-liquid phase separation, Journal of Membrane Science. 52 (1990) 239–261. doi:10.1016/S0376-7388(00)85130-3.
[63] D. Li, W.B. Krantz, A.R. Greenberg, R.L. Sani, Membrane formation via thermally induced phase separation (TIPS): Model development and validation, Journal of Membrane Science. 279 (2006) 50–60. doi:10.1016/j.memsci.2005.11.036.
[64] S. Liu, C. Zhou, W. Yu, Phase separation and structure control in ultra-high molecular weight polyethylene microporous membrane, Journal of Membrane Science. 379 (2011) 268–278. doi:10.1016/j.memsci.2011.05.073.
[65] A. Akbari, R. Yegani, Study on the Impact of Polymer Concentration and Coagulation Bath Temperature on the Porosity of Polyethylene Membranes Fabricated Via TIPS Method, Journal of Membrane and Separation Technology. 1 (2012) 100–107.
[66] F. Toquet, L. Guy, B. Schlegel, P. Cassagnau, R. Fulchiron, Effect of the naphthenic oil and precipitated silica on the crystallization of ultrahigh-molecular-weight polyethylene, Polymer. 97 (2016) 63–68. doi:10.1016/j.polymer.2016.05.021.
[67] Y. Hong, G. Xin-shi, Preparation of polyethylene–paraffin compound as a form-stable solid-liquid phase change material, Solar Energy Materials and Solar Cells. 64 (2000) 37–44. doi:10.1016/S0927-0248(00)00041-6.
[68] B. Zalba, J.M. Marín, L.F. Cabeza, H. Mehling, Review on thermal energy storage with phase change: materials, heat transfer analysis and applications, Applied Thermal Engineering. 23 (2003) 251–283. doi:10.1016/S1359-4311(02)00192-8.
[69] A. Sarı, Form-stable paraffin/high density polyethylene composites as solid–liquid phase change material for thermal energy storage: preparation and thermal properties, Energy Conversion and Management. 45 (2004) 2033–2042. doi:10.1016/j.enconman.2003.10.022.
[70] I. Krupa, A.S. Luyt, Thermal properties of polypropylene/wax blends, Thermochimica Acta. 372 (2001) 137–141. doi:10.1016/S0040-6031(01)00450-6.
[71] I. Krupa, G. Miková, A.S. Luyt, Polypropylene as a potential matrix for the creation of shape stabilized phase change materials, European Polymer Journal. 43 (2007) 895–907. doi:10.1016/j.eurpolymj.2006.12.019.
[72] C. Alkan, K. Kaya, A. Sarı, Preparation, Thermal Properties and Thermal Reliability of Form-Stable Paraffin/Polypropylene Composite for Thermal Energy Storage, J Polym Environ. 17 (2009) 254. doi:10.1007/s10924-009-0146-7.

[73] J.A. Molefi, A.S. Luyt, I. Krupa, Investigation of thermally conducting phase-change materials based on polyethylene/wax blends filled with copper particles, Journal of Applied Polymer Science. 116 (2010) 1766–1774. doi:10.1002/app.31653.

[74] J.A. Molefi, A.S. Luyt, I. Krupa, Comparison of LDPE, LLDPE and HDPE as matrices for phase change materials based on a soft Fischer–Tropsch paraffin wax, Thermochimica Acta. 500 (2010) 88–92. doi:10.1016/j.tca.2010.01.002.

[75] F. Chen, M.P. Wolcott, Miscibility studies of paraffin/polyethylene blends as form-stable phase change materials, European Polymer Journal. 52 (2014) 44–52. doi:10.1016/j.eurpolymj.2013.09.027.

[76] D. Nwabunma, T. Kyu, Polyolefin Blends, John Wiley & Sons, 2008.

[77] A. Genovese, G. Amarasinghe, M. Glewis, D. Mainwaring, R.A. Shanks, Crystallisation, melting, recrystallisation and polymorphism of n-eicosane for application as a phase change material, Thermochimica Acta. 443 (2006) 235–244. doi:10.1016/j.tca.2006.02.008.

[78] D. Langhe, Chapter 9 - Fractionated Crystallization in Polymer Blends, in: S. Thomas, M. Arif P., E.B. Gowd, N. Kalarikkal (Eds.), Crystallization in Multiphase Polymer Systems, Elsevier, 2018: pp. 239–267. doi:10.1016/B978-0-12-809453-2.00009-8.

[79] H. Sun, K.B. Rhee, T. Kitano, S.I. Mah, High-density polyethylene (HDPE) hollow fiber membrane via thermally induced phase separation. I. Phase separation behaviors of HDPE–liquid paraffin (LP) blends and its influence on the morphology of the membrane, Journal of Applied Polymer Science. 73 (1999) 2135–2142. doi:10.1002/(SICI)1097-4628(19990912)73:11<2135::AID-APP9>3.0.CO;2-X.

[80] H. Matsuyama, H. Okafuji, T. Maki, M. Teramoto, N. Kubota, Preparation of polyethylene hollow fiber membrane via thermally induced phase separation, Journal of Membrane Science. 223 (2003) 119–126. doi:10.1016/S0376-7388(03)00314-4.

[81] S.S. Kim, D.R. Lloyd, Thermodynamics of polymer/diluent systems for thermally induced phase separation: 2. Solid-liquid phase separation systems, Polymer. 33 (1992) 1036–1046. doi:10.1016/0032-3861(92)90020-W.

[82] S.P. Hlangothi, I. Krupa, V. Djoković, A.S. Luyt, Thermal and mechanical properties of cross-linked and uncross-linked linear low-density polyethylene–wax blends, Polymer Degradation and Stability. 79 (2003) 53–59. doi:10.1016/S0141-3910(02)00238-0.

[83] T.N. Mtshali, I. Krupa, A.S. Luyt, The effect of cross-linking on the thermal properties of LDPE/wax blends, Thermochimica Acta. 380 (2001) 47–54. doi:10.1016/S0040-6031(01)00636-0.

[84] V. Djoković, T.N. Mtshali, A.S. Luyt, The influence of wax content on the physical properties of low-density polyethylene–wax blends, Polymer International. 52 (2003) 999–1004. doi:10.1002/pi.1180.

[85] I. Krupa, A.S. Luyt, Mechanical properties of uncrosslinked and crosslinked linear low-density polyethylene/wax blends, J. Appl. Polym. Sci. 81 (2000) 973–980. doi:10.1002/app.1519.

[86] M.J. Hato, A.S. Luyt, Thermal fractionation and properties of different polyethylene/wax blends, Journal of Applied Polymer Science. 104 (2007) 2225–2236. doi:10.1002/app.25494.

[87] M.P. Molaba, D. Dudic, A.S. Luyt, Influence of the presence of medium-soft paraffin wax on the morphology and properties of iPP/silver nanocomposites, eXPRESS Polymer Letters. (2015). doi:10.3144/expresspolymlett.2015.82.

[88] C. Zhang, B. Zhu, G. Ji, Y. Xu, Studies on nonisothermal crystallization of ultra–high molecular weight polyethylene in liquid paraffin, Journal of Applied Polymer Science. 99 (2006) 2782–2788. doi:10.1002/app.22645.

[89] J.W. Park, J. Yoon, J. Cha, H.S. Lee, Determination of molecular weight distribution and composition dependence of monomeric friction factors from the stress relaxation of ultrahigh molecular weight polyethylene gels, Journal of Rheology. 59 (2015) 1173–1189. doi:10.1122/1.4928072.

[90] G. Groeninckx, M. Vanneste, V. Everaert, eds., 3. Crystallization, Morphological Structure, and Melting of Polymer Blends, in: Polymer Blends Handbook, Kluwer Academic Publishers, Dordrecht ; Boston, 2002: pp. 203–294.

[91] Z. Bartczak, A. Gałeski, Changes in interface shape during crystallization in two-component polymer systems, Polymer. 27 (1986) 544–548. doi:10.1016/0032-3861(86)90240-5.

[92] E. Martuscelli, C. Silvestre, L. Bianchi, Properties of thin films of isotactic polypropylene blended with polyisobutylene and ethylene-propylene-diene terpolymer rubbers, Polymer. 24 (1983) 1458–1468. doi:10.1016/0032-3861(83)90231-8.

[93] K. Friedrich, Analysis of crack propagation in isotactic polypropylene with different morphology, Physik Der Duroplaste Und Anderer Polymerer. (1978) 103–112.

[94] T. Nishi, T.T. Wang, Melting Point Depression and Kinetic Effects of Cooling on Crystallization in Poly(vinylidene fluoride)-Poly(methyl methacrylate) Mixtures, Macromolecules. 8 (1975) 909–915. doi:10.1021/ma60048a040.

[95] C.C. Puig, Enhanced crystallisation in branched polyethylenes when blended with linear polyethylene, Polymer. 42 (2001) 6579–6585. doi:10.1016/S0032-3861(01)00102-1.

[96] T.P. Gumede, A.S. Luyt, R.A. Pérez-Camargo, A. Iturrospe, A. Arbe, M. Zubitur, A. Mugica, A.J. Müller, Plasticization and cocrystallization in LLDPE/wax blends, Journal of Polymer Science Part B: Polymer Physics. 54 (2016) 1469–1482. doi:10.1002/polb.24039.

[97] A. Lustiger, R.L. Markham, Importance of tie molecules in preventing polyethylene fracture under long-term loading conditions, Polymer. 24 (1983) 1647–1654. doi:10.1016/0032-3861(83)90187-8.

[98] U. Gedde, 7. Crystalline polymers, in: Polymer Physics, Springer Netherlands, 1999: pp. 131–168. //www.springer.com/us/book/9780412590207 (accessed June 8, 2018).

[99] M. Hedenqvist, M.T. Conde Braña, U.W. Gedde, J. Martinez-Salazar, Fracture of binary blends of linear and branched polyethylene, Polymer. 37 (1996) 5123–5129. doi:10.1016/0032-3861(96)00237-6.

[100] H. Frensch, B.-J. Jungnickel, Some novel crystallization kinetic peculiarities in finely dispersing polymer blends, Colloid & Polymer Sci. 267 (1989) 16–27. doi:10.1007/BF01410144.

[101] A. Galeski, M. Pracella, E. Martuscelli, Polypropylene spherulite morphology and growth rate changes in blends with low-density polyethylene, Journal of Polymer Science: Polymer Physics Edition. 22 (1984) 739–747. doi:10.1002/pol.1984.180220415.

[102] Z. Bartczak, A. Galeski, M. Pracella, Spherulite nucleation in blends of isotactic polypropylene with high-density polyethylene, Polymer. 27 (1986) 537–543. doi:10.1016/0032-3861(86)90239-9.

[103] C. Koning, M. Van Duin, C. Pagnoulle, R. Jerome, Strategies for compatibilization of polymer blends, Progress in Polymer Science. 23 (1998) 707–757. doi:10.1016/S0079-6700(97)00054-3.

[104] U. Sundararaj, C.W. Macosko, Drop Breakup and Coalescence in Polymer Blends: The Effects of Concentration and Compatibilization, Macromolecules. 28 (1995) 2647–2657. doi:10.1021/ma00112a009.

[105] J. Huitric, M. Moan, P.J. Carreau, N. Dufaure, Effect of reactive compatibilization on droplet coalescence in shear flow, Journal of Non-Newtonian Fluid Mechanics. 145 (2007) 139–149. doi:10.1016/j.jnnfm.2007.06.001.

[106] D.R. Paul, Chapter 12 - Interfacial Agents ("Compatibilizers") for Polymer Blends, in: D.R. Paul, S. Newman (Eds.), Polymer Blends, Academic Press, 1978: pp. 35–62. doi:10.1016/B978-0-12-546802-2.50008-7.

[107] L.A. Utracki, Compatibilization of Polymer Blends, The Canadian Journal of Chemical Engineering. 80 (2002) 1008–1016. doi:10.1002/cjce.5450800601.

[108] A. Ajji, ed., 4. Interphase and compatibilization by addition of a compatibilizer, in: Polymer Blends Handbook, Kluwer Academic Publishers, Dordrecht ; Boston, 2002: pp. 295–338.

[109] S.B. Brown, ed., 5. Reactive compatibilization of polymer blends, in: Polymer Blends Handbook, Kluwer Academic Publishers, Dordrecht ; Boston, 2002: pp. 357–433.

[110] B. O'Shaughnessy, U. Sawhney, Reaction Kinetics at Polymer−Polymer Interfaces, Macromolecules. 29 (1996) 7230–7239. doi:10.1021/ma9601171.

[111] P. Marechal, Polyéthylènes basse densité PE-BD et PE-BDL, Techniques de l'ingénieur Matières thermoplastiques : monographies. base documentaire : TIB147DUO (2011).

[112] C. Penu, Polyéthylène haute densité PE-HD, Techniques de l'ingénieur Matières thermoplastiques : monographies. base documentaire : TIB147DUO (2011).

[113] B. GUÉRIN, Polyamides PA, Ref : TIP100WEB - "Plastiques et composites." (1994).

[114] M.K. Akkapeddi, ed., 15. Commercial polymer blends, in: Polymer Blends Handbook, Kluwer Academic Publishers, Dordrecht ; Boston, 2002: pp. 1023–1116.

[115] J. Huitric, P. Médéric, M. Moan, J. Jarrin, Influence of composition and morphology on rheological properties of polyethylene/polyamide blends, Polymer. 39 (1998) 4849–4856. doi:10.1016/S0032-3861(97)10255-5.

[116] L.A. Utracki, M.M. Dumoulin, P. Toma, Melt rheology of high density polyethylene/polyamide-6 blends, Polymer Engineering & Science. 26 (1986) 34–44. doi:10.1002/pen.760260108.

[117] H. Pernot, M. Baumert, F. Court, L. Leibler, Design and properties of co-continuous nanostructured polymers by reactive blending, Nat Mater. 1 (2002) 54–58. doi:10.1038/nmat711.

[118] A. Argoud, L. Trouillet-Fonti, S. Ceccia, P. Sotta, Morphologies in Polyamide 6/High Density Polyethylene blends with high amounts of reactive compatibilizer, European Polymer Journal. 50 (2014) 177–189. doi:10.1016/j.eurpolymj.2013.10.026.

[119] R. Scaffaro, M.C. Mistretta, F.P.L. Mantia, M. Gleria, R. Bertani, F. Samperi, C. Puglisi, On the Preparation and Characterization of Polyethylene/Polyamide Blends by Melt Processing in the Presence of an Ethylene/Acrylic Acid Copolymer and of New Phosphazene Compounds, Macromolecular Chemistry and Physics. 207 (2006) 1986–1997. doi:10.1002/macp.200600332.

[120] M. Xanthos, Interfacial agents for multiphase polymer systems: Recent advances, Polymer Engineering & Science. 28 (1988) 1392–1400. doi:10.1002/pen.760282108.

[121] M. Xanthos, S.S. Dagli, Compatibilization of polymer blends by reactive processing, Polymer Engineering & Science. 31 (1991) 929–935. doi:10.1002/pen.760311302.

[122] J. Duvall, C. Sellitti, C. Myers, A. Hiltner, E. Baer, Effect of compatibilization on the properties of polypropylene/polyamide-66 (75/25 wt/wt) blends, Journal of Applied Polymer Science. 52 (1994) 195–206. doi:10.1002/app.1994.070520207.

[123] S. Lim, J.L. White, Influence of a compatibilizing agent on the phase morphology of a polyethylene-polyamide 6 blend in a modular intermeshing co-rotating twin screw extruder, Polymer Engineering & Science. 34 (1994) 221–228. doi:10.1002/pen.760340308.

[124] I. Pesneau, A.A. Kadi, M. Bousmina, P. Cassagnau, A. Michel, From polymer blends to in situ polymer/polymer composites: Morphology control and mechanical properties, Polymer Engineering & Science. 42 (2002) 1990–2004. doi:10.1002/pen.11091.

[125] J.R. Araújo, M.R. Vallim, M.A.S. Spinacé, M. -A D. Paoli, Use of postconsumer polyethylene in blends with polyamide 6: Effects of the extrusion method and the compatibilizer, Journal of Applied Polymer Science. 110 (2008) 1310–1317. doi:10.1002/app.28441.

[126] Q. Su, M. Feng, S. Zhang, J. Jiang, M. Yang, Melt blending of polypropylene-blend- polyamide 6-blend-organoclay systems, Polym. Int. 56 (2007) 50–56. doi:10.1002/pi.2109.

[127] Z. Fang, Y. Xu, L. Tong, Effect of clay on the morphology of binary blends of polyamide 6 with high density polyethylene and HDPE-graft-acrylic acid, Polymer Engineering & Science. 47 (2007) 551–559. doi:10.1002/pen.20675.

[128] G. Filippone, N.T. Dintcheva, D. Acierno, F.P. La Mantia, The role of organoclay in promoting co-continuous morphology in high-density poly(ethylene)/poly(amide) 6 blends, Polymer. 49 (2008) 1312–1322. doi:10.1016/j.polymer.2008.01.045.

[129] G. Filippone, N.T. Dintcheva, F.P. La Mantia, D. Acierno, Using organoclay to promote morphology refinement and co-continuity in high-density polyethylene/polyamide 6 blends – Effect of filler content and polymer matrix composition, Polymer. 51 (2010) 3956–3965. doi:10.1016/j.polymer.2010.06.044.

[130] C.C. Chen, E. Fontan, K. Min, J.L. White, An investigation of instability of phase morphology of blends of nylons with polyethylenes and polystyrenes and effects of compatibilizing agents, Polymer Engineering & Science. 28 (1988) 69–80. doi:10.1002/pen.760280203.

[131] G. Serpe, J. Jarrin, F. Dawans, Morphology-processing relationships in polyethylene-polyamide blends, Polymer Engineering & Science. 30 (1990) 553–565. doi:10.1002/pen.760300908.

[132] B. Kyu Kim, S. Yun Park, S. Jin Park, Morphological, thermal and rheological properties of blends: Polyethylene/nylon-6, polyethylene/nylon-6/(maleic anhydride-g-polyethylene) and (maleic anhydride-g-polyethylene)/nylon-6, European Polymer Journal. 27 (1991) 349–354. doi:10.1016/0014-3057(91)90186-R.

[133] B. Jurkowski, K. Kelar, D. Ciesielska, Influence of chemical and mechanical compatibilization on structure and properties of polyethylene/polyamide blends, Journal of Applied Polymer Science. 69 (1998) 719–727. doi:10.1002/(SICI)1097-4628(19980725)69:4<719::AID-APP10>3.0.CO;2-K.

[134] M. Palabiyik, S. Bahadur, Mechanical and tribological properties of polyamide 6 and high density polyethylene polyblends with and without compatibilizer, Wear. 246 (2000) 149–158. doi:10.1016/S0043-1648(00)00501-9.

[135] L. Minkova, H. Yordanov, S. Filippi, N. Grizzuti, Interfacial tension of compatibilized blends of LDPE and PA6: the breaking thread method, Polymer. 44 (2003) 7925–7932. doi:10.1016/j.polymer.2003.09.054.

[136] C. Jiang, S. Filippi, P. Magagnini, Reactive compatibilizer precursors for LDPE/PA6 blends. II: maleic anhydride grafted polyethylenes, Polymer. 44 (2003) 2411–2422. doi:10.1016/S0032-3861(03)00133-2.

[137] S. Filippi, L. Minkova, N. Dintcheva, P. Narducci, P. Magagnini, Comparative study of different maleic anhydride grafted compatibilizer precursors towards LDPE/PA6 blends: Morphology and mechanical properties, Polymer. 46 (2005) 8054–8061. doi:10.1016/j.polymer.2005.06.090.

[138] B. Chatreenuwat, M. Nithitanakul, B.P. Grady, The effect of zinc oxide addition on the compatibilization efficiency of maleic anhydride grafted high-density polyethylene compatibilizer for high-density polyethylene/polyamide 6 blends, Journal of Applied Polymer Science. 103 (2007) 3871–3881. doi:10.1002/app.25565.

[139] F. Hamid, S. Akhbar, K.H.K. Halim, Mechanical and Thermal Properties of Polyamide 6/HDPE-g- MAH/High Density Polyethylene, Procedia Engineering. 68 (2013) 418–424. doi:10.1016/j.proeng.2013.12.201.

[140] S. Filippi, V. Chiono, G. Polacco, M. Paci, L.I. Minkova, P. Magagnini, Reactive compatibilizer precursors for LDPE/PA6 blends, 1. Ethylene/acrylic acid copolymers, Macromolecular Chemistry and Physics. 203 (2002) 1512–1525. doi:10.1002/1521-3935(200207)203:10/11<1512::AID-MACP1512>3.0.CO;2-G.

[141] J.M. Willis, B.D. Favis, Processing-morphology relationships of compatibilized polyolefin/polyamide blends. Part I: The effect of an lonomer compatibilizer on blend morphology, Polymer Engineering & Science. 28 (1988) 1416–1426. doi:10.1002/pen.760282111.

[142] J.M. Willis, V. Caldas, B.D. Favis, Processing-morphology relationships of compatibilized polyolefin/polyamide blends, Journal of Materials Science. 26 (1991) 4742–4750. doi:10.1007/bf00612413.

[143] R. González-Núnez, D. De Kee, B.D. Favis, The influence of coalescence on the morphology of the minor phase in melt-drawn polyamide-6/HDPE blends, Polymer. 37 (1996) 4689–4693. doi:10.1016/S0032-3861(96)00318-7.

[144] P. Leewajanakul, R. Pattanaolarn, J.W. Ellis, M. Nithitanakul, B.P. Grady, Use of zinc-neutralized ethylene/methacrylic acid copolymer ionomers as blend compatibilizers for nylon 6 and low-density polyethylene, Journal of Applied Polymer Science. 89 (2003) 620–629. doi:10.1002/app.11898.

[145] A. Lahor, M. Nithitanakul, B.P. Grady, Blends of low-density polyethylene with nylon compatibilized with a sodium-neutralized carboxylate ionomer, European Polymer Journal. 40 (2004) 2409–2420. doi:10.1016/j.eurpolymj.2004.07.004.

[146] T. Baouz, S. Fellahi, Interfacial modification of high density polyethylene/glass fiber reinforced and non reinforced polyamide 66 blends, Journal of Applied Polymer Science. 98 (2005) 1748–1760. doi:10.1002/app.22359.

[147] S. Charoenpongpool, M. Nithitanakul, B.P. Grady, Melt-neutralization of maleic anhydride grafted on high-density polyethylene compatibilizer for polyamide-6/high-density polyethylene blend: effect of neutralization level on compatibility of the blend, Polymer Bulletin. 70 (2013) 293–309. doi:10.1007/s00289-012-0805-z.

[148] H. Raval, S. Devi, Y.P. Singh, M.H. Mehta, Relationship between morphology and properties of polyamide-6 low-density polyethylene blends: effect of the addition of functionalized low-density polyethylene, Polymer. 32 (1991) 493–500. doi:10.1016/0032-3861(91)90455-R.

[149] A. Valenza, G. Geuskens, G. Spadaro, Blends of polyamide 6 and linear low density polyethylene functionalized with methacrylic acid derivatives, European Polymer Journal. 33 (1997) 957–962. doi:10.1016/S0014-3057(96)00174-7.

[150] C. Vocke, U. Anttila, J. Seppälä, Compatibilization of polyethylene/polyamide 6 blends with oxazoline-functionalized polyethylene and styrene ethylene/butylene styrene copolymer (SEBS), Journal of Applied Polymer Science. 72 (1999) 1443–1450. doi:10.1002/(SICI)1097-4628(19990613)72:11<1443::AID-APP7>3.0.CO;2-4.

[151] V. Chiono, S. Filippi, H. Yordanov, L. Minkova, P. Magagnini, Reactive compatibilizer precursors for LDPE/PA6 blends. III: ethylene–glycidylmethacrylate copolymer, Polymer. 44 (2003) 2423–2432. doi:10.1016/S0032-3861(03)00134-4.

[152] C.A. Orr, J.J. Cernohous, P. Guegan, A. Hirao, H.K. Jeon, C.W. Macosko, Homogeneous reactive coupling of terminally functional polymers, Polymer. 42 (2001) 8171–8178. doi:10.1016/S0032-3861(01)00329-9.

[153] M.E. Córdova, A.T. Lorenzo, A.J. Müller, L. Gani, S. Tencé-Girault, L. Leibler, The Influence of Blend Morphology (Co-Continuous or Sub-Micrometer Droplets Dispersions) on the Nucleation and Crystallization Kinetics of Double Crystalline Polyethylene/Polyamide Blends

Prepared by Reactive Extrusion, Macromol. Chem. Phys. 212 (2011) 1335–1350. doi:10.1002/macp.201100039.

[154] Z. Yin, C. Koulic, H.K. Jeon, C. Pagnoulle, C.W. Macosko, R. Jérôme, Effect of Molecular Weight of the Reactive Precursors in Melt Reactive Blending, Macromolecules. 35 (2002) 8917–8919. doi:10.1021/ma0206366.

[155] E.A. Eastwood, M.D. Dadmun, Multiblock Copolymers in the Compatibilization of Polystyrene and Poly(methyl methacrylate) Blends: Role of Polymer Architecture, Macromolecules. 35 (2002) 5069–5077. doi:10.1021/ma011701z.

[156] A.D. Todd, R.J. McEneany, V.A. Topolkaraev, C.W. Macosko, M.A. Hillmyer, Reactive Compatibilization of Poly(ethylene terephthalate) and High-Density Polyethylene Using Amino-Telechelic Polyethylene, Macromolecules. 49 (2016) 8988–8994. doi:10.1021/acs.macromol.6b02080.

[157] C.P. O'Brien, J.K. Rice, M.D. Dadmun, Reactive processing with difunctional oligomers to compatibilize polymer blends, European Polymer Journal. 40 (2004) 1515–1523. doi:10.1016/j.eurpolymj.2004.01.023.

[158] H. Shi, D. Shi, X. Wang, L. Yin, J. Yin, Y.-W. Mai, A facile route for preparing stable co-continuous morphology of LLDPE/PA6 blends with low PA6 content, Polymer. 51 (2010) 4958–4968. doi:10.1016/j.polymer.2010.08.023.

[159] A.R. Padwa, Compatibilized blends of polyamide-6 and polyethylene, Polymer Engineering & Science. 32 (1992) 1703–1710. doi:10.1002/pen.760322208.

Chapter 2 – Materials and methods

Table of contents

1. Materials

1.1. Polymer resins

The polypropylene (PP) used in this work was an isotactic homopolymer (PPH 7060, Total). It has a melting temperature of 165 °C and a density of 0.905 g/cm^3. Its melt flow index is 12 g/10min (230 °C, 2.16 kg), which corresponds to a zero shear viscosity of 3.10^3 Pa.s (180 °C).

A high-density polyethylene (HDPE) (Hostalen GF 7750 M2, LyonDellBasell) was also studied. It has a melting temperature of 135 °C and a density of 0.957 g/cm^3. Its melt flow index is 1 g/10min (190 °C, 2.16kg), or a zero shear viscosity of 9.10^3 Pa.s (180 °C).

A high molar mass, maleic anhydride-grafted polyethylene (PE-g-MA) (Exxelor PE 1040, ExxonMobil) was used both as a polymer resin and as a high molar mass additive. It has a melting temperature of 135 °C and a density of 0.960 g/cm^3. Its melt flow index is 1 g/10min (190 °C, 2.16 kg), which corresponds to a zero shear viscosity of 5.10^5 Pa.s (180 °C).

A polyamide 6 (PA6) (Akulon F136-DH, DSM) with a melting temperature of 220 °C and a density of 1.130 g.cm^{-3} was also used in this study. It has a viscosity number of 245 cm^3/g (ISO 307) i.e. a zero shear viscosity of 4.10^3 Pa.s (240 °C).

The molar masses of the polyolefins were determined with a Malvern Viscotek TDAmax high-temperature gel permeation chromatography (GPC)/size-exclusion chromatography (SEC) system. The molar mass of the polyamide 6 was determined by potentiometric titration of the amine and acid terminal groups. The values obtained were [COOH] = 32 mmol/kg and [NH_2] = 33 mmol/kg. The molar mass of polyamide 6 was therefore calculated to be approximately 30 000 g/mol. The molar masses obtained from these analyses are given in Table 1.

Table 1. Molar masses of the selected polyolefins (measured by HT-GPC/SEC) and of the polyamide 6 (measured by potentiometric titration)

Designation	Mp (Da)	Mn (Da)	Mw (Da)	Mw/Mn
PP	119 000	48 000	210 000	4.4
HDPE	56 000	19 000	111 000	5.9
HDPE-g-MA	39 000	17 000	50 000	2.9
PA6	-	30 000	-	-

1.2. Oligomers

1.2.1. Commercially available polyethylene oligomers

Readily available, functional as well as non-functional polyethylene oligomer additives were used as model molecules for this study. The first one was a linear primary carboxylic acid polyethylene (Unicid

700 acid, Baker Hughes). The other functional oligomers used were linear polyethylenes grafted with maleic anhydride derivatives (Ceramer 67 polymer and Ceramer 1608 polymer, Baker Hughes). The non-functional polyethylene oligomer used in the present work was a synthetic wax, linear and fully saturated homopolymer of ethylene (Polywax 725 polyethylene, Baker Hughes). The chemical structures of such oligomers are illustrated in Table 2.

Table 2. Chemical structures of Baker Hughes functional and non-functional oligomers (n + m + p ≈ 50, R = H or iPr)

Designation	Chemical structure
Polywax 725	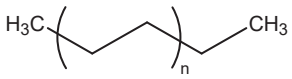
Unicid 700	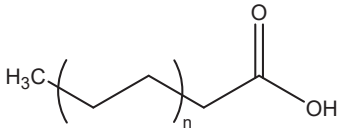
Ceramer 67	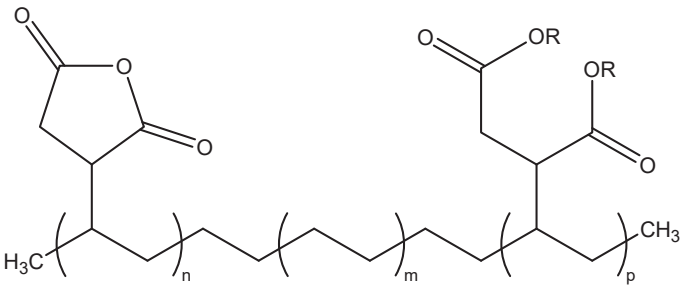
Ceramer 1608	

The molar mass of each commercial oligomers was determined using a Malvern Viscotek TDAmax high-temperature gel permeation chromatography (GPC)/size-exclusion chromatography (SEC) system. The measured values can be found in Table 3.

Table 3. Molar masses of the commercial polyethylene oligomers (measured by HT-GPC/SEC)

Designation	Mp (Da)	Mn (Da)	Mw (Da)	Mz (Da)	Mw/Mn
Polywax 725	900	800	900	1 000	1,1
Unicid 700	700	600	700	900	1,3
Ceramer 67	700	700	800	1 100	1,2
Ceramer 1608	1 100	800	1 300	2 000	1,6

The physical and chemical properties of these commercial oligomers are gathered in Table 4. The melting temperature as well as the acid and saponification numbers were obtained from the technical datasheets provided with the products. The viscosities were measured using an ARES-G2 strain-

controlled rheometer in parallel plate geometry (T = 180 °C, ε = 500% for Polywax 725, Unicid 700 and Ceramer 67, and ε = 100% for Ceramer 1608).

Table 4. Physical and chemical properties of the commercial polyethylene oligomers

Designation	Melting point (°C)	Acid value (mgKOH/g)	Sonification value (mgKOH/g)	Zero shear viscosity (Pa.s)
Polywax 725	104	-	-	0.007
Unicid 700	110	63	-	0.02
Ceramer 67	96	48	77	0.02
Ceramer 1608	75	154	215	2

It is worth noting that the maleic anhydride derivatives used for the functionalization of Ceramer products are among maleic anhydride, mono-isopropyl maleate (Z and E isomers) and maleic acid (Z and E isomers), as stated on the safety datasheets provided with the products. This was verified by analytical thermal desorption coupled with gas chromatography and mass spectroscopy (ATD-GC-MS), which is detailed in Appendix A. For simplification purposes, oligomers grafted with the above cited maleic anhydride derivatives will be referred to as maleic anhydride-grafted polyethylene oligomers in the rest of this document.

1.2.2. Polyethylene oligomers synthesized by the C2P2 laboratory

End-functionalized polyethylenes with low molar mass were synthesized by the Chemistry, Catalysis, Polymers and Processes laboratory (C2P2, Villeurbanne, France). The strategy for the functionalization of such polyethylenes involved catalyzed chain growth (CCG) on a main-group metal-based catalyst. This allowed the synthesis of polyethylenes with controlled molar masses between 500 and 5000 g/mol.[1,2] Very high functionalities were achieved and a wide range of end-functions were thus made available for use.[3,4] For the purpose of this study, several functional polyethylene oligomers were chosen with regards to their chemical affinity and/or potential reactivity towards functional groups available at the surface of the fillers. The chemical structures of those oligomers are specified in Table 5. Functional groups, functionalities and molar masses can be found in Table 6.

Table 5. Chemical structure of the functional oligomers synthesized by the C2P2 laboratory

Designation	Chemical structure
PE-Si(OMe)(Me)$_2$	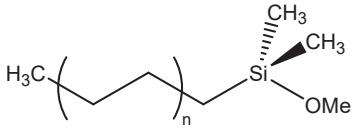

PE-Si(OMe)$_3$	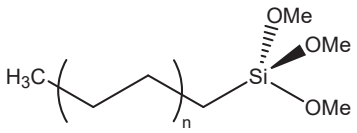
PE-NH$_2$	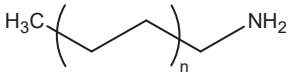

Table 6. List of the end-functionalized polyethylene oligomers synthesized for the study

Designation	Functional group	Molar mass (g/mol)*	Functionality (%)**
PE-Si(OMe)(Me)$_2$	Mono-alkoxysilane	1300	84
PE-Si(OMe)$_3$	Tri-alkoxysilane	1300	81
PE-NH$_2$	Amine	1700	97
PE-NH$_2$	Amine	4000	97

** Determined by ^{13}C NMR by the C2P2 laboratory*

*** Determined by ^{1}H NMR by the C2P2 laboratory*

1.2.3. Other oligomers

A tri-functional polyetheramine oligomer was also used in this study (Jeffamine T-403, Huntsman). It has a density of 0.978 g/cm^3 and is in the liquid state at room temperature with a zero-shear viscosity of η_0 = 0.07 Pa.s (at 25 °C). The chemical structure and properties of this oligomer are presented in Table 7.

Table 7. Chemical structure and properties of Jeffamine T-403 (x + y + z = 5-6)

Designation	Chemical structure	Molar mass (g/mol)	AHEW* (g/eq)
Jeffamine T-403	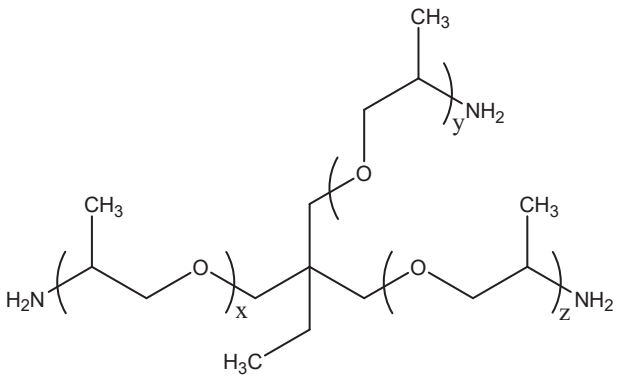	400	81

**AHEW = amine hydrogen equivalent weight*

1.3. Glass fibres

The fillers used in this work were chopped strand glass fibres (DS 2200-13P and DS 1128-10N, Binani 3B). These E-CR glass fibres are typically used for the reinforcement of thermoplastic composites. Details on the dimensions of the fibres as well as compatible thermoplastic resins are given in Table 8.

Table 8. Characteristics of the glass fibres

Designation	Reference	Compatible resins	Fibre length (mm)	Fibre diameter (µm)
GF1	DS 2200-13P	PE, PP	4	13
GF2	DS 1128-10N	PA	4	10

Such glass fibres are supplied in the form of fibre bundles which unbound upon blending with a polymeric media. For the purpose of this study, a chemical characterization of the surface of these fillers was carried out. Characterization methods as well as conclusions concerning the chemical composition of the sizing of the fibres are detailed in Section 2 of this chapter.

2. Surface characterization of glass fibres

2.1. Short literature review

Glass fibres are generally mostly comprised of silicon dioxide SiO_2, calcium oxide CaO and aluminium oxide Al_2O_3. The composition of E-CR glass also involves alkali metal oxides (Na_2O), alkaline earth metal oxides (MgO, K_2O) and transition metal oxides (TiO_2, Fe_2O_3, ZnO).[5]

The surface of glass fibres is usually treated with a thin (10-100 nm) coating called "sizing", which consists of an aqueous suspension of several components, the role of which is to facilitate the handling of the fibres and to ensure a good compatibility with the polymer matrix.[6] The formulation of such sizings involves film formers, lubricants, surfactants, antistatic agents and coupling agents. Figure 1 shows the typical composition of a glass fibre sizing according to Gorowa et al.[7]

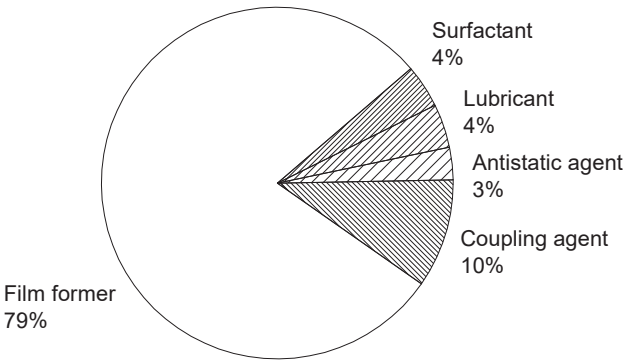

Figure 1. Typical composition of a glass fibre sizing [7]

The role of coupling agents is to ensure a strong anchoring of the sizing onto the surface of the glass fibre and to promote, along with the film former, a good matrix-filler interfacial adhesion. The most commonly used coupling agents are alkoxysilanes, which bond covalently with the glass substrate via naturally occurring silanol functions on the glass surface.[8] Functional end-groups allow the coupling agents to interact with the other components of the sizing through interpenetration, diffusion and chemical reaction.[9] Common functional end-groups include amines (e.g. aminopropyl silanes, APS), epoxides (e.g. glycidoxypropyl silanes, GPS) and vinyls (e.g. vinyl silanes, VS).[10] Typical coupling agents for glass fibres designed for polyolefin and polyamide systems are shown in Table 9.[11]

Table 9. Typical coupling agents used in sizings for glass fibres used in the reinforcement of thermoplastics

Designation	Chemical structure	Thermoplastic resin
γ-methacryloxy propyltrimethoxysilane	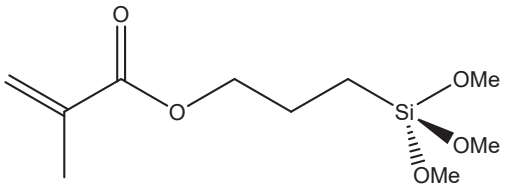	Polyethylene, polypropylene, polystyrene
N-bis (beta-hydroxy ethyl) γ-amino propyltriethoxysilane	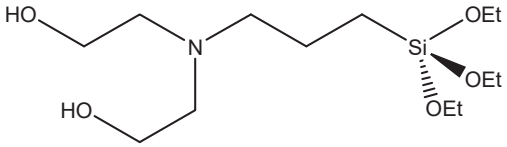	Polyamide

As already mentioned, commercial sizings based on silane coupling agents also involve numerous other additives. Those formulations are often proprietary multicomponent systems designed for specific applications, and it would therefore be difficult to determine their exact composition. Nevertheless, in the scope of this study, the use of functional polyethylene oligomers as matrix-filler interface agents requires some knowledge about the surface chemistry of said fillers. Therefore, several analyses were carried out in order to identify potential reactive groups at the surface of the selected glass fibres.

2.2. Direct analysis of the glass fibres

2.2.1. Thermogravimetric analysis (TGA)

TGA measurements were performed on a TA Instruments Q500 thermogravimetric analyser to determine the amount of sizing on glass fibres. Samples of commercial glass fibres were heated up to 800 °C at a rate of 10 °C/min under helium flow. Table 10 shows the mean weight loss measured over several analyses for the two types of glass fibres considered.

Table 10. Thermogravimetric analysis (TGA) of the glass fibres

Designation	Reference	Mean weight loss (%)	Degradation range (°C)
GF1	DS 2200-13P	0.53	250-450
GF2	DS 1128-10N	0.79	215-575

As expected, both references showed weight loss values around 0.5-1 wt%. They were attributed to the thermal degradation of the sizing as E-CR glass does not undergo thermal degradation in the temperature range considered for TGA measurements. The samples exhibited several degradation peaks, which probably correspond to the different components of the sizings. It was also noted that the

degradation of the sizing of DS 1128-10N fibres takes place over a significantly broader range of temperatures, indicating the presence of a component with higher thermal stability.

2.2.2. Scanning electron microscopy (SEM)

Scanning electron microscopy (SEM) observations of the fibres were done on a Zeiss Merlin electron microscope at the Centre Technologique des Microstructures (CTμ, Villeurbanne, France). The glass fibre bundles were gently dissociated and the glass fibres were spread over carbon tape on the sample holder. The samples were then sputter-coated with a 10 nm layer of copper. Observations were made both with a standard secondary electrons detector (SE) and a back-scattered electrons detector (BSE).

The BSE mode allows the observation of a chemical contrast between the different components of a sample. Since electrons are back-scattered more strongly from elements with a higher atomic number, "heavier" atoms appear brighter and "lighter" atoms appear darker. This observation mode is particularly relevant in the case of glass fibres since the sizing (organic polymers) is chemically very different from the glass substrate (silicon, calcium and aluminium oxides). Samples observed in the BSE mode were not sputter-coated, since it could have induced image artefacts due to the relatively high atomic number of copper.

The general surface aspect of sized glass fibres is shown in Figures 2-4. Observations in SE and BSE mode showed no significant difference between DS 1128-10N and DS 2200-13P fibres with regard to sizing distribution and patterns on the glass surface. It seemed that the distribution of the sizing was highly inhomogeneous along the fibres, especially in terms of sizing thickness, which is consistent with observations reported in the literature.[12] Some patterns, such as the ones observed in Figure 2, were attributed to capillary bridges formed between fibres upon bundling, leaving linear sizing aggregates on the surface.

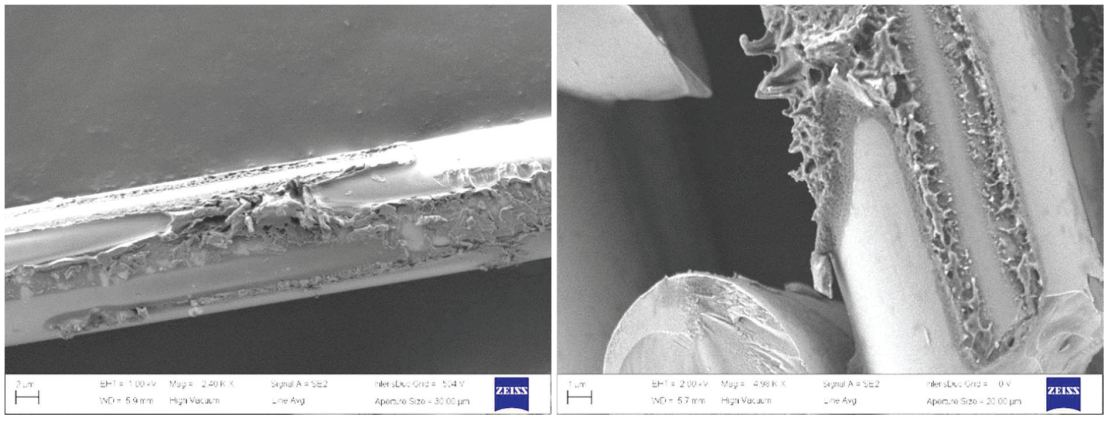

Figure 2. SEM pictures of glass fibres

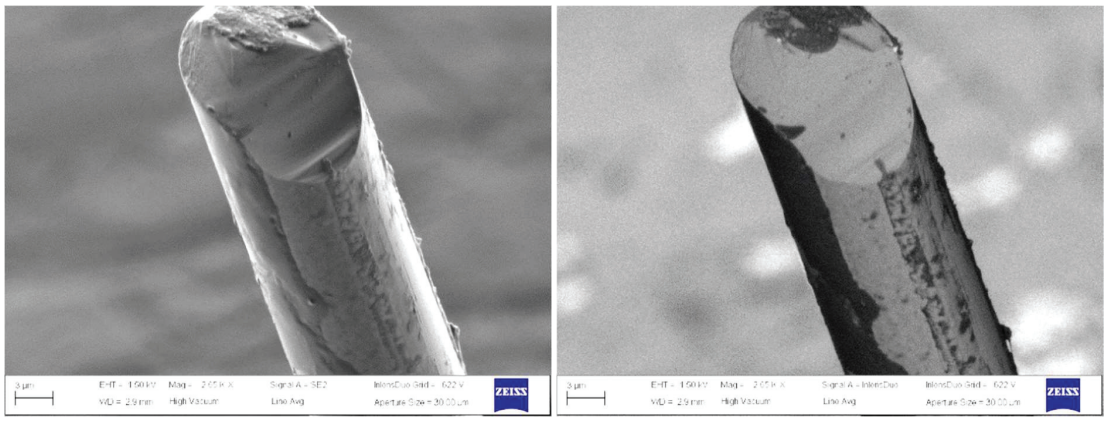

Figure 3. SEM pictures of a glass fibre under SE mode (left) and BSE mode (right)

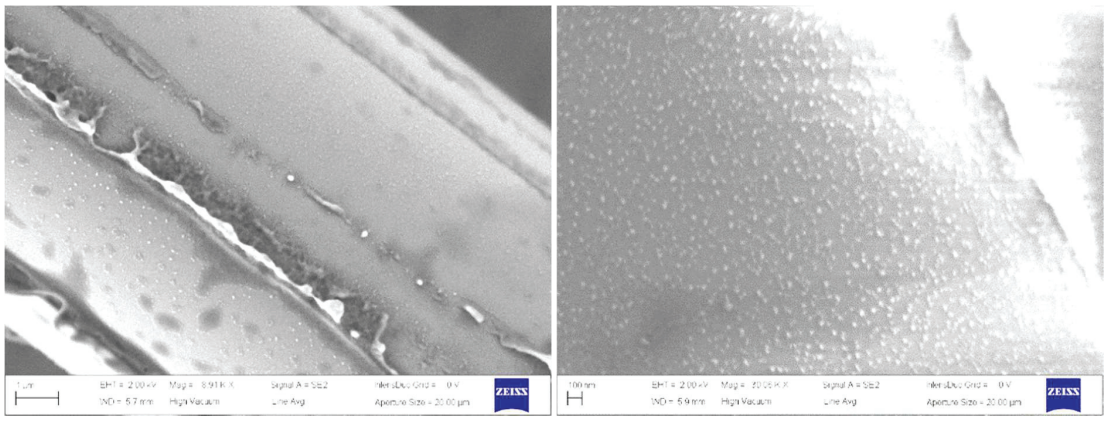

Figure 4. High magnification SEM picture of a glass fibre

Observations at higher magnifications (see Figure 4) showed small spots around 100-500nm in diameter, which could be due to dewetting of the sizing on the glass substrate. A certain roughness was also noticed besides sizing aggregates and spots. It could not be determined whether this roughness is due to the sizing deposition or if it is characteristic of glass substrates, although evidence of surface roughness on clean glass substrates has been reported.[13] This question is of interest as bare glass areas at the surface of the fibres would imply potential reactivity towards alkoxysilanes-functionalized polyethylene oligomers.

2.2.3. Time-of-flight secondary-ion mass spectroscopy (ToF-SIMS)

Time-of-flight secondary-ion mass spectroscopy (ToF-SIMS) analyses were subcontracted to the Science et Surface laboratory (Ecully, France) and conducted on an Ion-TOF SIMS 5 spectrometer.

Apart from the inorganic compounds naturally present in the glass substrate, the study of both references of glass fibres demonstrated the presence of organic compounds such as aliphatic and aromatic hydrocarbons (C_xH_y) as well as nitrogenous species (CN, CNO, C_xN).

The analysis report emphasized the presence of $C_xH_yO_2$ species characteristic of C_{15}-C_{18} linear saturated and unsaturated fatty acids on DS 2200-13P fibres. The presence of $C_xH_yO_z$ fragments indicative of bisphenol diglycidyl ethers on the surface of DS 1128-10N fibres was also pointed out.

2.2.4. Solid-state nuclear magnetic resonance (NMR)

^{1}H, ^{13}C, ^{29}Si and ^{31}P solid-state NMR spectroscopy was conducted on a Brüker Avance WB 500MHz spectrometer equipped with a MAS probe. Analyses were carried out directly on the glass fibres. They were rendered particularly difficult by the small amount of sizing present on the fibres and by the complex nature of those multi-component formulations. The NMR spectra obtained were therefore analysed qualitatively. They can be found in Appendix B.

2.2.4.1. Proton and carbon-13 NMR

^{1}H and ^{13}C solid-state NMR analyses of DS 1128-10N and DS 2200-13P glass fibres showed many peaks corresponding to aliphatic carbons and hydrogens ($-CH_2$ and $-CH_3$). This was considered consistent with the presence of potentially numerous polymeric components in the glass fibres sizings. No signal corresponding to aromatic compounds were found.

While ^{13}C NMR of DS 2200-13P fibres did not show any other peaks, ^{1}H NMR of this type of fibres exhibited strong signals at δ = 3.7 and 4.9 ppm which indicate the presence of an ether, ester and/or acrylate compound.

In the case of DS 1128-10N fibres, ^{1}H NMR exhibited a peak at δ = 3.4 ppm which suggests the presence of an amide (or polyamide) compound along with a shoulder at δ = 3.6 ppm which could indicate the presence of an ether. The ^{13}C NMR spectrum showed a narrow peak at δ = 70 ppm which could correspond to an ether or amine moiety as well as a very broad signal at δ = 180-260 ppm which is typical of compounds containing a carbonyl group such as carboxylic acids, esters and amides.

2.2.4.2. Silicon-29 NMR

Solid-state NMR of ^{29}Si was used to find evidence of the presence of alkoxysilanes coupling agents in the glass fibre sizings studied. Alkoxysilanes form "T" structures while the silicon dioxide (which constitutes the most part of the glass substrate) is arranged in "Q" structures.[14,15] Spectrum analysis was therefore complicated by the very low amount of T sites compared to Q sites as well as by their close chemical shifts in ^{29}Si NMR.

Table 11. Structures of different silicon sites and their typical chemical shifts in ^{29}Si NMR[16]

Site type	Structure	^{29}Si NMR shift range
Q^n (n = 4-x)	$Si(OR)_x(OSi)_{4-x}$	-95; -115 ppm
T^n (n = 3-x)	$R\text{-}Si(OR)_x(OSi)_{3-x}$	-60; -75 ppm
D^n (n = 2-x)	$R_2\text{-}Si(OR)_x(OSi)_{2-x}$	-20; -30 ppm
M^n (n = 1-x)	$R_3\text{-}Si(OR)_x(OSi)_{1-x}$	10 ppm

Spectrum analysis for DS 1128-10N and DS 2200-13P glass fibres revealed a main peak at δ = -90 ppm corresponding to the Q sites of the glass substrate, along with two small peaks at δ = -40 ppm and δ = -140 ppm which were identified as rotation bands. Because of the low sensitivity of solid-state ^{29}Si NMR as well as the presence of rotation bands at the chemical shifts corresponding to T structures, it was not possible to verify the presence of alkoxysilanes in the samples.

2.2.4.3. Phosphorus-31 NMR

^{31}P NMR spectra of both types of glass fibres exhibited a single broad peak at δ = 0 ppm, corresponding to the chemical shift of phosphoric acid and phosphate esters.[17] This was interpreted as evidence of the presence of a phosphate mono/di-ester compound such as those used as emulsifiers and defoamers in a wild range of formulations. The chemical shift of phosphates being relatively insensitive to the nature of the alkoxy groups attached, it is difficult to conclude as to the exact structure of this compound.

2.3. Analysis of sizing extracts

2.3.1. Sizing extraction

Considering that direct chemical analysis of the glass fibres was made difficult by the very small amount of material deposited on their surface, the sizing was extracted in order to be analysed independently. The extraction technique used was solid-liquid extraction with a Soxhlet extractor.[18]

Approximately 10 g of glass fibres were placed in the cellulose thimble and 200 mL of solvent were placed in the boiling flask. Solvents with different polarities and boiling temperatures were chosen for the extractions: ethanol (T_b = 79 °C), cyclohexane (T_b = 81 °C) and xylene (T_b = 141 °C). It is worth noting that xylene is a good solvent for hydrocarbon polymers and is commonly used in the formulation of paints and varnishes. The temperature was set at 120 °C for ethanol and cyclohexane and 180 °C in the case of xylene. The duration of the experiments was 72h.

After each extraction a rotary evaporator was used to remove the solvent from the liquid phase collected in the boiling flask. The remaining liquid samples recovered from this process were yellow-brownish and viscous substances that were later analysed using FTIR and NMR spectroscopy (see following Sections 2.3.2 and 2.3.3).

The glass fibres were recovered from the thimble to be analysed by TGA. The conditions for TGA measurements were the same as described in Section 2.2.1 of this chapter. The results of those analyses are presented in Table 12, where the weight loss is expressed as a percentage of the total weight of glass fibres in the sample and the amount of sizing extracted is expressed as a percentage of the total amount of sizing on the glass fibres (which was determined from the weight loss value before extraction).

Table 12. Mean weight loss values measured by TGA and corresponding amount of sizing extracted from the glass fibres

Solvent used for extraction	DS 2200-13P glass fibres		DS 1128-10N glass fibres	
	Weight loss (%)	Amount of sizing extracted (%)	Weight loss (%)	Amount of sizing extracted (%)
Before extraction	0.53		0.79	
Ethanol	0.34	35	0.67	14
Cyclohexane	0.36	30	0.67	14
Xylene	0.28	54	0.37	52

For both glass fibre types, the same amount of sizing was extracted whether ethanol of cyclohexane was used. Xylene allowed the extraction of around 50 % of the glass fibres sizing in both cases. It was also noted that the amount of sizing extracted did not increase much after 24h of extraction. One reason for the limited amount of material extracted would be that the glass fibres are arranged in bundles, which probably prevented the solvent from solubilizing all of the sizing.

2.3.2. Fourier-transform infrared spectroscopy (FTIR)

Fourier-transform infrared spectroscopy (FTIR) was performed on the extracted sizings using a Thermo Fisher Scientific Nicolet iS10 spectrometer equipped with a Start Omni Transmission module. The liquid samples were placed between two KBr discs to be analysed in transmittance mode. The collected data was processed by Fourier transform to obtain absorbance spectra. A summary of the main absorbance signals measured by FTIR as well as the corresponding bonds and possible attributions is presented in Table 13. The corresponding spectra are displayed in Appendix B.

Table 13. Main signals (cm^{-1}) observed by FTIR analysis for sizing samples extracted with different solvents

DS 2200-13P glass fibres			DS 1128-10N glass fibres			Bond	Attribution
Ethanol	Cyclohexane	Xylene	Ethanol	Cyclohexane	Xylene		
3473	3465	3569	3468	3468	3470	O-H	Alcohol, acid
			3319			N-H	Amine
2951	2953	2950	2951	2954	2953		
2923	2925	2925	2923	2926	2925	C-H	Methyl
2850	2855	2854	2850	2855	2855		
1742	1741	1740	1741	1742	1740	C=O	Carbonyl
			1581			$R\text{-}NH_2$	Amine
			1557				
1466	1464	1461	1466	1464	1461	$-CH_2-$	Aliphatic chain
1378	1378	1376	1377	1379	1377	$-CH_3$	Methyl
1346	1354	1357	1352	1356	1356		
1244	1247	1246	1247	1245	1249	Si-C	Alkoxysilane
1226	1226	1227	1227	1226	1226		Alcohol, acid,
1156	1157	1158	1163	1159	1157	C-O	ether, epoxy,
1107	1109	1108	1105	1108	1109	C-N	amine, amide,
	1059	1058		1058	1058	Si-O	siloxane,
1032		1029	1031		1029		alkoxysilane

The signals collected from FTIR analyses indicated the presence of -CH_2- and -CH_3 groups typical of aliphatic chains. Measurements also suggested the presence of a carbonyl group on both types of fibres but not much evidence was found as to what kind (amide, ester, carboxylic acid and/or ketone). Many peaks were found in the 1000-1250 cm^{-1} range and were thus difficult to attribute to specific bonds. Some peaks could be attributed to Si-C and Si-O bonds, but it is unlikely that alkoxysilanes coupling agents could be removed by the extraction process because of to their strong adsorption on the glass substrate.

The main information that was drawn from FTIR analyses was the presence of peaks corresponding to N-H and R-NH_2 bonds, thus indicating the presence of amine and/or amide compounds in the sizing of DS 1128-10N glass fibres, although removed only by extraction with ethanol.

2.3.3. Nuclear magnetic resonance (NMR)

^1H liquid-state nuclear magnetic resonance (NMR) analyses were performed on a Brüker Avance III 400MHz spectrometer equipped with a BBFO probe. Different deuterated solvents were used depending on the solvent used for sizing extraction: chloroform ($CDCl_3$) for samples extracted in ethanol and benzene was used (C_6D_6) in the case of cyclohexane and xylene.

Again, the interpretation of NMR spectra (which can be found in Appendix B) was difficult because of the complex nature of the sizing formulations. The multiplet signals obtained often overlapped each other, hence the NMR spectra were analysed qualitatively and peaks were rather attributed in terms of typical chemical shifts.

The NMR spectra of both types of glass fibres displayed similar signals. Numerous peaks between δ = 0.6 and 1.8 ppm were found in all samples, corresponding to aliphatic protons. Peaks found at δ = 2.2-2.3 ppm were attributed to alcohol and/or ether groups and peaks in the δ = 4.0-4.2 ppm range to the presence of ether and/or carbonyl groups.

2.4. Conclusions and hypotheses

The surface characterization of DS 2200-13P and DS 1128-10N glass fibres allowed to make hypotheses as to the composition of their sizing, although it was not possible to determine precisely the chemical nature of all constituents.

SEM observations showed an inhomogeneous sizing distribution on the surface of the fibres. As bare glass areas would imply potential reactivity towards alkoxysilanes compounds, polyethylene oligomers with dimethyl methoxy silane and trimethoxy silane functional groups were selected for the study on glass fibre-reinforced HDPE (see Chapter 5).

ToF-SIMS, FTIR, solid-state NMR and liquid-state NMR analyses indicated the presence of hydrocarbon polymer chains and carbonyl compounds on both types of glass fibres, as well as an

organophosphate compound. Analyses also suggested the presence of ether, ester and/or acrylate compounds on the surface of DS 2200-13P fibres. Lastly, amine and/or amide compounds were found on DS 1128-10N fibres as well as potential epoxy groups. Consequently, polyethylene oligomers with carboxylic acid, maleic anhydride and amine functional groups were also selected (see Chapter 5).

It was not possible to verify the presence of silane coupling agents in the sizing of the selected glass fibres. However, considering the potentially low concentration of such compounds as well as their strong adsorption on the glass substrate, they may not constitute suitable reaction sites for functional polyethylene oligomers.

All of the functional polyethylene oligomers selected for the experimental trials reported in Chapter 5 are listed in Section 1.2 of this chapter.

3. Sample preparation

3.1. Batch mixing

Samples were prepared using a 69cm^3 batch internal mixer (Haake Rheomix 600) equipped with roller rotors. Each sample consisted of a polymer resin blended with various amounts of oligomers (0-30 wt%) and/or glass fibres (0-70 vol%).

Blending was carried out at 180 °C in the case of HDPE and PP resins and 240 °C in the case of PA6, with a mixing speed of 50 rpm and a typical filling level of 70 %. During the mixing process the torque was recorded in order to monitor viscosity changes in the mix. The protocols which were used are detailed in the following paragraphs.

In the case of HDPE/PE oligomer and PP/PE oligomer blends (Chapter 3), the polymer was first introduced at t = 0 min and allowed to melt and the PE oligomer was added at t = 5 min, unless otherwise indicated. The mixing was stopped after stabilization of the mixing torque, which took approximately 10-15 min. A similar protocol was used for the trials presented in Chapter 4, where PE-g-MA and polyetheramine oligomers were incorporated within 2-5 min after the introduction of the polymer resin.

For the preparation of composites blends involving glass fibres (Chapter 5), both the HDPE matrix and the PE oligomer were initially introduced at t = 0 min and the glass fibres were incorporated at t = 5 min. The mixing was stopped after stabilization of the mixing torque, which took approximately 20 to 25 min.

The general aspect of the mixing torque curves corresponding to the addition of a PE oligomer or to the incorporation of glass fibres in polyolefins is shown in Figure 5.

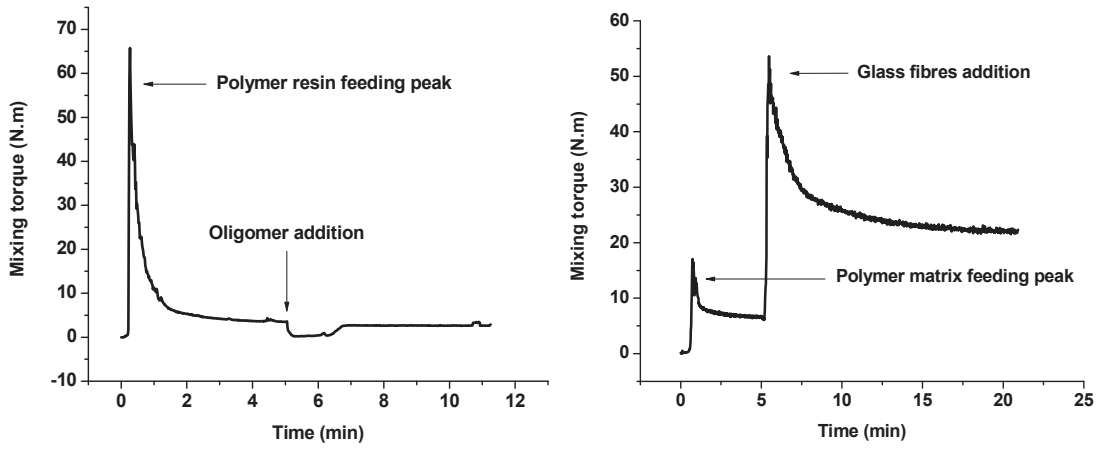

Figure 5. Typical mixing torque curves corresponding to the addition of a PE oligomer (left: PP + 10 wt% PE-COOH oligomer) or to the incorporation of glass fibres (right: HDPE + 40 vol% DS 2200-13P glass fibres)

3.2. Extrusion

Samples were prepared using a Leistritz ZSE18 co-rotating twin-screw extruder with a screw diameter of 18 mm and a length/diameter (L/D) ratio of 60. The screw profile which was used did not include any reverse pitch element, as illustrated in Figure 6. Formulations were extruded at a flow rate of 3 kg/h with a screw speed of 200 rpm. HDPE and PP-based blends were extruded at 180 °C, while blends involving PA6 were extruded at 240 °C.

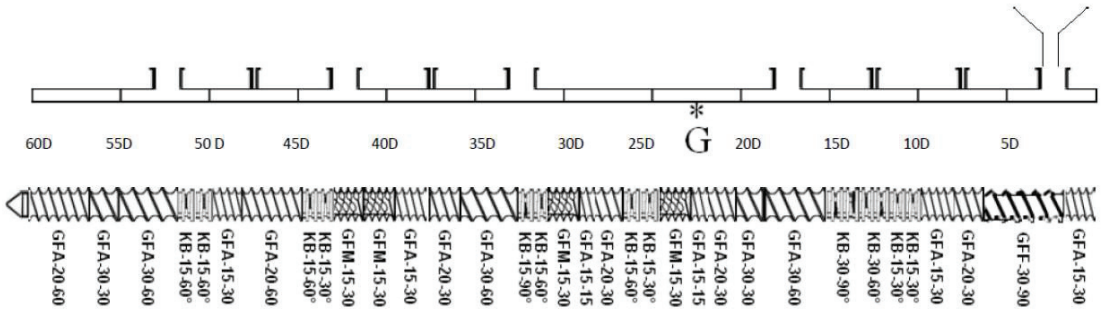

Figure 6. Diagram of the screw profile used for extrusions

The main component(s) of the blend was/were fed into the first block of the extruder through the main hopper. The secondary component(s) was/were incorporated through a secondary side feeder at block n°4 (L/D = 40), which was the case for HDPE/PA6 blends (Chapter 4) and HDPE/glass fibre composite blends (Chapter 5). In formulations involving the addition of a liquid component (e.g. Jeffamine T-403 in Chapter 4), that component was fed into the extruder using a peristaltic pump through an injection point at block n°4.

The following process variables were monitored: (i) pressure and (ii) temperature of the extruded material, measured at the die of the extruder, and (iii) mixing torque.

The extruded material was then air-cooled on a conveyor and chopped into pellets.

4. Characterization methods

4.1. Rheometry

4.1.1. Viscosity measurements

The rheological properties of the samples were measured using a TA Instruments Discovery HR-2 stress-controlled rheometer in parallel plate geometry. The specimens used for rheological measurements were prepared using a hydraulic press. They consisted of discs of 1 mm thickness and 25 mm diameter.

Firstly, a strain sweep oscillatory shear test was performed (with a set angular frequency of ω = 1 rad/s) in order to determine the linear viscoelastic domain of each blend. A frequency sweep oscillatory shear test was then carried out at a set strain depending on the type of sample (typically ε = 1 %, unless otherwise specified) to measure the viscoelastic properties of the blends. All frequency sweeps were carried out from high angular frequencies (starting at ω = 100 rad/s) to low angular frequencies (ending at ω = 0.01 rad/s). It is worth noting that viscoelastic properties measured at low angular frequencies therefore correspond to a residence time of 30-45 min within the rheometer. All rheological measurements were carried out under nitrogen flow at a temperature of 180 °C for both HDPE and PP systems, and 240 °C for blends based on PA6.

Samples with various oligomer concentrations were compared in terms of zero shear viscosity. For further discussion of the results, the absolute complex viscosity (simply referred to as "viscosity") of polymeric systems will be considered, such as:

$$|\eta^*(\omega)| = \sqrt{\left(\frac{G\prime(\omega)}{\omega}\right)^2 + \left(\frac{G\prime\prime(\omega)}{\omega}\right)^2} \qquad \text{with} \qquad G^*(\omega) = G'(\omega) + j \cdot G''(\omega)$$

where G*(ω) is the complex shear modulus, G'(ω) the shear storage modulus, G"(ω) the shear loss modulus, η*(ω) the complex viscosity and ω the angular frequency.

4.1.2. Diffusion experiments

The diffusion of polyethylene oligomers into HDPE and PP was assessed using bi-layer rotational rheometry, a technique well described in the work of Joubert et al.[19]

These measurements were carried out using a TA Instruments ARES-G2 strain-controlled rheometer in parallel plate geometry, with a diameter of 25 mm. The experimental setup is depicted in Figure 7, with the high viscosity component (HDPE or PP) as the lower layer and low viscosity component (PE oligomer) as the upper layer. Diffusion experiments were carried out at a temperature of 180 °C, which was the processing temperature chosen for both HDPE and PP-based systems.

To avoid contact between the upper rheometer plate and the lower polymer layer, a sufficiently thick layer of oligomer was intercalated. Measurements were done with a 1.5mm polymer layer and a 0.5mm layer of polyethylene oligomer, hence a 25 vol% (i.e. ≈ 25 wt%) concentration of polyethylene oligomer in the system.

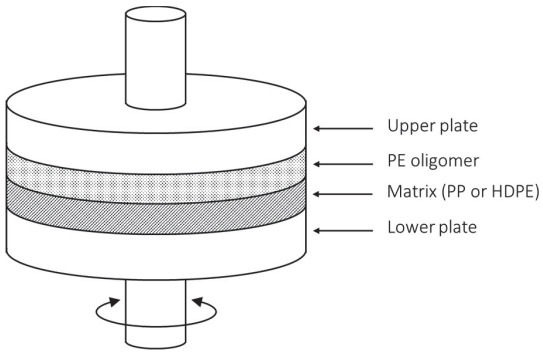

Figure 7. Experimental setup for diffusion measurements using bi-layer rotational rheometry

The shear storage and shear loss moduli (G' and G", respectively) of the system were measured as a function of time with a set angular frequency of ω = 10 rad/s. The strain value was adjusted during the experiment in order to remain within the linear domain of the interlayer mixture: ε = 100 % at the beginning of the experiment and progressively reduced to ε = 1 % after 5 min.

A typical example of the curves obtained from these diffusion experiments is depicted in Figure 8, where the viscosity measured at the beginning of the experiment corresponds to that of the low viscosity component and increases as molecular diffusion takes place.

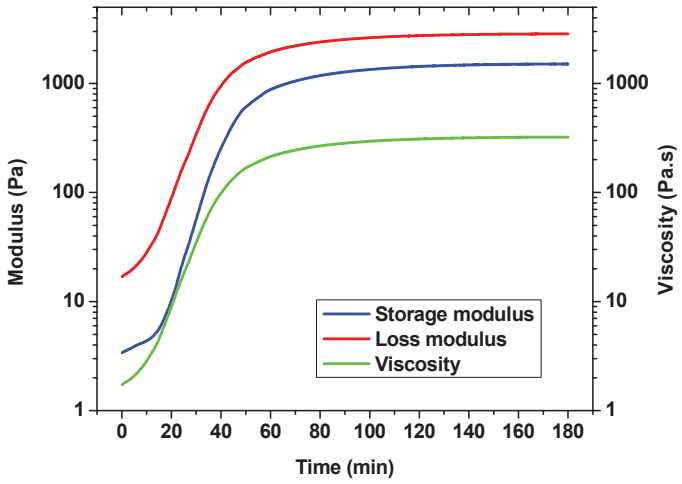

Figure 8. General aspect of G', G" and |η| curves obtained from diffusion experiments*

At the end of each diffusion experiment (i.e. when G', G" and |η*| reach a steady value), a frequency sweep oscillatory shear test was performed in order to measure the viscoelastic properties of the

resulting mixture. This was done to compare the viscoelastic properties of the samples resulting from the diffusion tests with that of mechanically blended samples at similar oligomer concentrations.

4.1.3. Activation energy measurements

The activation energies of HDPE, PP and Unicid 700 were measured to be used in the modelling of the viscoelastic behaviour of polyolefin blends. The WLF equation[20,21] is generally used as a model to determine the temperature dependency of the viscosity of polymers. However, the Arrhenius law is usually more suitable for low molar mass oligomers as well as semi-crystalline polymers processed at temperatures significantly higher than their glass transition temperature[22], which is presently the case for HDPE and PP.

The temperature dependency of the viscosity of the above cited components was determined by performing a temperature sweep oscillatory shear test. However, such measurements are only valid in the Newtonian regime. Consequently, while PE oligomers behave like Newtonian fluids on a wide frequency range, polymers such as HDPE and PP had to be analysed at low angular frequency (ω = 0.01 rad/s in this case) to be as close as possible to the Newtonian domain. The measurements were done using a Discovery HR-2 stress-controlled rheometer in parallel plate geometry. The viscosity of the samples was measured at set strain (ε = 1 % for polyolefin resins and ε = 500 % for polyethylene oligomers) and angular frequency, with temperatures ranging from 120 to 220 °C for polyethylene oligomers, 140 to 240 °C of high-density polyethylene and 170 to 270 °C for polypropylene.

Activation energies were then determined by plotting viscosity as a function of the reciprocal inverse of the temperature. The following Arrhenius law was used:

$$\ln(\eta) = \frac{E_a}{R} \cdot \frac{1}{T} + \ln(k)$$

where E_a is the activation energy, η is the measured viscosity, T is the temperature, R is the ideal gas constant (R = 8.314 J/mol/K) and k is a constant.

4.2. Differential scanning calorimetry (DSC)

A TA Instruments Q200 differential scanning calorimeter was used to determine the melting and crystallization temperatures of the blends as well as raw materials. Neat HDPE and HDPE/PE oligomer blends were heated to 180 °C, then cooled down to -150 °C and finally heated to 180 °C again. Neat PP and PP/PE oligomer blends were heated to 180 °C, then cooled down to -50 °C and finally heated to 180 °C again. Neat PA6 and PA6/oligomer blends were heated to 240 °C, then cooled down to 20 °C and finally heated to 240 °C again. All DSC runs were carried out at a scanning rate of 10 °C/min.

4.3. Hot stage optical microscopy (HSOM)

Hot stage optical microscopy (HSOM) was used in order to observe the crystallization process and crystalline morphology of PP/PE oligomer blends. HSOM consists of observations under a polarized light microscope with the sample placed inside a hot stage to allow thermal scanning of the material. HSOM observations were performed on a Leica DM 2770 M optical microscope equipped with a QImaging Qicam Fast 1394 digital camera. Thermal scanning was ensured by a Mettler Toledo FP82HT hot stage controlled by a Mettler Toledo FP90 central processor.

The blends were pressed into 30-60 µm films using a Polystat 200T bench-type hydraulic press. The films were placed inside the hot stage, firstly heated to 180 °C and allowed to melt. The samples were then cooled down to 50 °C at a rate of 5 °C/min. Pictures were taken at regular intervals of temperature. Figure 9 displays the typical aspect of a neat polypropylene sample during the crystallization process, as observed under a polarized light microscope.

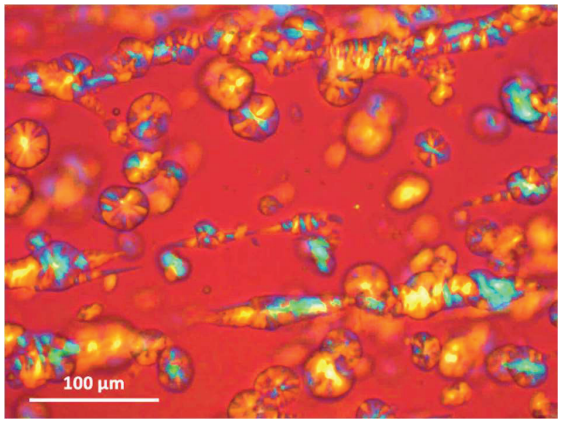

Figure 9. Picture of a thin film of PP at 125 °C under polarized light

The use of a waveplate allows the observation of HSOM pictures in colour., where non-crystalline objects appear magenta and crystalline objects appear yellow or blue. In the case of polymer samples, the magenta colour indicates the presence of an amorphous or molten phase. Under polarized light, polypropylene spherulites appear as birefringent discs growing radially, showing a typical Maltese cross pattern.[23] Eventually, polygonal structures can be observed when spherulites come into contact with each other. In the example shown in Figure 9, the developing PP crystalline phase (spherulites) can be observed exhibiting radial as well as epitaxial growth within the still molten polymer phase at 125 °C.

4.4. Scanning electron microscopy (SEM)

Scanning electron microscopy (SEM) observations were performed on a Zeiss Merlin electron microscope at the Centre Technologique des Microstructures (CTµ, Villeurbanne, France). Polymer blend and fibrous composite specimens were prepared using a hydraulic press to press the samples

into 1 mm-thick discs. The discs were then quenched in liquid nitrogen and fractured using pliers. Sections of appropriate size were cut and mounted on specimen holders, the fractured surface facing upwards.

Some of the polymer blend samples were also prepared with chemical etching of the surface to extract the lower molar mass components of the blends. This protocol, very similar to the one described by Michler[24], is the following:

1. The etchant was prepared by slowly mixing 5 ml of distilled water, 50 ml of sulfuric acid and 0.55 g of potassium permanganate under continuous stirring;
2. The samples were placed in a test tube with the etchant solution;
3. After 30min, the samples were removed, thoroughly rinsed with distilled water and dried.

All specimens were finally sputter-coated with a 10 nm layer of copper to ensure good electrical conductivity between the surface of the specimen and the specimen holder.

4.5. Tensile testing

The mechanical properties of the blends were determined by tensile testing. Those tests were performed on a Shimadzu Autograph AG-X Plus tensile tester equipped with a Shimadzu TRViewX digital video extensometer. The samples were moulded into type 5A test specimens (20 mm gauge length, 4 mm width and 2 mm thickness) according to the ISO-527 standard, using a Babyplast 610P hydraulic injection moulding machine.

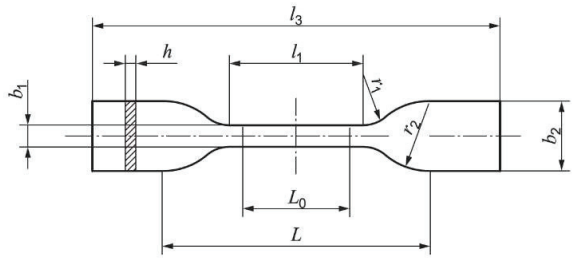

l_3	Overall length	≥75
b_2	Width at ends	12,5 ± 1
l_1	Length of narrow parallel-sided portion	25 ± 1
b_1	Width at narrow portion	4 ± 0,1
r_1	Small radius	8 ± 0,5
r_2	Large radius	12,5 ± 1
L	Initial distance between grips	50 ± 2
L_0	Gauge length	20 ± 0,5
h	Thickness	2 ± 0,2

Figure 10. Type 5A test specimen dimensions according to the ISO-527 standard

To comply with the ISO-527 standard, two different tensile test speeds were used: (i) 1mm/min to determine Young's modulus (E) and (ii) 30mm/min to measure yield stress (σ_y) and strain at break (ε_b). For each blend, ten specimens were tested at each testing speed. A typical stress-strain curve obtained from the tensile testing of neat HDPE is shown in Figure 11.

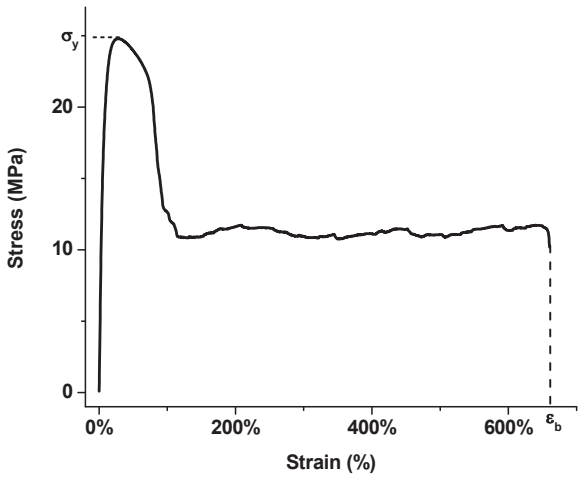

Figure 11. Typical stress-strain curve obtained from tensile testing (e.g. neat HDPE)

4.6. Dynamic mechanical analysis (DMA)

Dynamic mechanical analysis (DMA) was performed on some of the samples. Measurements were carried out using a TA Instruments ARES-G2 strain-controlled rheometer in rectangular torsion geometry. The dimensions of the rectangular parallelepiped test specimens were 15 × 5 × 1.5 mm (length × width × thickness).

A temperature sweep oscillatory shear test was carried out at a set strain of ε = 0.05 % and a set frequency of f = 1 Hz (ω ≈ 6.28 rad/s) in a temperature range of -60 °C to 130 °C and with a heating rate of 3 °C/min. The shear storage and shear loss moduli (G' and G", respectively) as well as the loss factor (tan δ) were measured as a function of the temperature. The loss factor is defined by the following equation.

$$\tan\delta = \frac{G''}{G'}$$

5. Bibliography

[1] J. Mazzolini, E. Espinosa, F. D'Agosto, C. Boisson, Catalyzed chain growth (CCG) on a main group metal: an efficient tool to functionalize polyethylene, Polymer Chemistry. 1 (2010) 793–800. doi:10.1039/B9PY00353C.

[2] I. German, W. Kelhifi, S. Norsic, C. Boisson, F. D'Agosto, Telechelic Polyethylene from Catalyzed Chain-Growth Polymerization, Angewandte Chemie International Edition. 52 (2013) 3438–3441. doi:10.1002/anie.201208756.

[3] W. Nzahou Ottou, S. Norsic, I. Belaid, C. Boisson, F. D'Agosto, Amino End-Functionalized Polyethylenes and Corresponding Telechelics by Coordinative Chain Transfer Polymerization, Macromolecules. 50 (2017) 8372–8377. doi:10.1021/acs.macromol.7b01396.

[4] S. Norsic, C. Thomas, F. D'Agosto, C. Boisson, Divinyl-End-Functionalized Polyethylenes: Ready Access to a Range of Telechelic Polyethylenes through Thiol–Ene Reactions, Angewandte Chemie International Edition. 54 (2015) 4631–4635. doi:10.1002/anie.201411223.

[5] A. Berthereau, E. Dallies, Fibres de verre de renforcement, Techniques de l'ingénieur Matériaux composites : présentation et renforts. base documentaire : TIB142DUO (2008).

[6] J.L. Thomason, L.J. Adzima, Sizing up the interphase: an insider's guide to the science of sizing, Composites Part A: Applied Science and Manufacturing. 32 (2001) 313–321. doi:10.1016/S1359-835X(00)00124-X.

[7] R.L. Gorowara, W.E. Kosik, S.H. McKnight, R.L. McCullough, Molecular characterization of glass fiber surface coatings for thermosetting polymer matrix/glass fiber composites, Composites Part A: Applied Science and Manufacturing. 32 (2001) 323–329. doi:10.1016/S1359-835X(00)00112-3.

[8] D.M. Laura, H. Keskkula, J.W. Barlow, D.R. Paul, Effect of glass fiber surface chemistry on the mechanical properties of glass fiber reinforced, rubber-toughened nylon 6, Polymer. 43 (2002) 4673–4687. doi:10.1016/S0032-3861(02)00302-6.

[9] A.T. DiBenedetto, Tailoring of interfaces in glass fiber reinforced polymer composites: a review, Materials Science and Engineering: A. 302 (2001) 74–82. doi:10.1016/S0921-5093(00)01357-5.

[10] F.R. Jones, A Review of Interphase Formation and Design in Fibre-Reinforced Composites, Journal of Adhesion Science and Technology. 24 (2010) 171–202. doi:10.1163/016942409X12579497420609.

[11] A. Bergeret, P. Krawczak, Liaison renfort/matrice Définition et caractérisation, Techniques de l'ingénieur Caractérisation et propriétés d'usage des composites. base documentaire : TIB144DUO (2006).

[12] J.L. Thomason, D.W. Dwight, The use of XPS for characterisation of glass fibre coatings, Composites Part A: Applied Science and Manufacturing. 30 (1999) 1401–1413. doi:10.1016/S1359-835X(99)00042-1.

[13] Y. Gabet, O. Gain, E. Espuche, Etude et optimisation des interfaces fibre-matrice polymère de composites structuraux à base thermoplastique, University of Lyon, 2018.

[14] M. Lelli, D. Gajan, A. Lesage, M.A. Caporini, V. Vitzthum, P. Miéville, F. Héroguel, F. Rascón, A. Roussey, C. Thieuleux, M. Boualleg, L. Veyre, G. Bodenhausen, C. Coperet, L. Emsley, Fast Characterization of Functionalized Silica Materials by Silicon-29 Surface-Enhanced NMR Spectroscopy Using Dynamic Nuclear Polarization, J. Am. Chem. Soc. 133 (2011) 2104–2107. doi:10.1021/ja110791d.

[15] M.-C. Brochier Salon, M.N. Belgacem, Competition between hydrolysis and condensation reactions of trialkoxysilanes, as a function of the amount of water and the nature of the organic

group, Colloids and Surfaces A: Physicochemical and Engineering Aspects. 366 (2010) 147–154. doi:10.1016/j.colsurfa.2010.06.002.
[16] H.C. Marsmann, R.R. Gupta, Chemical Shifts and Coupling Constants for Silicon-29, Springer-Verlag, Berlin Heidelberg, 2008. //www.springer.com/la/book/9783540452775 (accessed July 4, 2018).
[17] D.G. Gorenstein, Phosphorous-31 NMR: Principles and Applications, Academic Press, 2012.
[18] J. Leybros, P. Fremeaux, Extraction solide-liquide. II. Techniques et appareillage, Techniques de l'ingénieur. Génie des procédés. 2J2782 (1990) J2782.1-J2782.13.
[19] C. Joubert, P. Cassagnau, L. Choplin, A. Michel, Diffusion of plasticizer in elastomer probed by rheological analysis, Journal of Rheology. 46 (2002) 629–650. doi:10.1122/1.1470521.
[20] M.L. Williams, R.F. Landel, J.D. Ferry, The Temperature Dependence of Relaxation Mechanisms in Amorphous Polymers and Other Glass-forming Liquids, J. Am. Chem. Soc. 77 (1955) 3701–3707. doi:10.1021/ja01619a008.
[21] J.D. Ferry, Viscoelastic properties of polymers, 3rd ed., John Wiley & Sons, Inc., 1980.
[22] J.A. Dantzig, C.L. Tucker, Modeling in Materials Processing, Cambridge University Press, 2001.
[23] J. Varga, Supermolecular structure of isotactic polypropylene, J Mater Sci. 27 (1992) 2557–2579. doi:10.1007/BF00540671.
[24] G.H. Michler, 9.3.1. Chemical Etching, in: Electron Microscopy of Polymers, Springer, Berlin, Heidelberg, 2008: pp. 187–191. doi:10.1007/978-3-540-36352-1.

Chapter 3 – Rheology and crystallization behaviour of HDPE and PP in the presence of a functional PE oligomer

Table of contents

1. Introduction

The formulation of thermoplastic materials involves the blending of numerous additives and fillers in order to improve their technical features as well as their processability.[1] The aim of the REPEAT project is to value functional polyethylene oligomers as plasticizers and interface agents in thermoplastic composites. A large number of processing aids that are currently used in the formulation of polyolefins consists of hydrocarbon derivatives such as paraffinic, naphthenic and aromatic oils, paraffinic and microcrystalline waxes or saturated fatty acids.[2,3] The main difficulties associated with these blends are the very low viscosity ratio between the additive and the polymer resin in the molten state[4] as well as the potential phase separation occurring in the solid state due to the difference in the degree of crystallinity, crystallization temperature and crystalline microstructure between the constituents.[5]

During the blending of a miscible low viscosity oligomer with a high viscosity polymer, the homogenization of the system proceeds through two mechanisms: mixing and diffusion.[6] Lubrication occurs in the case of a slow diffusion of the additive into the polymer, causing the low viscosity component to segregate to the high shear rate zones of the mixing equipment. In the case of immiscible additives, no diffusion takes place and the homogenization on a macroscopic scale relies solely on the mixing ability of the blending equipment. Lubrication therefore occurs as a result of the absence of diffusion of the low viscosity component into the high viscosity component. Some studies have investigated the blending of miscible and immiscible low viscosity additives into polymers[4,7], and Scott and Macosko[8,9] have proposed a mechanism to describe the morphology developments during the initial stages of mixing. The viscosity ratios reported in those studies varied in the range of 10^{0} to 10^{-3}. In the present work, the blending of a low viscosity polyethylene oligomer with high viscosity polypropylene and high-density polyethylene was considered, involving viscosity ratios in the range of 10^{-5} to 10^{-6}. Morphology developments during the blending of such systems was studied by a batch processing approach (Section 2.1). Furthermore, recent studies[10–13] have highlighted the efficiency of bi-layer rheological measurements to investigate the diffusion of low viscosity plasticizers into polymers. This technique is very adequate in the case of miscible polymers and discriminating towards non-diffusive blends. It was therefore used as a model experiment to monitor the evolution of the viscoelastic properties in bi-layer systems (Section 2.2). Rheology constitutes a particularly powerful tool for the study of such blends and was therefore further used in combination with rheological predictive laws[14] in order to assess the miscibility of a functional polyethylene oligomer in the selected polyolefin resins in the molten state (Section 3).

It is also well known that the morphology of binary polymer blends has a decisive influence on the final properties of polymer materials. Most polymers are thermodynamically immiscible with each other, including polypropylene/polyethylene blends as well as some polyethylene/polyethylene blends, although some instances of partial miscibility resulting in macroscopically homogeneous blends have

been reported.[15–18] Many studies[15,19–23] have focused on the control of the morphology and crystallization kinetics of miscible and immiscible polymer blends with similar viscosities. However, a large number of processing aids that are used in the formulation of polyolefins consists of low viscosity hydrocarbon derivatives and more recently, blends of polyolefin with low molar mass paraffin compounds generated new interest for their use in the field of energy storage.[24–34] The second objective of the present work was therefore to investigate the miscibility aspects inherent to the crystallization of blends of low molar mass polyethylene oligomers with polypropylene and high-density polyethylene (Section 4). The crystallization behaviour of such blends was studied by dynamic scanning calorimetry in combination with optical microscopy under polarized light, and changes in the crystalline microstructure of the blends were observed by electron scanning microscopy.

2. Processing of HDPE/PE oligomer and PP/PE oligomer blends

2.1. Morphology developments upon blending: batch processing approach

Blends based on HDPE or PP with a functional PE-COOH oligomer (Unicid 700) were achieved using a batch internal mixer at a temperature of 180 °C. The PE oligomer concentrations tested were 1, 2.5, 5, 10, 20 and 30 wt%. In a first set of experiments, the polyolefin resin and the PE oligomer were introduced simultaneously at t = 0 min. The mixing torque was recorded to monitor viscosity variations in the systems and to get a better understanding of the morphology developments during blending. The torque curves obtained are presented in Figure 1.

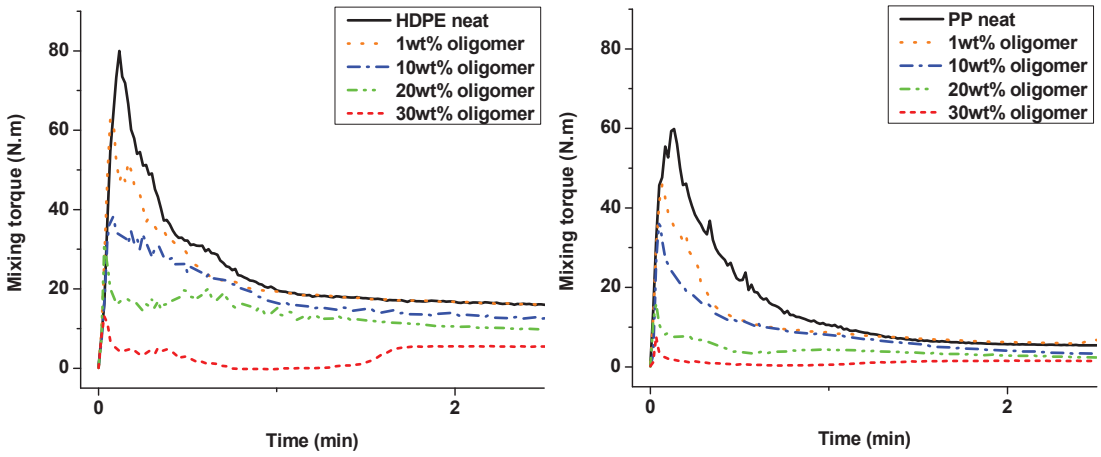

Figure 1. Mixing torque curves for HDPE/PE oligomer (left) and PP/PE oligomer (right) blends

Both graphs show a single torque peak for the blending of neat polyolefins. The introduction of a gradually increased amount of PE oligomer in the mix was characterized by a decrease of the maximum torque value as well as area under the curve, which corresponds to the energy that is necessary to melt and homogenize the system. It was also noted that the final mixing torque was reduced by the addition of the PE oligomer, indicating a reduction of the overall viscosity of the blend.

Studies have shown that during the initial stages of blending, the lower viscosity component segregates to the high shear zones of the mixing equipment, resulting in a lubricating effect.[4] This is especially true since the additive has a lower melting temperature than the polymer, thus melting first when put in contact with the hot surface of the mixer. The current understanding of this process is that in the initial stages of the blending process, the (low viscosity) minor component forms a continuous phase that coats the major component which is still in the form of solid pellets.[7] The available energy to melt the major component is subsequently decreased, resulting in longer times to homogenization, which emphasizes the importance of the viscosity ratio towards the processing conditions of binary blends.

In the case of HDPE systems, the time required to reach a stable torque value was not impacted by the addition of PE oligomer. However, at 20 wt% PE oligomer, the curve did not exhibit a single peak, due to the lubricating effect of the low viscosity oligomer. The lubricating effect was even more apparent at 30 wt% PE oligomer, where the mixing torque was reduced to 0 N.m for almost a minute, delaying the homogenization of the system. For PP blends, adding PE oligomer in various amounts did not impact the homogenization time either. Blends with 20-30 wt% PE oligomer again showed evidence of lubricating effect. However, variations in torque value were less apparent than in HDPE systems after the prime peak, due to the lower viscosity of PP compared to HDPE.

The lubricating effect was further investigated by introducing the polyolefin resin and the PE oligomer separately into the mixer: the polyolefin resin was first introduced in the mixer and allowed to melt and the PE oligomer was added after 5 min. The mixing torque variations corresponding to the incorporation of the PE oligomer are shown in Figure 2.

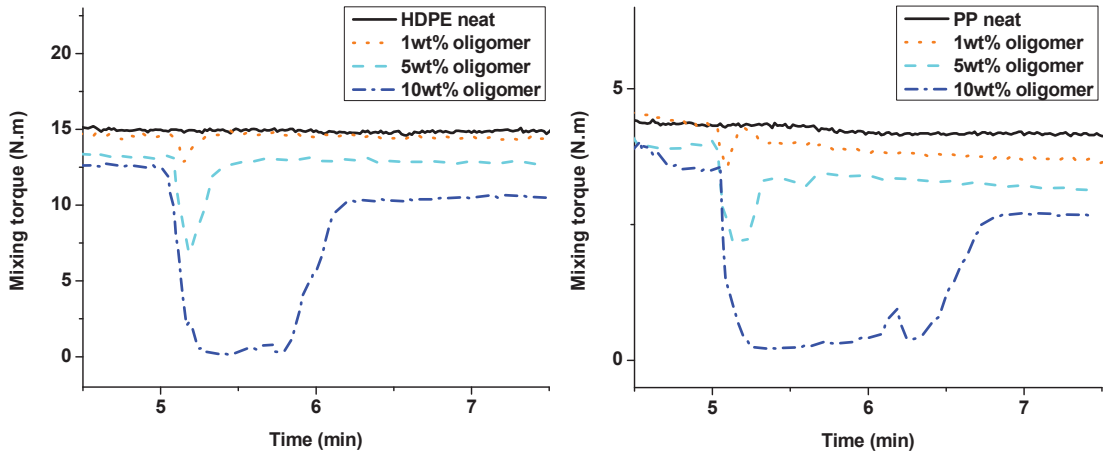

Figure 2. Mixing torque curves after the addition of PE oligomer in HDPE (left) or PP (right)

The concentration of PE oligomer was again linked to the gradual reduction of the final mixing torque (i.e. viscosity) of the blend. While the introduction of low amounts of PE oligomer (1-5 wt%) resulted in rapid homogenization, blends involving higher oligomer concentrations (≥ 10 wt%) were characterized by longer times to achieve homogenization, during which the mixing torque was nearly decreased to the minimum measurable value. It was therefore deduced that the persistence of the lubricating effect and delay in homogenization of the system was directly linked to the concentration of PE oligomer in the blend at a given viscosity ratio.

The raise of the torque value following the lubrication phenomenon is typical of a phase inversion arising from the melting and subsequent consolidation of the major component when an immiscible low viscosity component is introduced in the mixer.[4,35] The blends studied in this work can therefore be considered to behave like immiscible blends in the early stages of the blending process, although it was observed that times to achieve homogenization were much shorter than the values found in the literature for low amounts of PE oligomer.[4]

Finally, the comparison of the steady torque value before the addition of PE oligomer and after the homogenization of the system clearly shows a reduction of the overall viscosity of the blend (despite the increased filling level in the mixer), suggesting that PE oligomers behave like plasticizers in the melts.

All of these observations suggest that diffusion is the dominating mechanism in the homogenization of such systems. Besides, the homogenization occurring in a batch internal mixer can be further described by representing the velocity profile of a binary polymer blend between in a simple shear flow.[36] Such a system is depicted in Figure 3, where a low viscosity fluid is placed on top of a high viscosity fluid between a lower stationary plate and an upper moving plate.

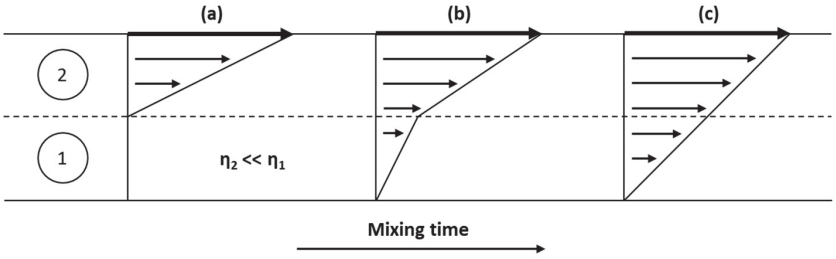

Figure 3. Evolution of the velocity profile during the homogenization a binary blend with a low viscosity ratio

In the first stages of the mixing process, the low viscosity component absorbs all the shear stress, as depicted in the velocity profile (a). The formation of a lubricating layer thus hinders the shear stress transfer to the high viscosity component. In the case of miscible fluids, mixing as well as diffusion occurring at the interface between fluids (1) and (2) contribute to the homogenization of the system, leading to the distribution of the velocity profile (b). This results in an increase of the overall viscosity of the system, which translates into a raise in the mixing torque value, as observed in Figure 2. Further mixing and diffusion finally lead to the complete homogenization of the system, which corresponds to profile (c).

2.2. Diffusion of a PE oligomer into HDPE and PP: model experiment

Studies have shown that during the blending of two miscible of immiscible polymers, the viscosity ratio is of foremost importance.[4,7] Low viscosity ratios were shown to have a dramatic impact on the mixing regime as well as the morphology development of the blends. It has also been shown that when blending of a very low viscosity component into a high viscosity polymer, the system behaviour is more sensitive to diffusion than mixing for viscosity ratios below 10^{-3}.[6] A model experiment is therefore proposed to investigate the homogenization process during the blending of polyolefin resins with polyethylene oligomers.

As explained in Chapter 2, the diffusion ability of the PE oligomer into HDPE and PP was measured by bi-layer rotational rheometry.[10] The high viscosity polyolefin resin was placed on the bottom

plate while the low viscosity PE oligomer was placed on top and the viscoelastic properties of the system were measured against time. Variations of the absolute complex viscosity during the diffusion of the PE oligomer into HDPE and PP are presented in Figure 4.

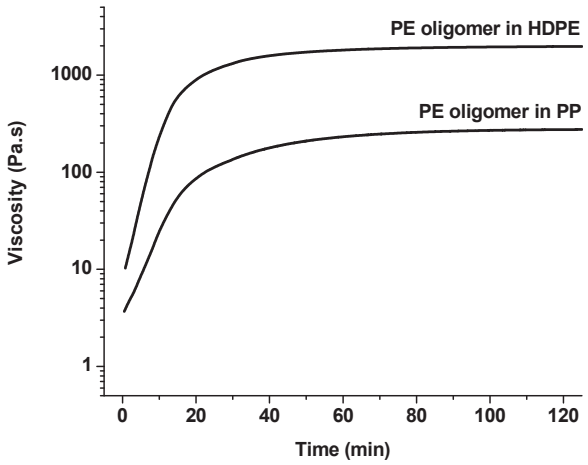

Figure 4. Variations of the absolute complex viscosity measured by bi-layer rotational rheometry during the diffusion of a PE oligomer into HDPE and PP resins (θ = 180 °C, ω = 10 rad/s, d = 25mm, e = 2 mm)

Considering the viscosity ratio between the polyolefins and the PE oligomer as well as the experimental setup, the viscosity measured at the beginning of the experiment should be similar to that of the neat PE oligomer, which is around 10^{-2} Pa.s. Because of the time required to place the samples in the rheometer and to reach the appropriate temperature, the viscosity measurements were started with a delay of about 1 min. The HDPE and PP systems thus generally exhibited viscosities around 10^{0}-10^{1} Pa.s at the beginning of the measurements, which was attributed to part of the low viscosity component having already diffused into the other component during the setting up of the experiment. Additionally, considering the slopes of the viscosity curves presented in Figure 4 for t = 0-15 min, it can be argued that the diffusion phenomenon is faster in the HDPE resin, which may partly explain the higher viscosity values measured at the beginning of the experiment for the HDPE/PE oligomer system.

Studies indicate that the diffusion of the low viscosity component into the polymer generates a concentration gradient, thus leading to viscosity variations. As the viscosity is directly linked to the transport behaviour between the two components[11], the measured viscosity of the system increases if diffusion occurs. All samples indeed displayed a rapid increase in viscosity in the first minutes of the experiment, indicating facile diffusion of the PE oligomers into the polyolefins. HDPE and PP systems were compared in terms of diffusion coefficient in the polymer phase, which was calculated according to the following equation[37,38]:

$$t_D = \frac{2{L_0}^2}{D}$$

where, L_0 is the thickness of the polymer phase, t_D is the diffusion time and D is the diffusion coefficient. The calculated diffusion coefficients for both HDPE and PP systems were around 5.10^{-10} m^2/s, with no significant difference between the different systems. Those values were found to be in the same order of magnitude as the typical values found in the literature for similar systems at similar temperatures and concentrations.[10,12,13]

After a sufficient amount of time, the viscosity of each sample reached a steady value as a result of the homogenization process. At the end of each experiment, the viscoelastic behaviour of the final medium was subsequently determined by a frequency sweep oscillatory shear test. The measurements revealed that the samples resulting from the diffusion experiments had a similar viscoelastic behaviour than that of blends processed using an internal mixer. Those results strongly suggest that the samples undergo an efficient homogenization process through diffusion without any mixing, which confirms previous results and demonstrates that diffusion is the dominating mechanism in the homogenization of such systems.

3. Miscibility and morphology in the molten state

3.1. Viscoelastic properties of the blends

HDPE/PE oligomer and PP/PE oligomer blends were prepared using a batch internal mixer at a temperature of 180 °C and characterized in terms of rheological behaviour by oscillatory shear rheometry in parallel plate geometry. Figure 5 shows the viscosity curves obtained for HDPE and PP systems with 0-30 wt% PE oligomer.

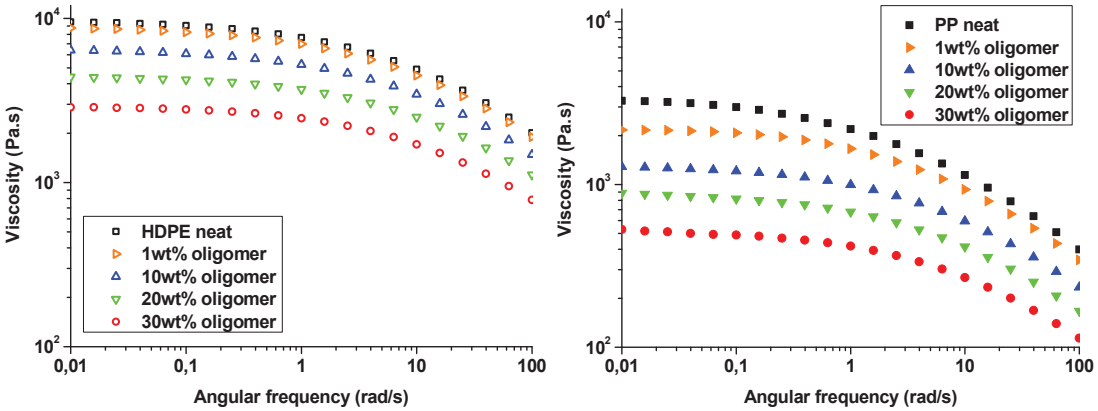

Figure 5. Viscosity curves for HDPE/PE oligomer (left) and PP/PE oligomer blends (right)

All blends exhibited a viscoelastic behaviour corresponding to that of typical polyolefins with a linear molecular structure. The blends containing PE oligomer had a viscoelastic behaviour analogous to that of the neat polyolefin, and frequency sweeps showed a gradual decrease in viscosity as the PE oligomer content was increased in both HDPE and PP systems, as shown in Figure 5.

The incorporation of low viscosity polyethylene oligomers into polyolefins can be considered to have a dilution effect[39], thus influencing the viscoelastic properties of the resulting blend. If PE oligomers were completely immiscible with the polyolefins, then the continuous polymer phase would dominate the rheological behaviour of the blends[40] and the viscosity of the blends would have likely remained unchanged. However, the miscibility cannot be ascertained only by observing the decrease of the viscosity of the blends.

It was noticed that in the case of PP blends with high oligomer concentrations, the storage modulus exhibited a deviation from the typical slope at low angular frequencies, indicating an alteration of the terminal relaxation behaviour of PP in the presence of large amounts of PE oligomer. The storage modulus curves of HDPE/PE oligomer and PP/PE oligomer blends are shown in Figure 6, where the blends with 0, 10 and 30 wt% PE oligomer are displayed as relevant examples of this phenomenon.

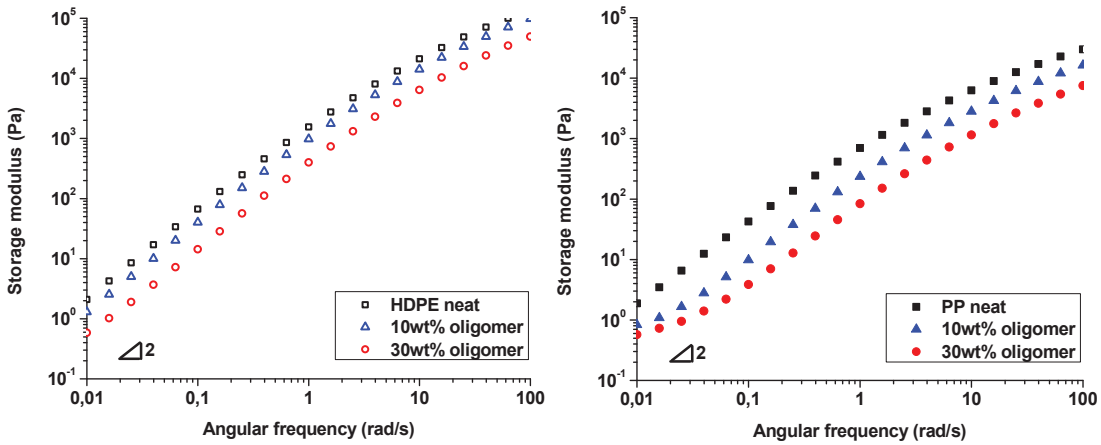

Figure 6. Storage modulus curves for HDPE/PE oligomer (left) and PP/PE oligomer (right) blends at 0, 10 and 30 wt%

This phenomenon was investigated by using another method of data representation. Cole-Cole diagrams have been successfully used in a number of studies[41–45] as an efficient tool to further investigate miscibility aspects of binary polymer blends. They consist in the representation of η'' versus η' which are calculated according to the following equations:

$$\eta'' = \frac{G\prime}{\omega} \qquad \text{and} \qquad \eta' = \frac{G\prime}{\omega}$$

where η' is the real viscosity, η'' is the imaginary viscosity (with $\eta^* = \sqrt{(\eta')^2 + (\eta'')^2}$), G' is the shear storage modulus, G'' is the shear loss modulus, and ω is the angular frequency. The Cole-Cole diagrams corresponding to the viscosity curves presented in Figure 5 are displayed in Figure 7.

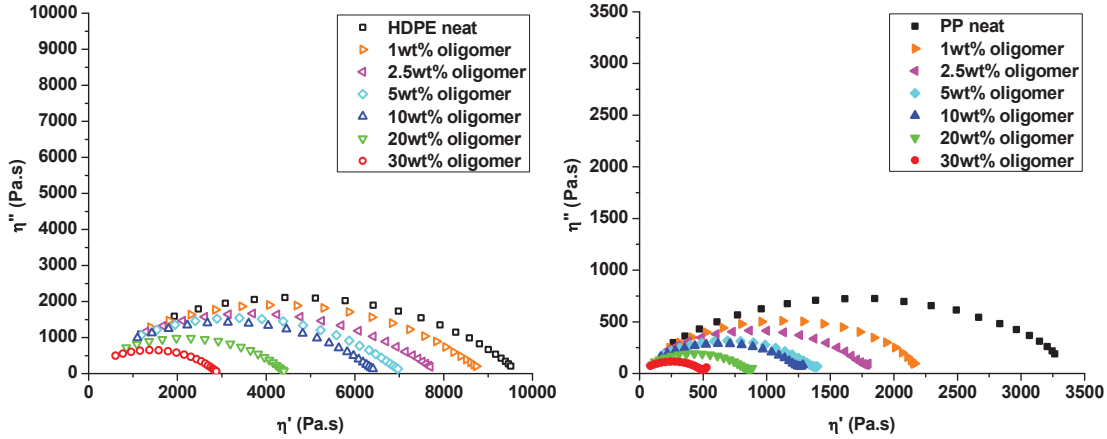

Figure 7. Cole-Cole diagrams for HDPE/PE oligomer (left) and PP/PE oligomer (right) blends

All HDPE/PE oligomer blends exhibited a semi-circular scatter which is characteristic of homogeneous blends.[41] PP systems on the other hand showed a tail on the right-hand side of the arc, starting with oligomer concentrations as low as 2.5 wt% and growing more visible as the amount of oligomer increased. An enlarged Cole-Cole diagram for the blend of PP with 30 wt% PE oligomer is shown in Figure 8 as a relevant example of this phenomenon.

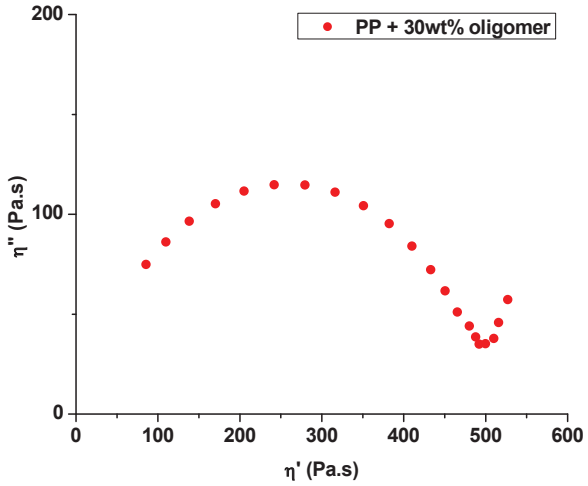

Figure 8. Cole-Cole diagram for PP with 30 wt% PE oligomer

Those results indicate that a phase separation occurs in blends of PP with PE oligomers[41,43–45], suggesting that the miscibility in such blends could be limited by the oligomer concentration. However, it would be difficult to quantify this phase separation and therefore to determine to what extent the oligomer contributes to the dilution of the polymer resin.

3.2. Rheological modelling

3.2.1. Carreau-Yasuda law

In their study of the viscoelastic properties of PP/oil blends, Gimenez et al.[14] and Ponsard-Fillette et al.[12] demonstrated that the viscoelastic behaviour of such mixtures could be described using the Carreau-Yasuda equation.[46] Assuming the applicability of the Cox-Merz rule, where $\dot{\gamma} \equiv \omega$, this equation can be written as follows:

$$\eta = \eta_0[1 + (\tau\omega)^a]^{\frac{m}{a}}$$

where η_0 is the zero-shear viscosity of the bulk polymer, τ corresponds to the relaxation time of the bulk polymer and m is the power law slope. The parameter a characterizes the transition between the power law and zero-shear regions.

Considering an entangled regime ($M > (M_c)_{bulk}.\varphi^{-1.25}$, with φ the volume fraction of polyolefin resin in the blend) the intrinsic viscosity $[\eta_0]$ can be drawn from the zero-shear viscosity of the bulk polyolefin resin.

$$[\eta_0] = (\eta_0)_{bulk}\,\varphi^4$$

The zero-shear viscosity of the blend is then determined by introducing a free volume correction parameter a_φ that takes into account the change in glass temperature inherent to the dilution.

$$(\eta_0)_{blend} = (\eta_0)_{bulk}\, \varphi^4\, a_\varphi$$

Similarly, in the entangled regime the relaxation time τ can be written as:

$$\tau = (\tau)_{bulk} \varphi^{1.75} a_\varphi$$

The following generalized Carreau-Yasuda equation was therefore used to model the viscosity reduction arising from the dilution of HDPE and PP resins by the PE oligomer:

$$\eta(\omega, \varphi) = (\eta_0)_{bulk}\, a_\varphi\, \varphi^4 \left[1 + \left(\tau_{bulk}\, a_\varphi\, \varphi^{1,75}\, \omega\right)^a\right]^{\frac{m}{a}}$$

Using the input parameters $(\eta_0)_{bulk}$, a_φ and φ, the Carreau-Yasuda model was fitted to the viscosity curve of neat HDPE and PP, as shown in Figure 9.

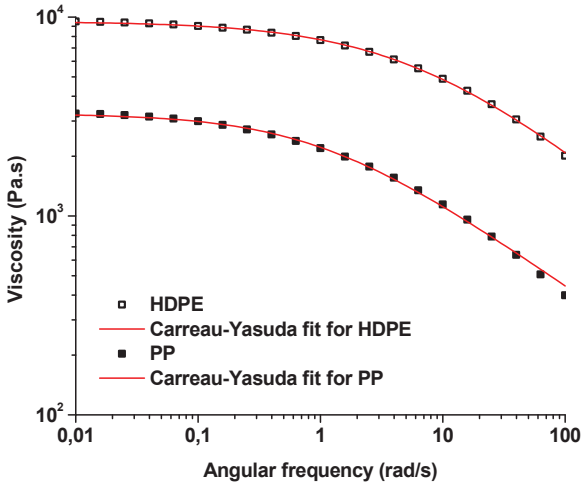

Figure 9. Fitting of the Carreau-Yasuda equation for the viscosity curves of neat HDPE and PP

The input parameters $(\eta_0)_{bulk}$, a_φ and φ, as well as the output parameters τ_{bulk}, a and m drawn from the fittings are given in Table 1.

Table 1. Parameters of the Carreau-Yasuda equation for bulk HDPE and PP

Polymer	$(\eta_0)_{bulk}$ (Pa.s)	a_φ (-)	φ (-)	τ_{bulk} (s)	a (-)	m (-)
HDPE	9.5×10^3	1	1	0.16	0.64	-0.51
PP	3.3×10^3	1	1	0.97	0.76	-0.43

These calculated parameters were then used as fixed input parameters in the Carreau-Yasuda model in order to predict the viscoelastic behaviour of the blends, as described in the following sections.

3.2.2. HDPE/PE oligomer blends

The PE oligomer considered in this study is a linear polyethylene with a chemical structure very close to that of HDPE and its glass transition temperature can be considered to be very similar to that of

HDPE. Consequently, the free volume correction parameter was not taken into account (i.e. $a_\varphi = 1$) for HDPE/PE oligomer blends.

The viscosity of each HDPE/PE oligomer blend was predicted using the previously calculated parameters and then compared to the measured viscosity. Figure 10 displays the predicted and measured viscosities for blends with 10 wt% and 30 wt% PE oligomer, which were taken as relevant examples. The predicted zero-shear viscosities were also compared to the measured zero-shear viscosities (see Figure 5) for all blends of HDPE with PE oligomer.

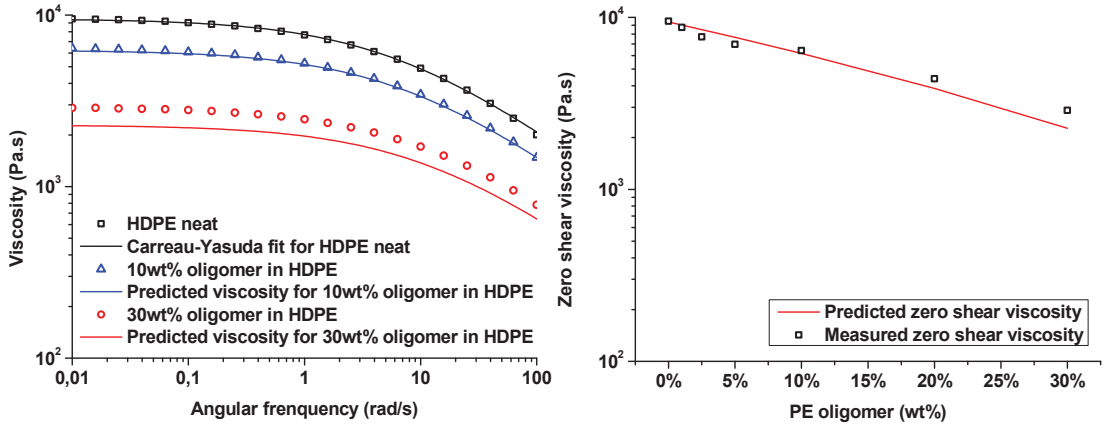

Figure 10. Modelled viscoelastic properties for HDPE/PE oligomer blends (10 wt% and 30 wt%) (left) and comparison of the predicted versus measured zero-shear viscosities for HDPE/PE oligomer blends (0-30 wt%) (right)

It appeared that the rheological behaviours predicted by the model fitted the experimental data quite well. Those results therefore indicate that HDPE systems behave like semi-dilute or concentrated polymer solutions[14,39] in the presence of PE oligomers, suggesting that the selected low molar mass oligomer is good solvents for HDPE in the molten state.

3.2.3. PP/PE oligomer blends

Because of the difference in glass transition temperatures between PP and PE oligomers, the free volume theory must be considered[47–49] to model the viscoelastic behaviour of PP systems. The free volume correction parameter a_φ must therefore be determined. This correction parameter is given by the following equation:[10,14]

$$a_\varphi = exp\left(\frac{-1}{RT}|E - E_0|\right)$$

where E is the activation energy of the blend and E_0 is the activation energy of the bulk polymer. Assuming the additive law of free volumes and considering the activation energy of the oligomer E_1, the activation energy of the blend can therefore be defined as:

$$\frac{1}{E} = \frac{\varphi}{E_0} + \frac{1-\varphi}{E_1}$$

The activation energies of PP and PE oligomers were determined by performing a temperature sweep oscillatory shear test in the Newtonian regime (ω = 0.01 rad/s) and plotting viscosity as a function of the reciprocal inverse of temperature, using an Arrhenius equation.[50] The measured activation energy values were E_0 = 41.7 kJ/mol for PP and E_1 = 21.4 kJ/mol for the PE oligomer. The activation energies and free volume correction parameters were calculated for each PP/PE oligomer blend and are given in Table 2.

Table 2. Activation energies and free volume correction parameters calculated for PP/PE oligomer blends (0-30 wt%)

PE oligomer content (wt%)	PP content (wt%)	φ (-)	E (kJ/mol)	aφ (-)
0	1.000	1.000	41.7	1.000
1	0.990	0.989	41.3	0.895
2.5	0.975	0.974	40.6	0.761
5	0.950	0.947	39.7	0.588
10	0.900	0.895	37.9	0.364
20	0.800	0.790	34.7	0.158
30	0.700	0.687	32.1	0.079

a_φ and φ, as well as the previously calculated parameters (τ_{bulk}, a and m) were used in the Carreau-Yasuda model to predict the viscosity of PP/PE oligomer blends. Figure 11 shows the predicted viscosity for blends of PP with 10 wt% and 30 wt% PE oligomer, which were taken as relevant examples, analogous to those presented in Figure 10. The predicted zero-shear viscosities were also compared to the measured zero-shear viscosities for all of the PP/PE oligomer blends.

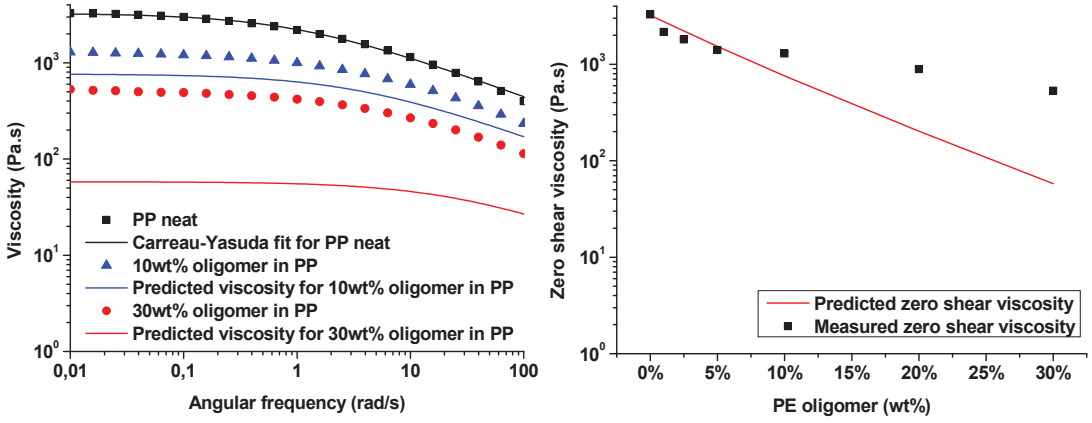

Figure 11. Modelled viscoelastic properties for PP/PE oligomer blends (10 wt% and 30 wt%) (left) and comparison of the predicted versus measured zero-shear viscosities for PP/PE oligomer blends (0-30 wt%) (right)

It was found that in the case of PP/PE oligomer blends, the model (which is based on the hypothesis of a homogeneous medium) did not fit the experimental data as well as for HDPE systems. While the zero-shear viscosities appeared to be well predicted for concentrations up to 5 wt% PE oligomer, blends with concentrations of 10 wt% PE oligomer and above showed higher viscosities than expected, meaning that the viscosity reduction arising from the dilution was overestimated by the model. For

instance, the measured zero-shear viscosity of the 30 wt% blend was found to be ten times higher than the predicted value. This could be caused by the appearance of separate domains of PE oligomer at high concentrations, which could be the result of the saturation of the PP above a certain concentration. This is consistent with previous observations on the viscoelastic behaviour of PP/PE oligomer blends (see Cole-Cole diagrams in Figure 7) which indicated a possible phase separation.

The present results therefore suggest that the PE oligomer is partially miscible in PP in the molten state and that the miscibility may be dependent on the blend composition. However, the mechanism leading to the saturation of the polymer phase and causing the observed variations in the viscosity reduction effect was not further investigated in the scope of this study. Some authors reported that the blending of PP with low molar mass paraffinic waxes were homogeneous on a macroscopic scale up to wax concentrations of about 5-10 wt%.[16,51] Such results could be consistent with the assumption that PP and PE oligomers are at least partially miscible in the melt.[52] However, the mechanisms leading to the saturation of the polymer phase and causing the observed variations in the viscosity reduction effect were not further investigated in the scope of this study.

4. Crystallization behaviour of HDPE and PP in the presence of a functional PE oligomer

As mentioned previously, the final properties of polymer blends are highly dependent on their morphology in the solid state, which ensues from the morphology developments during melt processing as well as from the molecular rearrangements that occur during the transition from the molten to the solid state. The experimental work presented in this section is therefore focused on the crystallization behaviour of HDPE/PE oligomer and PP/PE oligomer blends as well as the consequent morphology in the solid state.

As low concentrations might not have allowed the observation of potentially separate domains in the solid state, blends with large amounts of PE oligomer (10-30 wt%) were chosen for this part of the study in order to be able to detect the presence of said oligomers in the samples. The differential scanning calorimetry (DSC) curves of HDPE and PP systems with 30 wt% PE oligomer are shown in Figure 12 as examples of the crystallization behaviours observed at high concentrations.

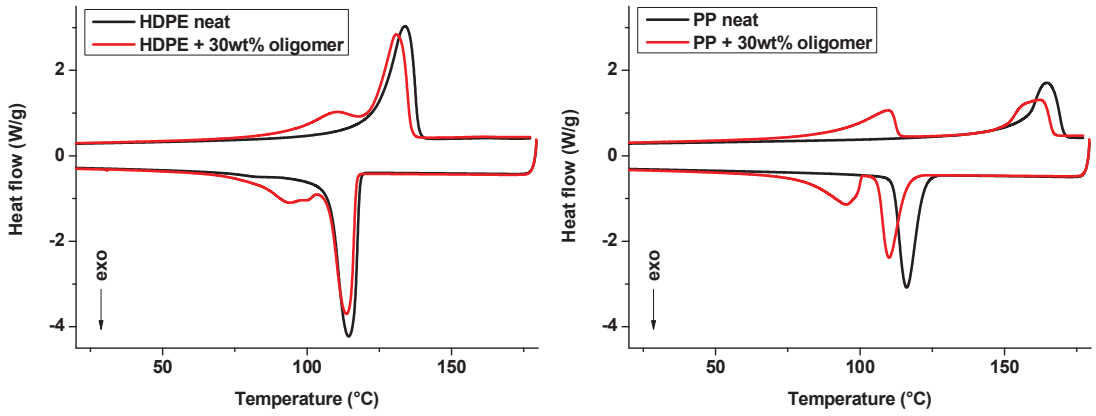

Figure 12. DSC curves for HDPE/PE oligomer (left) and PP/PE oligomer (right) blends at 0 and 30 wt% PE oligomer

The crystallization behaviours of HDPE and PP systems with various amounts of PE oligomer are discussed separately in the following sections.

4.1. HDPE/PE oligomer blends

In order to evaluate the effect of PE oligomers on the crystallization behaviour of HDPE, differential scanning calorimetry (DSC) was used to measure the crystallization temperature, melting temperature and degree of crystallinity of HDPE/PE oligomer blends. The corresponding heat flow curves are displayed in Figure 13.

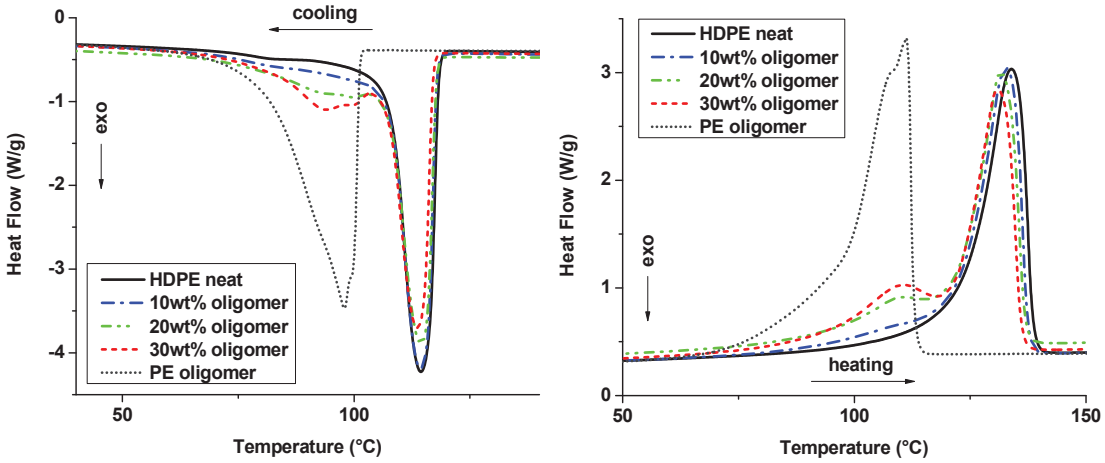

Figure 13. DSC curves recorded during the crystallization (left) and melting (right) of HDPE/PE oligomer blends

All samples displayed two melting and crystallization peaks, each corresponding to the melting and crystallization temperatures of neat components. It is worth noting that for all blends, each component exhibited a single crystallization exotherm, therefore showing no sign of fractionated crystallization.[53] Those results indicate that PE oligomers form a separate phase upon solidification of the blend.[21]

Several investigations found that HDPE was miscible with low molar mass linear hydrocarbon compounds in the molten state, but that those blends underwent a solid-liquid phase separation upon crystallization of the polymer resin.[25,28,54] Here, it was observed that the melting temperature of HDPE had slightly decreased with the addition of PE oligomer, which may be directly linked to the dilution[55] of HDPE by the PE oligomer as a result of their miscibility in the molten state.[56,57] However, the crystallization temperature of HDPE did not shift with the addition of the PE oligomer as it could be expected, indicating that the crystallization kinetics of the HDPE phase is not affected by dilution.

The overlapping of peaks in (due to the close melting and crystallization temperature of HDPE and PE oligomer) prevented the direct determination of the degree of crystallinity of the two separate components, even though the DSC analysis indicated separate melting and crystallization of HDPE and the PE oligomer in the blend. Additionally, it is difficult to ascertain the heat of fusion of PE oligomers, although values can be found in the literature for linear low molar mass linear alkanes and paraffinic waxes.[58] Considering that HDPE and PE oligomer have very similar molecular structures, the heat of fusion of purely crystalline HDPE (ΔH_f^0 = 293 J/g[58]) was used to determine the overall degree of crystallinity in all samples. The overall degree of crystallinity and heat of fusion measured by DSC for HDPE/PE oligomer blends as well as neat components can be found in Table 3. For each blend, the overall degree of crystallinity calculated with an additive rule of mixture from the degrees of crystallinity of the neat materials is given in the last column of the table.

Table 3. Overall heat of fusion and degree of crystallinity of HDPE/PE oligomer blends

Blend composition	ΔH_f(blend) (J/g)	X_m(blend) (%)	Calculated X_m (%)
100/0	198	68	68
90/10	208	71	70
80/20	214	73	71
70/30	226	77	73
100/0	253	86	86

Those measurements showed that the overall degree of crystallinity of the HDPE blends slightly increased with the addition of PE oligomer. It should be noted that PE oligomers have a much higher degree of crystallinity than HDPE. Therefore, the increase in overall degree of crystallinity did not allow to draw conclusions as to the consequences of the dilution of HDPE by PE oligomers on the crystallization behaviour of those blends. Nevertheless, it was observed that for each blend the overall degree of crystallinity measured by DSC was similar to the calculated value obtained from an additive rule of mixture. This suggests that the degree of crystallinity of each constituent is not influenced by blending and that both the HDPE and the PE oligomer crystallize separately.

The sample with 10 wt% PE oligomer did not exhibit a second crystallization peak. Instead, the crystallization exotherm was slightly lower than for neat HDPE around 90 °C. Although this is probably due to the weaker signal corresponding to the oligomer at lower concentrations, it could be associated with the concurrent melting of the two constituents. Blends with even lower oligomer concentrations might not have exhibited the same melting and crystallization behaviours, but this would be practically impossible to verify due to the very close melting and crystallization temperatures of HDPE and PE oligomers, meaning that the peak corresponding to the melting of the PE oligomer would be concealed by the onset of the melting peak of HDPE (and that the crystallization peak of the PE oligomer would be concealed by the offset of the crystallization peak of HDPE).

Samples with lower oligomer concentrations (≤ 10 wt%, not represented in Figure 5) did not exhibit a second crystallization or melting peak. Instead, the crystallization exotherm was slightly lower than for neat HDPE around 90 °C and the melting endotherm was slightly higher than for neat HDPE around 110 °C. Although this is probably due to the weaker signal corresponding to the PE oligomer at lower concentrations, it could also be associated with a concurrent crystallization phenomenon between the two constituents. Hato et al.[59] notably found that hard paraffin wax (with similar molar mass and melting temperature as the PE oligomer considered in the present study) was miscible with HDPE up to 20 wt% in the solid state as a result of potential co-crystallization. Additionally, Gumede et al.[60] recently found evidence that while solid-liquid phase separation essentially occurred upon cooling, linear portions of a highly branched LLDPE were able to co-crystallize with medium-soft paraffin wax in the wax-rich phase. However, considering that in the present case PE oligomer chains in their fully

extended conformation are about 6-7 nm long, they should only be able to co-crystallize with the thinner HDPE lamellae, the melting temperature of which is around 100°C.[61]

4.2. PP/PE oligomer blends

4.2.1. Crystallization behaviour – DSC analysis

PP/PE oligomer blends were analysed by differential scanning calorimetry (DSC), in the same manner as for HDPE/PE oligomer blends. The corresponding heat flow curves are displayed in Figure 14.

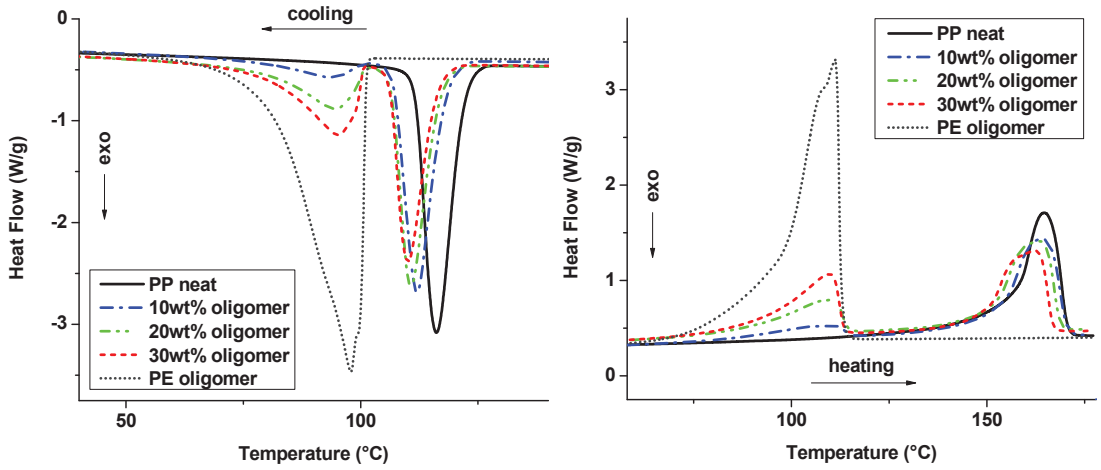

Figure 14. DSC curves recorded during the crystallization (left) and melting (right) of PP/PE oligomer blends

All samples exhibited two distinct melting and crystallization peaks, each corresponding to the melting and crystallization temperatures of the neat constituents, similarly to what was observed in the case of HDPE/PE oligomer blends, thus indicating phase separation upon crystallization.[21] The melting peaks of PP and PE oligomer were well separated and the degree of crystallinity of the two constituents could therefore be determined independently, with respect to their mass fraction in the blend. These valued are displayed in Table 4 along with the overall degree of crystallinity of each blend. Again, the heat of fusion of purely crystalline HDPE (ΔH_f^0 = 293 J/g) was used to determine the degree of crystallinity of the PE oligomer and a value of ΔH_f^0 = 207 J/g was used in the case of PP.[58]

Table 4. Heat of fusion and degree of crystallinity of PP and PE oligomer in PP/PE oligomer blends

Blend composition	ΔH_f (PE) (J/g)	X_m (PE) (%)	ΔH_f (PP) (J/g)	X_m (PP) (%)	X_m (blend) (%)
100/0	-	-	103	50	50
90/10	14	49	89	48	48
80/20	37	63	79	48	51
70/30	66	70	72	50	56
0/100	253	86	-	-	86

The addition of PE oligomer to PP generally resulted in an increase of the overall degree of crystallinity of the blends, while the degree of crystallinity of the PP phase remained globally unaffected. The degree of crystallinity of the PE oligomer increased with its concentration, which can be correlated with the increase of the overall degree of crystallinity of the blends. However, the degree of crystallinity of the PE oligomer in the blends was found lower than that of the neat PE oligomer, meaning that when introduced in PP a portion of the PE oligomer is unable to crystallize, which could be explained by a lack of mobility of the PE oligomer chains in the already solidified PP.[62]

Furthermore, it was observed that the crystallization temperature of PP had shifted downwards and that the melting peak of PP had broadened with the addition of PE oligomer. Those effects were more discernible at high concentrations, although already noticeable with 10 wt% PE oligomer. This indicates that the introduction of PE oligomers, even in low amounts, somehow has an impact on the melting and crystallization behaviour of PP. Several studies showed that low molar mass n-alkanes were miscible with PP in the molten state and acted as a diluent, while solid-liquid phase separation occurred upon crystallization of the PP.[5,26] Although it appears clearly here that two separate crystalline phases form upon cooling of the blend, the shift in crystallization temperature indicates that the presence of the PE oligomer influences the crystallization behaviour of PP as a result of dilution in the molten state.[55]

Evidence of melting point depression in the presence of hydrocarbon waxes and oils have also been reported in the literature in the case of PP[16,31] and PE[34,63]. According to Groeninckx et al.[62], dilution by a miscible amorphous component in the molten state results in a decrease of the free energy of the semi-crystalline polymer, which eventually leads to a shift of the equilibrium melting point.[56,64] Nevertheless, even if PE oligomers act as diluents in the molten state thanks to their low molar mass, no co-crystallization can take place between PP and PE oligomers because of their different crystalline structures.[31,32] The present results could therefore be an indication that some PE oligomer chains are retained in the amorphous phase of PP[51] as a result of the dilution of PP by the PE oligomer.

Additional DSC analyses were performed at a scanning rate of 5 °C/min on a PP/PE oligomer blend at a concentration of 5 wt% in an attempt to get a better understanding of the crystallization behaviour of less diluted PP systems. The corresponding heat flow curve is presented in Figure 15 and compared to that of neat PP as well as that of the blend with 30 wt% PE oligomer.

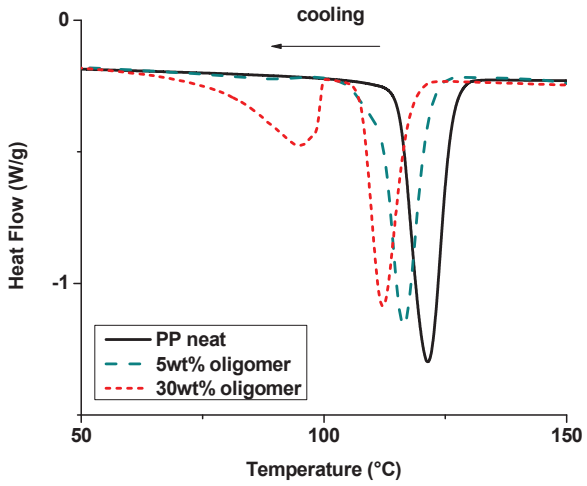

Figure 15. Crystallization behaviour of PP with 5 wt% and 30 wt% PE oligomer (cooling rate = 5 °C/min)

Again, the separate crystallization of PP and PE phases appeared clearly at 30 wt% PE oligomer. The sample with 5 wt% PE oligomer showed no crystallization peak corresponding to the oligomer. It was not obvious in this case whether the signal was too weak to be distinguished from the baseline or simply non-existent. The crystallization peak corresponding to PP exhibited a small shoulder on the left-hand side. This could be attributed either to the delayed crystallization of some PP chains due to the presence of PE oligomer, or to the concurrent crystallization of the two constituents as PP crystals may act as additional nucleation sites for the PE oligomer.[65] The fact that this shoulder is not observed at 30 wt% may simply be the result of the further decrease of the crystallization temperature range of PP with the increased concentration of PE oligomer.

Moreover, the downwards shift in crystallization temperature which had previously been noticed at higher oligomer concentrations (see Figure 14) appeared to be already quite pronounced at 5 wt%. This shows that the decrease in crystallization temperature is not a linear function of the oligomer content, which suggests that the dilution of PP involves only a small amount of PE oligomer. Those results are in agreement with the hypothesis that the low molar mass PE is at least partially miscible in polyolefins such as HDPE and PP. Nevertheless, even if polyethylene oligomers act as diluents in the melt thanks to their low molar mass, no co-crystallization can occur because of their different crystalline structure compared to PP.[31,32] It is therefore possible that due to their low molar mass, some PE oligomer chains are able to remain in the amorphous phase of PP upon crystallization.

4.2.2. Morphology developments upon crystallization – HSOM experiments

The morphology developments taking place upon the phase separation between the PP and the PE oligomer were further investigated by hot stage optical microscopy (HSOM) in combination with the DSC analyses. When cooled under a polarized light microscope, PP spherulites appear as birefringent discs growing radially as a result of crystallization.[66] Crystalline phases therefore appear white under

polarized light because of the positive birefringence of the spherulites, whereas amorphous or molten areas of the film appear black.

As explained in Chapter 2, the samples consisting of thin films of polymer were heated at 180 °C and cooled down to 50 °C at a rate of 5 °C/min in order to monitor the morphology of the crystalline phases. Particular interest was taken in the crystalline morphology of the samples in the 100-120 °C range, which is in between the crystallization peaks of PP and PE oligomer, as displayed on DSC curves (Figure 14). HSOM pictures of the samples at different temperatures are shown in Figure 16 (neat PP) and Figure 17 (PP with 30 wt% PE oligomer).

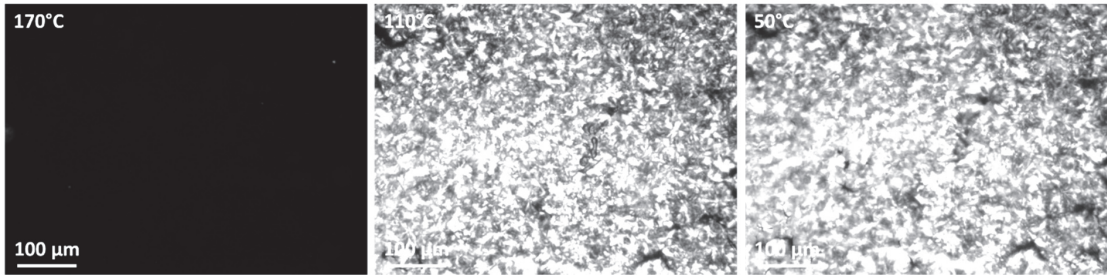

Figure 16. Pictures of neat PP at 170 °C, 110 °C and 50 °C under polarized light

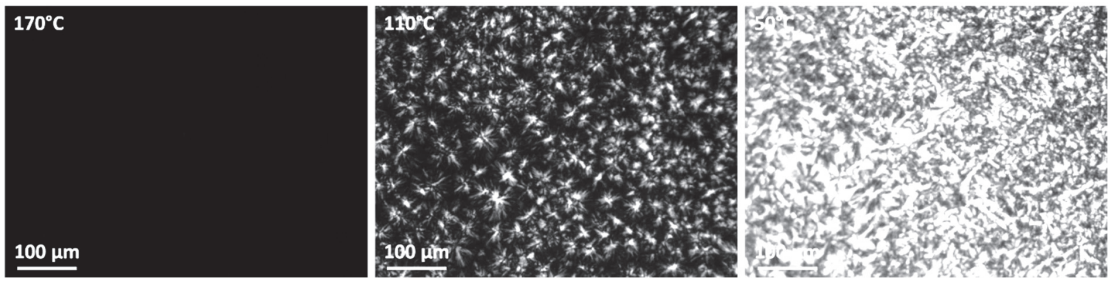

Figure 17. Pictures of the PP/PE oligomer (70/30) blend at 170 °C, 110 °C and 50 °C under polarized light

Here, both PP and the PE oligomer are in the molten state at 170 °C (no transmitted light) and in the solid state at 50 °C (maximum light intensity). The central picture taken at 110 °C corresponds to a stage where the PP, which is the major component of the blend, has crystallized while the PE oligomer remains molten.

The intensity of the light transmitted through the sample was correlated with the relative crystallinity of the blend.[67] The monochrome pictures taken during HSOM experiments were analysed in terms of grey value on an 8-bit greyscale that ranges from 0 (black) to 255 (white). The mean grey value of each picture was determined using an image processing software. The mean grey values obtained were then plotted against temperature so as to obtain a transmitted light intensity profile throughout the cooling process. The resulting normalized transmitted light intensity profiles of both samples are displayed in Figure 18.

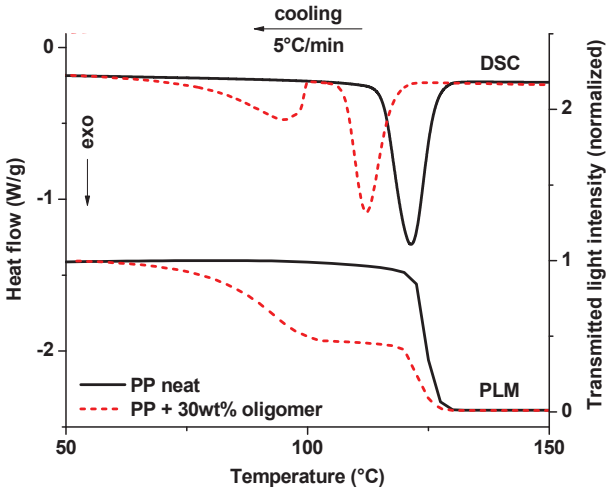

Figure 18. Evolution of the transmitted light intensity during the cooling of PP with 0 wt% and 30 wt% PE oligomer, measured by PLM and compared to the DSC curves for the corresponding samples

In neat PP the transmitted light intensity rose rapidly between 130 °C and 120 °C to reach approximately the maximum value, which corresponds to the crystallization peak of PP on the DSC thermogram. The sample consisting of PP with 30 wt% PE oligomer exhibited a slower increase in light intensity between 130 °C and 120 °C, as well as a plateau between 120 °C and 100 °C corresponding to the temperature range in which the PE oligomer is still molten. The presence of this plateau correlates with the separate crystallization of PP and the PE oligomer observed by DSC.

Enlarged sections of the pictures shown in Figure 17 are displayed in Figure 19. The two pictures represent the exact same area of the film corresponding to the PP/PE oligomer (70/30) blend at 110 °C and 50 °C. In these pictures, polygonal structures can be observed as a result of the PP spherulites coming into contact with each other.

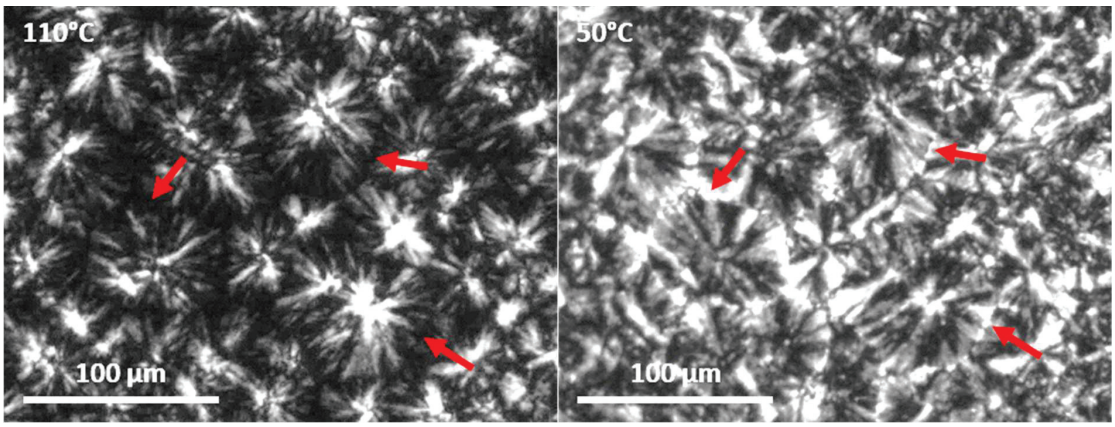

Figure 19. HSOM pictures of PP with 30 wt% PE oligomer taken at 110 °C and 50 °C under polarized light

Qualitative analysis of those pictures revealed that the inter-spherulitic region consisted of molten material at temperatures between the crystallization temperatures of PP and the PE oligomer (see Figure 19 at 110 °C). At temperatures below the crystallization temperature of the PE oligomer those

areas seemed to have crystallized, as the boundaries between PP spherulites appeared very bright (see Figure 19 at 50 °C). These observations were interpreted as evidence of the presence of the highly crystalline PE oligomer in the inter-spherulitic region.

Studies on the morphology of PP-PE interfaces have highlighted the fact that the PE phase could be deformed by the growth of PP spherulites upon crystallization, resulting in the presence of deformed PE occlusions in the ultimately crystallized blends.[68,69] Moreover, it was reported that the ultimate morphology of the PE phase is highly dependent on the viscosity of the PE, which determines its ability to flow between the growing PP spherulites.[70] Considering the very low viscosity of the PE oligomers used in this study, it can be assumed that the PE domains encountered should be highly deformed with numerous ramifications into the PP phase. Additionally, no spherical PE occlusions were observed in the PP phase.

On the other hand, in the case of a miscible polymer/diluent system there is no liquid-liquid phase separation and the final morphology of the blend should therefore be controlled by the solid-liquid phase separation occurring during the solidification of the semi-crystalline polymer[54], which may take place in the case of an amorphous diluent or if the diluent has a significantly lower crystallization temperature than the polymer. This was reported several times in the literature for blends of PP with low molar mass hydrocarbon compounds such as mineral oil or linear alkanes[5,26], in which cases the segregation of the low molar mass component may be mostly described as inter-spherulitic.[62]

Considering the dilution of the PP by the PE oligomer in the molten state, the qualitative analysis of HSOM pictures (Figure 19) suggests that upon crystallization of the PP, the liquid PE oligomer phase is excluded from the growing PP spherulites and forms separate domains.[21,52] However, it was not possible to determine from these observations whether some PE oligomer chains had remained within PP spherulites.

4.2.3. Crystalline morphology in the solid state – SEM observations

PP/PE oligomer blends were observed by scanning electron microscopy (SEM) in order to evaluate the impact of PE oligomer addition on the crystalline microstructure of PP in the solid state. The chemical etching of the samples, as described in Chapter 2, allowed the observation of the crystalline microstructure of both neat polyolefins and blends. The fracture morphologies corresponding to neat PP and PP with 30 wt% PE oligomer are presented in Figure 20 and Figure 21.

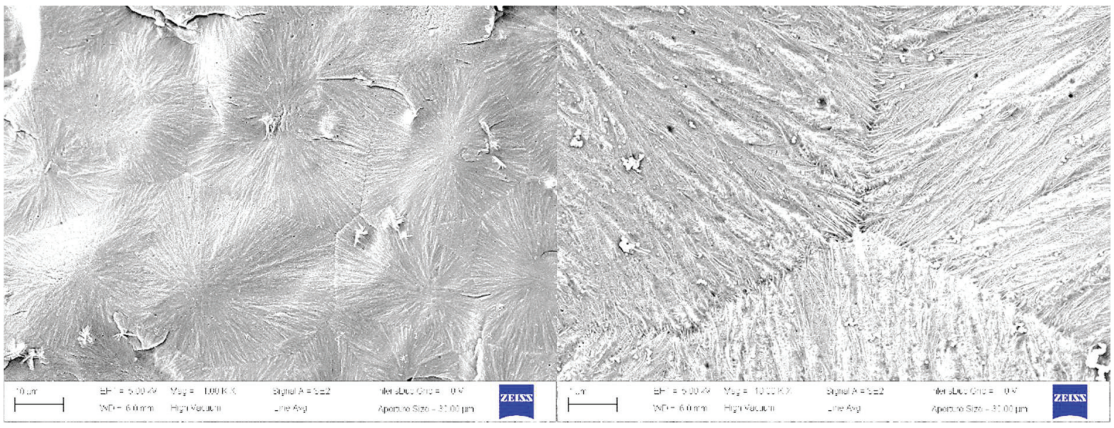

Figure 20. SEM pictures of neat PP

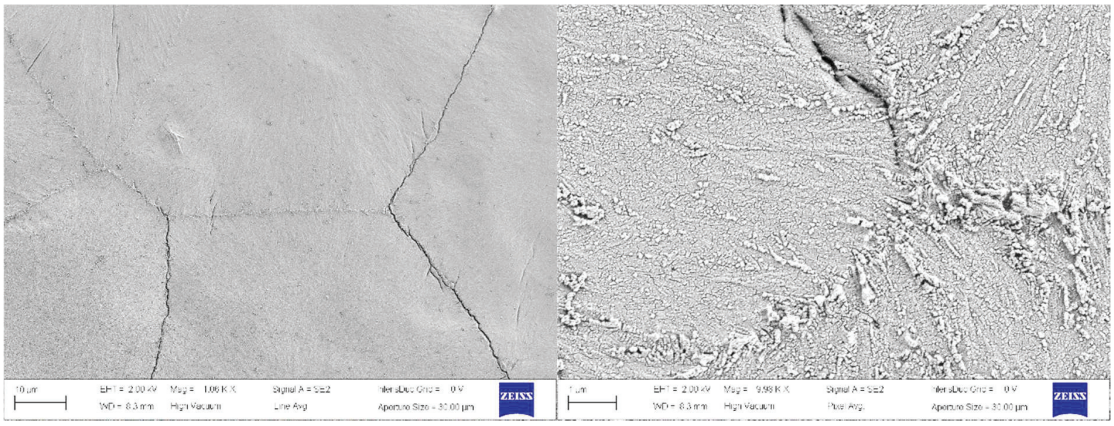

Figure 21. SEM pictures of PP + 30 wt% PE oligomer

SEM pictures of neat PP (Figure 20) revealed the spherulitic morphology of the polymer. The sample showed no discontinuity within the crystalline phase, with lamellae interweaving at the junction between spherulites. The PP/PE oligomer (70/30) blend (Figure 21) on the other hand exhibited an altered topography which was found to be very unlike the morphologies typically encountered in (immiscible) PP/PE blends, where the dispersed phase generally appears in the form of spherical domains.[21] Even though spherulites were still visible, the junctions between them seemed to form small aggregates of matter, and occasionally resulted in cracks.

Assuming from the previous experiments that the PE oligomer is driven out of the PP phase during the spherulitic growth, SEM pictures of blends with 30 wt% oligomer were expected to show large PE domains in the inter-spherulitic region. While it appeared that the presence of PE oligomer had affected the integrity of the junctions between PP spherulites, no conclusion could be drawn as to the exact location of the PE oligomer in the crystallized blend. Nevertheless, the brittleness of low molar mass polyethylenes in the solid state could explain the appearance of cracks if at least some of the PE oligomer is located in the inter-spherulitic region.

It is also worth noting that the fracture of PP/PE oligomer samples occasionally resulted in apparent spherulitic morphologies such as presented in Figure 22 for 90/10 and 70/30 blends.

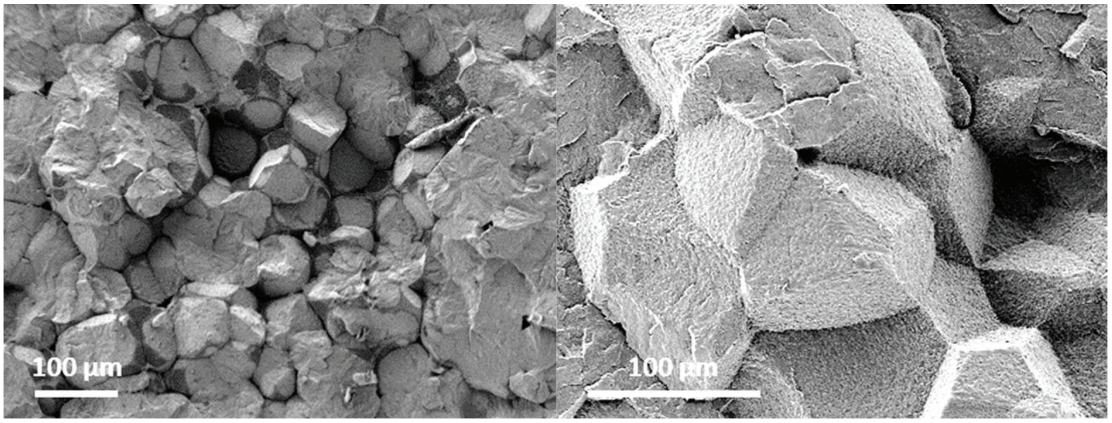

Figure 22. SEM pictures of PP/PE oligomer blends: 90/10 (left) and 70/30 (right)

SEM observations showed that most of the fracture had happened at the junctions between PP spherulites rather than inside them, suggesting that the presence of the PE oligomer had affected the integrity of the boundaries between PP spherulites. These fracture patterns have already been described in the literature in the case of the solid-liquid phase separation between PP and diluents such as mineral oil.[23,71] According to these studies, the fracture pattern (corresponding to the crystalline microstructure of the polymer) resulting from solid-liquid phase separation is dependent on the polymer/diluent combination, blend composition and cooling rate.

The presently observed morphologies may therefore be qualitatively explained by the solid-liquid phase separation arising from the inter-spherulitic segregation[62] of the PE oligomer during the growth of PP spherulites. The consequent weakening of the interface between PP spherulites was found to be strongly correlated with previous DSC and HSOM observations and may indeed be caused by the presence of the PE oligomer (which is very brittle in the solid state) in the inter-spherulitic region. Ultimately, the lack of cohesion in the crystalline microstructure induced by the presence of PE oligomer is likely to result in brittleness and probably lead to poor mechanical properties of the blends in the solid state.

4.3. Consequences of phase separation on mechanical properties in the solid state

In the absence of adequate compatibilization, blends of immiscible polymers usually result in poor mechanical properties. Many studies[15,18,20,22,72–74] have reported that the blending of different polyolefins resulted in either antagonistic or synergistic effects depending on the selected polymers, blend composition and processing conditions. Most studies[15,22,72,73] have reported that Young's modulus was merely a linear functions of the blend composition in miscible and immiscible blends of PP with various types of PE. However, it has also been found that this particular parameter was

dependent on the degree of crystallinity[75] in blends of linear polyethylenes with paraffinic waxes[18,76], where an increased wax concentration induced an increased crystallinity and resulted in an increase of Young's modulus. The yield stress parameter on the other hand was generally found to deviate (positively or negatively) from the linear additive law.

For the purpose of this study, the mechanical properties of HDPE/PE oligomer and PP/PE oligomer blends were measured by tensile testing, according to the protocol described in Chapter 2. The results showed that the yield stress σ_y and Young's modulus E of HDPE and PP systems remained unaffected by the presence of PE oligomer, at least up to 30 wt%, contrary to the strain at break ε_b values. The values of strain at break for HDPE/PE oligomer and PP/PE oligomer blends are presented in Figure 23.

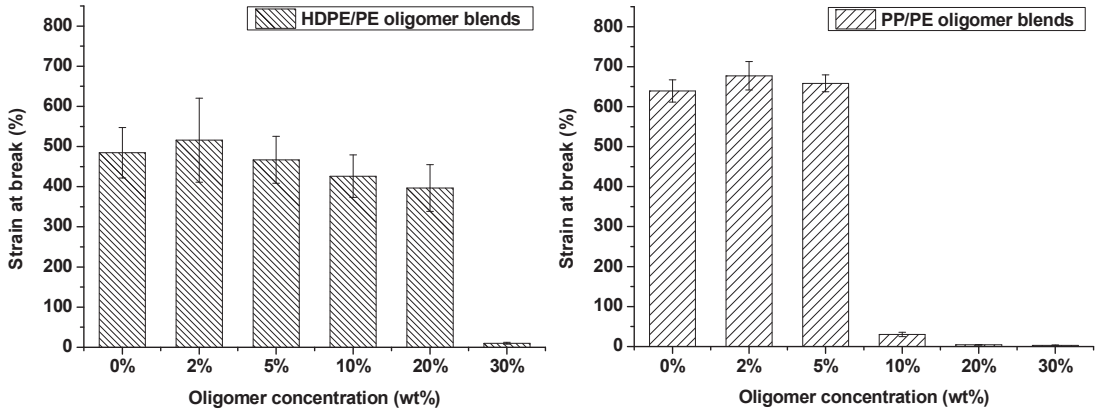

Figure 23. Elongation at break for HDPE/PE oligomer (left) and PP/PE oligomer (right) blends

It was found that the addition of PE oligomer did not significantly impact the elongation properties of HDPE for concentrations up to 20 wt%, and the elongation at break of PP was not significantly impacted either up to 5 wt%. However, it decreased dramatically with 30 wt% PE oligomer in HDPE and 10 wt% PE oligomer or more in PP, concentrations at which the samples underwent brittle fracture, which is typical of biphasic materials.[77]. The correlation of those results with previous observations suggests that poor mechanical properties arise from a weakening of the crystalline microstructure as a result of the presence of PE oligomer domains.

The degradation of the ultimate mechanical properties in the presence of low molar mass hydrocarbon compounds has been reported in other studies[18,78], where the decrease of stress and strain at break was closely related to the decreased number of tie chains[79,80] arising from the dilution of the polymer. However, in such systems where the miscibility appears to be limited by the composition of the blend, the presence of defects arising from phase separation may be the dominating mechanism explaining this biphasic material behaviour.

The results presented here as well as those from previous studies lead to the conclusion that an excessive concentration of low molar mass PE leads to the saturation of the polymer resin due to their limited miscibility in polyolefins such as HDPE and PP in the solid state, thus resulting in the

formation of a separate phase that accumulates in the inter-spherulitic region and becomes sufficiently sizeable to cause defects in the crystalline microstructure of the blend. It also appears that the concentration threshold from which the mechanical properties are altered is dependent on the type of polymer resin: around 5-10 wt% for PP and 20-30 wt% for HDPE.

It is also worth noting that in the case of PP systems, the degradation of the mechanical properties is concurrent with the presence of a second crystallization exotherm evidencing the separate crystallization of the PE oligomer at concentrations above 5 wt%. However, analogous observations on the DSC thermograms of HDPE systems would a priori lead to predict the degradation of mechanical properties to occur at concentrations between 10 wt% and 20 wt% of PE oligomer. This could be explained by the different microstructure of polyethylene in the presence of low molar mass hydrocarbon compounds ("leafy" morphology), as evidenced by Lloyd et al.[71], which may be more resistant to mechanical solicitations than that of polypropylene (spherulitic morphology).

5. Conclusion

This work was focused on the study of binary polyolefin blends with low viscosity ratios, where a low molar mass PE-COOH oligomer was incorporated in PP and HDPE. The rheological behaviour in the molten state as well as crystalline microstructure in the solid state were investigated along with the crystallization behaviour during the transition between those two states.

The functional PE oligomer was easily incorporated into the selected polyolefins thanks to rapid molecular diffusion and good miscibility in the molten state. However, the modelling of the viscoelastic behaviour of the blends using the Carreau-Yasuda equation suggested that the miscibility might be limited at high oligomer concentrations and that some kind of saturation phenomenon may occur, particularly in the case of PP-based systems which seemed to result in partially inhomogeneous melts above 5 wt% PE oligomer.

Additionally, it appeared clearly from DSC analyses as well as HSOM and SEM observations that HDPE/PE oligomer and PP/PE oligomer blends underwent solid-liquid phase separation upon cooling, leading to biphasic materials in the solid state. However, the hypothesis can be made that due to their close molecular structure, small amounts of PE oligomer chains are able to co-crystallize with HDPE, resulting in better compatibility in the solid state. On the other hand, the crystallization of PP/PE oligomer blends can be considered to lead to small amounts of PE oligomer chains being retained in the amorphous phase of PP as a result of the dilution phenomenon in the melt.

Further experimental work would be required to study the impact of the molar mass and/or viscosity of the PE oligomer on the viscoelastic and crystallization behaviours of such binary systems, as well as the resulting blend morphologies in the solid state. It would also be interesting to determine the solubility parameters of PE oligomers with various functional groups in order to compare them to that of the selected polyolefin resins and to correlate them with experimental results.

6. Bibliography

[1] B. Bitsch, Amélioration des thermoplastiques : Rôle du compoundeur, Techniques de l'ingénieur. Plastiques et composites. 2 (2003) AM3238.1-AM3238.14.

[2] G. Wypych, Handbook of Plasticizers, ChemTec Publishing, 2004.

[3] D.F. Cadogan, C.J. Howick, Plasticizers, in: Ullmann's Encyclopedia of Industrial Chemistry, American Cancer Society, 2000. doi:10.1002/14356007.a20_439.

[4] C.E. Scott, S.K. Joung, Viscosity ratio effects in the compounding of low viscosity, immiscible fluids into polymeric matrices, Polymer Engineering & Science. 36 (1996) 1666–1674. doi:10.1002/pen.10563.

[5] S.S. Kim, D.R. Lloyd, Thermodynamics of polymer/diluent systems for thermally induced phase separation: 2. Solid-liquid phase separation systems, Polymer. 33 (1992) 1036–1046. doi:10.1016/0032-3861(92)90020-W.

[6] P. Cassagnau, F. Fenouillot, Rheological study of mixing in molten polymers: 1-mixing of low viscous additives, Polymer. 45 (2004) 8019–8030. doi:10.1016/j.polymer.2004.09.027.

[7] H.E. Burch, C.E. Scott, Effect of viscosity ratio on structure evolution in miscible polymer blends, Polymer. 42 (2001) 7313–7325. doi:10.1016/S0032-3861(01)00240-3.

[8] C.E. Scott, C.W. Macosko, Model experiments concerning morphology development during the initial stages of polymer blending, Polymer Bulletin. 26 (1991) 341–348. doi:10.1007/BF00587979.

[9] C.E. Scott, C.W. Macosko, Morphology development during the initial stages of polymer-polymer blending, Polymer. 36 (1994) 461–470. doi:10.1016/0032-3861(95)91554-K.

[10] C. Joubert, P. Cassagnau, L. Choplin, A. Michel, Diffusion of plasticizer in elastomer probed by rheological analysis, Journal of Rheology. 46 (2002) 629–650. doi:10.1122/1.1470521.

[11] C. Bétron, V. Bounor-Legaré, C. Pinel, G. Scalabrino, L. Djakovitch, P. Cassagnau, Diffusion of modified vegetables oils in thermoplastic polymers, Materials Chemistry and Physics. 200 (2017) 107–120. doi:10.1016/j.matchemphys.2017.07.059.

[12] M. Ponsard-Fillette, C. Barrès, P. Cassagnau, Viscoelastic study of oil diffusion in molten PP and EPDM copolymer, Polymer. 46 (2005) 10256–10268. doi:10.1016/j.polymer.2005.08.015.

[13] R. Bella, P. Cassagnau, F. Fenouillot, L. Falk, C. Lacoste, Diffusion of liquids in molten polymers: Mutual diffusion coefficient dependence on liquid miscibility and polymer molar mass, Polymer. 47 (2006) 5080–5089. doi:10.1016/j.polymer.2006.05.024.

[14] J. Gimenez, P. Cassagnau, A. Michel, Bulk polymerization of ε-caprolactone: Rheological predictive laws, Journal of Rheology. 44 (2000) 527.

[15] T. Kyu, P. Vadhar, Cocrystallization and miscibility studies of blends of ultrahigh molecular weight polyethylene with conventional polyethylenes, Journal of Applied Polymer Science. 32 (1986) 5575–5584. doi:10.1002/app.1986.070320625.

[16] I. Krupa, A.S. Luyt, Thermal properties of polypropylene/wax blends, Thermochimica Acta. 372 (2001) 137–141. doi:10.1016/S0040-6031(01)00450-6.

[17] M.T. Conde Braña, U.W. Gedde, Morphology of binary blends of linear and branched polyethylene: composition and crystallization-temperature dependence, Polymer. 33 (1992) 3123–3136. doi:10.1016/0032-3861(92)90224-K.

[18] S.P. Hlangothi, I. Krupa, V. Djoković, A.S. Luyt, Thermal and mechanical properties of cross-linked and uncross-linked linear low-density polyethylene–wax blends, Polymer Degradation and Stability. 79 (2003) 53–59. doi:10.1016/S0141-3910(02)00238-0.

[19] E. Martuscelli, M. Pracella, M. Avella, R. Greco, G. Ragosta, Properties of polyethylene-polypropylene blends: Crystallization behavior, Makromol. Chem. 181 (1980) 957–967. doi:10.1002/macp.1980.021810417.

[20] R. Greco, G. Mucciariello, G. Ragosta, E. Martuscelli, Properties of polyethylene-polypropylene blends, J Mater Sci. 15 (1980) 845–853. doi:10.1007/BF00552093.

[21] J. Li, R.A. Shanks, R.H. Olley, G.R. Greenway, Miscibility and isothermal crystallisation of polypropylene in polyethylene melts, Polymer. 42 (2001) 7685–7694. doi:10.1016/S0032-3861(01)00248-8.

[22] P. Vadhar, T. Kyu, Effects of mixing on morphology, rheology, and mechanical properties of blends of ultra-high molecular weight polyethylene with linear low-density polyethylene, Polymer Engineering & Science. 27 (1987) 202–210. doi:10.1002/pen.760270305.

[23] R.A. Shanks, J. Li, L. Yu, Polypropylene–polyethylene blend morphology controlled by time–temperature–miscibility, Polymer. 41 (2000) 2133–2139. doi:10.1016/S0032-3861(99)00399-7.

[24] Y. Hong, G. Xin-shi, Preparation of polyethylene–paraffin compound as a form-stable solid-liquid phase change material, Solar Energy Materials and Solar Cells. 64 (2000) 37–44. doi:10.1016/S0927-0248(00)00041-6.

[25] H. Matsuyama, H. Okafuji, T. Maki, M. Teramoto, N. Kubota, Preparation of polyethylene hollow fiber membrane via thermally induced phase separation, Journal of Membrane Science. 223 (2003) 119–126. doi:10.1016/S0376-7388(03)00314-4.

[26] D. Li, W.B. Krantz, A.R. Greenberg, R.L. Sani, Membrane formation via thermally induced phase separation (TIPS): Model development and validation, Journal of Membrane Science. 279 (2006) 50–60. doi:10.1016/j.memsci.2005.11.036.

[27] S. Liu, C. Zhou, W. Yu, Phase separation and structure control in ultra-high molecular weight polyethylene microporous membrane, Journal of Membrane Science. 379 (2011) 268–278. doi:10.1016/j.memsci.2011.05.073.

[28] A. Akbari, R. Yegani, Study on the Impact of Polymer Concentration and Coagulation Bath Temperature on the Porosity of Polyethylene Membranes Fabricated Via TIPS Method, Journal of Membrane and Separation Technology. 1 (2012) 100–107.

[29] B. Zalba, J.M. Marín, L.F. Cabeza, H. Mehling, Review on thermal energy storage with phase change: materials, heat transfer analysis and applications, Applied Thermal Engineering. 23 (2003) 251–283. doi:10.1016/S1359-4311(02)00192-8.

[30] A. Sarı, Form-stable paraffin/high density polyethylene composites as solid–liquid phase change material for thermal energy storage: preparation and thermal properties, Energy Conversion and Management. 45 (2004) 2033–2042. doi:10.1016/j.enconman.2003.10.022.

[31] I. Krupa, G. Miková, A.S. Luyt, Polypropylene as a potential matrix for the creation of shape stabilized phase change materials, European Polymer Journal. 43 (2007) 895–907. doi:10.1016/j.eurpolymj.2006.12.019.

[32] C. Alkan, K. Kaya, A. Sarı, Preparation, Thermal Properties and Thermal Reliability of Form-Stable Paraffin/Polypropylene Composite for Thermal Energy Storage, J Polym Environ. 17 (2009) 254. doi:10.1007/s10924-009-0146-7.

[33] J.A. Molefi, A.S. Luyt, I. Krupa, Investigation of thermally conducting phase-change materials based on polyethylene/wax blends filled with copper particles, Journal of Applied Polymer Science. 116 (2010) 1766–1774. doi:10.1002/app.31653.

[34] F. Chen, M.P. Wolcott, Miscibility studies of paraffin/polyethylene blends as form-stable phase change materials, European Polymer Journal. 52 (2014) 44–52. doi:10.1016/j.eurpolymj.2013.09.027.

[35] C.W. Macosko, Morphology development and control in immiscible polymer blends, Macromol. Symp. 149 (2000) 171–184. doi:10.1002/1521-3900(200001)149:1<171::AID-MASY171>3.0.CO;2-8.
[36] J.-F. Agassant, P. Avenas, P.J. Carreau, B. Vergnes, M. Vincent, Polymer Processing, 2nd ed., Hanser, 2017.
[37] Z. Tadmor, C. Gogos, 2. The Balance Equations and Newtonian Fluid Dynamics, in: Principles of Polymer Processing, 2nd edition, Wiley, 2006: pp. 25–78.
[38] Z. Tadmor, C. Gogos, 11. Reactive Polymer Processing and Compounding, in: Principles of Polymer Processing, 2nd edition, Wiley, 2006: pp. 603–676.
[39] G. Marin, E. Menezes, V.R. Raju, W.W. Graessley, Propriétés viscoélastiques linéaires de solutions de polybutadiène en régime semi-dilué et concentré, Rheol Acta. 19 (1980) 462–476. doi:10.1007/BF01524019.
[40] P. Cassagnau, T. Nietsch, M. Bert, A. Michel, Reactive blending by in situ polymerization of the dispersed phase, Polymer. 40 (1999) 131–138. doi:10.1016/S0032-3861(98)00210-9.
[41] A. Ajji, L. Choplin, R.E. Prud'homme, Rheology and phase separation in polystyrene/poly(vinyl methyl ether) blends, Journal of Polymer Science Part B: Polymer Physics. 26 (1988) 2279–2289. doi:10.1002/polb.1988.090261108.
[42] L.A. Utracki, Viscoelastic behavior of polymer blends, Polymer Engineering & Science. 28 (1988) 1401–1404. doi:10.1002/pen.760282109.
[43] Y.J. Kim, G.S. Shin, I.T. Lee, B.K. Kim, Miscible and immiscible blends of ABS with PMMA. I. Morphology and rheology, Journal of Applied Polymer Science. 47 (1993) 295–304. doi:10.1002/app.1993.070470209.
[44] R. Li, W. Yu, C. Zhou, Phase Behavior and its Viscoelastic Responses of Poly(methyl methacrylate) and Poly(styrene-co-maleic anhydride) Blend Systems, Polym. Bull. 56 (2006) 455–466. doi:10.1007/s00289-005-0499-6.
[45] D. Chopra, M. Kontopoulou, D. Vlassopoulos, S.G. Hatzikiriakos, Effect of maleic anhydride content on the rheology and phase behavior of poly(styrene-co -maleic anhydride)/ poly(methyl methacrylate) blends, Rheol. Acta. 41 (2002) 10–24. doi:10.1007/s003970200001.
[46] K. Yasuda, R.C. Armstrong, R.E. Cohen, Shear flow properties of concentrated solutions of linear and star branched polystyrenes, Rheol Acta. 20 (1981) 163–178. doi:10.1007/BF01513059.
[47] M.H. Cohen, D. Turnbull, Molecular Transport in Liquids and Glasses, The Journal of Chemical Physics. 31 (1959) 1164–1169. doi:10.1063/1.1730566.
[48] J.S. Vrentas, C.M. Vrentas, Predictive methods for self-diffusion and mutual diffusion coefficients in polymer–solvent systems, European Polymer Journal. 34 (1998) 797–803. doi:10.1016/S0014-3057(97)00205-X.
[49] M.P. Tonge, R.G. Gilbert, Testing free volume theory for penetrant diffusion in rubbery polymers, Polymer. 42 (2001) 1393–1405. doi:10.1016/S0032-3861(00)00518-8.
[50] J.A. Dantzig, C.L. Tucker, Modeling in Materials Processing, Cambridge University Press, 2001.
[51] M.P. Molaba, D. Dudic, A.S. Luyt, Influence of the presence of medium-soft paraffin wax on the morphology and properties of iPP/silver nanocomposites (PDF Download Available), EXPRESS Polymer Letters. (2015). doi:10.3144/expresspolymlett.2015.82.
[52] F. Avalos, M.A. Lopez-Manchado, M. Arroyo, Crystallization kinetics of polypropylene: 1. Effect of small additions of low-density polyethylene, Polymer. 37 (1996) 5681–5688. doi:10.1016/S0032-3861(96)00429-6.
[53] D. Langhe, Chapter 9 - Fractionated Crystallization in Polymer Blends, in: S. Thomas, M. Arif P., E.B. Gowd, N. Kalarikkal (Eds.), Crystallization in Multiphase Polymer Systems, Elsevier, 2018: pp. 239–267. doi:10.1016/B978-0-12-809453-2.00009-8.

[54] H. Sun, K.B. Rhee, T. Kitano, S.I. Mah, High-density polyethylene (HDPE) hollow fiber membrane via thermally induced phase separation. I. Phase separation behaviors of HDPE–liquid paraffin (LP) blends and its influence on the morphology of the membrane, Journal of Applied Polymer Science. 73 (1999) 2135–2142. doi:10.1002/(SICI)1097-4628(19990912)73:11<2135::AID-APP9>3.0.CO;2-X.

[55] U. Gedde, 8. Crystallization Kinetics, in: Polymer Physics, Springer Netherlands, 1999: pp. 169–198. //www.springer.com/us/book/9780412590207 (accessed June 8, 2018).

[56] P.J. Flory, Principles of Polymer Chemistry, Cornell University Press, 1953.

[57] F.N. Andrade, R. Fulchiron, F. Collas, T.F.L. McKenna, Condensed Mode Cooling for Ethylene Polymerization: Part V—Reduction of the Crystallization Rate of HDPE in the Presence of Induced Condensing Agents, Macromolecular Chemistry and Physics. (2019). doi:10.1002/macp.201800563.

[58] B. Wunderlich, Table of Thermal Properties of Linear Macromolecules and Related Small Molecules—The ATHAS Data Bank, in: Thermal Analysis of Polymeric Materials, 1st ed., Springer, 2005: pp. 777–799.

[59] M.J. Hato, A.S. Luyt, Thermal fractionation and properties of different polyethylene/wax blends, Journal of Applied Polymer Science. 104 (2007) 2225–2236. doi:10.1002/app.25494.

[60] T.P. Gumede, A.S. Luyt, R.A. Pérez-Camargo, A. Iturrospe, A. Arbe, M. Zubitur, A. Mugica, A.J. Müller, Plasticization and cocrystallization in LLDPE/wax blends, Journal of Polymer Science Part B: Polymer Physics. 54 (2016) 1469–1482. doi:10.1002/polb.24039.

[61] B. Wunderlich, Thermal Analysis of Polymeric Materials, 1st ed., Springer, 2005.

[62] G. Groeninckx, M. Vanneste, V. Everaert, eds., 3. Crystallization, Morphological Structure, and Melting of Polymer Blends, in: Polymer Blends Handbook, Kluwer Academic Publishers, Dordrecht ; Boston, 2002: pp. 203–294.

[63] F. Toquet, L. Guy, B. Schlegel, P. Cassagnau, R. Fulchiron, Effect of the naphthenic oil and precipitated silica on the crystallization of ultrahigh-molecular-weight polyethylene, Polymer. 97 (2016) 63–68. doi:10.1016/j.polymer.2016.05.021.

[64] T. Nishi, T.T. Wang, Melting Point Depression and Kinetic Effects of Cooling on Crystallization in Poly(vinylidene fluoride)-Poly(methyl methacrylate) Mixtures, Macromolecules. 8 (1975) 909–915. doi:10.1021/ma60048a040.

[65] H. Frensch, B.-J. Jungnickel, Some novel crystallization kinetic peculiarities in finely dispersing polymer blends, Colloid & Polymer Sci. 267 (1989) 16–27. doi:10.1007/BF01410144.

[66] J. Varga, Supermolecular structure of isotactic polypropylene, J Mater Sci. 27 (1992) 2557–2579. doi:10.1007/BF00540671.

[67] E. Koscher, R. Fulchiron, Influence of shear on polypropylene crystallization: morphology development and kinetics, Polymer. 43 (2002) 6931–6942. doi:10.1016/S0032-3861(02)00628-6.

[68] A. Galeski, M. Pracella, E. Martuscelli, Polypropylene spherulite morphology and growth rate changes in blends with low-density polyethylene, Journal of Polymer Science: Polymer Physics Edition. 22 (1984) 739–747. doi:10.1002/pol.1984.180220415.

[69] Z. Bartczak, A. Gałeski, Changes in interface shape during crystallization in two-component polymer systems, Polymer. 27 (1986) 544–548. doi:10.1016/0032-3861(86)90240-5.

[70] J.W. Teh, A. Rudin, J.C. Keung, A review of polyethylene–polypropylene blends and their compatibilization, Adv. Polym. Technol. 13 (1994) 1–23. doi:10.1002/adv.1994.060130101.

[71] D.R. Lloyd, K.E. Kinzer, H.S. Tseng, Microporous membrane formation via thermally induced phase separation. I. Solid-liquid phase separation, Journal of Membrane Science. 52 (1990) 239–261. doi:10.1016/S0376-7388(00)85130-3.

[72] R.E. Robertson, D.R. Paul, Stress–strain behavior of polyolefin blends, J. Appl. Polym. Sci. 17 (1973) 2579–2595. doi:10.1002/app.1973.070170823.
[73] M.M. Dumoulin, P.J. Carreau, L.A. Utracki, Rheological properties of linear low density polyethylene/polypropylene blends. Part 2: Solid state behavior, Polym Eng Sci. 27 (1987) 1627–1633. doi:10.1002/pen.760272109.
[74] K. Cho, B.H. Lee, K.-M. Hwang, H. Lee, S. Choe, Rheological and mechanical properties in polyethylene blends, Polymer Engineering & Science. 38 (1998) 1969–1975. doi:10.1002/pen.10366.
[75] S. Humbert, O. Lame, R. Séguéla, G. Vigier, A re-examination of the elastic modulus dependence on crystallinity in semi-crystalline polymers, Polymer. 52 (2011) 4899–4909. doi:10.1016/j.polymer.2011.07.060.
[76] I. Krupa, A.S. Luyt, Mechanical properties of uncrosslinked and crosslinked linear low-density polyethylene/wax blends, J. Appl. Polym. Sci. 81 (2000) 973–980. doi:10.1002/app.1519.
[77] P. Galli, J.C. Haylock, T. Simonazzi, Manufacturing and properties of polypropylene copolymers, in: Polypropylene - Structure, Blends and Composites, Springer, Dordrecht, 1995: pp. 1–24. doi:10.1007/978-94-011-0521-7_3.
[78] V. Djoković, T.N. Mtshali, A.S. Luyt, The influence of wax content on the physical properties of low-density polyethylene–wax blends, Polymer International. 52 (2003) 999–1004. doi:10.1002/pi.1180.
[79] A. Lustiger, R.L. Markham, Importance of tie molecules in preventing polyethylene fracture under long-term loading conditions, Polymer. 24 (1983) 1647–1654. doi:10.1016/0032-3861(83)90187-8.
[80] M. Hedenqvist, M.T. Conde Braña, U.W. Gedde, J. Martinez-Salazar, Fracture of binary blends of linear and branched polyethylene, Polymer. 37 (1996) 5123–5129. doi:10.1016/0032-3861(96)00237-6.

Chapter 4 – Study of a reactive system involving functional PE oligomers as a new compatibilization strategy for immiscible HDPE/PA6 blends

Table of contents

1. Introduction

Polyethylene and polyamide are some of the most widely spread thermoplastic polymers, with a large variety of industrial applications.[1–3] The blending of these polymers is primarily motivated by combination of the good technical properties of polyamide with the cost-effectiveness and moisture resistance of polyethylene.[4] However, polyethylene and polyamide have significantly different crystalline structures and polarities due to their very different chemical nature, thus resulting in highly incompatible blends usually exhibiting coarse biphasic morphologies.[5,6] The compatibilization of such immiscible systems has therefore been the subject of a considerable number of investigations, with the aim of achieving various controlled morphologies depending on the targeted applications.

An adequate compatibilization of two incompatible polymers should promote the reduction of interfacial tension between the two phases and prevent coalescence, resulting in the formation of a stable morphology as well as a narrow domain size distribution.[7] The addition of various functional polymers as coupling agents in immiscible polymer blends has been studied extensively as an effective way to achieve reactive compatibilization.[8,9] However, the use of high molar mass compatibilizer precursors may result in poor compatibilization as a result of their low chain mobility and potential inability to migrate to the interface. As mentioned in Chapter 1, the issue of molar mass was overcome by Todd et al.[10] and O'Brien et al.[11] by introducing low molar mass compatibilizer precursors to form a high molar mass multi-block copolymer compatibilizer in situ. However, no such example has been reported in the case of polyethylene/polyamide compatibilization.

A very well-known and well-documented strategy for the compatibilization of polyethylene/polyamide blends is the use of maleic anhydride-grafted polyethylenes (PE-g-MA), which are miscible in polyethylene and react with the amine end-groups of polyamide.[12–14] Additionally, low molar mass polyolefin oligomers grafted with maleic anhydride groups have been used successfully by several authors as a means to obtain stable morphologies in polyethylene/polyamide blends.[15,16] On the other hand, multi-functional oligomers such as polyetheramines have generated interest as efficient crosslinkers[17,18] as well as for the chemical modification of various polymers, including polyamides, resulting in remarkable viscoelastic and mechanical properties.[19–21]

The primary objective of the present work was therefore to compatibilize immiscible HDPE/PA6 blends using a reactive system involving (i) a polyethylene oligomer grafted with maleic anhydride groups (Ceramer) as well as (ii) a tri-functional polyetheramine oligomer (Jeffamine T). The experimental work reported in this chapter is divided into four sections. The first part (Section 2) is dedicated to the characterization of Ceramer/Jeffamine T systems in terms of viscoelastic and mechanical behaviour. Then (Section 3), such a reactive system is investigated as a potential route towards the compatibilization of immiscible HDPE/PA6 blends and compared to the sole use of Ceramer 1608 as well as to the use of a high molar mass PE-g-MA (Exxelor) which is commonly used as a compatibilizer precursor. Finally, the last two sections are focused on the study of the physical and chemical interactions between the

selected functional oligomers and PA6 (Section 4) and HDPE (Section 5) homopolymers, as well as on the resulting viscoelastic and mechanical properties of those blends.

2. Study of Ceramer/Jeffamine reactive systems

The compatibilization strategy investigated in this chapter involves a reactive system based on two types of functional oligomers. The first type consists of polyethylene oligomers grafted with maleic anhydride derivatives (Ceramer) and the other is a tri-functional polyetheramine oligomer (Jeffamine T). The results presented in this first experimental section are focused on the characterization of Ceramer/Jeffamine T compounds in terms of viscoelastic and mechanical behaviour in order to determine their chemical structure.

2.1. Reaction between Ceramer and Jeffamine T oligomers

The amount of functional groups in the oligomers was determined from the acid and saponification values (in the case of Ceramer) or from the amine hydrogen equivalent weight (in the case of Jeffamine T) found in the technical datasheets provided with the products. The calculated values are summarized in Table 1. In the last column, the amount of functional groups is expressed in moles of functional groups per mole of oligomer, which corresponds to the mean number of functional groups per oligomer chain. Additional information on the chemical structure and physical properties of those functional oligomers can be found in Chapter 2.

Table 1. Amount of functional groups in Ceramer and Jeffamine T oligomers

Oligomer	Type of functional group	Amount of functional groups (mmol/g)	Amount of functional groups (mol/mol)
Ceramer 67	Maleic anhydride	0.7	0.5
Ceramer 1608	Maleic anhydride	1.9	1.5
Jeffamine T-403	Amine	6.8	3.0

The compositions of Ceramer/Jeffamine T mixtures (see Table 2) were adjusted accordingly, in order achieve quasi-stoichiometric ratios of amine and maleic anhydride functional groups. For simplification purposes, these oligomers may be referred to as C67 (Ceramer 67), C1608 (Ceramer 1608) and T403 (Jeffamine T-403) herein after.

Table 2. Composition of Ceramer 67/Jeffamine T-403 and Ceramer 1608/Jeffamine T-403 mixtures

Ceramer oligomer	Mixture composition (Ceramer/Jeffamine T-403)
Ceramer 67	90/10
Ceramer 1608	75/25

The reactive systems were first studied by directly mixing the two types of oligomers in a counter-rotating twin-screw micro-compounder (Haake MiniLab). This compounding equipment has a capacity of 7 cm^3 and integrates a backflow channel to allow recirculation. Ceramer pellets were first introduced at a temperature of 130 °C and a mixing speed of 50 rpm under recirculation. Jeffamine was then injected

and the system was mixed for 15 min under recirculation. The mixture was finally recovered from the micro-compounder in order to be analysed.

A reaction mechanism is proposed in Figure 1. It involves the reaction between the maleic anhydride groups of the Ceramer and the amine groups of the Jeffamine T, yielding a compound characterized by a cyclic imide moiety along with water as a by-product.

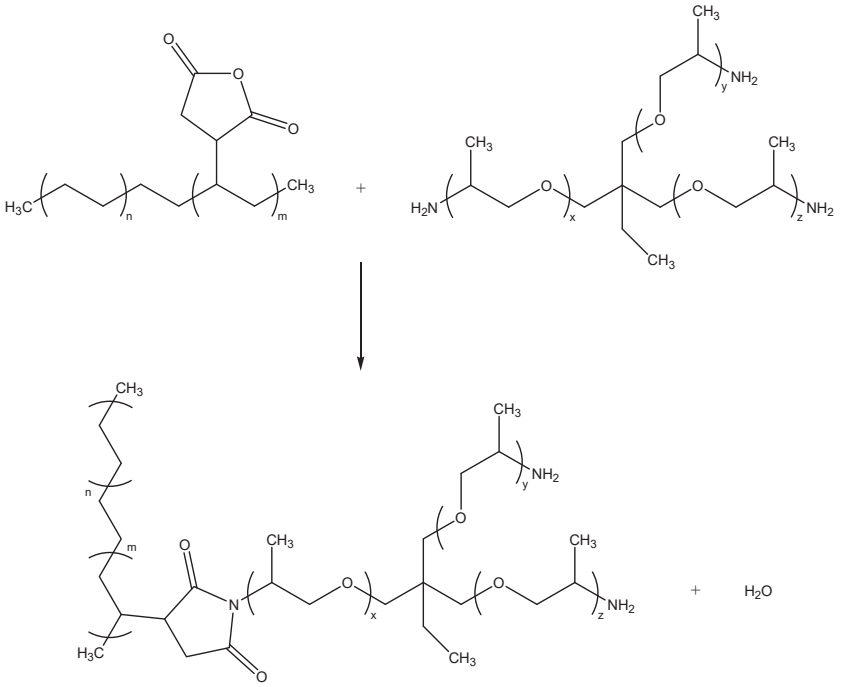

Figure 1. Reaction between Ceramer and Jeffamine T oligomers

As explained in Chapter 2, Ceramer oligomers are actually obtained from the grafting of various maleic anhydride derivatives onto a polyethylene backbone, according to the information provided by the manufacturer. Those derivatives include: maleic anhydride, mono-isopropyl maleate, di-isopropyl maleate and 2-butenedioic acid. The reaction between the amine groups of Jeffamine T and such derivatives is very similar to the one illustrated in Figure 1, and it can be noted that the reaction between isopropyl maleate groups and amine groups generate isopropanol as a by-product.

2.2. Characterization of Ceramer/Jeffamine compounds

The samples produced by micro-compounding were characterized by means of differential scanning calorimetry (DSC) as well as rheometry. The experimental protocols are similar to those described in Chapter 2 and are further detailed in the following paragraphs.

DSC analyses were carried out in a temperature range of -70 to 120 °C at a scanning rate of 10 °C/min. Considering that polyethylene and Ceramer oligomers have similar structures, the heat of fusion of purely crystalline polyethylene (ΔH_f^0 = 293 J/g[22]) was used to determine the overall degree of

crystallinity in all samples. The crystallization temperature (T_c), melting temperature (T_m), melting enthalpy (ΔH_f) and degree of crystallinity (X_m) of each sample are summarized in Table 3 (Section 2.2.1) and Table 4 (Section 2.2.2).

Viscosity measurements (frequency sweep oscillatory shear tests in parallel plate geometry) were performed at a temperature of 130 °C and a set strain of ε = 500 % for C67 and C67/T403, ε = 100 % for C1608 and ε = 0.1 % in the case of C1608/T403.

2.2.1. Ceramer 67/Jeffamine T-403

After micro-compounding, the C67/T403 sample was recovered in the form of a low viscosity liquid at 130 °C and quickly turned into a waxy solid at room temperature, similarly to unreacted Ceramer 67 and Ceramer 1608 oligomers.

DSC measurements of the samples (see Table 3) showed that the crystallization and melting temperatures of Ceramer 67 remained unaffected by the reaction with Jeffamine T-403, and that the degree of crystallinity was only slightly decreased.

Table 3. DSC analysis of the Ceramer 67/Jeffamine T-403 compound

Sample	Tc (°C)	Tm (°C)	ΔHf (J/g)	Xm (%)
T403	-	-	0	0
C67	84	89	246	84
C67/T403	85	89	232	79

Rheological analysis of the sample at 130 °C (see Figure 2) showed that the viscosity of Ceramer 67 had increased from 0.02 Pa.s to 0.06 Pa.s with the addition of Jeffamine T-403, while its rheological behaviour was still similar to that of a Newtonian liquid.

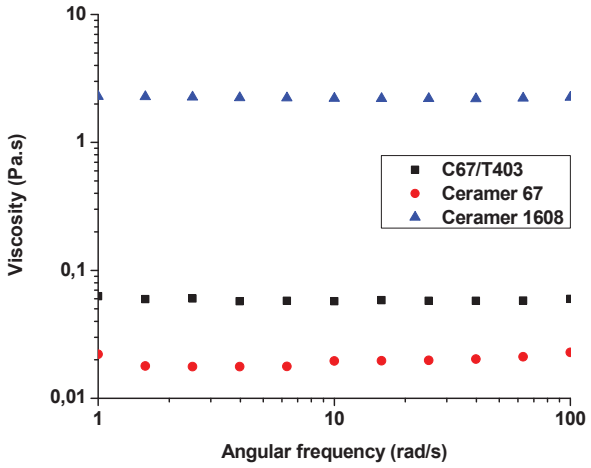

Figure 2. Viscosity of the C67/T403 compound compared to that of Ceramer 67 and Ceramer 1608 oligomers

This increase in viscosity can be attributed to an increase of the average molar mass of Ceramer 67 as a result of the reaction with Jeffamine T-403, according the reaction mechanism proposed in Figure 1.

Considering the low maleic anhydride content of Ceramer 67, the DSC and rheometry results suggest that the addition of Jeffamine T-403 does not significantly alter the molecular arrangement of Ceramer 67 chains. The reaction with Jeffamine T-403 can therefore be considered to only result in an increase of the molar mass through the grafting of one, two or three polyethylene oligomer chains onto the tri-functional polyetheramine.

2.2.2. Ceramer 1608/Jeffamine T-403

The C1608/T403 sample recovered from micro-compounding was found to be in the form of a rubbery and translucent solid at 130 °C which became brittle at room temperature. A visual comparison of C1608/T403 and C67/T403 compounds is provided in Figure 3.

Figure 3. Photographs of C1608/T403 (left) and C67/T403 (right) compounds in the form of 1 mm-thick discs

DSC analyses (see Table 4) showed that the main melting and crystallization peaks of Ceramer 1608 had disappeared with the incorporation of Jeffamine T-403, leaving only a very small endotherm and exotherm. The measured degree of crystallinity was consequently found to be severely decreased, indicating that Ceramer 1608 had become mainly amorphous with the addition of Jeffamine T-403.

Table 4. DSC analysis of the Ceramer 1608/Jeffamine T-403 compound

Sample	Tc (°C)	Tm (°C)	ΔHf (J/g)	Xm (%)
T403	-	-	0	0
C1608	53	69	83	28
C1608/T403	32	62	16	6

Rheological measurements at 130 °C showed that the C1608/T403 sample behaved like a solid, while the rheological behaviour of Ceramer 1608 was that of a Newtonian liquid with η_0 = 2 Pa.s (see Figure 2). Consequently, a dynamical mechanical analysis (DMA) was performed on the C1608/T403 sample, following the protocol described in Chapter 2 (temperature sweep oscillatory shear stress in rectangular torsion geometry between -60 and 130 °C at a set strain of ε = 0.05 % and a set frequency of f = 1 Hz). A rupture of the test specimen was observed around 130-135 °C. The results of the DMA and rheological measurements are shown in Figure 4.

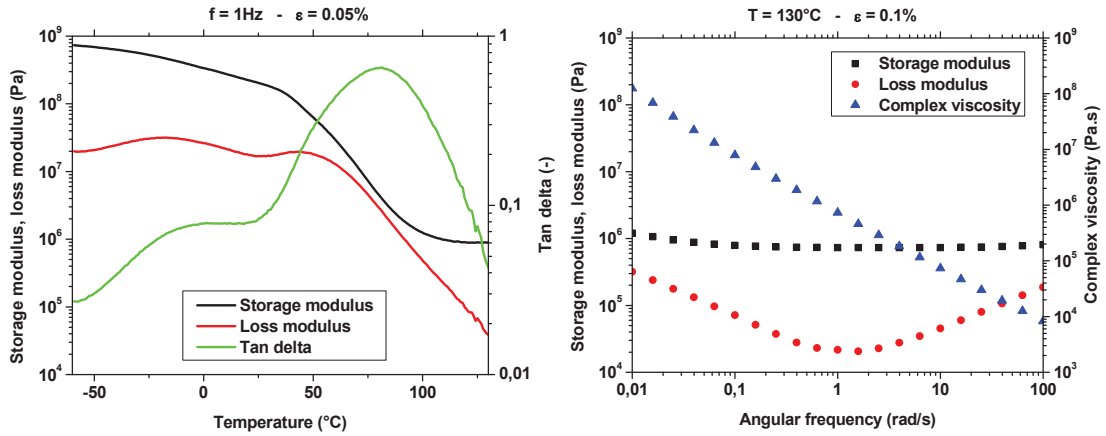

Figure 4. Characterization of the C1608/T403 compound by temperature sweep oscillatory shear test in rectangular torsion geometry (right) and frequency sweep oscillatory shear test in parallel plate geometry (left)

It was observed from the frequency sweep test that the storage modulus of the C1608/T403 sample is higher than the loss modulus and that the viscosity curve exhibits no plateau at low frequencies, which are usually typical characteristics of crosslinked rubbers.[23] It can also be noted that the measured values of storage modulus are similar to that of polymers such as synthetic rubbers. DMA on the sample showed a main transition at $T_\alpha \equiv T_g$ = +81 °C, which is much higher than that of the neat oligomers: the glass transition temperature of Jeffamine T-403 was measured at -71 °C by DSC and the glass transition temperature of Ceramer oligomers can be considered to be similar to that of polyethylene, which is around -110 °C.

These results therefore suggest that the reaction between Ceramer 1608 and Jeffamine T-403 may have yielded a crosslinked network, due to the higher number of maleic anhydride groups on the polyethylene oligomer. It is worth noting that the formation of a Ceramer-Jeffamine T network is only possible is the Ceramer oligomer is at least di-functional, provided that enough functional groups from both oligomers react effectively. The crosslink density of such a system can be estimated from the rheological measurements presented in Figure 4 by using the theory of ideal crosslinked rubber networks, which is well described in the work of Ferry.[23] The number-average molar mass in between cross-links (also called "critical molar mass") $\overline{M_c}$ is thus defined by the following equation:

$$\overline{M_c} = \frac{\rho . R . T}{G_e}$$

where ρ is the density of the material, R is the ideal gas constant (R = 8.314 J/mol/K), T is the temperature and G_e is the elastic modulus of the material. The density of the Ceramer1608/Jeffamine T-403 compound was approximated to that of the Ceramer 1608 (i.e. ρ ≈ 960 kg/m^3) and the mean value of storage modulus (measured by rheometry at 130 °C) was 8.10^5 Pa. Hence, the calculated critical molar mass value was approximately $\overline{M_c}$ ≈ 4000 g/mol.

In the case of a di-functional PE-g-MA oligomer, in stoichiometric conditions (i.e. a mixture composition of 78/22) and with a conversion rate of 100 %, the critical molar mass of the network would be defined by $\overline{M_c} = \frac{2}{3}\overline{M_{T403}} + \overline{M_{C1608}}$, thus giving an approximate value of $\overline{M_c} \approx 1000$ g/mol. Considering the quasi-stoichiometric ratio of amine and maleic anhydride groups in the present case, the calculated value of critical molar mass suggests an effective reaction between Ceramer 1608 and Jeffamine T-403 yielding a crosslinked network. A schematic representation of the network formed from the reaction between the two oligomers (a di-functional PE-g-MA and a tri-functional polyetheramine) is proposed in Figure 5.

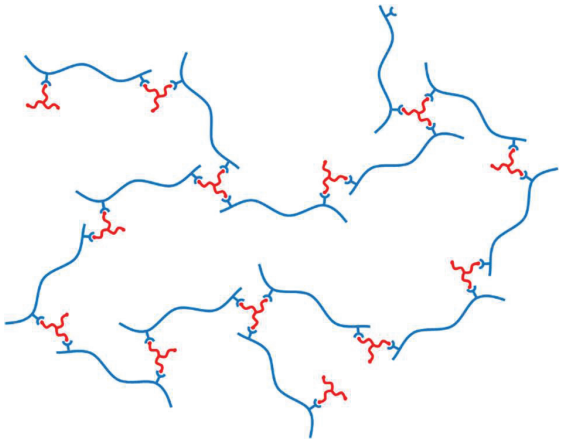

Figure 5. Proposed representation of the network formed from the reaction between Ceramer 1608 and Jeffamine T-403

The structure of such a network depends on the molar mass and number of functional groups of each reactive oligomer. In the present case, the number of maleic anhydride groups on Ceramer 1608 chains is not known exactly and may vary from one chain to another. Calculations (see Table 1) indicate that each Ceramer 1608 chain should bear 1-2 maleic anhydride groups, compared to 0-1 grafts in the case of Ceramer 67.

Finally, it is worth noting that several other Ceramer and Jeffamine oligomers are currently commercially available, meaning that the properties of such crosslinked compounds could be easily adjusted by tuning the critical molar mass of the network.

3. Compatibilization of a HDPE/PA6 blend using a C1608/T403 reactive system

In this part of the study, a reactive system involving two functional oligomers as compatibilizer precursors was investigated in order to compatibilize HDPE/PA6 blends produced by extrusion. The selected oligomers were Ceramer 1608 and Jeffamine T-403, whose interactions with HDPE and PA6 homopolymers are investigated separately in Sections 4 and 5. The compatibilizing efficiency of this reactive system was compared to that of a high molar mass PE-g-MA compatibilizer precursor commonly used in the industry: Exxelor PE 1040. HDPE/PA6 blends containing various amounts of PE-g-MA and polyetheramine additives were therefore tested in terms of morphology, viscoelastic behaviour and mechanical properties, which are good indicators of compatibilization efficiency.

3.1. Blend composition and processing

The molar mass and amount of functional groups of the selected compatibilizer precursors are summarized in Table 5.

Table 5. Properties of the selected compatibilizer precursors

Compatibilizer precursor	Molar mass (g/mol)	Amount of functional groups (mmol/g)	Amount of functional groups (mol/mol)
Jeffamine T-403	400	6.8	3.0
Ceramer 1608	800	1.9	1.5
Exxelor PE 1040	17 000	0.1	1.7

The blends investigated in this part of the study were based on a 70/30 blend of polyethylene and polyamide. Thus, for each blend the weight fraction of PA6 was set at 30 wt% while the remaining 70 wt% consisted of HDPE and compatibilizer precursors.

The blends were prepared using a co-rotating twin-screw extruder (L/D = 60) at a temperature of 240 °C and a flow rate of 3 kg/h. Following the protocol described in Chapter 2, dry-blends of neat HDPE and PE-g-MA were fed through the main hopper into the first block of the extruder, while PA6 was introduced through a side feeder at block n°4 (L/D = 20). In the case of the HDPE/PA6/C1608/T403 blend, Jeffamine T-403 was added by injection at block n°4.

Considering the difficulties associated with the injection of Jeffamine T-403 at very low flow rates, the weight fraction of Jeffamine T-403 was set at 1 wt%. The weight fraction of Ceramer 1608 was consequently set at 4 wt% to account for the amount of amine functional groups in the blend. The two other blends without Jeffamine T-403 were used as control samples. The compositions of the blends are summarized in Table 6.

Table 6. Compositions of the HDPE/PA6 blends with various compatibilizer precursors

Compatibilizer precursor	Blend composition (HDPE/PA6/PE-g-MA*/T403)
-	70/30/0/0
Ceramer 1608 + Jeffamine T-403	65/30/4/1
Ceramer 1608	66/30/4/0
Exxelor PE 1040	60/30/10/0

**PE-g-MA = Ceramer 1608 (C1608) or Exxelor PE 1040 (E1040)*

It is worth noting that several blending methods were tested in an attempt to optimize the extrusion process through the preparation of various polymer/oligomer premixes. However, it was found that such variations of the extrusion process had no significant influence on the properties of HDPE/PA6/C1608/T403 blends, hence the protocol described above was used. Those extrusion trials are reported in Appendix C.

3.2. Evaluation of compatibilization efficiency

The viscoelastic behaviour of each blend was characterized by rheometry at 240 °C, according the protocol described in Chapter 2. The corresponding storage modulus curves are displayed in Figure 6. It is worth noting that, as mentioned in the experimental section (see Chapter 2), frequency sweeps were carried out from high to low angular frequencies, thus viscoelastic properties measured at low angular frequencies (ω = 0.1-0.01 rad/s) correspond to a residence time of 30-45 min within the rheometer. Variations of storage and loss modulus values measured at low frequencies may therefore be due to further evolution of the system during rheological measurements in the case of reactive blends.

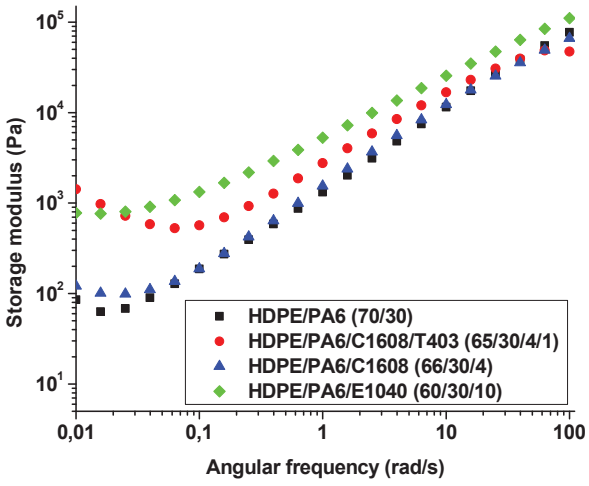

Figure 6. Storage modulus curves for HDPE/PA6 blends with various types and amounts of compatibilizer precursors

The viscoelastic behaviour of HDPE/PA6 blends was not significantly affected by the incorporation of Ceramer 1608. Both HDPE/PA6 (70/30) and HDPE/PA6/C1608 (66/30/4) blends were characterized by a storage modulus lower than the loss modulus, thus exhibiting a behaviour similar to that of the molten

homopolymers. The increase in storage modulus at low frequencies was found to be consistent with observations made by other authors in the case of uncompatibilized blends where polyamide is dispersed in a continuous polyethylene phase.[24] The 65/30/4/1 blend (containing both Ceramer 1608 and Jeffamine T-403) presented a similar behaviour at high frequencies but exhibited a more pronounced increase in storage and loss modulus at low frequencies.

On the other hand, the presence of 10 wt% Exxelor PE 1040 resulted in a significant increase in viscosity with similar storage modulus and loss modulus values, indicating a viscoelastic behaviour similar to that of a gel, which is more commonly encountered in the case of branched or even crosslinked polymers.[25–27] This behaviour can be attributed to the strong chemical interactions of the high molar mass PE-g-MA with PA6 as well as molecular entanglement with HDPE, therefore suggesting the possible formation of a three-dimensional network.

The morphology of these blends was subsequently determined by SEM and compared to that of the uncompatibilized HDPE/PA6 blend. The corresponding SEM pictures are shown in Figure 7.

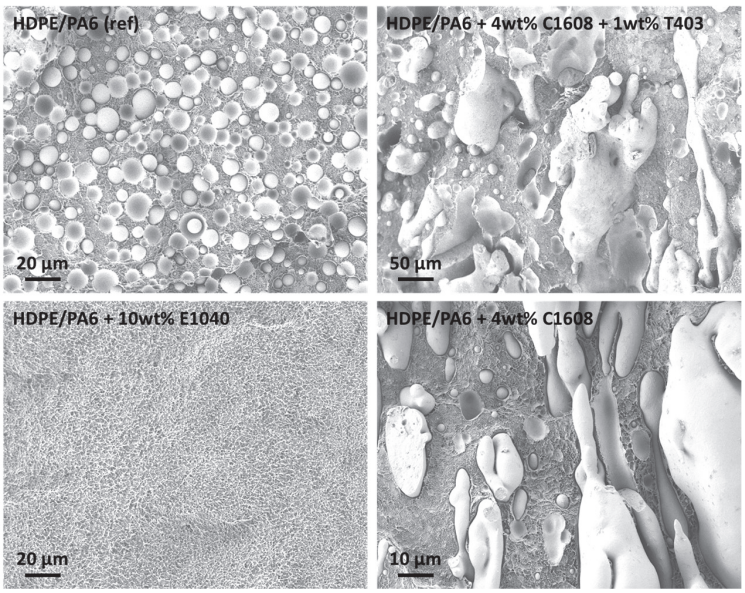

Figure 7. SEM pictures of HDPE/PA6 blends with various types and amounts of compatibilizer precursors: Ceramer 1608 + Jeffamine T-403 (top right), Ceramer 1608 (bottom right) and Exxelor PE 1040 (bottom left)

The uncompatibilized HDPE/PA6 blend exhibited a dispersed morphology (spherical domains of PA6 dispersed in a continuous HDPE phase) with a typical domain diameter of 1-10 µm and poor interfacial adhesion between the two phases. These observations are in accordance with the morphologies commonly encountered in such immiscible systems.[28,29]

The blends with Ceramer 1608 (66/30/4/0) or both Ceramer 1608 and Jeffamine T-403 (65/30/4/1) exhibited two types of coexisting morphologies: (i) spherical domains of PA6 with diameters ranging from roughly 1 µm to 10 µm (i.e. dimensions similar to those observed in the uncompatibilized

HDPE/PA6 blend) along with (ii) elongated domains of PA6 extending over lengths ranging from several micrometres to several millimetres. The coexistence of spherical and elongated domains of PA6 suggests that low molar mass compatibilizer precursors tend to favour droplet coalescence instead of hindering it, thus resulting in flattened interfaces, as observed in a previous study.[16] Furthermore, the interfacial adhesion between HDPE and PA6 was observed to be quite poor with many occurrences of debonding, demonstrating an ineffective compatibilization in both cases. The Palierne model could be useful to quantify variations of the interfacial tension between HDPE-rich and PA6-rich phases. However, it would be practically impossible to apply here because of the presence of elongated domains in HDPE/PA6/C1608 and HDPE/PA6/C1608/T403 blends.

Lastly, the incorporation of 10 wt% Exxelor PE 1040 resulted in a macroscopically homogeneous morphology, indicating an efficient compatibilization of the HDPE/PA6 blend.

The mechanical properties of the blends were determined by tensile testing (according to the protocol described in Chapter 2) in order to supplement SEM observations on the compatibilization efficiency of the investigated compatibilizer precursors. The measured values of Young's modulus (E), yield stress (σ_y) and strain at break (ε_b) are presented in Table 7. A graphical comparison of those blends in terms of yield stress and strain at break is proposed in Figure 8.

Table 7. Mechanical properties of HDPE/PA6 blends with various types and amounts of compatibilizer precursors

Blend	E (MPa)	σ_y (MPa)	ε_b (%)
HDPE/PA6 (ref)	770 ± 30	28 ± 1	10 ± 0
4wt% C1608 + 1wt% T403	660 ± 90	22 ± 0	10 ± 0
4wt% C1608	710 ± 30	26 ± 1	10 ± 0
10wt% E1040	780 ± 60	33 ± 0	50 ± 10

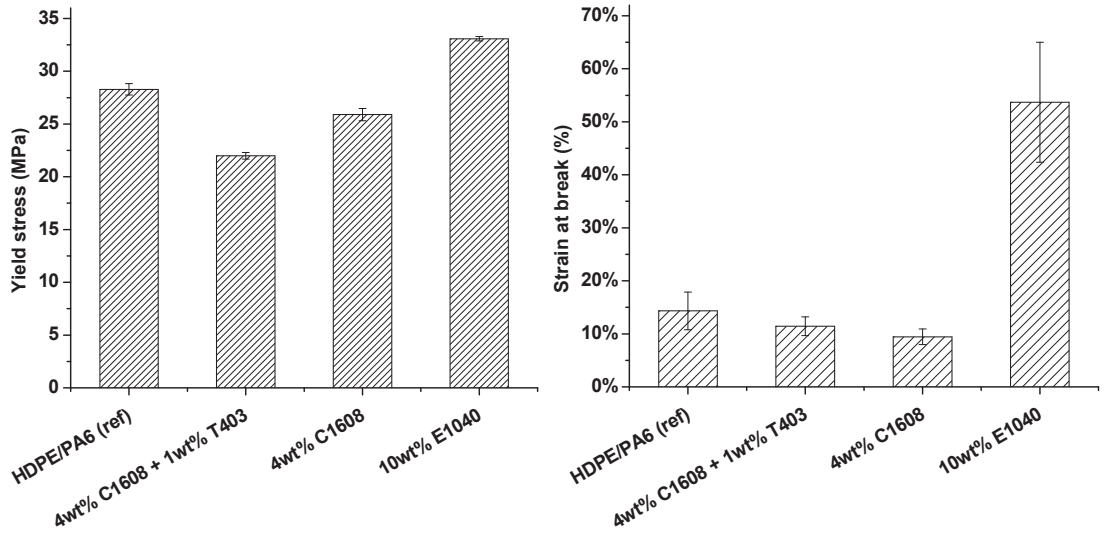

Figure 8. Yield stress (left) and strain at break (right) for HDPE/PA6 blends with various types and amounts of compatibilizer precursors

The typical stress-strain curves (recorded by tensile testing at 30 mm/min) corresponding to each blend are displayed in Figure 9 to further illustrate the mechanical behaviour of HDPE/PA6 blends in the presence of Ceramer 1608 (C1608), Jeffamine T-403 (T403) and Exxelor PE 1040 (E1040).

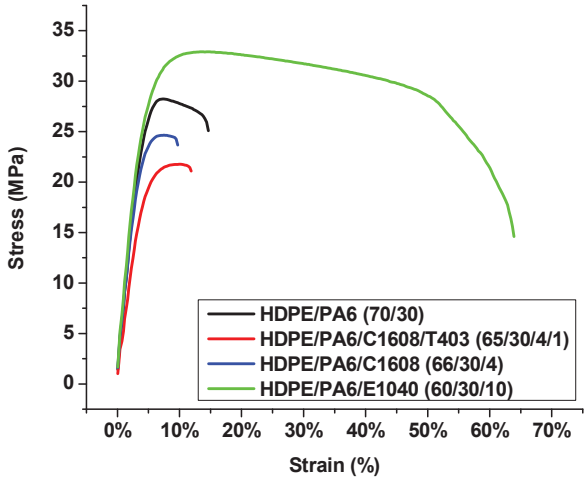

Figure 9. Typical stress-strain curves for HDPE/PA6 blends with various types and amounts of compatibilizer precursors

No significant variation of Young's modulus was observed with any of the PE-g-MA compatibilizer precursors, although the presence of both Ceramer 1608 and Jeffamine T-403 resulted in slightly lower values. The low values of strain at break measured in the case of the first three blends are indicative of biphasic materials, which is typical of uncompatibilized blends of immiscible polymers.[30] On the contrary, the use of Exxelor PE 1040 as a compatibilizer precursor resulted in a significant increase in strain at break as well as a slight increase in yield stress, suggesting an improvement of the interfacial adhesion between polyethylene and polyamide phases as a result of effective compatibilization.[12,31,32]

These results are consistent with previous rheological measurements and SEM observations showing that the incorporation of a high molar mass PE-g-MA leads to strong interactions between HDPE and PA6, while the use of a PE-g-MA oligomer or a reactive PE-g-MA/polyetheramine system results in unstable dispersed morphologies with poor interfacial adhesion between HDPE and PA6 phases. Considering the reactivity of such functional oligomers towards polyamide (see Section 4), their poor compatibilizing ability can therefore be attributed to a lack of interaction with the polyethylene phase, compared to a higher molar mass compatibilizer precursor.

4. Chemical interactions between Ceramer and Jeffamine functional oligomers and PA6

As explained in Chapter 1, maleic anhydride-grafted polyethylenes (PE-g-MA) are commonly used as compatibilizer precursors in polyethylene/polyamide blends because of their reactivity towards the amine end-groups of polyamide as well as their miscibility with polyethylene resins.[12–14] On the other hand, various polyetheramines have been used in other studies for the chemical modification of polyamides.[19,20] The objective of the experimental work presented in this part of the study was therefore to get a better understanding of the chemical interactions between the selected functional oligomers and PA6.

4.1. Reactivity towards PA6

4.1.1. Reactivity of Ceramer 1608 towards PA6

Blends of PA6 with various amounts of Ceramer 1608 (see Table 8) were achieved using a batch internal mixer at a temperature of 240 °C.

Table 8. Composition of PA6/Ceramer 1608 blends

Oligomer type	Overall oligomer concentration (wt%)	Blend composition (PA6/C1608)
Ceramer 1608	0	100/0
	1	99/1
	2	98/2
	3	97/3
	4	96/4
	5	95/5
	10	90/10

The PA6 was initially introduced and allowed to melt, then the oligomer was added around t = 5 min. The mixing torque curves corresponding to the 2 wt% and 10 wt% blends are displayed in Figure 10 as relevant examples. For each blend, the first peak corresponds to the introduction and melting of PA6.

After blending, PA6/Ceramer 1608 samples were characterized by rheometry following the protocol described in Chapter 2 for viscosity measurements. Regarding the viscosity curves shown in Figure 10, it should be noted that the rheological characterization of polyamides can be affected by the presence of water which evaporates during measurements at high temperatures, thus shifting the polycondensation equilibrium towards longer polyamide chains.[28] As a consequence, the measured viscosity usually tends to increase at low frequencies (particularly since rheological measurements were carried out from high to low angular frequencies, thus resulting in residence times of approximately 30-45 min within the rheometer) instead of approaching a Newtonian plateau. In order to avoid this phenomenon, samples were dried under vacuum for 24h at 70°C to remove water prior to rheological measurements.

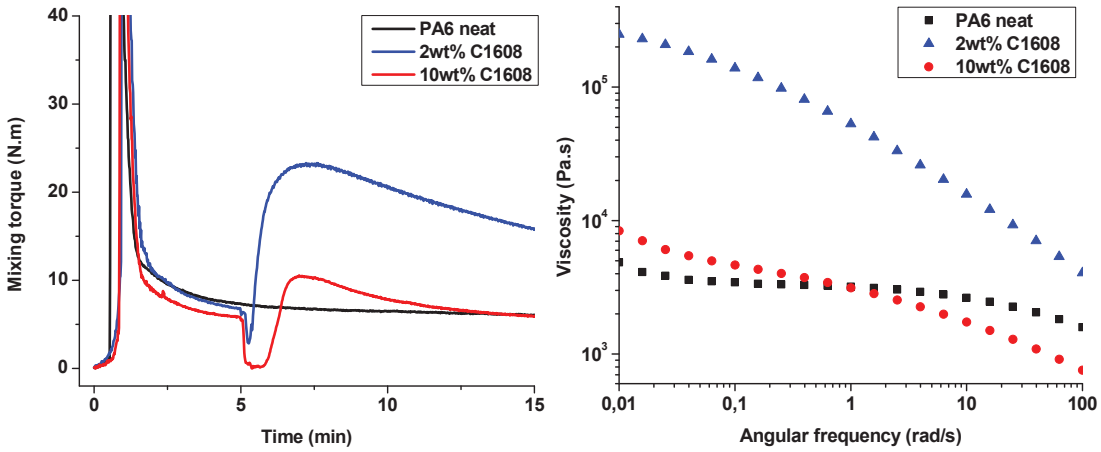

Figure 10. Mixing torque curves (left) and viscosity curves (right) for blends of PA6 with various amounts of Ceramer 1608

The introduction of Ceramer 1608 resulted in a drop in mixing torque values, showing a lubricating effect similar to that observed in the case of polyethylene-based blends (see Chapter 3). Homogenization times were found to be dependent on the oligomer concentration, which is consistent with previous observations made in Chapter 3. During homogenization, the mixing torque raised rapidly and exceeded that of neat PA6, indicating a reaction between the two components.

As explained in Chapter 1, the blending of PA with a PE-g-MA leads to a reaction between maleic anhydride groups and the terminal amines of PA, which is illustrated in Figure 11.

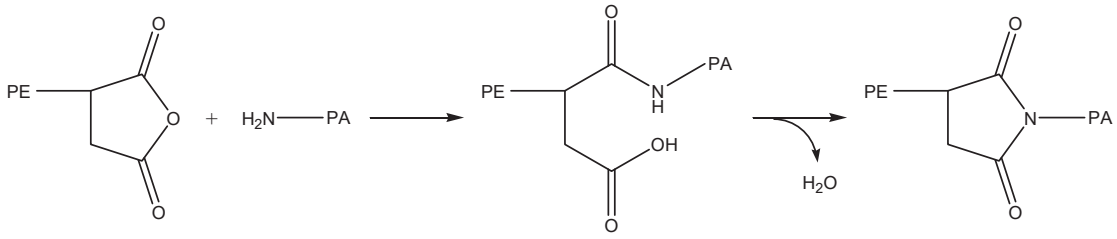

Figure 11. Mechanism for the reaction between Ceramer 1608 and Polyamide 6[33]

Such a reaction results in the grafting of PA6 chains onto Ceramer 1608 to form a polyethylene-g-polyamide copolymer. In practice, this corresponds to an increase of the molar mass of PA6, which is consistent with the increased viscosity of the 2 wt% blend (Figure 10). However, it can be observed that the mixing torque value at the reaction peak is higher with 2 wt% Ceramer 1608 than with 10 wt%, and rheological measurements of the corresponding blends confirmed that the viscosity of the 98/2 blend was much higher than that of the 90/10 one.

As mentioned in Chapter 2, the concentration of amine end-groups in PA6 was measured by potentiometric titration, which gave a value of 33 mmol(NH_2)/kg, while the concentration of maleic anhydride groups in Ceramer 1608 is 1.9×10^3 mmol(MA)/kg. The concentration of amine and maleic anhydride functional groups was therefore calculated as a function of the weight fraction of Ceramer

1608 in the blend and compared to the mixing torque values recorded at the reaction peak for each blend. Those values are displayed in Figure 12.

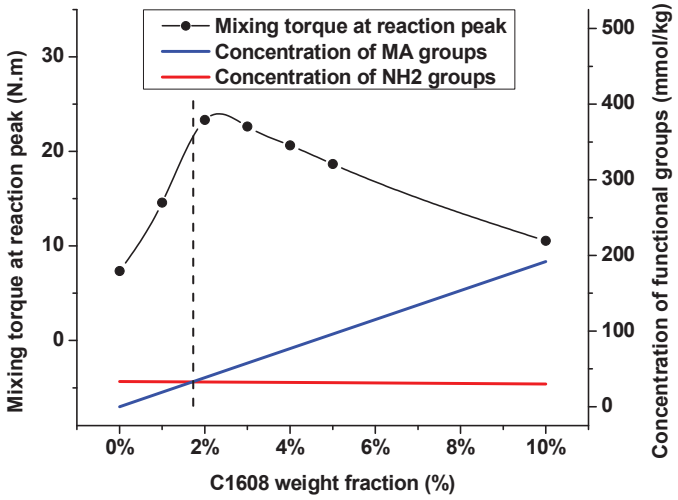

Figure 12. Mixing torque at the reaction peak for PA6/Ceramer 1608 blends compared with the concentration of amine and maleic anhydride functional groups in each blend

Calculations showed that stoichiometric conditions would be achieved at 1.7 wt% Ceramer 1608, which corresponds approximately to the 2 wt% blend for which the mixing torque at the reaction peak is the highest. Meanwhile, blends with unreacted functional groups (i.e. an excess of either amine or maleic anhydride functional groups) resulted in lower mixing torque values at the reaction peak.

The results presented here suggest that the molar mass of PA6 is indeed increased as a consequence of the reaction with Ceramer 1608, leading to an increase of the viscosity and thus of the mixing torque value during blending. While the highest molar mass is attained when all the amine end-groups have reacted (i.e. stoichiometric conditions), further incorporation of Ceramer 1608 results in a decrease of the blend viscosity. This can be explained by two phenomena: (i) a lesser increase in molar mass due to the grafting of fewer PA6 chains onto each PE-g-MA oligomer (excess of maleic anhydride functional groups), and/or (ii) the plasticization of the blend by unreacted PE-g-MA chains.

The increase of the molar mass of PA6 was quantified in the case of the blend with 2 wt% Ceramer 1608, as the rheological behaviour of this blend is not affected by an excess of Ceramer 1608 (quasi-stoichiometric conditions). In the absence of potential dilution by unreacted oligomer chains, the entangled regime was considered ($M > M_c$), where the zero-shear viscosity increases with the 3.4 power of the molar mass[23], yielding the following equation:

$$\frac{\eta_{PA6+2\%C1608}}{\eta_{PA6\ neat}} = k.\left(\frac{\overline{M}_{PA6+2\%C1608}}{\overline{M}_{PA6\ neat}}\right)^{3.4}$$

where η_i is the zero-shear viscosity of the blend and $\overline{M_i}$ is the number-average molar mass of PA6 with and without the addition of 2 wt% Ceramer 1608. The viscosity of the PA6/C1608 (98/2) blend was

measured to be fifty times higher than that of neat PA6, which corresponds to a threefold increase in molar mass according to this equation. Considering the initial molar mass of PA6 (30 000 g/mol), the copolymer obtained from the reaction with Ceramer 1608 should therefore have an approximate molar mass of 90 000 g/mol.

4.1.2. Reactivity of Jeffamine T-403 towards PA6

Blends of PA6 with various amounts of Jeffamine T-403 (Table 9) were achieved using a batch internal mixer at a temperature of 240 °C.

Table 9. Composition of PA6/Jeffamine T-403 blends

Oligomer type	Overall oligomer concentration (wt%)	Blend composition (PA6/T403)
Jeffamine T-403	0	100/0
	1	99/1
	3	97/3

The PA6 was initially introduced and allowed to melt, then the oligomer was added around t = 3 min. The mixing torque curves recorded during blending are displayed in Figure 13 along with the corresponding viscosity curves (measured by rheometry according to the protocol described in Chapter 2) for those samples.

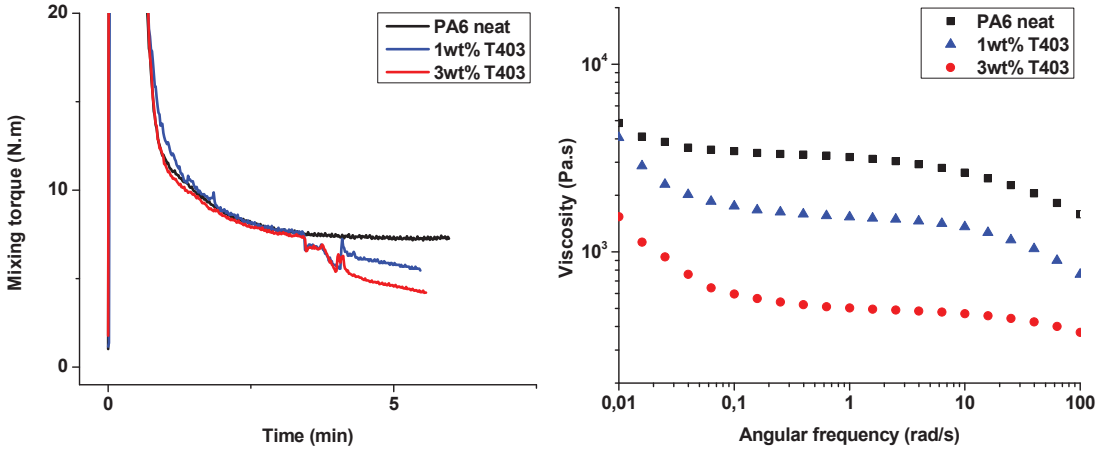

Figure 13. Mixing torque curves (left) and viscosity curves (right) for blends of PA6 with various amounts of Jeffamine T-403

The introduction of Jeffamine T-403 resulted in short homogenization times. The homogenization of Jeffamine T-403 was characterized by a decrease of the mixing torque, with ultimate values inferior to that of neat PA6. Rheological measurements confirmed that the viscosity of PA6 had decreased incrementally as a result of the addition of incremental amounts of Jeffamine T-403.

In their work on the chemical modification of polyamide, Auclerc et al.[19] proposed a mechanism to describe the chemical interactions between PA6 and Jeffamine T-403. The blending of those

components involves two types of reactions that are: (i) amidification between the amine groups of Jeffamine T-403 and the carboxylic acid end-groups of PA6 and (ii) transamidification on the amide moieties of PA6. This mechanism is illustrated in Figure 14.

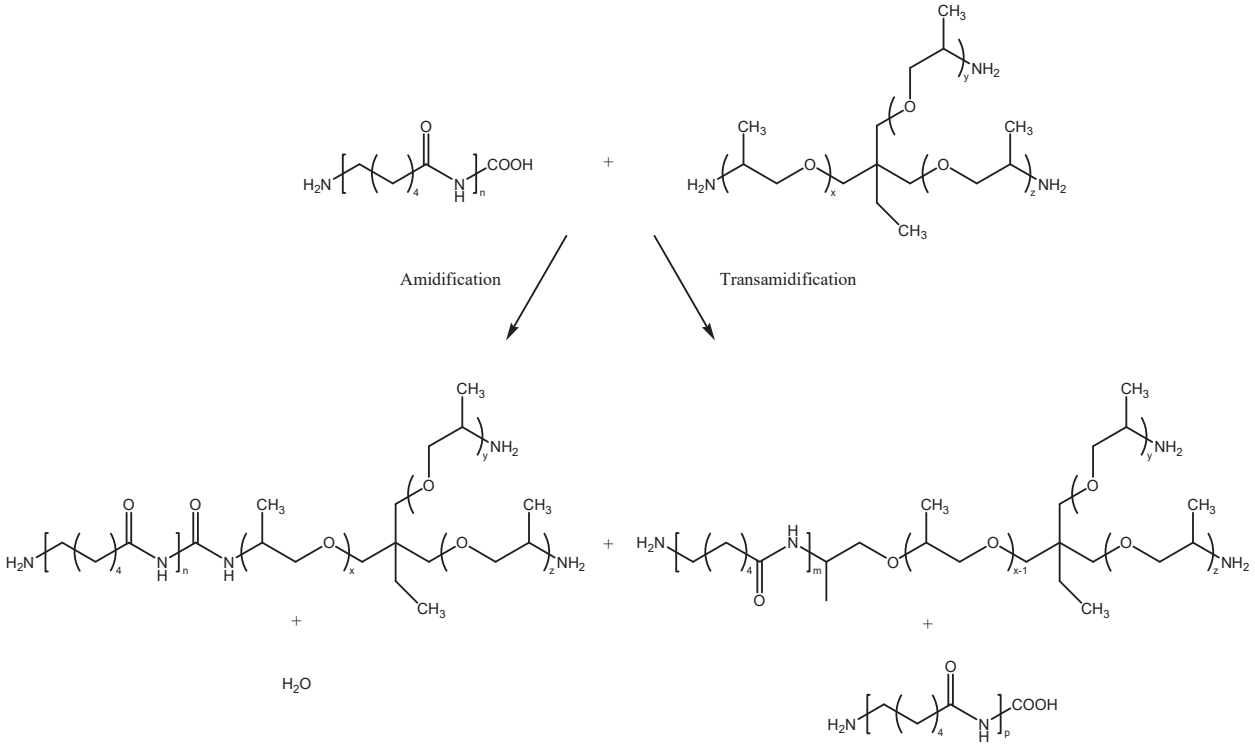

Figure 14. Proposed mechanism for the chemical reactions between polyamide 6 and Jeffamine T-403[19]

While the amidification reaction may lead to an increase of the molar mass of PA6 through chain extension and branching, the transamidification reaction on the other hand results in a decrease of the molar mass because of chain scission. A reduction of the molar mass is indeed consistent with the rheological behaviour observed for blends of PA6 with Jeffamine T-403, suggesting that chain scission as a result of transamidification is the prevalent mechanism. Nevertheless, the kinetics of those reactions were not investigated in this study and the blending of PA6 with Jeffamine T-403 may lead to complex mixtures of linear and branched polyamide chains, the chemical structures of which were not further characterized.

4.2. Properties of PA6/C1608/T403 ternary systems

PA6 was blended with Ceramer 1608 and Jeffamine T-403 using a batch internal mixer at a temperature of 240 °C. This system was studied at different overall oligomer concentrations (3 wt% and 15 wt%) and PA6/C1608 and PA6/T403 blends were also prepared as control samples. The compositions of these blends are summarized in Table 10.

Table 10. Composition of PA6/C1608/T403 blends

Oligomer type	Overall oligomer concentration (wt%)	Blend composition (PA6/C1608/T403)
-	-	100/0/0
Ceramer 1608 + Jeffamine T-403	3	97/2/1
Ceramer 1608 + Jeffamine T-403	15	85/12/3
Ceramer 1608 (control sample)	12	88/12/0
Jeffamine T-403 (control sample)	3	97/0/3

PA6 was initially introduced and allowed to melt. Ceramer 1608 was then incorporated around t = 2 min and Jeffamine T-403 was finally added around t = 4 min. The mixing torque curves as well as the viscosity curves for those blends are displayed in Figure 15.

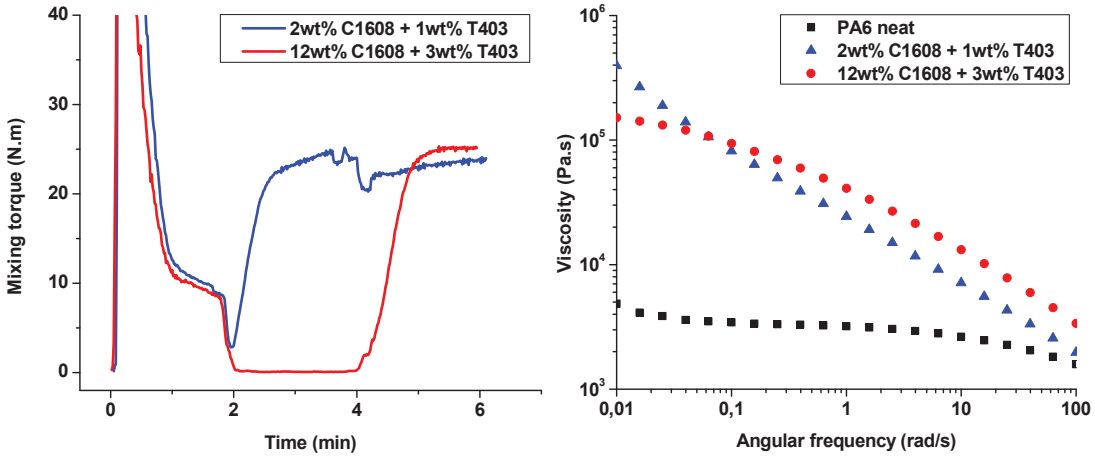

Figure 15. Mixing torque curves (left) and viscosity curves (right) for PA6/C1608/T403 blends

The successive variations of the mixing torque recorded in the case of the 97/2/1 blend were found to be consistent with the observations made in Sections 4.1.1 and 4.1.2 that the addition of small amounts of Ceramer 1608 resulted in an strong increase of the mixing torque while the addition of Jeffamine T-403 resulted in a decrease of the mixing torque. This suggests that the reactions described previously indeed take place with an increased molar mass of PA6 through grafting with Ceramer 1608 and a decrease of the molar mass through chain scission in the presence of Jeffamine T-403.

While the blend with 2 wt% Ceramer 1608 was rapidly homogenized, the incorporation of 12 wt% Ceramer resulted in a persistent lubricating effect, contrary to what was previously observed with 10 wt% Ceramer 1608 in PA6 (see Section 4.1.1). This could be attributed to the initially lower filling level of the mixing equipment in the case of blends involving large amounts of oligomers (15 wt% in this case). Consequently, in the case of the 85/12/3 blend the 3 wt% of Jeffamine T-403 were incorporated while the homogenization of Ceramer 1608 was not completed. This resulted in a strong increase of the mixing torque with a final value similar to that of the other blend (i.e. much higher than for neat PA6), although previous results (see Sections 4.1.1 and 4.1.2) showed that similar amounts of Ceramer 1608 (10 wt%)

and Jeffamine T-403 (3 wt%) both led to a decrease of the ultimate mixing torque of PA6. It can therefore be concluded that in such ternary blends, all three constituents interact with each other to form a complex mixture of linear and branched polyamide chains with various molar masses as a result of all the reaction mechanisms at play, which are described in Sections 2.1 and 4.1.

Ultimate mixing torque values were found to be similar for both blends and rheological measurements confirmed the similar viscoelastic behaviour of the two blends at high frequencies (10-100 rad/s). However, different trends were observed at low frequencies (0.01-10 rad/s). This difference in viscoelastic behaviour between 97/2/1 and 85/12/3 blends is better illustrated with the storage modulus and loss modulus curves presented in Figure 16.

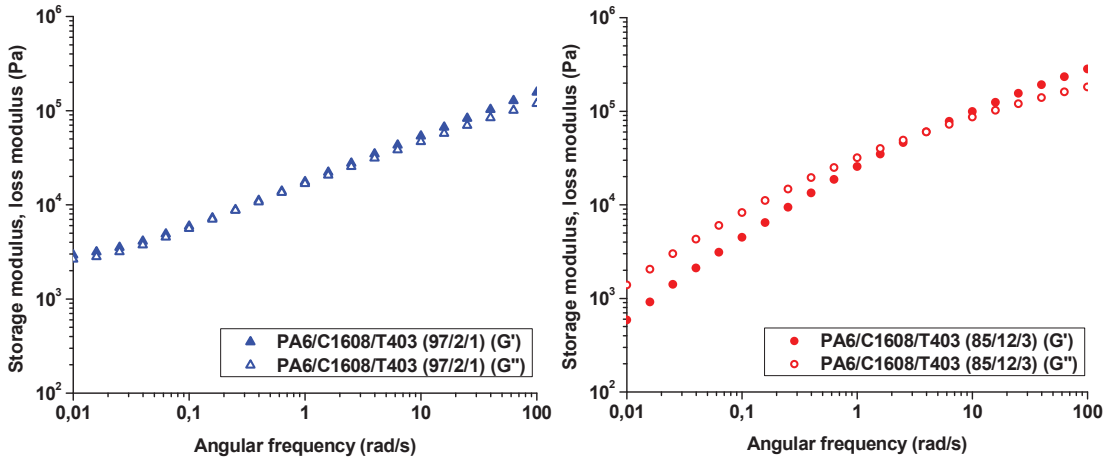

Figure 16. Storage modulus (G') and loss modulus (G") curves for PA6/C1608/T403 blends: 97/2/1 (left) and 85/12/3 (right)

The viscoelastic behaviour of the 97/2/1 blend was found to be similar to that of a gel[27], with a storage modulus slightly higher than the loss modulus. This could be interpreted as evidence of the formation of a network between the three constituents of the blend, considering the quasi-stoichiometric conditions in which the Ceramer 1608 is introduced.

On the contrary, the viscoelastic behaviour of the 85/12/3 blend was rather similar to that of a molten thermoplastic, although the moduli crossover point[34] had shifted towards lower frequencies compared to neat PA6 ($\omega_{co\ (85/12/3)} \approx 4$ rad/s and $\omega_{co\ (neat\ PA6)} > 100$ rad/s). This phenomenon can be explained either by an increased molar mass of polyamide chains[23] or by the presence of dispersed domains in the blend.[35] However, considering the large excess of Ceramer 1608 prior to the addition of Jeffamine T-403, it is more likely that a significant amount of Ceramer 1608 would remain available to react with Jeffamine T-403 and possibly form C1608/T403 domains.

The morphology of the blends was determined by SEM in order to verify those hypotheses. The corresponding pictures are shown in Figure 17.

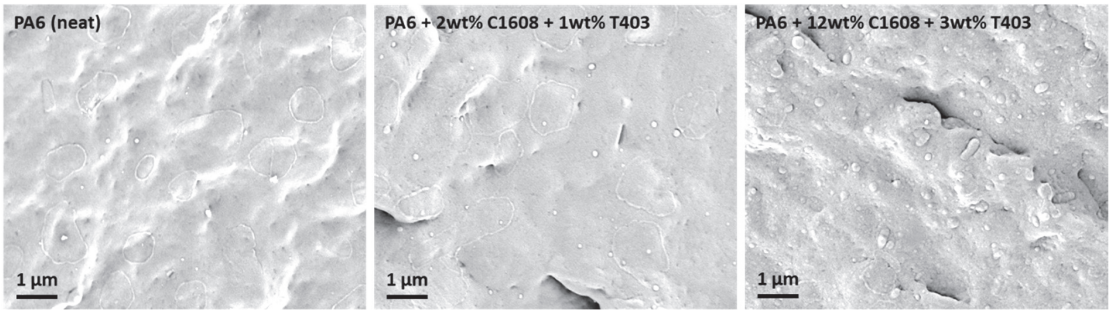

Figure 17. SEM pictures of PA6/C1608/T403 blends: 100/0/0 (left), 97/2/1 (middle) and 85/12/3 (right)

SEM observations of the 85/12/3 blend showed well dispersed and mostly spherical domains with dimensions ranging from 50 nm to 700 nm. This morphology was attributed to the presence of C1608/T403 domains dispersed in a continuous PA6 phase, which is consistent with the hypothesis that the unreacted Ceramer 1608 chains react with Jeffamine T-403. The interfacial adhesion between the two phases appeared to be excellent, which was expected because of the strong chemical interactions involving the three constituents. However, it cannot be concluded that in such systems Ceramer 1608 and Jeffamine T-403 oligomers are exclusively located in the dispersed phase, considering the structures of the compounds formed through their respective reaction(s) with PA6.

The 97/2/1 blend on the other hand showed only very few domains with diameters of approximately 50 nm to 200 nm. Considering the concentrations of Ceramer 1608 and Jeffamine T-403 in the blend, it is likely that both oligomers mostly react with PA6, leaving only little amounts of unreacted oligomer chains to form C1608/T403 domains. This would indeed explain the differences in number and size of the dispersed domains between the two blends.

In addition to rheological measurements and SEM observations, the impact of chemical modification on the mechanical properties of PA6 was evaluated by tensile testing, following the protocol detailed in Chapter 2. To that end, the blend with 12 wt% Ceramer 1608 and 3 wt% Jeffamine T-403 (85/12/3) was compared to neat PA6 (100/0/0) as well as to the blends containing only Ceramer 1608 (88/12/0) or Jeffamine T-403 (97/0/3). Young's modulus (E), yield stress (σ_y), stress at break (σ_b) and strain at break (ε_b) were measured by tensile testing and are presented in Table 11.

Table 11. Mechanical properties of PA6/C1608/T403 blends

Blend (PA6/C1608/T403)	E (MPa)	σ_y (MPa)	σ_b (MPa)	ε_b (%)
100/0/0	2100 ± 200	64 ± 1	52 ± 1	270 ± 20
88/12/0	1800 ± 100	54 ± 1	62 ± 1	210 ± 20
97/0/3	2200 ± 100	60 ± 1	49 ± 1	310 ± 20
85/12/3	1800 ± 100	52 ± 1	75 ± 1	230 ± 20

The addition of functional oligomers did not significantly impact the elongation at break or the Young's modulus of PA6, indicating that the ductility and stiffness of the material were preserved[36] thanks to the chemical interactions and excellent interfacial adhesion between PA6 and the dispersed phase.

Tensile testing results also showed a slight decrease in yield stress, which was attributed to the presence of polyolefin and polyether blocks that are inherently weaker than polyamide chains.

The typical stress-strain curves (recorded by tensile testing at 30 mm/min) corresponding to each blend are displayed in Figure 18 to further illustrate the impact of the addition of functional oligomers on the mechanical properties of PA6, especially in terms of yield stress and stress at break.

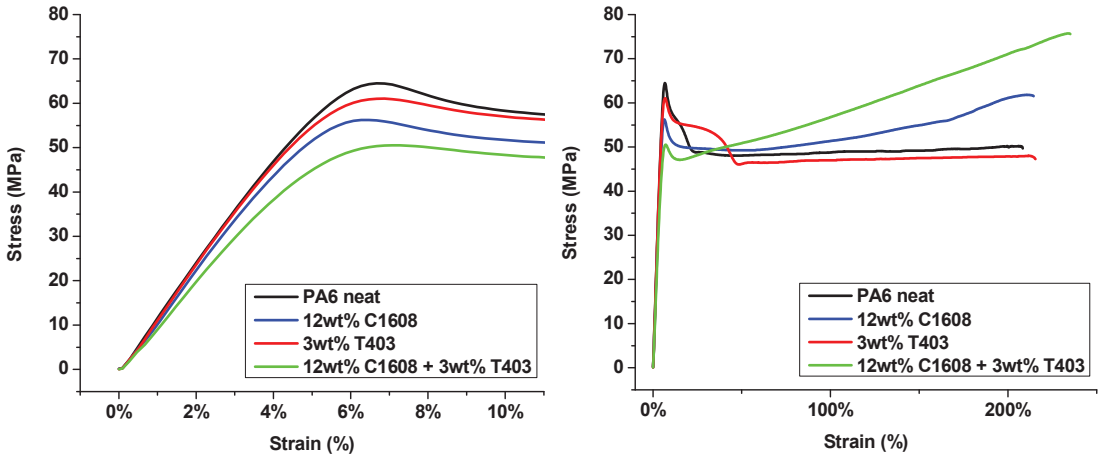

Figure 18. Typical stress-strain curves of PA6/C1608/T403 blends

88/12/0 and 85/12/3 blends exhibited a particular behaviour during plastic deformation, which was found to be similar to the strain-hardening behaviour typically encountered in rubber particle-toughened polymers for instance.[37,38] In the case of the 85/12/3 blend, toughening can be attributed to the formation of C1608/T403 domains with strong interactions with the polyamide phase, as well as to the potential formation of a network between the three constituent. On the other hand, the mechanical behaviour of the 88/12/0 blend under tensile strain is probably the result of the increased molar mass of the polyamide chains, which is usually responsible for higher stress at break.[39,40]

5. Behaviour of Ceramer and Jeffamine oligomers in HDPE

The aim of part of the study was to assess the compatibility of the C1608/T403 reactive system with HDPE. The miscibility of Ceramer 67, Ceramer 1608 and Jeffamine T-403 oligomers with HDPE was investigated as well as the morphology developments and rheological behaviour arising from the blending of both types of functional oligomers with HDPE. Lastly, the use of a high molar mass PE-g-MA was also investigated as a means to improve the compatibility between the C1608/T403 compound and the HDPE resin.

5.1. Miscibility of the functional oligomers with HDPE

Blends of HDPE with 5 wt% of each oligomer (Ceramer 67, Ceramer 1608 and Jeffamine T-403) were achieved using a batch internal mixer at a temperature of 180 °C. The compositions of these blends are summarized in Table 12.

Table 12. Composition of HDPE/oligomer blends

Oligomer type	Overall oligomer concentration (wt%)	Blend composition (HDPE/oligomer)
-	-	100/0
Ceramer 67	5	95/5
Ceramer 1608	5	95/5
Jeffamine T-403	5	95/5

The HDPE was initially introduced and allowed to melt, then the oligomer was added around t = 2 min. The mixing torque curves recorded during blending are displayed in Figure 19 along with the viscosity curves measured by rheometry at 180 °C (following the protocol described in Chapter 2 for viscosity measurements).

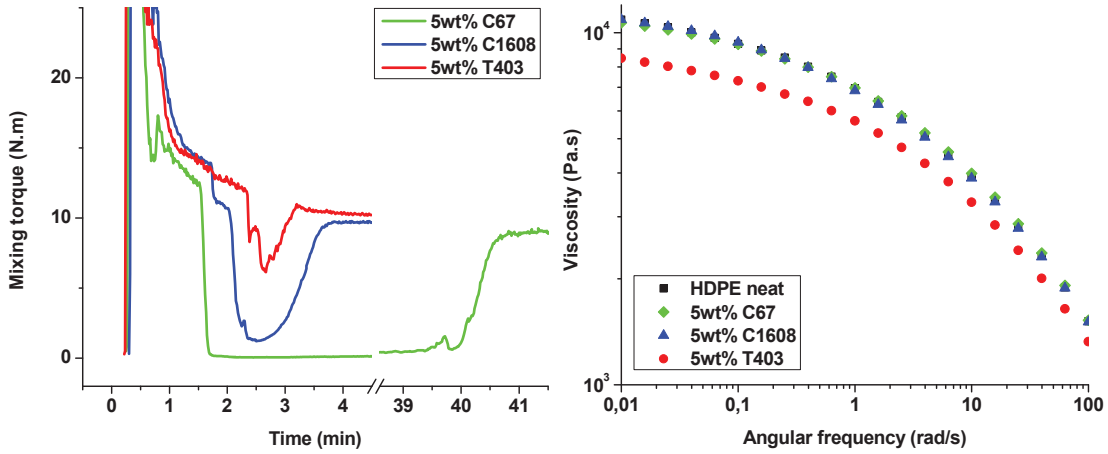

Figure 19. Mixing torque curves (left) and viscosity curves (right) for blends of HDPE with 5 wt% oligomer (Ceramer 67, Ceramer 1608 and Jeffamine T-403)

The introduction of the oligomers resulted in a sudden drop in the mixing torque value corresponding to a lubricating effect[41], similarly to what was described in Chapter 3 for the addition of a low viscosity PE oligomer into HDPE and PP resins. HDPE/C1608 and HDPE/T403 blends showed very short homogenization times (1-2 min), while the time to achieve homogenization of the HDPE/C67 blend was nearly 40 minutes.

As already discussed in Chapter 3, during the blending of low viscosity compounds into polymer matrices, lower viscosity ratios result in longer times to achieve homogenization.[41,42] Considering that the viscosity of Ceramer 1608 (2 Pa.s) is a hundred times higher than that of Ceramer 67 (0.02 Pa.s), the results presented here are consistent with those conclusions.

However, the lubricating effect observed in the case of Ceramer 67 is much more persistent than what was previously observed in the case of the Unicid 700 oligomer which has a similar viscosity. According to Cassagnau and Fenouillot[43], the mixing behaviour of a binary blend is more sensitive to diffusion than to mixing when the viscosity ratio is lower than 10^{-3}, which is presently the case. Seeing that Unicid 700 and Ceramer 67 have comparable viscosities and degrees of functionality, it could therefore be argued that the diffusion of PE oligomers into HDPE depends on the chemical nature of their functional group, which may influence miscibility.

Nevertheless, considering the viscosity and chemical structure of Jeffamine T-403, the short homogenization time observed in the case of the HDPE/T403 blend can be explained neither by a higher viscosity ratio nor by a greater chemical affinity. The rapid diffusion of Jeffamine T-403 into HDPE might therefore be due to its lower molar mass compared to that of Ceramer oligomers.

Rheological characterization of the blends showed that the viscosity of HDPE was unaffected by the presence of Ceramer 67 or Ceramer 1608 oligomers (in Figure 19 the curves corresponding to the HDPE/C67 and HDPE/C1608 blends are superimposed over the neat HDPE curve), although it was previously shown (see Chapter 3) that the addition of 5 wt% PE oligomer to HDPE caused a viscosity reduction as a result of dilution. This suggests that Ceramer oligomers have a poorer solvation ability towards HDPE, meaning that they may form dispersed domains within a HDPE continuous phase. This would explain why the viscosity of HDPE/C67 and HDPE/C1608 blends is dominated by the viscosity of HDPE.

The introduction of 5 wt% of Jeffamine T-403 on the other hand resulted in a perceptible decrease of the viscosity. Consequently, the theoretical viscoelastic behaviour of the HDPE/T403 (95/5) blend was predicted using the Carreau-Yasuda equation[44–46] in the same manner as in Chapter 3. The free volume correction parameter was not taken into account in this case (hence $a_\varphi = 1$). The other parameters of the Carreau-Yasuda equation (drawn from the fitting of the viscosity curve of neat HDPE) are given in Table 13. The modelled viscosity curves for both neat HDPE and the HDPE/T403 blend are shown in Figure 20.

Table 13. Parameters of the Carreau-Yasuda equation drawn from the fitting of the viscosity curve of neat HDPE and used for the prediction of the viscoelastic behaviour of the HDPE/T403 (95/5) blend

Blend	$(\eta_0)_{bulk}$ (Pa.s)	a_φ (-)	φ (-)	τ_{bulk} (s)	a (-)	m (-)
HDPE/T403 (95/5)	10.9×10^3	1	0.95	0.79	0.59	-0.42

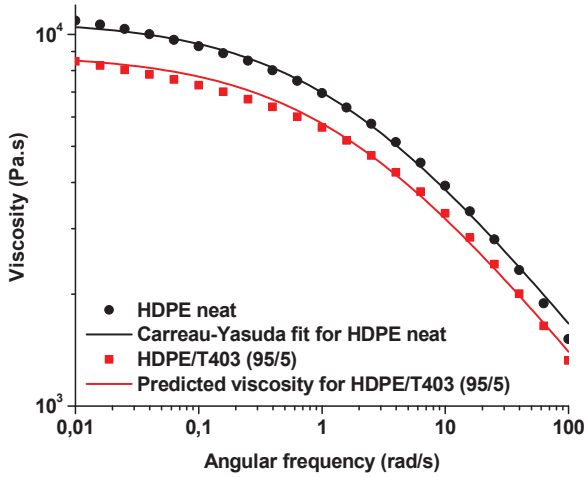

Figure 20. Predicted vs. measured viscoelastic behaviour of the HDPE/T403 (95/5) blend

It appeared that the viscoelastic behaviour predicted with the Carreau-Yasuda equation fitted the experimental data quite well, indicating an effective dilution of HDPE by the Jeffamine T-403 oligomer.[44,47] This was considered consistent with the rapid diffusion of Jeffamine T-403 into HDPE leading to shorter homogenization times compared to HDPE/C67 and HDPE/C1608 blends.

The morphology of the blends in the solid state was determined by SEM observations, which are presented in Figure 21.

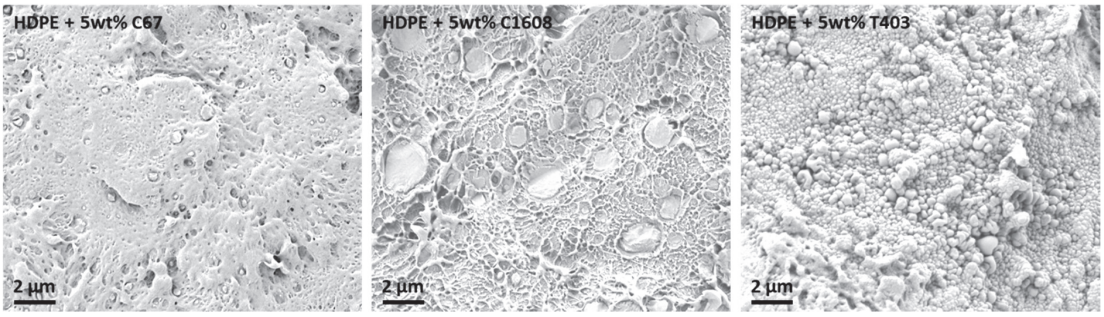

Figure 21. SEM pictures of HDPE/C67 (left), HDPE/C1608 (middle) and HDPE/T403 (right) blends

Samples containing 5 wt% Ceramer (both C1608 and C67) exhibited biphasic morphologies with spherical oligomer domains dispersed in a continuous HDPE phase, which is typical of a liquid-liquid phase separation[48], therefore indicating a poor miscibility in the molten state. Nevertheless, the domains were well dispersed and no debonding was observed, also suggesting a low surface tension between Ceramer oligomers and HDPE because of their close chemical structure. The diameter of the

dispersed domains was 50 nm to 500 nm in the case of Ceramer 67 and 100 nm to 3 µm with Ceramer 1608. This may be attributed to the higher maleic anhydride content of Ceramer 1608 (inducing higher incompatibility due to the increased polarity of the oligomer compared to Ceramer 67) as well as to its higher viscosity, as the viscosity ratio of the blend is known to have a direct influence on the morphology of the dispersed phase.[28,49]

The morphology of the HDPE/T403 blend was found to be very different with no dispersed domains observed. Instead, the sample exhibited a textured surface similar to that described by Lloyd et al.[50] as a result of solid-liquid phase separation in polymer-diluent mixtures. This appears to be a reasonable explanation for the observed morphology considering the miscibility between Jeffamine T-403 and HDPE in the molten state as well as the fact that Jeffamine T-403 remains an amorphous liquid upon the crystallization of HDPE (see Chapter 1). Figure 22 shows a SEM picture of the HDPE/T403 sample at higher magnification.

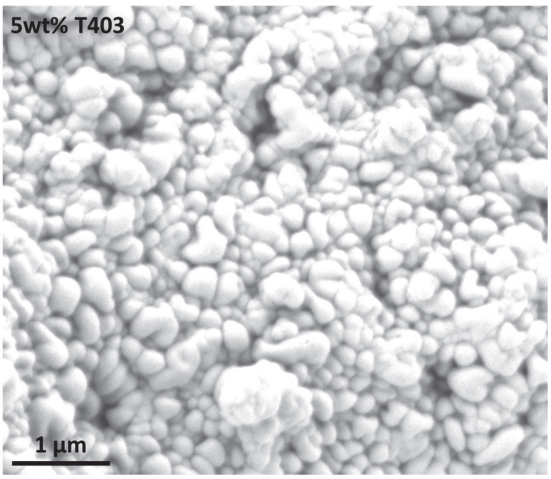

Figure 22. SEM picture of a HDPE/Jeffamine T-403 (95/5) blend

On this SEM picture, a "fuzzy sphere" morphology[50] with dimensions in the range of 100 nm to 1 µm is observable, which could correspond to a spherulitic morphology induced by solid-liquid phase separation between HDPE and Jeffamine T-403 upon cooling, similarly to what was observed in the case of PP/PE oligomer systems (see Chapter 3).

5.2. In-situ formation of a C1608/T403 compound in HDPE

Ceramer 1608 and Jeffamine T-403 were incorporated to HDPE using a batch internal mixer at a temperature of 180 °C. The weight ratio between the two oligomers was set at 3/1 in order to remain in quasi-stoichiometric conditions, hence a blend with 6 wt% Ceramer 1608 and 2 wt% Jeffamine T-403 was prepared. A control sample with the same overall oligomer content (8 wt% Ceramer 1608) was also prepared. The compositions of these blends are summarized in Table 14.

Table 14. Composition of HDPE/C1608/T403 blends

Oligomer type	Overall oligomer concentration (wt%)	Blend composition (HDPE/C1608/T403)
-	-	100/0/0
Ceramer 1608	8	92/8/0
Ceramer 1608 + Jeffamine T-403	8	92/6/2

The HDPE was initially introduced and allowed to melt. Ceramer 1608 was then added around t = 2 min and Jeffamine T-403 was finally added around t = 4 min. The mixing torque curves as well as the corresponding viscosity curves are displayed in Figure 23.

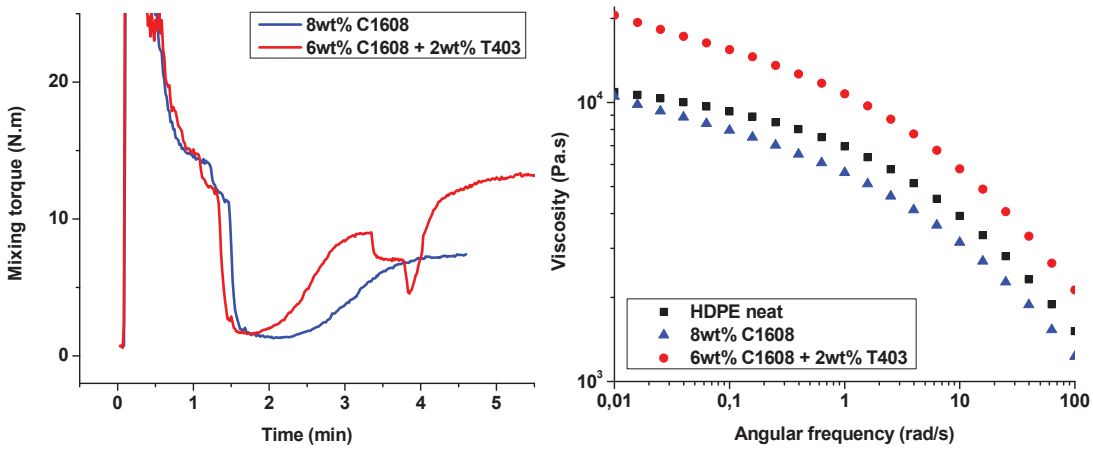

Figure 23. Mixing torque curves (left) and viscosity curves (right) for HDPE/C1608/T403 blends

The mixing torque graph shows that the incorporation of 6-8 wt% Ceramer 1608 to HDPE resulted in the same lubricating effect as observed with 5 wt% Ceramer 1608 (see Section 5.1), with the homogenization time and mixing torque value after homogenization both varying with the oligomer concentration, as expected considering the results obtained in Chapter 3. The corresponding viscosity curve of the HDPE/C1608 (92/8) blend showed a slight viscosity reduction compared to what can be observed in Figure 19, indicating a potential dilution of HDPE by the oligomer. However, the absence of a Newtonian plateau at low frequencies, which is characteristic of the presence of a dispersed phase, suggested a phase separation between HDPE and Ceramer 1608 at the same time.

In the case of the HDPE/C1608/T403 (92/6/2) blend, the incorporation of Jeffamine T-403 (t ≈ 4 min) to the HDPE/C1608 mixture resulted in a very short homogenization time as well as an increase of the ultimate mixing torque value. This was correlated with the higher viscosity of the HDPE/C1608/T403 blend compared to neat HDPE. Additionally, the absence of a Newtonian plateau at low frequencies also indicated the presence of a dispersed phase.

SEM pictures of theses samples are shown in Figure 24.

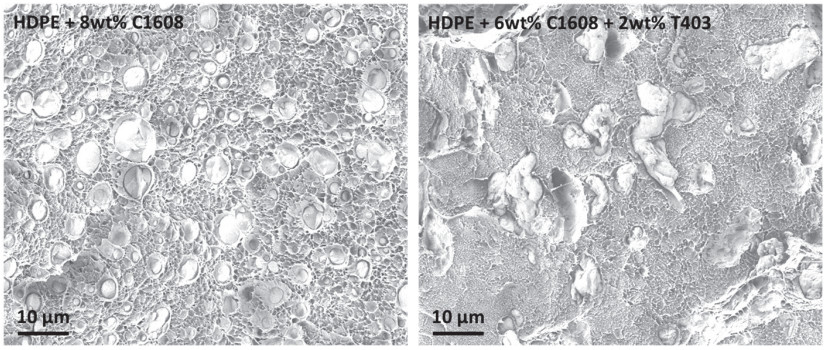

Figure 24. SEM pictures of HDPE/C1608/T403 blends: 92/8/0 (left) and 92/6/2 (right)

The HDPE/C1608 (92/8) blend exhibited a morphology similar to that observed with 5 wt% Ceramer 1608 (see Section 5.1), with slightly larger droplet diameters (roughly 100 nm to 10 µm) because of the higher oligomer concentration. This confirmed the phase separation between HDPE and Ceramer 1608.

SEM observations of the HDPE/C1608/T403 (92/6/2) blend revealed a dispersed phase consisting of irregularly shaped domains with dimensions ranging from 1 µm to 20 µm. This was interpreted as evidence of the in-situ formation of a compound resulting from the reaction between Ceramer 1608 and Jeffamine T-403. However, the frequent debonding of the dispersed domains on the surface of the sample indicated a poor interfacial adhesion between HDPE and the C1608/T403 compound.

5.3. Incorporation of a high molar mass PE-g-MA in HDPE/C1608/T403 blends

In order to improve the compatibility between the C1608/T403 compound and HDPE, samples containing a high molar mass polyethylene grafted with maleic anhydride groups were prepared. A commercially available PE-g-MA additive, Exxelor PE 1040 (E1040), was selected for this purpose.

6 wt% Ceramer 1608 and 2 wt% Jeffamine T-403 were incorporated to three different polyethylene-based resins: (i) HDPE, (ii) Exxelor PE 1040 or (iii) a 50/50 blend of HDPE and Exxelor PE 1040. The compositions of these blends are summarized in Table 15.

Table 15. Composition of HDPE/E1040/C1608/T403 blends

Polyethylene phase	Overall oligomer concentration (wt%)	Blend composition (HDPE/E1040/C1608/T403)
HDPE	8	92/0/6/2
HDPE + Exxelor PE 1040	8	46/46/6/2
Exxelor PE 1040	8	0/92/6/2

The polyethylene (HDPE and/or Exxelor PE 1040) was introduced in the batch internal mixer at a temperature of 180 °C and allowed to melt before adding 6 wt% Ceramer 1608 after 2 min. Jeffamine T-403 was added after homogenization of Ceramer 1608. The mixing torque curves recorded during blending as well as the viscosity curves measured by rheometry are displayed in Figure 25.

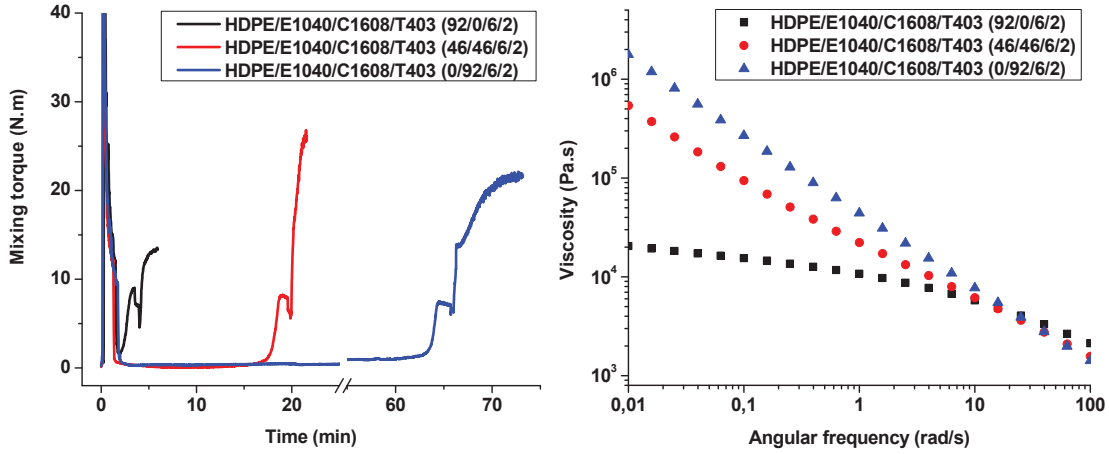

Figure 25. Mixing torque curves (left) and viscosity curves (right) for HDPE/E1040/C1608/T403 blends

The homogenization time following the addition of Ceramer 1608 (prior to the incorporation of Jeffamine T-403) varied dramatically depending on the composition of the polyethylene phase and was characterized by a persistent lubricating effect in the presence of Exxelor PE 1040: 2 min in neat HDPE, 19 min in the HDPE/E1040 (50/50) blend and 64 min in neat E1040. This was attributed to the higher viscosity of Exxelor PE 1040 which is six times higher than that of HDPE, as the lower viscosity ratios in HDPE/E1040/C1608 and E1040/C1608 blends ($R_{v\,(C1608/E1040)} \approx 10^{-5}$) compared to the HDPE/C1608 blend ($R_{v\,(C1608/HDPE)} \approx 10^{-4}$) is probably the main cause for the longer homogenization times observed.

The incorporation of Jeffamine T-403 in the blends containing Exxelor PE 1040 resulted in much higher final mixing torque and viscosity values compared to the blends containing only HDPE. This was attributed to the strong interaction between Jeffamine T-403 and Exxelor PE 1040 as a result of the reaction between amine and maleic anhydride functional groups, which is similar to the one described in Section 2.1 with Jeffamine T-403 and Ceramer 1608.

It should also be noted that a C1608/T403 weight ratio of 3/1 induces a slight excess of amine groups over the maleic anhydride groups of Ceramer 1608, making it possible for Jeffamine T-403 to react with Exxelor PE 1040 as well. The amounts of functional groups in the E1040/C1608/T403 (92/6/2) blend are given in Table 16 as an example.

Table 16. Calculated amounts of functional groups in the E1040/C1608/T403 (92/6/2) blend

Component	Weight fraction (%)	Type of functional group	Amount of functional groups in the blend (mmol/g)
Exxelor PE 1040	92	Maleic anhydride	0.098
Ceramer 1608	6	Maleic anhydride	0.114
Jeffamine T-403	2	Amine	0.136

Considering the amount of maleic anhydride and amine functional groups in the blends, it can therefore be suggested that Jeffamine T-403 is able to react with both Ceramer 1608 and Exxelor PE 1040, leading

to the formation of a network between the three constituents. However, the structure of this network cannot be determined exactly, as there is no indication that Jeffamine T-403 reacts preferentially with one PE-g-MA or the other.

SEM observations were carried out to assess the morphology of the blends and verify the presence of potential C1608/T403 domains. SEM pictures of the three blends are shown in Figure 26.

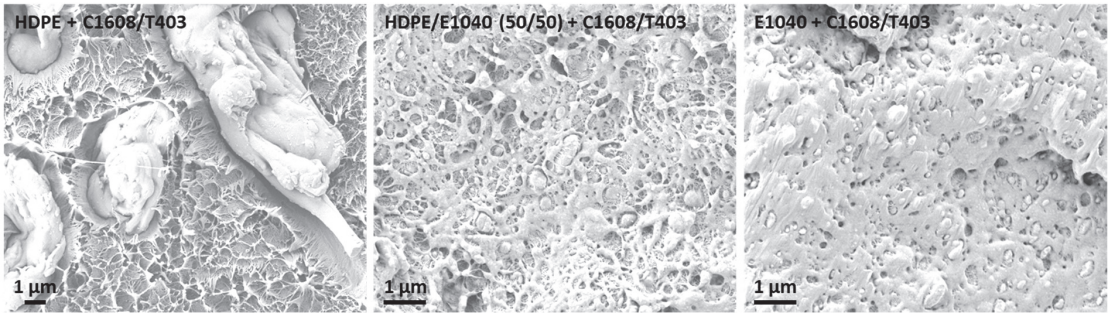

Figure 26. SEM pictures of HDPE/E1040/C1608/T403 blends: 92/0/6/2 (left), 46/46/6/2 (middle) and 0/92/6/2 (right)

As already shown in Figure 24, the introduction of Ceramer 1608 and Jeffamine T-403 in HDPE resulted in formation of a dispersed phase with irregular shapes and dimensions. Dispersed domains were also observed in the other two samples, showing that a C1608/T403 compound was also formed in situ. However, the presence of a high molar mass PE-g-MA (Exxelor PE 1040) resulted in a much better dispersion along with an improved interfacial adhesion between the polyethylene continuous phase and the C1608/T403 domains. In that case, the dispersed domains were mostly spherical with diameters ranging from 50 nm to 1 µm in HDPE/E1040/C1608/T403 and 20-500 nm in E1040/C1608/T403. These observations led to the conclusion that the C1608/T403 compound strongly interacted with the polyethylene phase because of the amine-maleic anhydride reaction between Jeffamine T-403 and Exxelor PE 1040. A schematic representation of the network formed between Jeffamine T-403, Ceramer 1608 and Exxelor PE 1040 is proposed in Figure 27 to account for the morphologies observed by SEM.

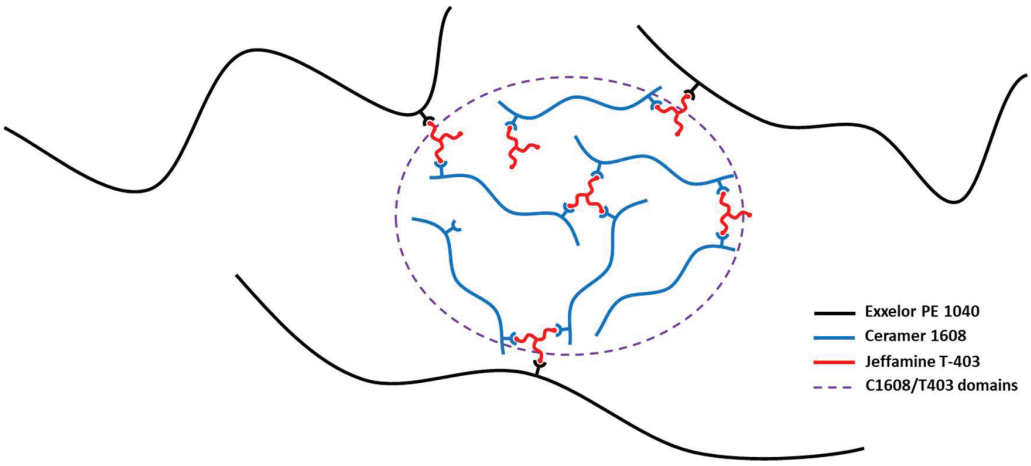

Figure 27. Proposed representation of the interactions between Exxelor PE 1040 and the dispersed C1608/T403 domains

Only the interactions through covalent bonding between Exxelor PE 1040 and C1608/T403 domains are represented here, although chemical interactions between those constituents may exist outside these domains. Unreacted constituents (such as HDPE or unreacted oligomer chains) were not represented for simplification purposes.

6. Conclusion

The objective of the experimental work developed in this chapter was to investigate new strategies for the compatibilization of immiscible polyethylene/polyamide blends. This study was focused on the use of a reactive system involving two types of functional oligomers, namely (i) a polyethylene oligomer grafted with maleic anhydride groups (Ceramer) as well as (ii) a tri-functional polyetheramine (Jeffamine T), both of which are commercially available materials.

In the first experimental part, it was found that the association of a PE-g-MA oligomer with a tri-functional polyetheramine oligomer resulted in compounds with very different characteristics depending on the physical and chemical properties of the PE-g-MA used, and the results suggested that the reaction between Ceramer 1608 and Jeffamine T-403 yielded a crosslinked network. It is worth noting that several other Ceramer and Jeffamine oligomers are commercially available, meaning that the properties of such Ceramer-Jeffamine networks could be finely tuned by adjusting several parameters such as the molar mass of the oligomers (number of ether repeat units of Jeffamine and number of ethylene repeat units of Ceramer) and the number of functional groups of each oligomer (type of Jeffamine as well as maleic anhydride content in the case of Ceramer).

A reactive system consisting of Ceramer 1608 and Jeffamine T-403 was therefore investigated as a potential route towards the compatibilization of an immiscible HDPE/PA6 (70/30) blend. The results showed that the use of Ceramer 1608 or of a Ceramer 1608/Jeffamine T-403 reactive system did not result in efficient compatibilization, while the use of a high molar mass PE-g-MA (Exxelor PE 1040) led to homogeneous materials with improved mechanical properties. This suggests that the poor compatibilizing ability of oligomeric compatibilizer precursors is due to their lack of interaction with the polyethylene phase. Nevertheless, the study of the physical and chemical interactions between the selected functional oligomers and HDPE and PA6 homopolymers led to some interesting results, which are detailed in the following paragraphs.

In Section 4, it was demonstrated that Ceramer 1608 and Jeffamine T-403 functional oligomers have strong interactions with PA6 through several reaction mechanisms, resulting in remarkable mechanical properties. Further mechanical testing should therefore be carried out on polyamide/Ceramer/Jeffamine compounds, especially in terms of impact strength, as their strain-hardening behaviour could make them good candidates for impact resistance applications. The results presented in that part of the study also indicate that the viscoelastic and mechanical properties of the resulting compounds are strongly influenced by the composition of the blends and could therefore be more finely adjusted with additional experimental work.

The results presented in Section 5 indicated that the compound formed from the reaction between a maleic anhydride grafted polyethylene oligomer (Ceramer 1608) and a tri-functional polyetheramine oligomer (Jeffamine T-403) was incompatible with HDPE. However, the interfacial adhesion between

the dispersed domains and the polyethylene continuous phase could be improved with the addition of a high molar mass polyethylene grafted with maleic anhydride functionalities (Exxelor PE 1040). Further work would be needed to determine the minimum amount of Exxelor PE 1040 necessary to obtain a good interface with the C1608/T403 compound, and the composition of the quaternary blend could be finely adjusted in order to achieve specific morphologies. Besides, it would be interesting to investigate the mechanical properties blends with such morphologies, considering the interactions between the continuous phase and the dispersed domains.

Considering the results presented in this chapter, additional experimental efforts would be required to focus on the use of PE-g-MA and polyetheramine oligomers with different molar masses and number of functional groups in order to achieve an efficient compatibilization of polyethylene/polyamide blends. In this perspective, it is worth noting that several Ceramer and Jeffamine oligomers are currently commercially available. Furthermore, the use of high molar mass PE-g-MA in addition to the functional oligomers could also be an interesting lead. Besides, the optimization of the blend composition in terms of polyethylene/polyamide ratio, concentration of oligomers and amounts of reactive groups in the blend is an issue that would require tackling.

7. Bibliography

[1] P. Marechal, Polyéthylènes basse densité PE-BD et PE-BDL, Techniques de l'ingénieur Matières thermoplastiques : monographies. base documentaire : TIB147DUO (2011).

[2] C. Penu, Polyéthylène haute densité PE-HD, Techniques de l'ingénieur Matières thermoplastiques : monographies. base documentaire : TIB147DUO (2011).

[3] B. GUÉRIN, Polyamides PA, Ref : TIP100WEB - "Plastiques et composites." (1994).

[4] M.K. Akkapeddi, ed., 15. Commercial polymer blends, in: Polymer Blends Handbook, Kluwer Academic Publishers, Dordrecht ; Boston, 2002: pp. 1023–1116.

[5] J. Huitric, P. Médéric, M. Moan, J. Jarrin, Influence of composition and morphology on rheological properties of polyethylene/polyamide blends, Polymer. 39 (1998) 4849–4856. doi:10.1016/S0032-3861(97)10255-5.

[6] L.A. Utracki, M.M. Dumoulin, P. Toma, Melt rheology of high density polyethylene/polyamide-6 blends, Polymer Engineering & Science. 26 (1986) 34–44. doi:10.1002/pen.760260108.

[7] A. Argoud, L. Trouillet-Fonti, S. Ceccia, P. Sotta, Morphologies in Polyamide 6/High Density Polyethylene blends with high amounts of reactive compatibilizer, European Polymer Journal. 50 (2014) 177–189. doi:10.1016/j.eurpolymj.2013.10.026.

[8] M. Xanthos, Interfacial agents for multiphase polymer systems: Recent advances, Polymer Engineering & Science. 28 (1988) 1392–1400. doi:10.1002/pen.760282108.

[9] M. Xanthos, S.S. Dagli, Compatibilization of polymer blends by reactive processing, Polymer Engineering & Science. 31 (1991) 929–935. doi:10.1002/pen.760311302.

[10] A.D. Todd, R.J. McEneany, V.A. Topolkaraev, C.W. Macosko, M.A. Hillmyer, Reactive Compatibilization of Poly(ethylene terephthalate) and High-Density Polyethylene Using Amino-Telechelic Polyethylene, Macromolecules. 49 (2016) 8988–8994. doi:10.1021/acs.macromol.6b02080.

[11] C.P. O'Brien, J.K. Rice, M.D. Dadmun, Reactive processing with difunctional oligomers to compatibilize polymer blends, European Polymer Journal. 40 (2004) 1515–1523. doi:10.1016/j.eurpolymj.2004.01.023.

[12] J. Duvall, C. Sellitti, C. Myers, A. Hiltner, E. Baer, Effect of compatibilization on the properties of polypropylene/polyamide-66 (75/25 wt/wt) blends, Journal of Applied Polymer Science. 52 (1994) 195–206. doi:10.1002/app.1994.070520207.

[13] S. Lim, J.L. White, Influence of a compatibilizing agent on the phase morphology of a polyethylene-polyamide 6 blend in a modular intermeshing co-rotating twin screw extruder, Polymer Engineering & Science. 34 (1994) 221–228. doi:10.1002/pen.760340308.

[14] I. Pesneau, A.A. Kadi, M. Bousmina, P. Cassagnau, A. Michel, From polymer blends to in situ polymer/polymer composites: Morphology control and mechanical properties, Polymer Engineering & Science. 42 (2002) 1990–2004. doi:10.1002/pen.11091.

[15] Z. Ke, D. Shi, J. Yin, R.K.Y. Li, Y.-W. Mai, Facile Method of Preparing Supertough Polyamide 6 with Low Rubber Content, Macromolecules. 41 (2008) 7264–7267. doi:10.1021/ma800495t.

[16] H. Shi, D. Shi, X. Wang, L. Yin, J. Yin, Y.-W. Mai, A facile route for preparing stable co-continuous morphology of LLDPE/PA6 blends with low PA6 content, Polymer. 51 (2010) 4958–4968. doi:10.1016/j.polymer.2010.08.023.

[17] A. Linemann, T. Briffaud, Polyamides branches a extremites insaturees, CA2503662C, 2013.

[18] G. Daun, L. Wittenbecher, M. Henningsen, D. Flick, J.-P. Geisler, J. Schillgalies, E. Jacobi, Blends comprising epoxy resins and mixtures of amines with guanidine derivatives, CA2729895C, 2016.

[19] M. Auclerc, V. Bounor-Legaré, P. Cassagnau, Modification chimique de polyamide par extrusion réactive, University of Lyon, 2018.
[20] A. Chambet, V. Bounor-Legaré, P. Cassagnau, Nouvelles voies de renforcement des polyamides par extrusion réactive, 2014.
[21] A. Lucas, V. Bounor-Legaré, P. Cassagnau, Renforcement de copolyester thermoplastique par extrusion réactive, thesis, Lyon, 2017.
[22] B. Wunderlich, Table of Thermal Properties of Linear Macromolecules and Related Small Molecules—The ATHAS Data Bank, in: Thermal Analysis of Polymeric Materials, 1st ed., Springer, 2005: pp. 777–799.
[23] J.D. Ferry, Chapter 10. Molecular theory for undiluted amorphous polymers and concentrated solutions; network and entanglements, in: Viscoelastic Properties of Polymers, 3rd ed., John Wiley & Sons, Inc., 1980: pp. 224–263.
[24] K. Lamnawar, A. Maazouz, Rheology and morphology of multilayer reactive polymers: effect of interfacial area in interdiffusion/reaction phenomena, Rheol Acta. 47 (2008) 383–397. doi:10.1007/s00397-007-0244-1.
[25] J.D. Ferry, Chapter 2. Illustration of viscoelastic behavior of polymeric systems, in: Viscoelastic Properties of Polymers, 3rd ed., John Wiley & Sons, Inc., 1980: pp. 33–55.
[26] K.-W. Lem, C.D. Han, Rheological properties of polyethylenes modified with dicumyl peroxide, Journal of Applied Polymer Science. 27 (1982) 1367–1383. doi:10.1002/app.1982.070270426.
[27] H.H. Winter, F. Chambon, Analysis of Linear Viscoelasticity of a Crosslinking Polymer at the Gel Point, Journal of Rheology. 30 (1986) 367–382. doi:10.1122/1.549853.
[28] C. Épinat, L. Trouillet-Fonti, P. Sotta, Predicting phase inversion based on the rheological behavior in Polyamide 6/Polyethylene blends, Polymer. 137 (2018) 132–144. doi:10.1016/j.polymer.2018.01.019.
[29] T. Inoue, ed., 8. Morphology of polymer blends, in: Polymer Blends Handbook, Kluwer Academic Publishers, Dordrecht ; Boston, 2002: pp. 565–594.
[30] S.F. Xavier, 12. Properties and performance of polymer blends, in: L.A. Utracki (Ed.), Polymer Blends Handbook, Kluwer Academic Publishers, Dordrecht ; Boston, 2002: pp. 861–950.
[31] S. Jose, S.V. Nair, S. Thomas, J. Karger-Kocsis, Effect of reactive compatibilisation on the phase morphology and tensile properties of PA12/PP blends, Journal of Applied Polymer Science. 99 (2006) 2640–2660. doi:10.1002/app.22806.
[32] S. Charoenpongpool, M. Nithitanakul, B.P. Grady, Melt-neutralization of maleic anhydride grafted on high-density polyethylene compatibilizer for polyamide-6/high-density polyethylene blend: effect of neutralization level on compatibility of the blend, Polymer Bulletin. 70 (2013) 293–309. doi:10.1007/s00289-012-0805-z.
[33] C.A. Orr, J.J. Cernohous, P. Guegan, A. Hirao, H.K. Jeon, C.W. Macosko, Homogeneous reactive coupling of terminally functional polymers, Polymer. 42 (2001) 8171–8178. doi:10.1016/S0032-3861(01)00329-9.
[34] P.J. Carreau, D.C.R.D. Kee, R.P. Chhabra, Rheology of Polymeric Systems: Principles and Applications, Hanser Pub Inc, Munich ; New York : Cincinnati, 1997.
[35] R.G. Larson, 6. Particulate suspensions, in: The Structure and Rheology of Complex Fluids, Oxford University Press, New York - Oxford, 1999: pp. 261–323.
[36] I.M. Ward, J. Sweeney, 2. The Mechanical Properties of Polymers: General Considerations, in: Mechanical Properties of Solid Polymers, John Wiley & Sons, 2012: pp. 19–29.
[37] G.H. Michler, 10. Micromechanical Mechanisms of Toughness Enhancement in Nanostructured Amorphous and Semicrystalline Polymers, in: Mechanical Properties of Polymers Based on Nanostructure and Morphology, CRC Press, 2016. doi:10.1201/9781420027136.

[38] A.A. Collyer, Rubber Toughened Engineering Plastics, Springer Science & Business Media, 2012.
[39] R.W. Nunes, J.R. Martin, J.F. Johnson, Influence of molecular weight and molecular weight distribution on mechanical properties of polymers, Polymer Engineering & Science. 22 (1982) 205–228. doi:10.1002/pen.760220402.
[40] S. Henning, Michler, 7. Micromechanical Deformation Mechanisms in Polyolefins: Influence of Polymorphism and Molecular Weight, in: Mechanical Properties of Polymers Based on Nanostructure and Morphology, CRC Press, 2016. doi:10.1201/9781420027136.
[41] C.E. Scott, S.K. Joung, Viscosity ratio effects in the compounding of low viscosity, immiscible fluids into polymeric matrices, Polymer Engineering & Science. 36 (1996) 1666–1674. doi:10.1002/pen.10563.
[42] H.E. Burch, C.E. Scott, Effect of viscosity ratio on structure evolution in miscible polymer blends, Polymer. 42 (2001) 7313–7325. doi:10.1016/S0032-3861(01)00240-3.
[43] P. Cassagnau, F. Fenouillot, Rheological study of mixing in molten polymers: 1-mixing of low viscous additives, Polymer. 45 (2004) 8019–8030. doi:10.1016/j.polymer.2004.09.027.
[44] J. Gimenez, P. Cassagnau, A. Michel, Bulk polymerization of ε-caprolactone: Rheological predictive laws, Journal of Rheology. 44 (2000) 527.
[45] M. Ponsard-Fillette, C. Barrès, P. Cassagnau, Viscoelastic study of oil diffusion in molten PP and EPDM copolymer, Polymer. 46 (2005) 10256–10268. doi:10.1016/j.polymer.2005.08.015.
[46] K. Yasuda, R.C. Armstrong, R.E. Cohen, Shear flow properties of concentrated solutions of linear and star branched polystyrenes, Rheol Acta. 20 (1981) 163–178. doi:10.1007/BF01513059.
[47] G. Marin, E. Menezes, V.R. Raju, W.W. Graessley, Propriétés viscoélastiques linéaires de solutions de polybutadiène en régime semi-dilué et concentré, Rheol Acta. 19 (1980) 462–476. doi:10.1007/BF01524019.
[48] D.R. Lloyd, S.S. Kim, K.E. Kinzer, Microporous membrane formation via thermally-induced phase separation. II. Liquid—liquid phase separation, Journal of Membrane Science. 64 (1991) 1–11. doi:10.1016/0376-7388(91)80073-F.
[49] H.E.H. Meijer, J.M.H. Janssen, P.D. Anderson, 3. Mixing of immiscible liquids, in: Mixing and Compounding of Polymers; Theory and Practice, 2nd edition, Carl Hanser Verlag GmbH & Co. KG, 2009: pp. 41–182.
[50] D.R. Lloyd, K.E. Kinzer, H.S. Tseng, Microporous membrane formation via thermally induced phase separation. I. Solid-liquid phase separation, Journal of Membrane Science. 52 (1990) 239–261. doi:10.1016/S0376-7388(00)85130-3.

Chapter 5 – Use of functional PE oligomers as interface agents in glass fibre-reinforced HDPE

Table of contents

1. Introduction

Glass fibre-reinforced thermoplastics constitute an important category of composite materials, as many industrial applications require both excellent mechanical properties and light weight, while reducing costs at the same time.[1,2] For these reasons, they have been the subject of considerable industrial and scientific interest for the past decades and therefore studied in many aspects.

The reinforcement of polymers, which corresponds to the enhancement of their mechanical properties, mainly relies on the quality of the interfacial interactions between the reinforcing filler and the polymer matrix to ensure a proper load transfer under mechanical solicitation.[3] In the case of glass fibres, a good matrix-filler interfacial adhesion is commonly obtained by surface treatment of the fibres with the appropriate sizing.[4] Consequently, most investigations on the improvement of polymer-glass fibre interfacial adhesion have focused on the development of efficient sizing formulations involving silane coupling agents[5,6] rather than on oligomeric or polymeric additives.

On the other hand, one of the major issues with discontinuous glass fibre-reinforced thermoplastics is certainly their processing, which requires the incorporation of high amounts of rigid, non-spherical particles, thus resulting in very high viscosity suspensions. From a rheological point of view, most investigations on the viscoelastic behaviour of such fibrous composites are conducted in dilute regimes, although some studies on concentrated fibre suspensions are available.[7–10] Additionally, while the use of dispersants is documented in the case of highly filled systems involving micron- or submicron-sized fillers (ceramics, minerals, metal oxides, etc.)[11–14], it seems that the reduction of interparticle interactions in concentrated fibre suspensions has not been studied extensively.

As a consequence, the aim of the experimental work reported in this chapter was to investigate the use of functional polyethylene oligomers as dispersing and coupling agents in HDPE reinforced with discontinuous glass fibres (GF), with the underlying objectives of improving both the processability and the mechanical properties of such systems. In the first experimental part of this study (Section 3.1), the dispersing ability of a functional PE oligomer was assessed by batch processing approach along with rheological analysis of HDPE/GF systems. The impact of this functional PE oligomer on the mechanical properties of such composite blends was then determined to serve as a proof of concept for further trials (Section 3.2). Lastly, a screening of PE oligomers with various functional groups was carried out in order evaluate the influence of glass fibre-coupling agent chemical interactions on the mechanical properties of HDPE/GF composite blends (Section 4).

2. Short literature review

Polymers can be reinforced with a wide variety of fillers[1], an important class of which are glass fibres. Such reinforcement fillers come in various forms, such as mats, rovings, chopped strands or milled fibres, depending on the targeted application.[15] The main advantage of discontinuous glass fibres is the possibility to associate them with thermoplastics using conventional processing and forming methods such as extrusion and injection moulding.[16] More specifically, chopped strand glass fibres (with a typical diameter of 10-20 μm and a typical length of 3-5 mm[17]) allow for this type of processes while providing strong mechanical reinforcement, compared to milled fibres or other typical reinforcement fillers.[10] However, the processing of polymers filled with chopped strand glass fibres may be challenging as these particles are characterized by very high aspect ratios, thus deeply influencing the flow properties of such suspensions.

2.1. Rheology of suspensions and dispersion of glass fibres

The rheological behaviour of filler polymers depends on both the characteristics of the filler (aspect ratio, stiffness, surface chemistry) and the characteristics of the polymer matrix (viscosity, chemical nature) as well as the interactions between those constituents.[18] Setting aside chemical interactions and matrix viscosity, the viscosity of particle suspensions is known to increase with increasing the volume fraction and/or the aspect ratio[19–23], as illustrated in Figure 1.

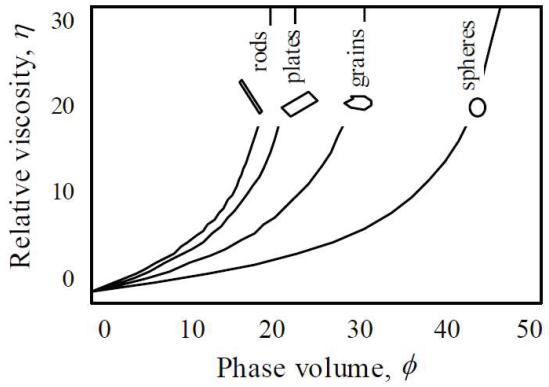

Figure 1. Relative viscosity as a function of volume fraction for various particle shapes[19]

Therefore, lower volume fractions are achievable with prolate or rod-like particles (such as glass fibres) compared to their spherical counterparts.[24,25] The consequences of this are both theoretical, as the maximum packing fraction is an important parameter in most mathematical models describing the rheological behaviour of particle suspensions, and practical, as it prevents compounders from achieving very high glass fibre contents in reinforced polymers.

While the flow properties of polymers is hardly affected by the presence of fibres at low volume fractions[9,23], their viscoelastic behaviour may change dramatically at higher volume fractions and

aspect ratios as the probability of fibre-fibre interactions increases.[22,26,27] Indeed, the flow properties of non-Brownian suspensions, such as glass fibre suspension, are influenced by viscous interactions (hydrodynamic forces exerted by the polymer matrix on the particles) as well as colloidal interactions.[28,29] The latter typically consist in interparticle interactions arising from the contacts between particles, which are influenced by several parameters such as the size and shape of the particles, as well as their surface chemistry.[30]

Such interactions may be used to induce repulsion (i.e. overcome attracting forces) between the particles in suspension by introducing appropriate chemical species in the system. A common strategy to achieve this is the use of polymeric dispersants to provide steric stabilization to the particles.[30] This strategy requires strong anchoring to the surface of the particles[11], which can occur through several modes depending on the structure of the dispersant, as illustrated in the work of Lewis[28] (see Figure 2).

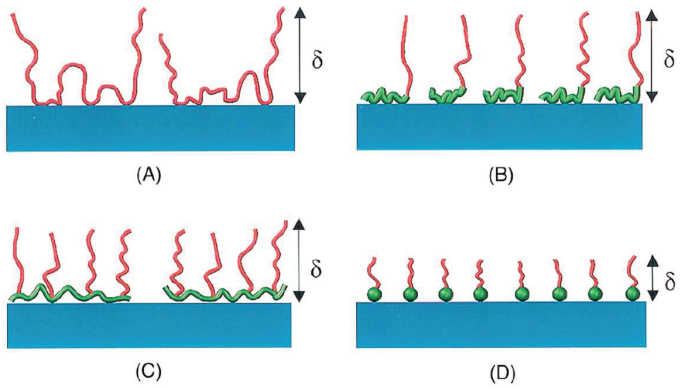

Figure 2. Schematic representation of the adlayer conformation depending on the molecular structure of the adsorbed polymeric dispersant: (A) homopolymer, (B) diblock copolymer with a short anchor block, (C) graft copolymer with an anchored backbone and (D) surfactant structure with a functional anchoring group[28]

Consequently, the chemical nature and structure of the dispersant should be carefully chosen depending on the type of filler as well as the type of dispersion medium.[12,31,32] Several mechanisms for the adsorption of polymeric dispersants onto various filler surfaces are well described in the literature.[13] Among these mechanisms, chemisorption is usually preferred as it provides a strong and durable chemical interaction between the adsorbed species and the filler through covalent bonding.[33]

Nevertheless, while polymer dispersants have been the subject of substantial research efforts in the case of systems involving micron- or submicron-sized fillers, it seems that the reduction of interparticle interactions during the processing of fibre-reinforced polymers has not been investigated extensively. The main reasons for this might be that discontinuous fibres are less prone to agglomeration compared to other reinforcing fillers[34] and that favourable matrix-filler interactions leading to an efficient dispersion are usually ensured by surface treatment ("sizing") of the fibres.[4,15]

2.2. Reinforcement of polymers with glass fibres

From a practical point of view, the reinforcement of polymers is defined as the enhancement of mechanical properties such as stiffness, tensile strength, tear strength, cracking resistance, fatigue resistance or abrasion resistance.[35] In that respect, glass fibres are good candidates as reinforcement fillers thanks to their interesting mechanical properties and moderate cost.[1] However, the major issue with glass fibres is their incompatibility with organic matrices such as polymers due to their chemical nature. Indeed, in composite materials, reinforcement arises from weak and/or strong matrix-filler interactions providing sufficient wetting and adhesion, and the role of the matrix-filler interface is to ensure the transfer of the mechanical load from the matrix to the filler.[3] In the case of glass fibres, good compatibility with the polymer matrix is provided by surface treatment involving the deposition of a thin coating called "sizing".[36]

As briefly discussed in Chapter 2, the formulation of such glass fibre sizings is usually quite complex and involves numerous components[37], the most important of which are film formers and coupling agents. It appears from the literature that current research trends are mostly directed towards the development of silane coupling agents to improve polymer-glass fibre interfacial adhesion.[5,6,38,39] Several authors have proposed models to describe the interpenetrated network structures formed in the interphase between the glass fibre and the sizing, thereby putting forward the availability of the coupling agents at the interface with the polymer matrix.[40–42]

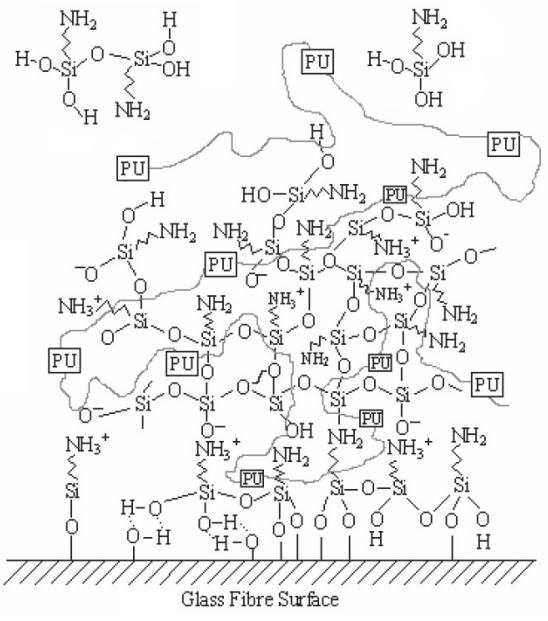

Figure 3. Schematic representation of a glass fibre-sizing interphase: an interpenetrating network between the coupling agent (hydrolysed γ-aminopropyltriethoxysilane) and the film former (polyurethane)[42]

However, considering their relatively low concentration in commercial sizings, there can be reasonable doubt that such silane coupling agents may not provide sufficient anchoring sites at the surface of glass

fibres. In that respect, other authors have suggested that the reactivity of the film former, which constitutes the major part of the sizing, may play a greater role in polymer-glass fibre interfacial adhesion.[43,44]

To this day, it seems that most investigations have focused on the development of surface treatments for glass fibres prior to their association with polymer matrices. Although this is probably an efficient strategy, considering that sizings are also designed to facilitate the manufacturing and handling of said glass fibres[15], some additional research effort could be directed towards the development of oligomeric or polymeric coupling agents to be incorporated directly upon the processing of glass fibre-reinforced polymers. It is worth noting that maleic anhydride-grafted polymers (e.g. PP-g-MA) and copolymers (e.g. SEBS-g-MA) have been successfully used in some studies together with or as an alternative to silane coupling agents in order to promote the interfacial adhesion between glass fibres and polymer matrices.[45–48] Additionally, the use of coupling agents is already the subject of numerous studies in the case of polymers reinforced with natural fibres[49,50] or carbon fibres[51,52], although the coupling agents investigated are usually limited to maleic anhydride-grafted polyolefins.

3. Impact of matrix-filler chemical interactions on the processability and mechanical properties of glass fibre-reinforced HDPE

The fillers investigated in this study were chopped strand glass fibres which are typically used in the reinforcement of thermoplastic composites. The physical characteristics of such glass fibres are recalled in Table 1.

Table 1. Characteristics of the glass fibres used in this study

Designation	Reference	Compatible resins	Fibre length (mm)	Fibre diameter (µm)
GF1	DS 2200-13P	PE, PP	4	13
GF2	DS 1128-10N	PA	4	10

As indicated in Table 1, the two types of glass fibres are designed for the reinforcement of different polymeric systems; GF1 for polyolefins and GF2 for polyamides. Type-2 glass fibres should therefore not be suitable for the reinforcement of the HDPE-based systems presently investigated due to unfavourable chemical interactions.

The surface characterization of these glass fibres (which is detailed in Chapter 2) suggested the presence of amine and/or amide as well as potential epoxy compounds in the composition of the GF2 sizing. A carboxylic acid-functionalized oligomer, Unicid 700 (U700), was therefore used as a dispersing/coupling agent. It can be noted that similar fatty acid compounds have been successfully used to promote the dispersion of zirconia particles in polymers and other non-polar media.[53–57]

3.1. Processability assessment by a batch processing and rheological approach

In this part of the study, systems involving a HDPE polymer matrix and two types of chopped strand glass fibres (GF) were investigated by a batch processing approach. This method was used in the work of Rueda[58] to quantify the maximum packing fraction of solids and assess the processability of PP/ferrite and PP/glass fibre composite blends. The objective of the experimental work presented here was to determine the impact of the chemical interactions between glass fibres and a polyethylene matrix on the processability and rheological behaviour of such highly filled suspensions in the presence of a functional PE oligomer used as a dispersant.

3.1.1. Batch processing

HDPE/GF and HDPE/U700/GF composite blends were achieved using a batch internal mixer at a temperature of 180 °C. Following the protocol described in Chapter 2, the HDPE matrix and the PE oligomer were introduced simultaneously at t = 0 min and the glass fibres were added at t = 5 min. The mixing torque was recorded during the blending process.

The amount of glass fibres incorporated varied from 5 vol% to 60 vol% (roughly 10 wt% to 80 wt%) and the concentration of Unicid 700 was set at 5 wt% of the polymer phase. The amount of functional PE oligomer per unit of glass fibre surface area was consequently decreased with the increasing fraction of glass fibres. While it could be argued that the amount of dispersant should be set according to the filler content, this was done in order to avoid any saturation of the HDPE matrix by the PE oligomer (see conclusions from Chapter 3). Another reason to do that is to keep the viscosity of the polymer phase constant, as it may affect the state of dispersion as well as fibre breakage upon mixing[59,60], although it was previously shown (see Chapter 3) that the addition of a PE oligomer to HDPE resulted in viscosities in the same order of magnitude as that of neat HDPE.

In Figure 4, the mixing torque recorded after complete homogenization of each composite blend (i.e. when the system has reached a steady state) is displayed as a function of the volume fraction (φ) of glass fibres. The corresponding weight fractions are indicated on the top X axis.

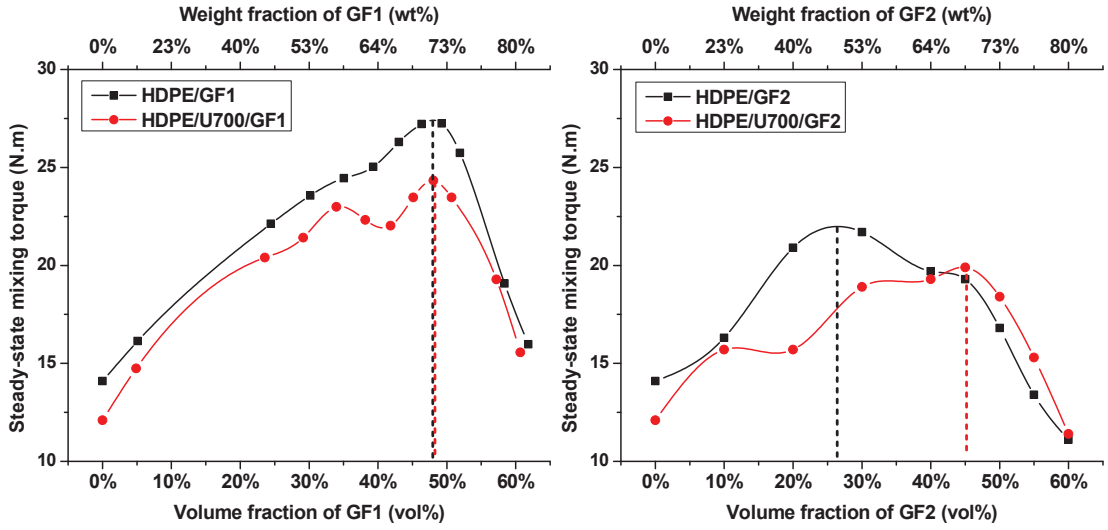

Figure 4. Steady-state mixing torque for HDPE/GF1 (left) and HDPE/GF2 (right) composite blends with and without U700

As expected, the steady-state mixing torque increased with the glass fibre content over a wide range of volume fractions. However, above a certain volume fraction, the steady-state mixing torque decreased with the increasing glass fibre content. The composite blends obtained for volume fractions beyond the maximum value of steady-state mixing torque progressively became incohesive and the glass fibres were no longer well dispersed as a result of insufficient wetting by the polymer matrix.

In highly filled systems, the maximum packing fraction of solids (φ_m) is defined as the maximum packing arrangement of particles while still retaining a continuous material.[34] However, in the case of non-ideal particles such as glass fibres, the maximum volume fraction that is achievable while still retaining a continuous polymer phase is usually well below that value. The volume fraction of glass fibres at which the steady-state mixing torque reached its maximum value was therefore assimilated to a critical volume fraction (φ_c). It is worth noting that in rheological terms, φ_c is usually refers to the percolation threshold,

which is defined as the volume fraction at which the particles start to form a three-dimensional network, thus resulting in the viscosity of the suspension tending towards infinity. However, the difference between φ_c and φ_m can be rather difficult to assess for some systems, especially in the case of fillers with high aspect ratios.[30]

For each system, the volume fraction corresponding to the maximum value of steady-state mixing torque is illustrated by a dotted line on Figure 4. The corresponding critical volume fractions φ_c measured by this method are given in Table 2.

Table 2. Critical volume fractions (φ_c) measured from the steady-state mixing torque curves

System	φ_c
HDPE/GF1	0.48
HDPE/U700/GF1	0.48
HDPE/GF2	0.27
HDPE/U700/GF2	0.45

It can be noted that in the absence of Unicid 700 the critical volume fraction is higher in the case of GF1 (compared to GF2), which was attributed to the fact that the sizing of type-1 glass fibres was designed for the reinforcement of polyolefin-based systems. Consequently, the critical volume fraction remains unchanged with the addition of Unicid 700 as the filler already has a good affinity with the polymer matrix. On the other hand, a shift in the maximum steady-state mixing torque in the presence of Unicid 700 is observed in the case of type-2 glass fibres.

In theory, the critical volume fraction should on depend on particle characteristics[61] such as aspect ratio or size distribution, which may be dependent on processing conditions (especially the aspect ratio in the case of glass fibres). However, previous studies showed that the maximum packing fraction could also be dependent on the chemical species adsorbed on the surface of the filler.[58] The present results therefore indicate that Unicid 700 may act similarly to a coupling agent between type-2 glass fibres and the HDPE matrix, thus leading to favourable matrix-filler interactions and increasing the wetting of glass fibres by the polymer matrix. They also suggest that such functional oligomer may act as a dispersant adsorbed onto the surface of glass fibres, thus reducing attractive forces by ensuring steric stabilization of the fibre suspension.[28]

It was also observed that the presence of the PE-COOH oligomer in such systems resulted in lower mixing torque after complete homogenization, indicating a reduction of the overall viscosity of the blend, which could be attributed both to the plasticizing of the polymer phase by the low molar mass PE oligomer in the melt and to the reduction of interparticle interactions.

3.1.2. Rheological analysis

As explained previously, the rheological behaviour of filled polymers depends on both the characteristics of the filler (aspect ratio, stiffness, surface chemistry) and the characteristics of the polymer matrix

(viscosity, chemical nature) as well as on the interactions between those constituents.[18] In such non-Newtonian suspensions of non-Brownian particles (glass fibres in this case), the flow regime is determined by the volume fraction (φ) of particles.[62,63] In their study on the rheological behaviour of polypropylene filled with short glass fibres, Rueda et al.[10] determined the onsets of the different concentration regimes in terms of volume fraction of glass fibres, based on the theories of Doi-Edwards and Onsager. These concentration regimes are closely linked to the aspect ratio of the fillers, which is known to have a controlling influence on the flow properties of highly filled polymers.[20,21,23]

The aspect ratio (p) of rod-like particles such as glass fibres can be defined as the ratio of the characteristic length (L) to the characteristic diameter (D).[64] In the present work, type-2 glass fibres have a diameter of 10 μm and an initial length of 4 mm. However, after breakage (upon processing with HDPE) the characteristic length of glass fibres in HDPE/GF2 and HDPE/U700/GF2 composite blends was determined to be roughly 200 μm. Consequently, the aspect ratio of the glass fibres in those systems was calculated to be approximately $p \approx 20$. The values of φ defining the transitions between the different concentration regimes were calculated accordingly and are given in Table 3.

Table 3. Transitions between concentration regimes calculated in terms of glass fibre volume fraction, according to the theories of Doi-Edwards and Onsager[10]

Regime transition	Dilute to semi-dilute $\varphi = (1/p)^2$	Semi-dilute to isotropic concentrated $\varphi = 1/p$	Isotropic concentrated to nematic $\varphi = 3.3/p$
φ (p ≈ 20)	0.003	0.05	0.17

According to those values, the glass fibres in composite blends with up to 17 vol% GF2 should be randomly oriented while interparticle interactions should generate anisotropy above 17 vol% GF2, thus influencing the rheological properties of those systems.[65]

HDPE/GF2 and HDPE/U700/GF2 composite blends prepared by batch mixing were characterized by rheometry. Following the protocol described in Chapter 2, frequency sweep oscillatory tests were performed at a temperature of T = 180 °C and a set strain of ε = 0.05 %. The corresponding storage modulus curves are displayed in Figure 5 and the two systems are compared in Figure 6.

As expected, the storage modulus increased with the addition of fibres. However, contrary to previous observations that the steady-state mixing torque (which is related to viscosity) decreased above a critical volume fraction (φ_c) of glass fibres, the viscosity of the composite blends measured by rheometry kept increasing with the filler content.

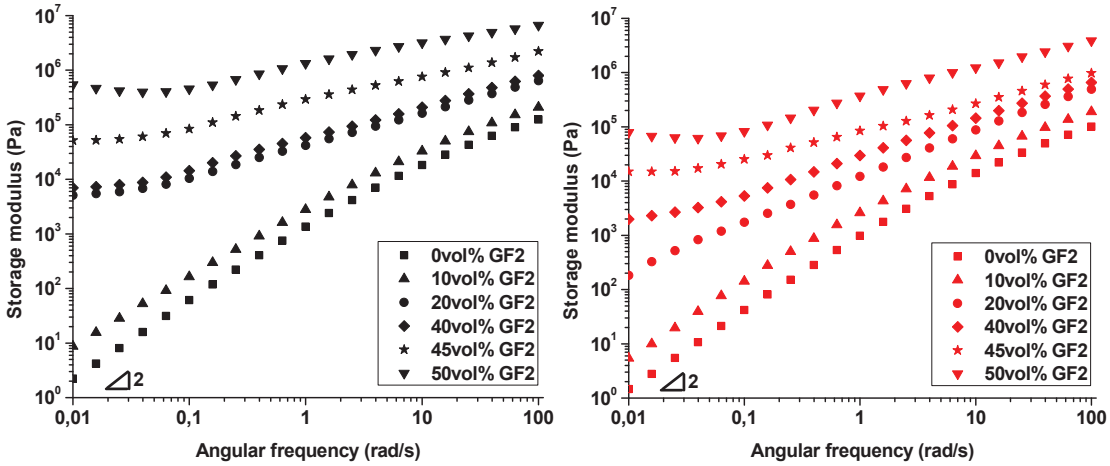

Figure 5. Storage modulus curves for HDPE/GF2 (left) and HDPE/U700/GF2 (right) composite blends

While HDPE/GF2 and HDPE/U700/GF2 systems followed similar trends, two main observations can be drawn from the storage modulus curves. Firstly, the volume fraction of glass fibres at which the viscoelastic behaviour shifted from a Newtonian behaviour (with a typical slope of 2 at low frequencies) to a percolated network behaviour (with G' tending to a plateau at low frequencies) was found to be different for the two systems. In the case of HDPE/GF2 composite blends, this shift took place between 10 vol% and 20 vol% GF2, which corresponds to the transition between the isotropic concentrated regime and the nematic regime, according to the values given in Table 3. For composite blends containing Unicid 700, the shift appeared to take place above 20 vol% GF2, indicating that the presence of the functional PE-COOH oligomer may decrease interparticle interactions through steric stabilization of the glass fibres.

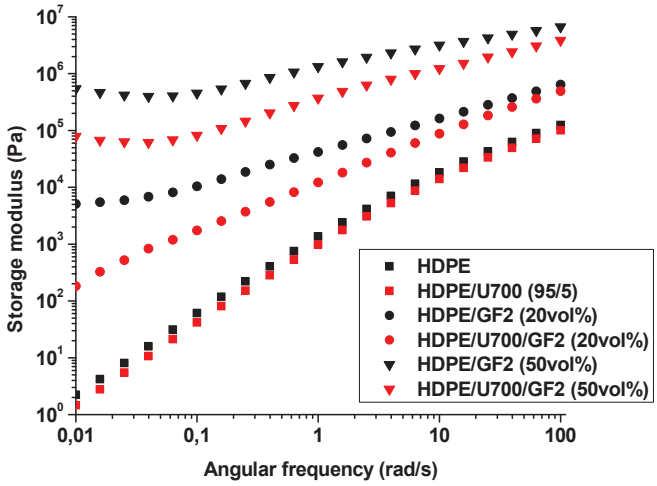

Figure 6. Storage modulus curves for HDPE/GF2 and HDPE/U700/GF2 composite blends at 0, 20 and 50 vol% GF2

The second observation, which is illustrated in Figure 6, is the decrease of the storage modulus with the addition of Unicid 700. However, considering the very similar storage modulus values between neat

HDPE and the HDPE/U700 (95/5) blend, the storage modulus changes observed in filled systems cannot be considered to be solely due to the plasticizing of the HDPE matrix in the molten state. This suggests that the addition of a functional PE-COOH oligomer to HDPE/GF2 systems leads to a reduction of fibre-fibre interactions through steric stabilization, which is consistent with the observations made in previous studies involving similar fatty acid as dispersants in concentrated suspensions.[11,53,54,66,67]

Lastly, it was also observed that the moduli crossover point (i.e. the frequency ω_{co} at which G' = G") was shifted towards lower frequencies with the increasing volume fraction of glass fibres, as illustrated in Figure 7 for HDPE/GF2 composite blends.

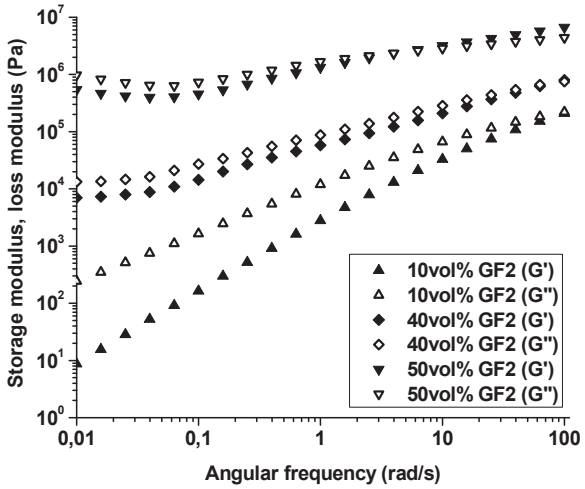

Figure 7. Storage modulus (G') and loss modulus curves (G") for HDPE/GF2 composite blends at 10, 40 and 50 vol% GF2

The crossover point is closely linked to the characteristic elastic time (λ) of the system. Such relationship is described by the following equation:[68]

$$\lambda = \frac{G'}{G''.\omega}$$

The characteristic elastic time $\lambda = 1/\omega_{co}$ (for G' = G") was therefore determined for both HDPE/GF2 and HDPE/U700/GF2 composite blends (see Figure 8).

Variations of the characteristic elastic time were observed to follow a trend which could be described by a model analogous to the Krieger-Dougherty model for particle suspensions.[69,70] The model used to fit the experimental data was defined by the following equation:

$$\lambda_r = \frac{\lambda}{\lambda_{HDPE}} = \left(1 - \frac{\phi}{\phi_c}\right)^{-k\phi_c}$$

where λ_r is the relative (normalized) characteristic elastic time, λ is the characteristic elastic time of the composite blend, λ_{HDPE} is the characteristic elastic time of the HDPE matrix, φ is the volume fraction of glass fibres, φ_c is the critical volume fraction of glass fibres and k is an empirical parameter relating to

the intrinsic viscosity of the glass fibres. The normalized values of characteristic elastic time ($\lambda_r = \lambda/\lambda_{HDPE}$) are plotted against the volume fraction of glass fibres in Figure 8.

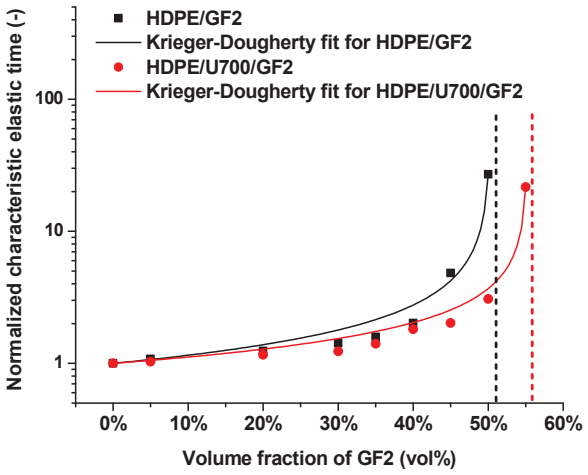

Figure 8. Normalized characteristic elastic time for HDPE/GF2 and HDPE/U700/GF2 composite blends

The values of the φ_c and k parameters obtained from the fitting of this equation are given in Table 4.

Table 4. Values φ_c and k obtained from the fitting of the equation derived from the Krieger-Dougherty model

System	φ_c	k
HDPE/GF2	0.50	1.27
HDPE/U700/GF2	0.57	1.01

The critical volume fraction (φ_c) was found to be higher in the presence of the functional PE-COOH oligomer, which is consistent with the observations made in Section 3.1.1 that such functional oligomer may act as a dispersant by reducing interparticle interactions through steric stabilization of the glass fibres.[28]

Although the values of relative characteristic elastic time did not exactly match the model, it is worth noting that HDPE/GF2 and HDPE/U700/GF2 systems are quite different from the ideal hard sphere suspensions described by the Krieger-Dougherty model, meaning that discrepancies between the model and the experimental data were to be expected.

3.2. Preliminary extrusion trials on a laboratory scale

Following the batch processing trials, HDPE/GF composite blends were prepared by extrusion in order to assess the impact of Unicid 700 (U700) on the maximum filler level as well as on the mechanical properties of HDPE/GF systems. Considering the results from Section 3.1, only type-2 glass fibres (designed for the reinforcement of polyamides) were studied as their chemical incompatibility with the polyethylene matrix made them a good indicator of the dispersing/coupling effect of Unicid 700. In order to dissociate the plasticizing effect of this low molar mass PE-COOH oligomer (on the polymer

phase) from matrix-filler chemical interactions, a non-functional PE oligomer, Polywax 725 (W725), was also used in a series of control samples.

3.2.1. Effect of the functional group on processability

HDPE/GF2, HDPE/W725/GF2 and HDPE/U700/GF2 composite blends were prepared using a co-rotating twin-screw extruder (L/D = 60) at a temperature of 180 °C and a flow rate of 3 kg/h, according to the protocol described in Chapter 2. Dry-blends of HDPE and PE oligomers (U700, W725 or none) were fed through the main hopper into the first block of the extruder, while the glass fibres (GF2) were introduced through a side feeder at block n°4 (L/D = 20).

The concentration of PE oligomers was set at 5 wt% of the polymer phase and the fraction of glass fibres incorporated varied from 5 vol% to 70 vol% (roughly 10 wt% to 85 wt%), similarly to the batch-processed composite blends.

The process variables recorded during the extrusion of the blends are represented in Figure 9. They correspond to the mean values measured once the process had reached a steady state. The mixing torque is expressed as a percentage of the maximum torque that the motor of the extruder is capable of providing. The pressure variable corresponds to the value measured at the die of the extruder.

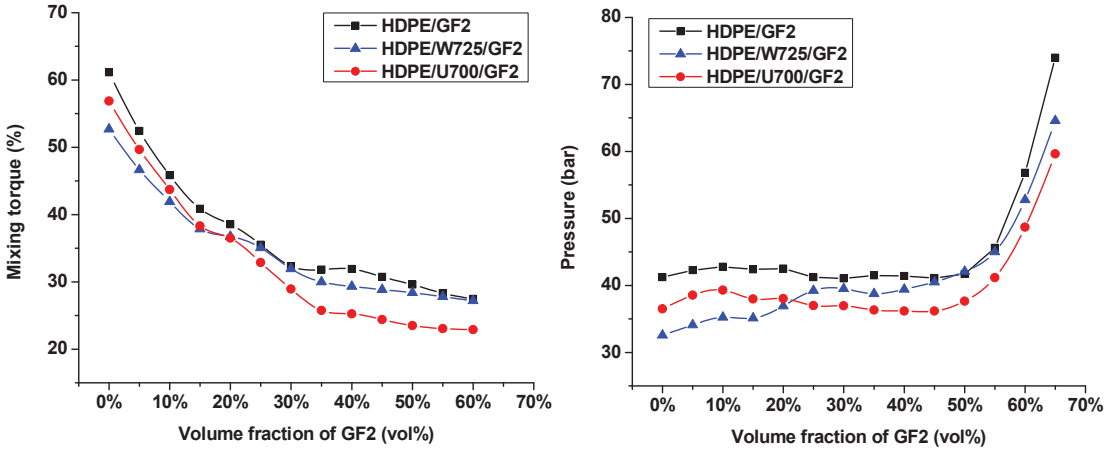

Figure 9. Process variables recorded during the extrusion of HDPE/GF2 blends: mixing torque (left) and pressure (right)

A maximum volume fraction of 65 vol% was achieved, regardless of the composition of the polymer phase. Further increase in the filler level resulted in an overload of the extruder.

The recorded mixing torque and pressure values indicate that the overall viscosity of the composite blends was reduced with the addition of PE oligomers, thus slightly improving processability. Furthermore, it was observed that the two PE oligomers did not have the same impact on processability depending on the filler level. Indeed, the mixing torque and pressure values were found to be lower in the presence of Polywax 725 up to 15-20 vol% glass fibres, while a more significant improvement of processability was observed in the presence of Unicid 700 at higher volume fractions. This suggests that

the effect of the non-functional PE oligomer is limited to the plasticizing of the polymer phase in the melt, while the introduction of the PE-COOH oligomer has an impact on interparticle interactions in highly filled systems.

3.2.2. Effect of the functional group on mechanical properties

The mechanical properties of the HDPE/GF2 composite blends obtained by extrusion were measured in order to assess the impact of the functional and non-functional PE oligomers on the matrix-filler interfacial adhesion.[71,72] Young's modulus (E), yield stress (σ_y) and strain at break (ε_b) were determined by tensile testing according to the protocol described in Chapter 2. The measured values are given in Table 5 and graphically represented in Figure 10.

Due to the limitations of the injection moulding equipment (because of the very high viscosity of these highly filled materials), only the composite blends with 0-30 vol% GF2 were tested.

Table 5. Mechanical properties of HDPE/GF2, HDPE/W725/GF2 and HDPE/U700/GF2 composite blends depending on the volume fraction of GF2

HDPE/GF2			
Volume fraction of GF2 (vol%)	**E (MPa)**	**σ_y (MPa)**	**ε_b (%)**
0	600 ± 100	25.9 ± 0.8	650 ± 90
5	1300 ± 100	26.5 ± 0.6	100 ± 10
10	2500 ± 300	27.3 ± 0.4	90 ± 10
15	3400 ± 300	27.1 ± 0.3	80 ± 10
20	4100 ± 0	25.4 ± 0.5	70 ± 10
25	4600 ± 200	25.6 ± 0.4	30 ± 0
30	5400 ± 200	25.8 ± 0.3	10 ± 0
HDPE/W725/GF2			
Volume fraction of GF2 (vol%)	**E (MPa)**	**σ_y (MPa)**	**ε_b (%)**
0	700 ± 0	25.5 ± 0.1	220 ± 70
5	1600 ± 100	27.2 ± 0.5	120 ± 10
10	2600 ± 100	27.7 ± 0.3	110 ± 10
15	3500 ± 500	27.0 ± 0.4	90 ± 10
20	4400 ± 400	26.2 ± 0.2	70 ± 10
25	4300 ± 600	26.5 ± 0.3	30 ± 0
30	5400 ± 200	26.1 ± 0.7	10 ± 0
HDPE/U700/GF2			
Volume fraction of GF2 (vol%)	**E (MPa)**	**σ_y (MPa)**	**ε_b (%)**
0	800 ± 0	25.6 ± 0.2	210 ± 20
5	2400 ± 100	29.0 ± 0.5	100 ± 10
10	3200 ± 100	29.2 ± 0.5	80 ± 0
15	4400 ± 200	29.4 ± 0.6	60 ± 10
20	5700 ± 100	30.0 ± 0.9	50 ± 0
25	6700 ± 300	32.6 ± 0.9	20 ± 0
30	7800 ± 400	36.4 ± 0.6	10 ± 0

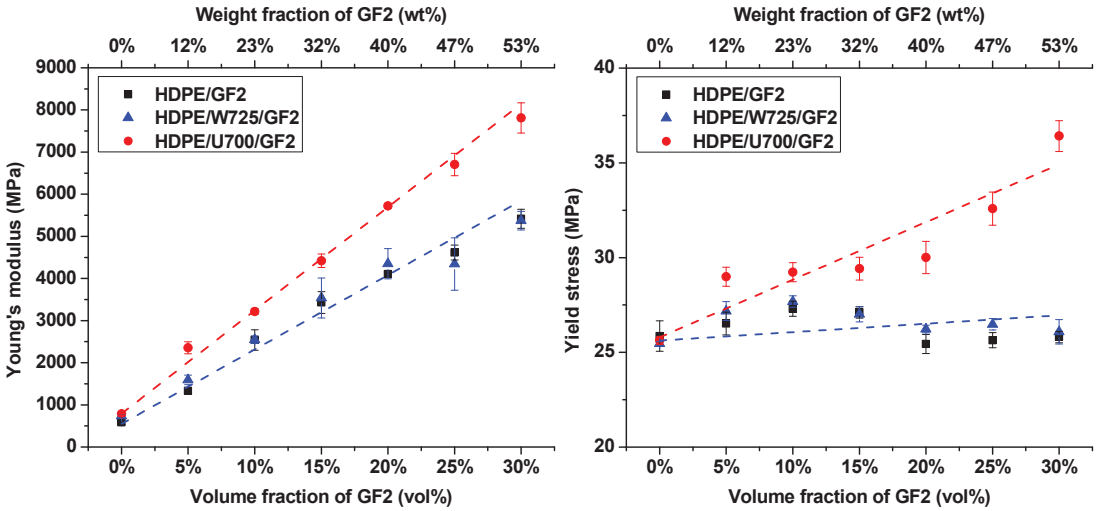

Figure 10. Young's modulus (left) and yield stress (right) of HDPE/GF2, HDPE/W725/GF2 and HDPE/U700/GF2 composite blends as a function of the volume fraction of GF2

As expected, the incorporation of glass fibres resulted in an increase of Young's modulus while decreasing the elongation at break. The yield stress of HDPE/GF2 and HDPE/W725/GF2 systems did not show significant variations, which was attributed to the poor quality of the matrix-filler interphase as a result of the incompatibility between type-2 glass fibres and polyolefin compounds.[4]

While the presence of a non-functional PE oligomer (Polywax 725) did not impact the mechanical properties of HDPE/GF2 composite blends, the use of a functional PE-COOH oligomer (Unicid 700) resulted in a significant improvement of mechanical properties. It was also observed that the difference in Young's modulus and yield stress values between HDPE/U700/GF2 composite blends and the other systems increased with the filler content. For instance, at a volume fraction of 30 vol% GF2, Young's modulus was increased by 44 % and yield stress was increased by 41 % in the case of the HDPE/U700/GF2 blend compared to HDPE/GF2.

Such improvement of the mechanical properties can be attributed either to an improved interfacial adhesion between the polymer matrix and the glass fibres or to an increase in fibre length.[71–73] In this case, the increase in fibre length could be the result of either less fibre breakage during the blending process due to the decreased viscosity of the polymer phase (plasticizing effect in the molten state) and/or to modified fibre-fibre interactions (dispersing effect). However, considering the minor decrease in matrix viscosity as well as the decrease in the viscosity of composite blends (see Section 3.1.2), an increase in fibre length is very unlikely. It can therefore be considered that the fibre length distribution is very similar in all three systems. Consequently, the improvement of mechanical properties was attributed to the improved matrix-filler interfacial adhesion as a result of favourable chemical interactions between the functional PE-COOH oligomer and type-2 glass fibres.

Additionally, these results show that the impact of the functional PE-COOH oligomer is more significant at higher filler contents, which is consistent with the general idea that the impact of polymeric

dispersants becomes more significant when increasing the solid content in suspensions.[30] Consequently, the volume fraction of glass fibres was set at 30 vol% for further trials (see Section 4).

3.2.3. Effect of the oligomer concentration on mechanical properties

From an industrial point of view, it is obviously in the compounder's best interest to use as little additives as possible to achieve optimal properties, as their cost may be greater than that of the polymer matrix or that of the filler.[2] Previous studies on the use of fatty acids as dispersants in zirconia suspensions and zirconia-filled polyethylene showed that the dispersant concentration should be finely tuned in order to achieve optimal rheological properties and that an excess of dispersant could actually be detrimental from a processing point of view. For instance, in their investigations on the use of fatty acids as dispersants in polyethylene/zirconia systems, Hanemann et al.[74,75] found that the optimum dispersant concentration was 2.2 mg/m² (referring to the specific surface area of filler) for filler contents of 50 vol% and more, which corresponds to a carboxylic acid functional group concentration of 7.7 µmol/m² in the case of stearic acid. This optimum concentration value is obviously dependent on the type of filler that is used, especially in terms of surface chemistry.

HDPE/W725/GF2 and HDPE/U700/GF2 composite blends with various amounts of PE oligomers were prepared by extrusion in order to study the effect of the PE oligomer concentration on the mechanical properties of such systems. Considering the results from the previous section, the filler content was set at 30 vol% GF2 (roughly 53 wt%), which is the volume fraction of glass fibres for which the effect of the functional PE-COOH oligomer is the most significant. The PE oligomer concentrations investigated were 0.5, 2 and 5 wt% of the polymer phase.

The concentrations of functional PE-COOH oligomer (Unicid 700) and corresponding concentrations of carboxylic acid functional groups with respect to the surface area of glass fibres were thus calculated. They are indicated in Table 6 in the case of a HDPE/U700/GF2 composite blend with 30 vol% GF2.

Table 6. Concentrations of Unicid 700 and corresponding concentrations of carboxylic acid groups, with respect to the surface area of glass fibres, depending on the concentration of Unicid 700 in the blend at 30 vol% GF2

Oligomer concentration (wt%)	Concentration of Unicid 700 (mg/m²), relative to the surface area of GF	Concentration of COOH (µmol/m²), relative to the surface area of GF
0	0	0
0.5	28	31
2	111	124
5	277	311

Young's modulus (E), yield stress (σ_y) and strain at break (ε_b) were determined by tensile testing according to the protocol described in Chapter 2. The measured values are given in Table 7 and graphically represented in Figure 11.

Table 7. Mechanical properties of HDPE/W725/GF2 and HDPE/U700/GF2 composite blends (30 vol% GF2) depending on the concentration of PE oligomer

HDPE/W725/GF2			
Oligomer concentration (wt%)	**E (MPa)**	**σ_y (MPa)**	**ε_b (%)**
0	5400 ± 200	25.8 ± 0.3	14 ± 2
0.5	5300 ± 400	25.9 ± 1.1	14 ± 1
2	5600 ± 600	26.2 ± 0.4	13 ± 1
5	5400 ± 200	26.1 ± 0.7	14 ± 2
HDPE/U700/GF2			
Oligomer concentration (wt%)	**E (MPa)**	**σ_y (MPa)**	**ε_b (%)**
0	5400 ± 200	25.8 ± 0.3	14 ± 2
0.5	5500 ± 500	26.9 ± 0.5	14 ± 1
2	5800 ± 600	29.2 ± 1.1	10 ± 1
5	7800 ± 400	36.4 ± 0.8	11 ± 1

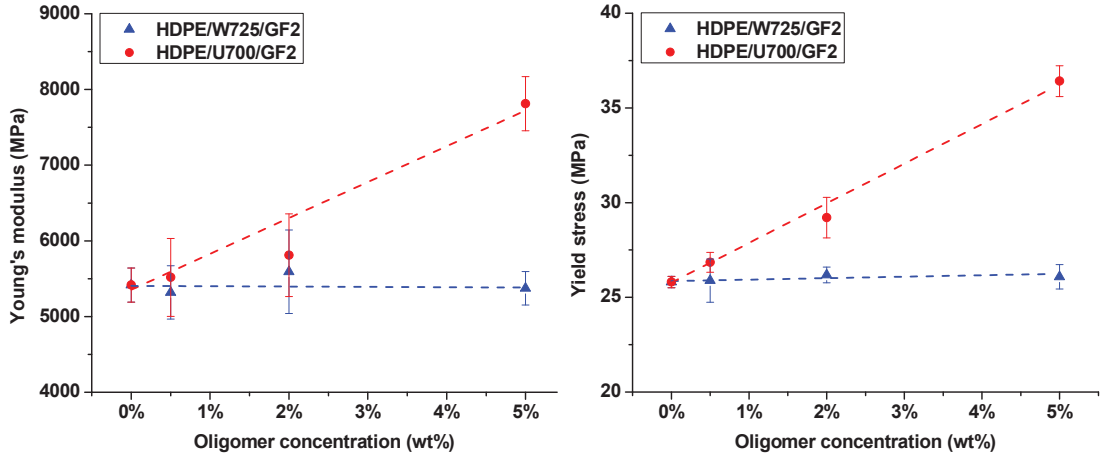

Figure 11. Young's modulus (left) and yield stress (right) of HDPE/W725/GF2 and HDPE/U700/GF2 composite blends (30 vol% GF2) as a function of the concentration of PE oligomer

The mechanical properties of HDPE/W725/GF2 systems remained unaffected by the variations of the Polywax 725 concentration, which is consistent with previous observations (see Section 3.2.2) that the presence of a non-functional PE oligomer does not improve the mechanical properties of HDPE/GF2 systems. In the case of HDPE/U700/GF2 systems, the mechanical properties were significantly improved with 5 wt% Unicid 700 but remained rather similar to that of HDPE/W725/GF2 systems at lower concentrations (0.5 wt% and 2 wt%).

As a consequence, the concentration of PE oligomers was set at 5 wt% of the polymer phase for the following trials (see Section 4) in order to achieve a sufficient improvement of the mechanical properties of HDPE/GF2 composite blends.

4. Enhancement of the mechanical properties of HDPE/GF composite blends: screening of functional PE oligomers

As explained previously, the reinforcement of a polymer relies on the interactions between the polymer matrix and the reinforcing filler.[35] It was shown in previous Section 3 that a PE oligomer with an appropriate functional group can be used to improve the matrix-filler interface in HDPE/GF systems. However, in order to achieve a good dispersion of the glass fibres as well as a satisfactory improvement of mechanical properties, such functional PE oligomers should be strongly anchored to the surface of glass fibres in order to avoid desorption.[28] For this reason, several PE oligomers with various types of functional groups were tested in this part of the study.

4.1. Selected functional PE oligomers

As mentioned previously, type-2 glass fibres are designed for the reinforcement of polyamides, according to the information provided by the manufacturer.

SEM observations (see Chapter 2) of the glass fibres revealed an inhomogeneous sizing distribution on the surface of the glass fibres. It was therefore hypothesized that there may be bare glass areas at the surface of those glass fibres; hence a potential reactivity towards alkoxysilane compounds.[76] Such functional PE oligomers were also selected accordingly.

Additionally, the surface characterization of the glass fibres (see Chapter 2) suggested the presence of amine and/or amide as well as potential epoxy compounds in the composition of the sizing of type-2 glass fibres. Consequently, PE oligomers with adequate functional groups (carboxylic acid, maleic anhydride and amine) were selected to be incorporated in HDPE/GF2 systems.

The list of commercial and tailor-made functional PE oligomers/polymers selected for this study is detailed in Table 8.

Table 8. List of functional PE oligomers and polymers used for the reinforcement of HDPE/GF2 composite blends

Designation	Functional group	Molar mass (g/mol)	Functionality (%)
Polywax 725	-	800	-
Unicid 700	Carboxylic acid	600	63[(1)]
Ceramer 1608	Maleic anhydride	800	150[(1)]
Exxelor PE 1040	Maleic anhydride	17 000	170[(2)]
PE-NH_2	Amine	1 700	97[(3)]
PE-NH_2	Amine	4 000	97[(3)]
PE-Si(OMe)(Me)$_2$	Mono-alkoxysilane	1 300	84[(3)]
PE-Si(OMe)$_3$	Tri-alkoxysilane	1 300	81[(3)]

[(1)] Determined from the acid and saponification values provided with the technical datasheets

[(2)] Determined from the maleic anhydride graft level reported on the technical datasheet

[(3)] Determined by ^{1}H NMR by the C2P2 laboratory

As explained in Chapter 2, the PE oligomers with amine and alkoxysilane functional groups were synthesized by the C2P2 laboratory, while the others are commercially available products. Apart from Ceramer 1608 and Exxelor PE 1040, all selected PE oligomers were mono-end-functional.

It is worth noting that two amine-functionalized PE oligomers with different molar masses (respectively 1700 and 4000 g/mol) were tested in order to study the impact of this parameter on the coupling ability of such functional oligomers.

The impact of those functional PE oligomers on the mechanical properties of HDPE/GF2 composite blends was compared to that of a high molar mass PE-g-MA (Exxelor PE 1040), as this type of compounds is commonly used to promote matrix-filler interfacial adhesion in reinforced polymer composites[49,51,52] and has been successfully used in some studies involving glass fibres.[47,48,77] However, it should be noted that

Lastly, Polywax 725 was used as a non-functional PE oligomer in control samples for the same reasons as stated in Section 3.2.

4.2. Mechanical properties

As some of the PE oligomers (those synthesized by the C2P2 laboratory) were only available in limited amounts, the HDPE/GF2 composite blends investigated in this part of the study were prepared using a batch internal mixer at a temperature of 180 °C following the protocol described in Chapter 2. Considering the results presented in Sections 3.2.2 and 3.2.3, the amount of glass fibres was set at 30 vol% of the total volume and the concentration of PE oligomer was set at 5 wt% of the polyethylene phase (HDPE + PE oligomer).

The mechanical properties of the composite blends were determined by tensile testing according to the protocol described in Chapter 2. The measured values of Young's modulus (E), yield stress (σ_y) and strain at break (ε_b) are given in Table 9. Young's modulus and yield stress are graphically represented in Figure 12.

Table 9. Mechanical properties of HDPE/GF2 composite blends with various functional PE oligomers and polymers

PE oligomer	E (MPa)	σ_y (MPa)	ε_b (%)
Reference	4900 ± 200	28 ± 1	12 ± 1
PE (W725)	5100 ± 200	29 ± 1	10 ± 1
PE-COOH (U700)	6200 ± 200	33 ± 2	6 ± 0
PE-g-MA (C1608)	6500 ± 200	37 ± 2	6 ± 0
PE-g-MA (E1040)	6800 ± 200	55 ± 2	4 ± 0
PE-NH_2 (1700 g/mol)	6200 ± 200	38 ± 2	4 ± 0
PE-NH_2 (4000 g/mol)	6600 ± 200	41 ± 2	4 ± 0
PE-Si(OMe)(Me)$_2$	5500 ± 200	29 ± 0	8 ± 1
PE-Si(OMe)$_3$	5100 ± 200	27 ± 0	12 ± 2

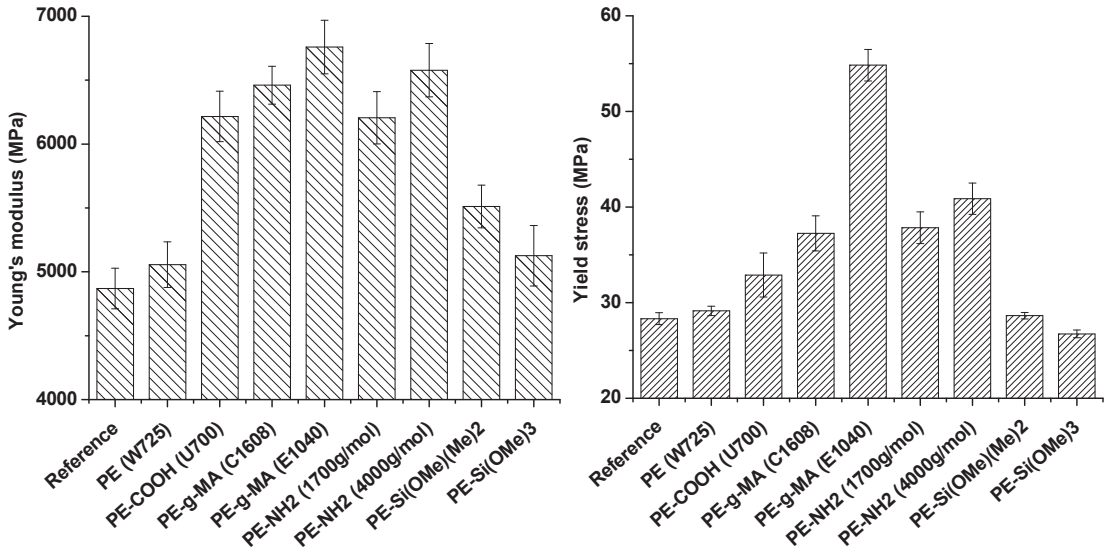

Figure 12. Young's modulus (left) and yield stress (right) values for HDPE/GF2 composite blends with various functional PE oligomers and polymers

A first observation of the data obtained for HDPE/GF2, HDPE/W725/GF2 and HDPE/U700/GF2 composite blends confirmed the trend observed in Sections 3.2.2 and 3.2.3, with a significant enhancement of the mechanical properties only in the presence of the functional PE-COOH oligomer (ΔE = +1.3 GPa and $\Delta\sigma_y$ = +5 MPa). However, this improvement was not as pronounced as previously observed. This could be due to the different processing method (batch mixing vs. extrusion) used for the preparation of the composite blends, which is known to influence both the morphology of polymer blends[78] and the breakage of glass fibres.[79–81] In the present case, batch processing should result in less fibre breakage, thus modifying the length distribution of glass fibres, which may reduce the relative impact of improving the matrix-filler interfacial adhesion.[71,73]

Secondly, the introduction of PE oligomers with alkoxysilane functional groups did not result in a significant improvement of the mechanical properties. This was attributed to the fact that there may not be enough reactive silanol sites available at the surface of the glass fibres, due to sufficient coverage by the sizing. A more surprising observation is the higher Young's modulus and yield stress in the presence of the PE-Si(OMe)$(Me)_2$ oligomer compared to the composite blend with the PE-Si$(OMe)_3$ oligomer, whereas the reactivity of such alkoxysilane compounds should increase with the number of hydrolysable alkoxy groups.[82] This may be explained by the instability of trimethoxysilane compounds, which can undergo condensation with themselves or with neighbouring alkoxysilanes in the presence of moisture[83,84], thus hindering the reaction with the glass substrate.

On the contrary, the addition of PE oligomers with carboxylic acid, maleic anhydride or amine functional groups to HDPE/GF2 systems resulted in a significant enhancement of mechanical properties, with ΔE = +1.3 to +1.6 GPa and $\Delta\sigma_y$ = +5 to +10 MPa. This shows that the introduction of PE oligomers with adequate functional groups leads to an improvement of the matrix-filler interfacial

adhesion[71,72] due to strong anchoring to the surface of glass fibres. Those results therefore suggest that such functional PE oligomers may act as coupling agents in glass fibre-reinforced polyethylene[47,48], although no coupling reaction occurs between the PE oligomer and the HDPE matrix, as it is usually the case in glass fibre sizings between silane coupling agents and film formers or more reactive polymer matrices.[39,85,86]

Lastly, it was found that the mechanical properties of HDPE/GF2 composite blends could be further improved by tuning the molar mass of the functional PE oligomers. In the case of PE-NH_2 oligomers, an increase of ΔE = +0.4 GPa and $\Delta\sigma_y$ = +3 MPa was observed when increasing the molar mass from 1500 to 4000 g/mol, although this may seem insignificant considering the standard deviation values. Nevertheless, a more significant improvement of the mechanical properties was observed when using a maleic anhydride-grafted polymer (Exxelor PE 1040, 17 000 g/mol) instead of an oligomer (Ceramer 1608, 800 g/mol) with a similar degree of functionality, especially in terms of yield stress. As already mentioned in Chapters 3 and 4, the high molar mass of Exxelor PE 1040 implies molecular entanglement with HDPE, whereas PE oligomer chains are too short.[87] This suggests that the limited improvement of mechanical properties provided by functional PE oligomers may be due to insufficient interactions (i.e. molecular entanglement in the melt and co-crystallization in the solid state) with the HDPE matrix, despite a rapid molecular diffusion upon blending and an efficient anchoring to the surface of glass fibres.

5. Conclusion

In this chapter, the influence of functional PE oligomers on the rheological and mechanical properties of HDPE/GF composite blends was investigated. Several conclusions could be drawn as to the impact of such compounds on matrix-filler interactions in the melt as well as in the solid state.

In the first part of this study, it was observed that the surface chemistry of chopped strand glass fibres had a controlling influence on the maximum volume fraction achievable while still retaining a cohesive material, depending on the sizing applied by the manufacturer. It was subsequently demonstrated that a PE oligomer with adequate functional groups (carboxylic acid in this case) could be successfully used as a dispersant in an initially chemically unfavourable HDPE/GF2 system, in which the glass fibres had been designed for the reinforcement of polyamides. The critical volume fraction of glass fibres was consequently shifted towards higher values and the viscosity of the composite blends was decreased, which could not be solely attributed to the plasticizing of the HDPE matrix by the PE oligomer in the melt. These observations were attributed both to improved matrix-filler interactions in the presence of the PE oligomer as well as reduced interparticle interactions due to steric stabilization of the glass fibres, especially at high volume fractions.

The second part of this study was focused on enhancing the reinforcement of HDPE/GF2 composite blends. Evidence was found that PE oligomers with the appropriate functional groups (carboxylic acid, maleic anhydride and amine in this case) could be used as coupling agents, thereby improving the interfacial adhesion between the glass fibres and the HDPE matrix. Alkoxysilane compounds, which are commonly used as coupling agents in polymer/glass fibre systems, did not have any significant impact on mechanical properties, which could be due to a lack of available silanol groups at the surface of glass fibres.

Those results lead to the conclusion that functional PE oligomers could be used as dispersants as well as coupling agents in glass fibre-reinforced polyethylene without requiring prior surface modification of the glass fibres (aside from the sizing applied by the manufacturer). However, considering the results from Chapter 3 as well as the tests carried out with functional polymers commonly used on an industrial scale, it is clear that the main drawback of such functional PE oligomers is the lack of strong interactions with the polymer matrix in the solid state due to their low molar mass, although it is clearly an advantage regarding processability in the melt. Consequently, further investigations on glass fibre-reinforced polyethylenes should focus on functional PE oligomers with molar masses in the range of 5000-10000 g/mol. Additionally, it could be interesting to investigate telechelic PE oligomers in composite systems in which the reactivity of both the filler and the polymer matrix could be exploited, such as glass fibre-reinforced polyamides.

6. Bibliography

[1] A. Mortensen, Concise Encyclopedia of Composite Materials, 2nd Edition, Elsevier Science, 2006.
[2] M. Xanthos, 18. Compounding (theory and practice), in: Mixing and Compounding of Polymers; Theory and Practice, 2nd edition, Carl Hanser Verlag GmbH & Co. KG, 2009: pp. 703–722.
[3] W.T.Y. Tze, D.J. Gardner, C.P. Tripp, S.C. O'Neill, Cellulose fiber/polymer adhesion: effects of fiber/matrix interfacial chemistry on the micromechanics of the interphase, Journal of Adhesion Science and Technology. 20 (2006) 1649–1668. doi:10.1163/156856106779024427.
[4] A. Bergeret, P. Krawczak, Liaison renfort/matrice Définition et caractérisation, Techniques de l'ingénieur Caractérisation et propriétés d'usage des composites. base documentaire : TIB144DUO (2006).
[5] J. Thomason, Glass Fibre Sizing : A Review of the Scientific Literature, Create Space Independent Publishing Platform, 2012.
[6] J. Thomason, Glass Fibre Sizing : A Review of Size Formulation Patents, Create Space Independent Publishing Platform, 2015.
[7] R.O. MASCHMEYER, C.T. HILL, The Rheology of Concentrated Suspensions of Fibers, in: Fillers and Reinforcements for Plastics, AMERICAN CHEMICAL SOCIETY, 1974: pp. 95–105. doi:10.1021/ba-1974-0134.ch010.
[8] T. Kitano, T. Kataoka, Y. Nagatsuka, Dynamic flow properties of vinylon fibre and glass fiber reinforced polyethylene melts, Rheol Acta. 23 (1984) 408–416. doi:10.1007/BF01329193.
[9] R. Guo, J. Azaiez, C. Bellehumeur, Rheology of fiber filled polymer melts: Role of fiber-fiber interactions and polymer-fiber coupling, Polymer Engineering & Science. 45 (2005) 385–399. doi:10.1002/pen.20285.
[10] M.M. Rueda, R. Fulchiron, G. Martin, P. Cassagnau, Rheology of polypropylene filled with short-glass fibers: From low to concentrated filled composites, European Polymer Journal. 93 (2017) 167–181. doi:10.1016/j.eurpolymj.2017.05.025.
[11] S. Zürcher, T. Graule, Influence of dispersant structure on the rheological properties of highly-concentrated zirconia dispersions, Journal of the European Ceramic Society. 25 (2005) 863–873. doi:10.1016/j.jeurceramsoc.2004.05.002.
[12] F. Nsib, N. Ayed, Y. Chevalier, Selection of dispersants for the dispersion of carbon black in organic medium, Progress in Organic Coatings. 55 (2006) 303–310. doi:10.1016/j.porgcoat.2005.11.006.
[13] S. Farrokhpay, A review of polymeric dispersant stabilisation of titania pigment, Advances in Colloid and Interface Science. 151 (2009) 24–32. doi:10.1016/j.cis.2009.07.004.
[14] M. Rueda, R. Fulchiron, P. Cassagnau, A. Prebé, G. Martin, Structuring of non-Brownian ferrite particles in molten polypropylene: Viscoelastic analysis, Journal of Rheology. 60 (2016) 1245–1255. doi:10.1122/1.4963801.
[15] A. Berthereau, E. Dallies, Fibres de verre de renforcement, Techniques de l'ingénieur Matériaux composites : présentation et renforts. base documentaire : TIB142DUO (2008).
[16] S.K. De, J.R. White, Short Fibre-Polymer Composites, Elsevier, 1996.
[17] F.R. Jones, N.T. Huff, 19 - The structure and properties of glass fibers, in: A.R. Bunsell (Ed.), Handbook of Properties of Textile and Technical Fibres (Second Edition), Woodhead Publishing, 2018: pp. 757–803. doi:10.1016/B978-0-08-101272-7.00019-5.
[18] A.P.R. Eberle, D.G. Baird, P. Wapperom, Rheology of Non-Newtonian Fluids Containing Glass Fibers: A Review of Experimental Literature, Ind. Eng. Chem. Res. 47 (2008) 3470–3488. doi:10.1021/ie070800j.

[19] H.A. Barnes, 15. The flow of suspensions, in: Handbook Of Elementary Rheology, University of Wales Institute of Non-Newtonian Fluid Mechanics, 2000: pp. 119–140.
[20] R.O. Maschmeyer, C.T. Hill, Rheology of Concentrated Suspensions of Fibers in Tube Flow. III. Suspensions with the Same Fiber Length Distribution, Transactions of the Society of Rheology. 21 (1977) 195–206. doi:10.1122/1.549454.
[21] A. Ramazani S. A., A. Ait-Kadi, M. Grmela, Rheology of fiber suspensions in viscoelastic media: Experiments and model predictions, Journal of Rheology. 45 (2001) 945–962. doi:10.1122/1.1378026.
[22] A. m. a. Huq, J. Azaiez, Effects of length distribution on the steady shear viscosity of semiconcentrated polymer-fiber suspensions, Polymer Engineering & Science. 45 (2005) 1357–1368. doi:10.1002/pen.20415.
[23] C. Mobuchon, P.J. Carreau, M.-C. Heuzey, M. Sepehr, G. Ausias, Shear and extensional properties of short glass fiber reinforced polypropylene, Polymer Composites. 26 (2005) 247–264. doi:10.1002/pc.20088.
[24] T. Kitano, T. Kataoka, T. Shirota, An empirical equation of the relative viscosity of polymer melts filled with various inorganic fillers, Rheol Acta. 20 (1981) 207–209. doi:10.1007/BF01513064.
[25] D.B. Genovese, Shear rheology of hard-sphere, dispersed, and aggregated suspensions, and filler-matrix composites, Advances in Colloid and Interface Science. 171–172 (2012) 1–16. doi:10.1016/j.cis.2011.12.005.
[26] M. Pishvaei, C. Graillat, P. Cassagnau, T.F. McKenna, Modelling the zero shear viscosity of bimodal high solid content latex: Calculation of the maximum packing fraction, Chemical Engineering Science. 61 (2006) 5768–5780. doi:10.1016/j.ces.2006.04.024.
[27] M. Keshtkar, M.C. Heuzey, P.J. Carreau, Rheological behavior of fiber-filled model suspensions: Effect of fiber flexibility, Journal of Rheology. 53 (2009) 631–650. doi:10.1122/1.3103546.
[28] J.A. Lewis, Colloidal Processing of Ceramics, Journal of the American Ceramic Society. 83 (2000) 2341–2359. doi:10.1111/j.1151-2916.2000.tb01560.x.
[29] C.W. Macosko, Rheology: Principles, Measurements and Applications, Wiley-VCH, 1994.
[30] M.M. Rueda, M.-C. Auscher, R. Fulchiron, T. Périé, G. Martin, P. Sonntag, P. Cassagnau, Rheology and applications of highly filled polymers: A review of current understanding, Progress in Polymer Science. 66 (2017) 22–53. doi:10.1016/j.progpolymsci.2016.12.007.
[31] W.M. Sigmund, N.S. Bell, L. Bergström, Novel Powder-Processing Methods for Advanced Ceramics, Journal of the American Ceramic Society. 83 (2004) 1557–1574. doi:10.1111/j.1151-2916.2000.tb01432.x.
[32] Q. Ran, P. Somasundaran, C. Miao, J. Liu, S. Wu, J. Shen, Adsorption Mechanism of Comb Polymer Dispersants at the Cement/Water Interface, Journal of Dispersion Science and Technology. 31 (2010) 790–798. doi:10.1080/01932690903333580.
[33] F.M. Fowkes, M.A. Mostafa, Acid-Base Interactions in Polymer Adsorption, Ind. Eng. Chem. Prod. Res. Dev. 17 (1978) 3–7. doi:10.1021/i360065a002.
[34] D.M. Bigg, Rheological behavior of highly filled polymer melts, Polymer Engineering & Science. 23 (1983) 206–210. doi:10.1002/pen.760230408.
[35] E.M. Dannenberg, The Effects of Surface Chemical Interactions on the Properties of Filler-Reinforced Rubbers(2012). doi:10.5254/1.3547460.
[36] J.L. Thomason, L.J. Adzima, Sizing up the interphase: an insider's guide to the science of sizing, Composites Part A: Applied Science and Manufacturing. 32 (2001) 313–321. doi:10.1016/S1359-835X(00)00124-X.

[37] R.L. Gorowara, W.E. Kosik, S.H. McKnight, R.L. McCullough, Molecular characterization of glass fiber surface coatings for thermosetting polymer matrix/glass fiber composites, Composites Part A: Applied Science and Manufacturing. 32 (2001) 323–329. doi:10.1016/S1359-835X(00)00112-3.

[38] E.P. Plueddemann, Silane Coupling Agents, Springer US, Boston, MA, 1991. doi:10.1007/978-1-4899-2070-6_2.

[39] A.T. DiBenedetto, Tailoring of interfaces in glass fiber reinforced polymer composites: a review, Materials Science and Engineering: A. 302 (2001) 74–82. doi:10.1016/S0921-5093(00)01357-5.

[40] D. Wang, F.R. Jones, ToF-SIMS and XPS studies of the interaction of silanes and matrix resins with glass surfaces, Surface and Interface Analysis. 20 (1993) 457–467. doi:10.1002/sia.740200520.

[41] J.L. Thomason, D.W. Dwight, The use of XPS for characterisation of glass fibre coatings, Composites Part A: Applied Science and Manufacturing. 30 (1999) 1401–1413. doi:10.1016/S1359-835X(99)00042-1.

[42] X. Liu, J.L. Thomason, F.R. Jones, XPS and AFM Study of Interaction of Organosilane and Sizing with E-Glass Fibre Surface, The Journal of Adhesion. 84 (2008) 322–338. doi:10.1080/00218460802004386.

[43] B.J.R. Scholtens, J.C. Brackman, Influence of the Film Former on Fibre-Matrix Adhesion and Mechanical Properties of Glass-Fibre Reinforced Thermoplastics, The Journal of Adhesion. 52 (1995) 115–129. doi:10.1080/00218469508015189.

[44] M. Dey, J.M. Deitzel, J.W. Gillespie, S. Schweiger, Influence of sizing formulations on glass/epoxy interphase properties, Composites Part A: Applied Science and Manufacturing. 63 (2014) 59–67. doi:10.1016/j.compositesa.2014.04.006.

[45] D. Bikiaris, P. Matzinos, A. Larena, V. Flaris, C. Panayiotou, Use of silane agents and poly(propylene-g-maleic anhydride) copolymer as adhesion promoters in glass fiber/polypropylene composites, Journal of Applied Polymer Science. 81 (2001) 701–709. doi:10.1002/app.1487.

[46] S.C. Tjong, S.-A. Xu, R.K.-Y. Li, Y.-W. Mai, Mechanical behavior and fracture toughness evaluation of maleic anhydride compatibilized short glass fiber/SEBS/polypropylene hybrid composites, Composites Science and Technology. 62 (2002) 831–840. doi:10.1016/S0266-3538(02)00037-4.

[47] J.-H. Lin, C.-L. Huang, C.-F. Liu, C.-K. Chen, Z.-I. Lin, C.-W. Lou, Polypropylene/Short Glass Fibers Composites: Effects of Coupling Agents on Mechanical Properties, Thermal Behaviors, and Morphology, Materials. 8 (2015). doi:10.3390/ma8125451.

[48] G. Luo, W. Li, W. Liang, G. Liu, Y. Ma, Y. Niu, G. Li, Coupling effects of glass fiber treatment and matrix modification on the interfacial microstructures and the enhanced mechanical properties of glass fiber/polypropylene composites, Composites Part B: Engineering. 111 (2017) 190–199. doi:10.1016/j.compositesb.2016.12.016.

[49] T.J. Keener, R.K. Stuart, T.K. Brown, Maleated coupling agents for natural fibre composites, Composites Part A: Applied Science and Manufacturing. 35 (2004) 357–362. doi:10.1016/j.compositesa.2003.09.014.

[50] X. Li, L.G. Tabil, S. Panigrahi, Chemical Treatments of Natural Fiber for Use in Natural Fiber-Reinforced Composites: A Review, J Polym Environ. 15 (2007) 25–33. doi:10.1007/s10924-006-0042-3.

[51] K.H. Wong, D. Syed Mohammed, S.J. Pickering, R. Brooks, Effect of coupling agents on reinforcing potential of recycled carbon fibre for polypropylene composite, Composites Science and Technology. 72 (2012) 835–844. doi:10.1016/j.compscitech.2012.02.013.

[52] C. Unterweger, J. Duchoslav, D. Stifter, C. Fürst, Characterization of carbon fiber surfaces and their impact on the mechanical properties of short carbon fiber reinforced polypropylene composites, Composites Science and Technology. 108 (2015) 41–47. doi:10.1016/j.compscitech.2015.01.004.

[53] P.C. Hidber, T.J. Graule, L.J. Gauckler, Influence of the dispersant structure on properties of electrostatically stabilized aqueous alumina suspensions, Journal of the European Ceramic Society. 17 (1997) 239–249. doi:10.1016/S0955-2219(96)00151-3.

[54] V.M.B. Moloney, D. Parris, M.J. Edirisinghe, Rheology of Zirconia Suspensions in a Nonpolar Organic Medium, Journal of the American Ceramic Society. 78 (1995) 3225–3232. doi:10.1111/j.1151-2916.1995.tb07958.x.

[55] D.-M. Liu, Effect of Dispersants on the Rheological Behavior of Zirconia-Wax Suspensions, Journal of the American Ceramic Society. 82 (1999) 1162–1168. doi:10.1111/j.1151-2916.1999.tb01890.x.

[56] S.Y. Yang, C.K. Huang, B.C. Lin, W.C.J. Wei, Kneading and molding of ceramic microparts by precision powder injection molding (PIM), Journal of Applied Polymer Science. 100 (2006) 892–899. doi:10.1002/app.23010.

[57] M.-C. Auscher, R. Fulchiron, T. Périé, P. Cassagnau, Morphological and rheological properties of zirconia filled polyethylene, Polymer. 132 (2017) 174–179. doi:10.1016/j.polymer.2017.10.068.

[58] M.M. Rueda, R. Fulchiron, P. Cassagnau, Rheology and processing of highly filled materials, 2017.

[59] Y. Shimizu, S. Arai, T. Itoyama, H. Kawamoto, Experimental analysis of the kneading disk region in a co-rotating twin screw extruder: Part 2. glass-fiber degradation during compounding, Advances in Polymer Technology. 16 (1997) 25–32. doi:10.1002/(SICI)1098-2329(199721)16:1<25::AID-ADV3>3.0.CO;2-L.

[60] B. Olalla, C. Carrot, R. Fulchiron, I. Boudimbou, E. Peuvrel-disdier, Analysis of the influence of polymer viscosity on the dispersion of magnesium hydroxide in a polyolefin matrix, Rheol Acta. 51 (2012) 235–247. doi:10.1007/s00397-011-0580-z.

[61] C. Carrot, J.-C. Majesté, B. Olalla, R. Fulchiron, On the use of the model proposed by Leonov for the explanation of a secondary plateau of the loss modulus in heterogeneous polymer–filler systems with agglomerates, Rheol Acta. 49 (2010) 513–527. doi:10.1007/s00397-010-0432-2.

[62] R.G. Larson, The Structure and Rheology of Complex Fluids, Oxford University Press, New York - Oxford, 1999.

[63] F. Chinesta, G. Ausias, Rheology of Non-spherical Particle Suspensions, Elsevier, 2015.

[64] N. Phan-Thien, 1. Introduction to supension rheology, in: Rheology of Non-Spherical Particle Suspensions, Elsevier, 2015: pp. 1–17.

[65] J. Férec, G. Ausias, 4. Rheological modeling of non-dilute rod suspensions, in: Rheology of Non-Spherical Particle Suspensions, Elsevier, 2015: pp. 77–117.

[66] M.M. Rueda, R. Fulchiron, G. Martin, P. Cassagnau, Linear and non-linear nature of the flow of polypropylene filled with ferrite particles: from low to concentrated composites, Rheol Acta. 56 (2017) 635–648. doi:10.1007/s00397-017-1025-0.

[67] M.A. Osman, A. Atallah, T. Schweizer, H.C. Öttinger, Particle–particle and particle-matrix interactions in calcite filled high-density polyethylene—steady shear, Journal of Rheology. 48 (2004) 1167–1184. doi:10.1122/1.1784782.

[68] P.J. Carreau, D.C.R.D. Kee, R.P. Chhabra, Rheology of Polymeric Systems: Principles and Applications, Hanser Pub Inc, Munich ; New York : Cincinnati, 1997.

[69] R.G. Larson, 6. Particulate suspensions, in: The Structure and Rheology of Complex Fluids, Oxford University Press, New York - Oxford, 1999: pp. 261–323.

[70] M. Pishvaei, C. Graillat, T.F. McKenna, P. Cassagnau, Rheological behaviour of polystyrene latex near the maximum packing fraction of particles, Polymer. 46 (2005) 1235–1244. doi:10.1016/j.polymer.2004.11.047.

[71] V.B. Gupta, R.K. Mittal, P.K. Sharma, G. Mennig, J. Wolters, Some studies on glass fiber-reinforced polypropylene. Part II: Mechanical properties and their dependence on fiber length, interfacial adhesion, and fiber dispersion, Polymer Composites. 10 (1989) 16–27. doi:10.1002/pc.750100104.

[72] K. Joseph, S. Varghese, G. Kalaprasad, S. Thomas, L. Prasannakumari, P. Koshy, C. Pavithran, Influence of interfacial adhesion on the mechanical properties and fracture behaviour of short sisal fibre reinforced polymer composites, European Polymer Journal. 32 (1996) 1243–1250. doi:10.1016/S0014-3057(96)00051-1.

[73] S.-Y. Fu, B. Lauke, Effects of fiber length and fiber orientation distributions on the tensile strength of short-fiber-reinforced polymers, Composites Science and Technology. 56 (1996) 1179–1190. doi:10.1016/S0266-3538(96)00072-3.

[74] T. Hanemann, R. Heldele, T. Mueller, J. Hausselt, Influence of Stearic Acid Concentration on the Processing of ZrO2-Containing Feedstocks Suitable for Micropowder Injection Molding, International Journal of Applied Ceramic Technology. 8 (2011) 865–872. doi:10.1111/j.1744-7402.2010.02519.x.

[75] T. Hanemann, R. Heldele, Fatty Acid Surfactant Structure–Feedstock Flow Properties: Correlation for High-Pressure Ceramic Injection Molding, International Journal of Applied Ceramic Technology. 8 (2011) 1296–1304. doi:10.1111/j.1744-7402.2011.02612.x.

[76] E.P. Plueddemann, 1. General concepts, in: Silane Coupling Agents, Springer US, Boston, MA, 1991: pp. 1–30. doi:10.1007/978-1-4899-2070-6_2.

[77] Y. Li, Y. Lin, M. Nie, Q. Wang, X. Zhang, New Insight into the Interfacial Enhancement of Polypropylene Glass Fiber Composites via a Compatibilizer: The Role of Injection Screw Temperature, Journal of Macromolecular Science, Part B. 55 (2016) 138–148. doi:10.1080/00222348.2015.1125064.

[78] J.-F. Agassant, P. Avenas, P.J. Carreau, B. Vergnes, M. Vincent, 6. Twin-screw extrusion and applications, in: Polymer Processing, 2nd ed., Hanser, 2017: pp. 433–520.

[79] F. Inceoglu, J. Ville, N. Ghamri, J.L. Pradel, A. Durin, R. Valette, B. Vergnes, Correlation between processing conditions and fiber breakage during compounding of glass fiber-reinforced polyamide, Polymer Composites. 32 (2011) 1842–1850. doi:10.1002/pc.21217.

[80] A. Durin, P. De Micheli, J. Ville, F. Inceoglu, R. Valette, B. Vergnes, A matricial approach of fibre breakage in twin-screw extrusion of glass fibres reinforced thermoplastics, Composites Part A: Applied Science and Manufacturing. 48 (2013) 47–56. doi:10.1016/j.compositesa.2012.12.011.

[81] J. Ville, F. Inceoglu, N. Ghamri, J.L. Pradel, A. Durin, R. Valette, B. Vergnes, Influence of Extrusion Conditions on Fiber Breakage along the Screw Profile during Twin Screw Compounding of Glass Fiber-reinforced PA, IPP. 28 (2013) 49–57. doi:10.3139/217.2659.

[82] E.P. Plueddemann, 2. Chemistry of silane coupling agents, in: Silane Coupling Agents, Springer US, Boston, MA, 1991: pp. 31–54. doi:10.1007/978-1-4899-2070-6_2.

[83] B. Arkles, J.R. Steinmetz, J. Zazyczny, P. Mehta, Factors contributing to the stability of alkoxysilanes in aqueous solution, Journal of Adhesion Science and Technology. 6 (1992) 193–206. doi:10.1163/156856192X00133.

[84] M.-C. Brochier Salon, M.N. Belgacem, Competition between hydrolysis and condensation reactions of trialkoxysilanes, as a function of the amount of water and the nature of the organic group, Colloids and Surfaces A: Physicochemical and Engineering Aspects. 366 (2010) 147–154. doi:10.1016/j.colsurfa.2010.06.002.

[85] D.M. Laura, H. Keskkula, J.W. Barlow, D.R. Paul, Effect of glass fiber surface chemistry on the mechanical properties of glass fiber reinforced, rubber-toughened nylon 6, Polymer. 43 (2002) 4673–4687. doi:10.1016/S0032-3861(02)00302-6.

[86] M. Abdelmouleh, S. Boufi, M.N. Belgacem, A. Dufresne, Short natural-fibre reinforced polyethylene and natural rubber composites: Effect of silane coupling agents and fibres loading, Composites Science and Technology. 67 (2006) 1627–1639. doi:10.1016/j.compscitech.2006.07.003.

[87] J.D. Ferry, Chapter 10. Molecular theory for undiluted amorphous polymers and concentrated solutions; network and entanglements, in: Viscoelastic Properties of Polymers, 3rd ed., John Wiley & Sons, Inc., 1980: pp. 224–263.

General conclusion

General conclusion

The formulation of thermoplastic materials involves the blending of numerous additives and fillers in order to improve their technical features as well as their processability, and the demand for new materials with specific properties designed to meet more restrictive and more diversified requirements is growing. As a consequence, the development of new molecules to promote the dispersion of fillers in thermoplastic matrices or to compatibilize blends of incompatible polymers has been the subject of substantial research efforts over the past decades. Considering those challenges, the aim of the REPEAT II project was to use end-functionalized polyethylene oligomers as interface agents in reinforced thermoplastics and in immiscible polymer blends. Within the framework of this project, the objective of this thesis was to investigate several aspects of the incorporation of such functional polyethylene oligomers into polyolefin resins, polyethylene-polyamide blends and glass fibre-reinforced polyethylene systems.

The objective of the experimental work presented in Chapter 3 was to get a better understanding of the morphology developments occurring during the melt processing and crystallization of binary systems where a low molar mass functional PE oligomer was incorporated into HDPE and PP resins. The rheological behaviour of such systems in the molten state as well as their crystalline microstructure in the solid state were therefore investigated, along with their crystallization behaviour during the transition between those two states.

One of the difficulties associated with the processing of such blends is the very low viscosity ratio between the low molar mass oligomer and the polymer. Batch processing as well as bi-layer rheological measurements were therefore used to investigate mixing and diffusion aspects. It was found that the PE oligomer was easily incorporated into the selected polyolefins thanks to rapid molecular diffusion and good miscibility in the molten state. However, rheological modelling using the Carreau-Yasuda equation as a predictive model suggested that the miscibility between PE oligomers and polyolefin resins is limited at high oligomer concentrations and that some kind of saturation phenomenon may occur, particularly in the case of PP-based systems which seemed to result in partially inhomogeneous melts above 5 wt% PE oligomer.

Miscibility aspects as well as the crystallization behaviour of such blends were then studied by dynamic scanning calorimetry in combination with optical microscopy under polarized light, and changes in the crystalline microstructure of the blends in the solid state were observed by electron scanning microscopy. It appeared clearly that HDPE/PE oligomer and PP/PE oligomer blends underwent solid-liquid phase separation upon cooling, leading to biphasic materials in the solid state. However, the hypothesis can be made that due to their close molecular structure, small amounts of PE oligomer chains are able to co-crystallize with HDPE, resulting in better compatibility in the solid state compared to PP-based systems. On the other hand, it can be considered that the crystallization of PP/PE oligomer blends leads to small amounts of PE oligomer chains being retained in the amorphous phase of PP (as a result of the dilution phenomenon in the melt), leading to poor compatibility and brittle behaviour in the solid state.

Considering the results obtained in this chapter as well as those reported in other studies, it would be interesting to investigate similar systems with different oligomers, using the same tools. In this perspective, the molar mass of the oligomers as well as the nature of the functional group(s) are parameters that should be considered for further experimental work.

In the following Chapter 4, new strategies for the compatibilization of immiscible HDPE/PA6 blends were investigated. This study was focused on the use of a reactive system involving two functional oligomers as compatibilizer precursors, namely (i) a polyethylene oligomer grafted with maleic anhydride groups (Ceramer 1608) as well as (ii) a tri-functional polyetheramine (Jeffamine T-403), both of which are commercially available materials.

The results showed that the use of Ceramer 1608 or of the Ceramer 1608/Jeffamine T-403 reactive system did not result in efficient compatibilization. On the other hand, the use of a high molar mass PE-g-MA, which is commonly used in the compatibilization of such systems, led to homogeneous materials with improved mechanical properties. This suggests that the poor compatibilizing ability of oligomeric compatibilizer precursors is due to their lack of interaction with the polyethylene phase as a result of their low molar mass. Nevertheless, the study of the physical and chemical interactions between the selected functional oligomers and HDPE and PA6 homopolymers led to some interesting results, which are detailed in the following paragraphs.

First, it was found that the association of a PE-g-MA oligomer (Ceramer 1608 or Ceramer 67) with a tri-functional polyetheramine oligomer (Jeffamine T-403) resulted in compounds with very different characteristics depending on the physical and chemical properties of the oligomers, and the results suggested that the reaction between Ceramer 1608 and Jeffamine T-403 yielded a crosslinked network. It is worth noting that several other similar oligomers are commercially available (especially in the Jeffamine product range), meaning that the properties of such Ceramer-Jeffamine networks could be easily tuned by adjusting parameters such as the molar mass of and the number of functional groups of each oligomer.

Then, it was demonstrated that Ceramer 1608 and Jeffamine T-403 functional oligomers have strong interactions with polyamide through several reaction mechanisms, which resulted in remarkable mechanical properties. Thus, impact strength testing should be carried out on such blends as their strain-hardening behaviour could make them good candidates for impact resistance applications. The results presented in that part of the study also indicate that the viscoelastic and mechanical properties of the resulting compounds are strongly influenced by the composition of the blends and could therefore be more finely adjusted with additional experimental work.

Lastly, the incorporation of Ceramer 1608 and Jeffamine T-403 into HDPE led to the formation of dispersed domains, which were found to be incompatible with HDPE. However, interfacial adhesion with the HDPE resin was improved with the addition of a high molar mass PE-g-MA (Exxelor PE 1040 in this case). Considering those results, further work would be necessary to determine the minimum

amount of Exxelor PE 1040 necessary to obtain a good interface between the Ceramer1608/Jeffamine T-403 domains and the HDPE resin, which could result in interesting mechanical properties. Besides, the composition of such quaternary blend could be finely adjusted in order to achieve specific morphologies.

In the light of these results, further experimental work would be required on the use of functional polyethylene and polyetheramine oligomers with different molar masses and numbers of functional groups in order to achieve an efficient compatibilization of polyethylene/polyamide blends. In this perspective, the use of high molar mass polyethylenes grafted with maleic anhydride functional groups in addition to functional oligomers could also be an interesting lead. Besides, the optimization of the blend composition in terms of polyethylene/polyamide ratio as well as the adjustment of the concentration of the different functional oligomers are issues that would require tackling.

In the last chapter, functional PE oligomers were investigated as dispersing and coupling agents in HDPE reinforced with discontinuous glass fibres (GF), with the aim of improving both the processability and the mechanical properties of these systems.

In the first part of this chapter, the dispersing ability of a functional PE oligomer was assessed by batch processing approach along with rheological analysis of HDPE/GF systems. It was demonstrated that a PE oligomer with adequate functional groups could be successfully used as a dispersant in such composite blends. Indeed, the maximum volume fraction of glass fibres achievable while still maintaining a cohesive material was shifted towards higher values and the processability was improved. These observations were attributed both to improved matrix-filler interactions in the presence of the PE oligomer and to reduced interparticle interactions due to steric stabilization of the glass fibres, especially at high volume fractions.

The second part of this chapter was focused on enhancing the reinforcement of HDPE/GF2 composite blends. Preliminary trials as well as a screening of PE oligomers with various functional groups brought evidence that PE oligomers with the appropriate functional groups (carboxylic acid, maleic anhydride and amine in that case) could be used as coupling agents, thereby improving the interfacial adhesion between the glass fibres and the HDPE matrix. On the other hand, although alkoxysilane compounds are commonly used as coupling agents in polymer/glass fibre systems, alkoxysilane-functionalized PE oligomers did not have any significant impact on the mechanical properties of HDPE/GF2 systems.

Those results led to the conclusion that functional PE oligomers could be used as interface agents in glass fibre-reinforced polyethylene without requiring prior surface modification of the glass fibres (aside from the sizing applied by the manufacturer). However, considering the results from Chapter 3 as well as the tests carried out with functional polymers commonly used on an industrial scale, it is clear that the main drawback of such functional PE oligomers is their lack of strong interactions with the polymer matrix in the solid state due to their low molar mass, although their very low viscosity

could be an advantage as regards processability in the melt. Consequently, further investigations on glass fibre-reinforced polyethylenes should probably focus on functional PE oligomers with molar masses in the range of 5000-10000 g/mol. Additionally, it would be interesting to investigate telechelic PE oligomers in composite systems in which the reactivity of both the filler and the polymer matrix could be exploited, such as glass fibre-reinforced polyamides.

Appendices

Table of contents

1. Appendix A – Characterization of Ceramer 1608 by ATD-GC-MS

1.1. Introduction

According to the safety datasheets provided by the supplier (Baker Hughes), the maleic anhydride derivatives used for the functionalization of Ceramer products are among maleic anhydride, mono-isopropyl maleate and maleic acid. In the case of Ceramer 1608, this was verified by analytical thermal desorption coupled with gas chromatography and mass spectroscopy (ATD-GC-MS).

1.2. Method

Gas chromatography (GC) was performed on a PerkinElmer Clarus 680 gas chromatograph equipped with a Sigma-Aldrich SLB-35ms capillary column as well as a PerkinElmer TurboMatrix 350 ATD thermal desorber. This equipment was coupled with a PerkinElmer Clarus SQ 8T mass spectrometer for mass spectroscopy (MS). During thermal desorption, the sample was heated at 200 °C for 10 min and the temperature of the focusing trap was -40 °C. The volatile compounds were then heated to 300 °C at a rate of 10 °C/min to be injected into the GC column.

1.3. Results

1.3.1. Gas chromatography (GC)

The chromatograph obtained from GC is shown in Figure 1.

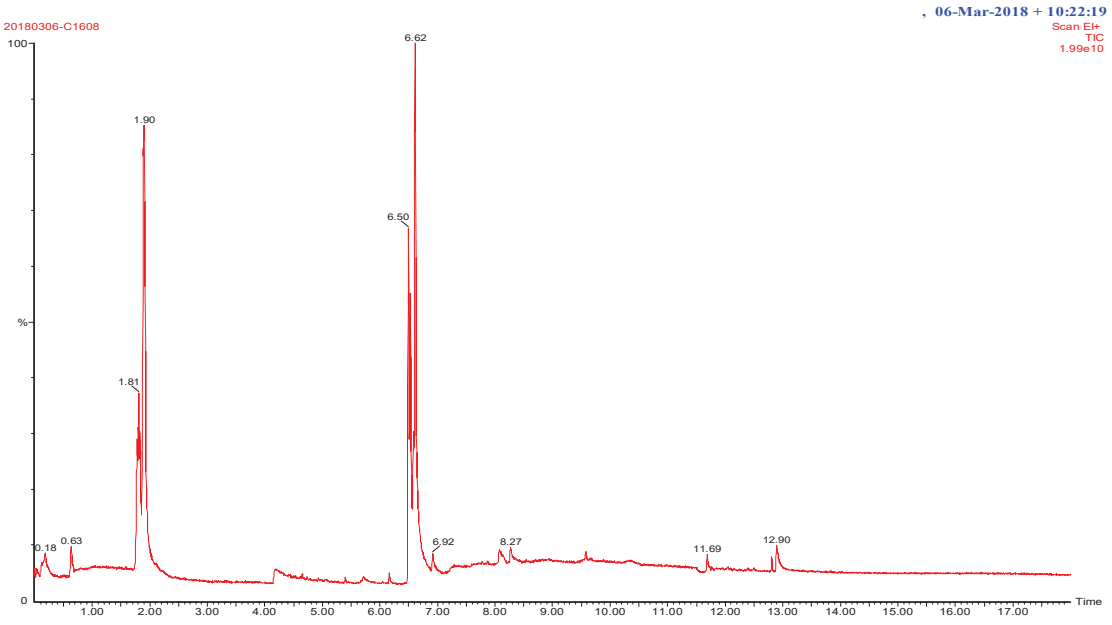

Figure 1. Chromatograph obtained from the ATD-GC-MS analysis of Ceramer 1608

1.3.2. Mass spectroscopy (MS)

The mass spectra corresponding to the relevant peaks displayed in Figure 1 are shown in Figures 2-6. The molecular structures of the volatile compounds featured on each figure were obtained from the mass spectral library of the TurboMass™ software used on the mass spectrometer.

The peak at m/z = 1.90 was attributed to the presence of isopropyl alcohol (Figure 2).

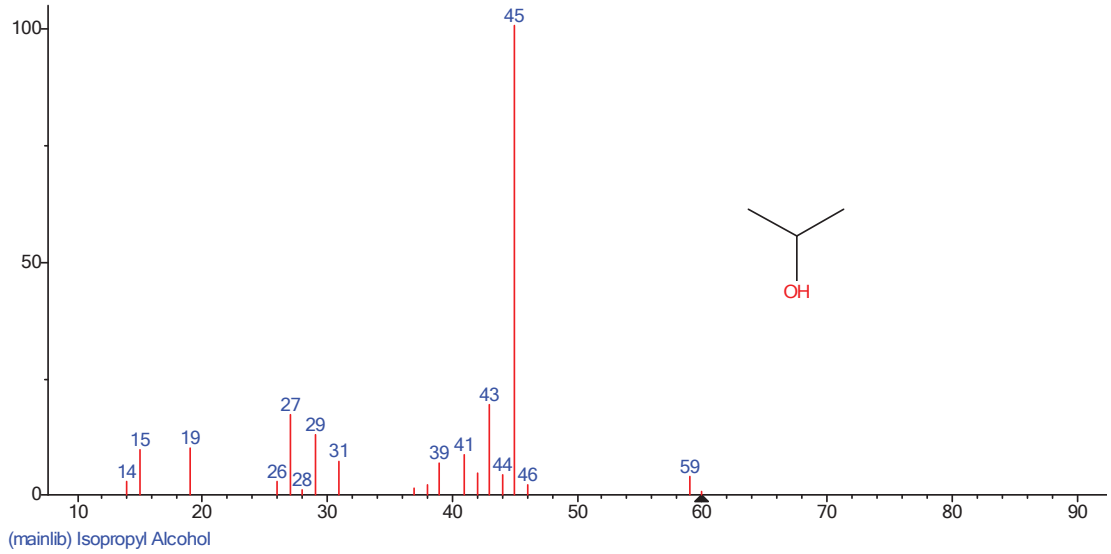

Figure 2. Mass spectrum corresponding to the peak at m/z = 1.90

The peak at m/z = 4.19 was attributed to the presence of maleic anhydride (Figure 3).

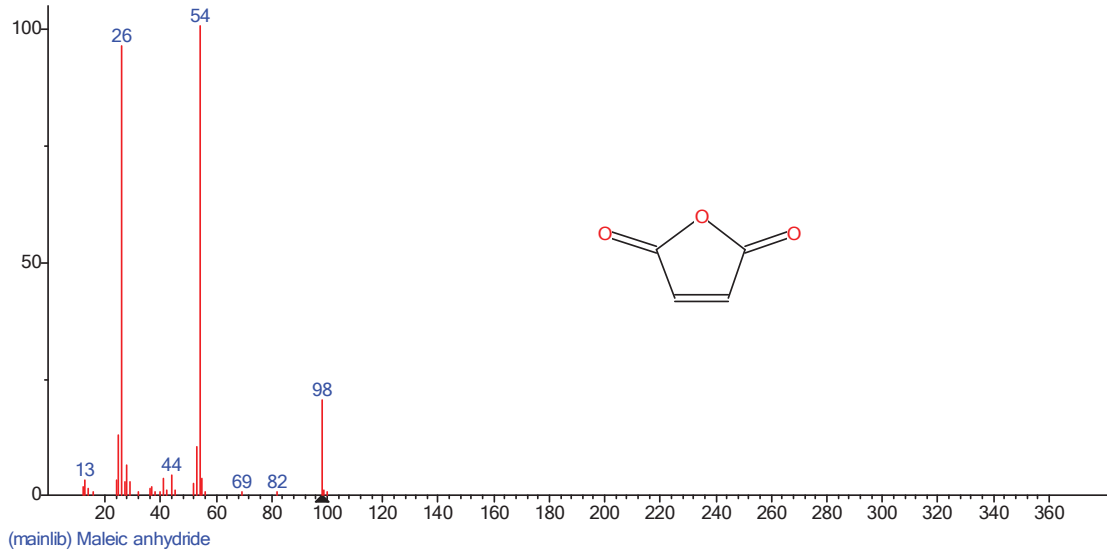

Figure 3. Mass spectrum corresponding to the peak at m/z = 4.19

The peak at m/z = 6.50 was attributed to the presence of di-isopropyl succinate (Figure 4).

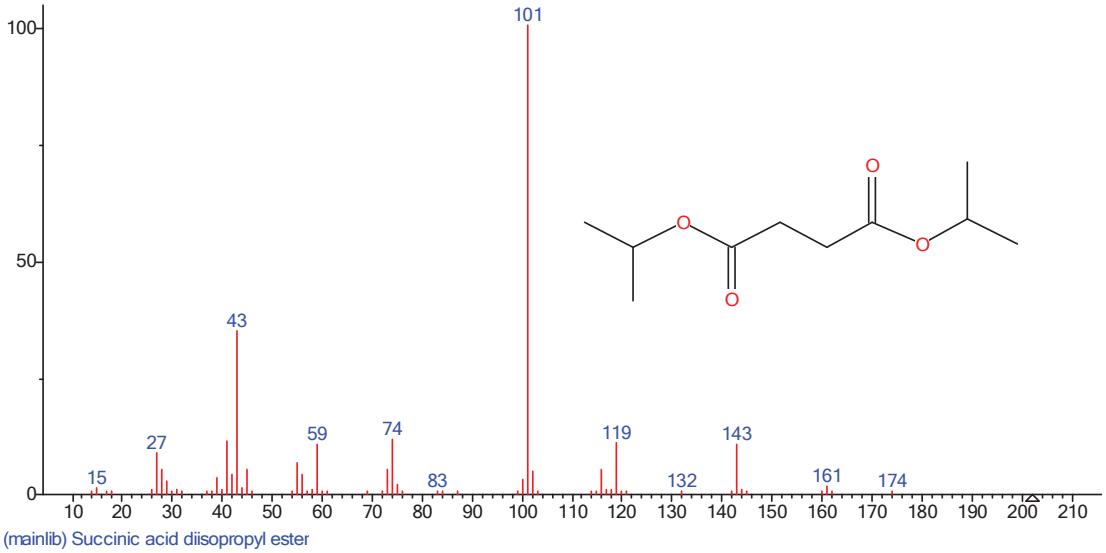

Figure 4. Mass spectrum corresponding to the peak at m/z = 6.50

The peak at m/z = 6.62 was attributed to the presence of di-isopropyl maleate (Figure 5).

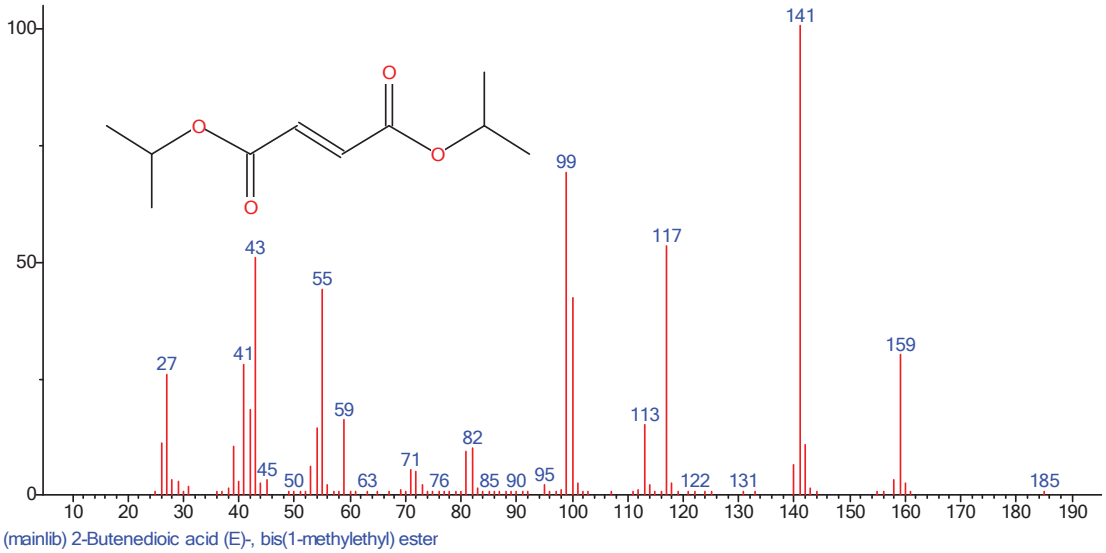

Figure 5. Mass spectrum corresponding to the peak at m/z = 6.62

The peak at m/z = 8.04 was attributed to the presence of mono-isopropyl succinate (mass spectrum not represented here). The peak at m/z = 8.27 was attributed to the presence of mono-isopropyl maleate (Figure 6).

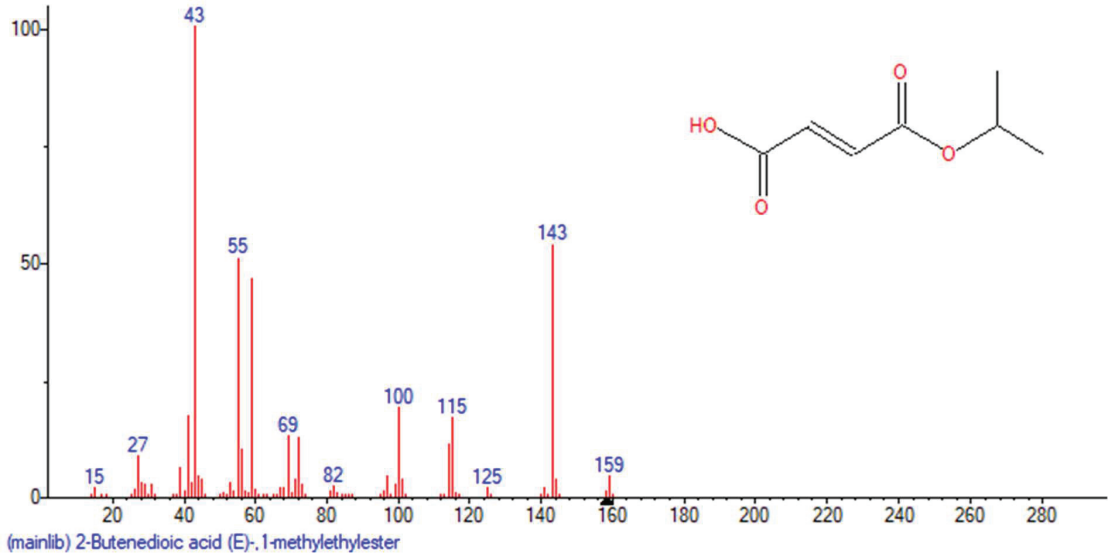

Figure 6. Mass spectrum corresponding to the peak at m/z = 8.27

1.4. Conclusion

The characterization by ATD-GC-MS indicated that the maleic anhydride derivative used for the functionalization of Ceramer 1608 was mainly di-isopropyl maleate. The presence of maleic anhydride and mono-isopropyl maleate was also confirmed, although in much lower amounts. The presence of maleic acid could not be detected.

2. Appendix B – Surface characterization of glass fibres

2.1. Introduction

The spectra obtained from the nuclear magnetic resonance (NMR) and infrared (IR) analyses performed either on sizing extracts or directly on the glass fibres are given in the following sections. The interpretation of those analysis results is detailed in Chapter 2.

2.2. Direct analysis of the glass fibres

^{1}H, ^{13}C, ^{29}Si and ^{31}P solid-state NMR spectroscopy was conducted at the C2P2 laboratory on a Brüker Avance WB 500MHz spectrometer equipped with a 4mm MAS probe. Those analyses were carried out directly on the glass fibres. The spectra obtained from those analyses are shown in Figures 7-10.

2.2.1. Proton solid-state NMR

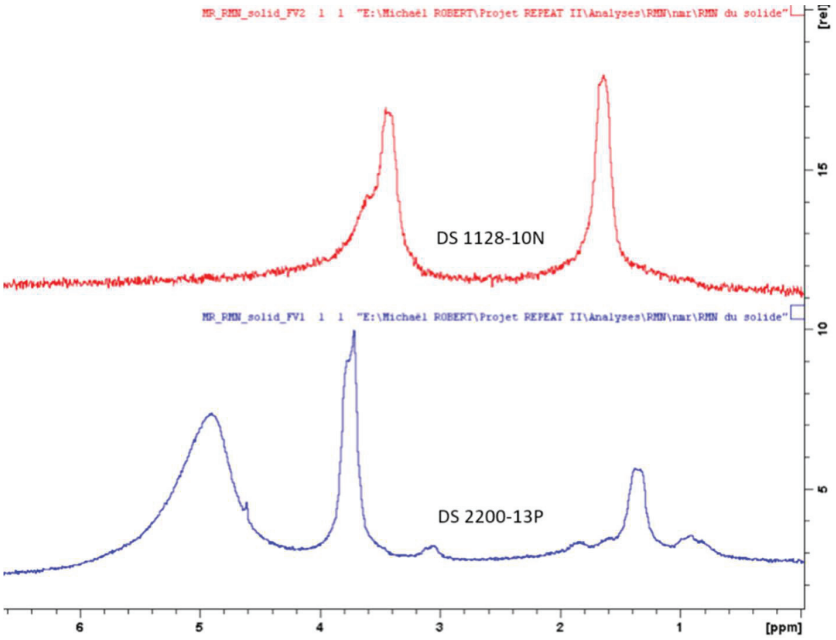

Figure 7. Spectra obtained from the ^{1}H solid-state NMR analysis of DS 2200-13P and DS 1128-10N glass fibres

2.2.2. Carbon-13 solid-state NMR

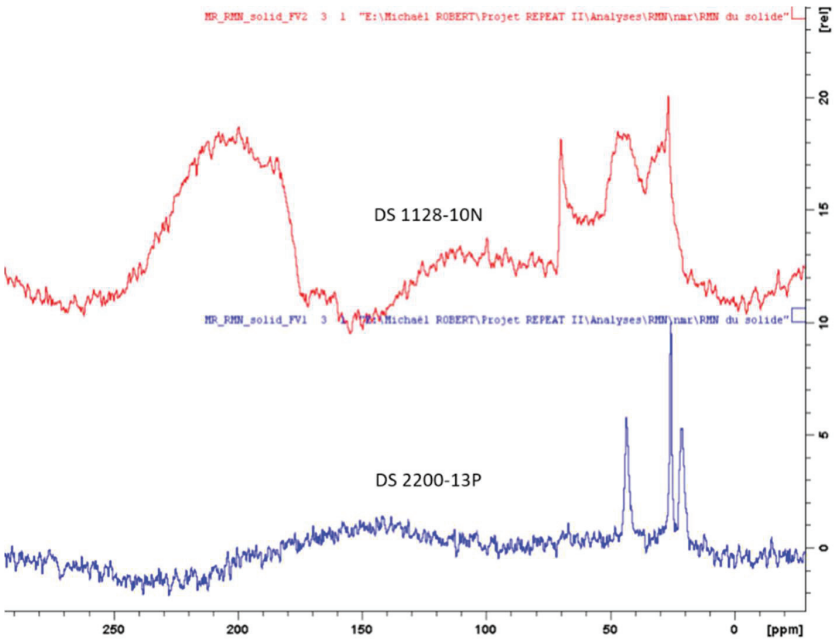

Figure 8. Spectra obtained from the ^{13}C solid-state NMR analysis of DS 2200-13P and DS 1128-10N glass fibres

2.2.3. Silicon-29 solid-state NMR

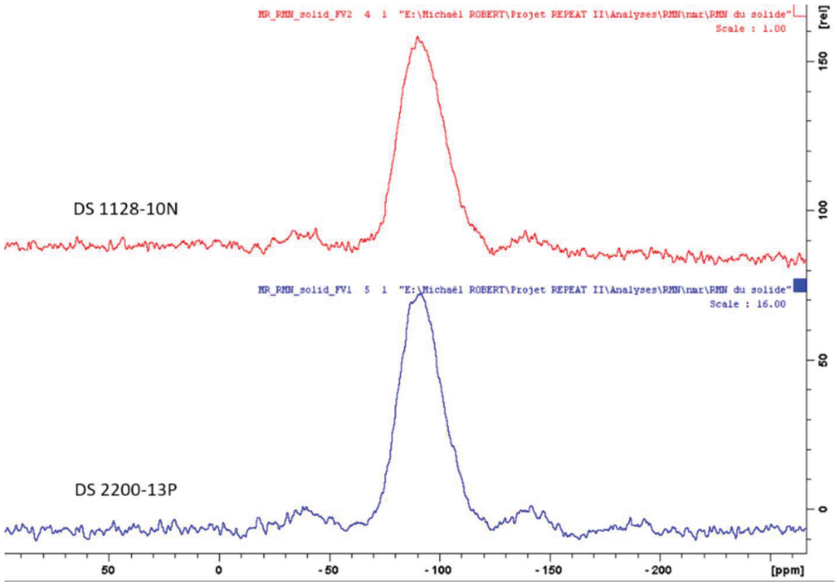

Figure 9. Spectra obtained from the ^{29}Si solid-state NMR analysis of DS 2200-13P and DS 1128-10N glass fibres

2.2.4. Phosphorus-31 solid-state NMR

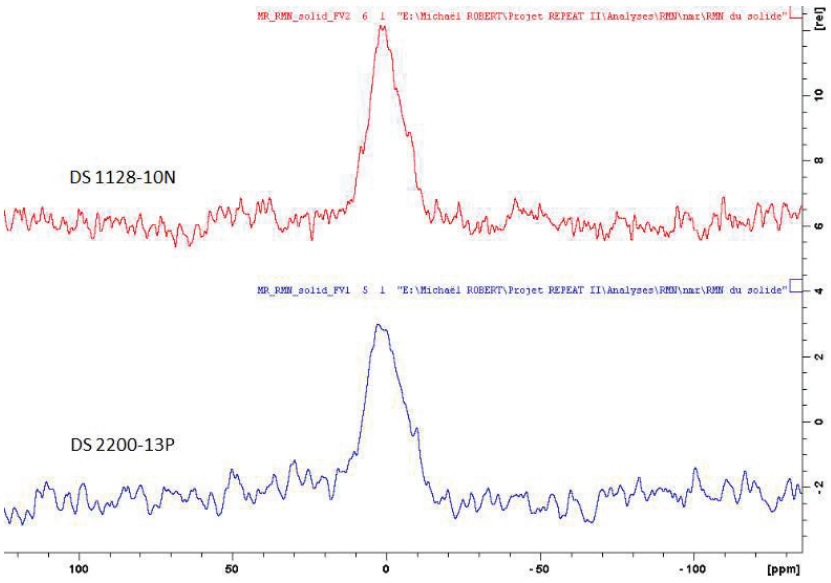

Figure 10. Spectra obtained from the ^{31}P solid-state NMR analysis of DS 2200-13P and DS 1128-10N glass fibres

2.3. Analysis of sizing extracts

2.3.1. Fourier-transform infrared spectroscopy (FTIR)

FTIR spectroscopy was performed on the extracted sizings using a Thermo Fisher Scientific Nicolet iS10 spectrometer equipped with a Start Omni Transmission module. The liquid samples were placed between two KBr discs to be analysed in transmittance mode. The collected data was processed by Fourier transform to obtain the absorbance spectra displayed in Figure 11. The type of glass fibre and the solvent used for solid-liquid extraction (with a Soxhlet extractor) are indicated on each spectrum.

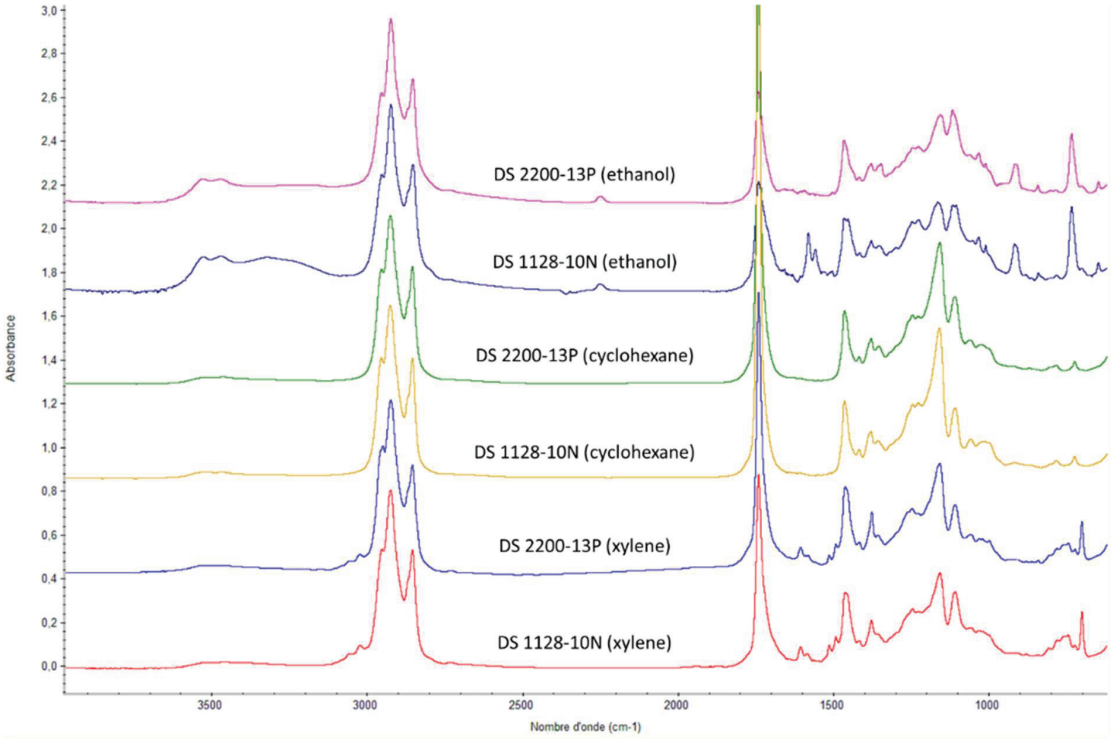

Figure 11. Spectra obtained from the FTIR analysis of DS 2200-13P and DS 1128-10N glass fibre sizing extracts obtained by solid-liquid extraction using a Soxhlet extractor with different solvents (ethanol, cyclohexane and xylene)

2.3.2. Liquid-state nuclear magnetic resonance (NMR)

^{1}H liquid-state NMR analyses were performed on a Brüker Avance III 400MHz spectrometer equipped with a BBFO probe. Different deuterated solvents were used depending on the solvent used for sizing extraction; chloroform ($CDCl_3$) for samples extracted in ethanol and benzene (C_6D_6) in the case of cyclohexane and xylene. The type of glass fibre and the solvent used for solid-liquid extraction (with a Soxhlet extractor) are indicated on each spectrum displayed in Figure 12.

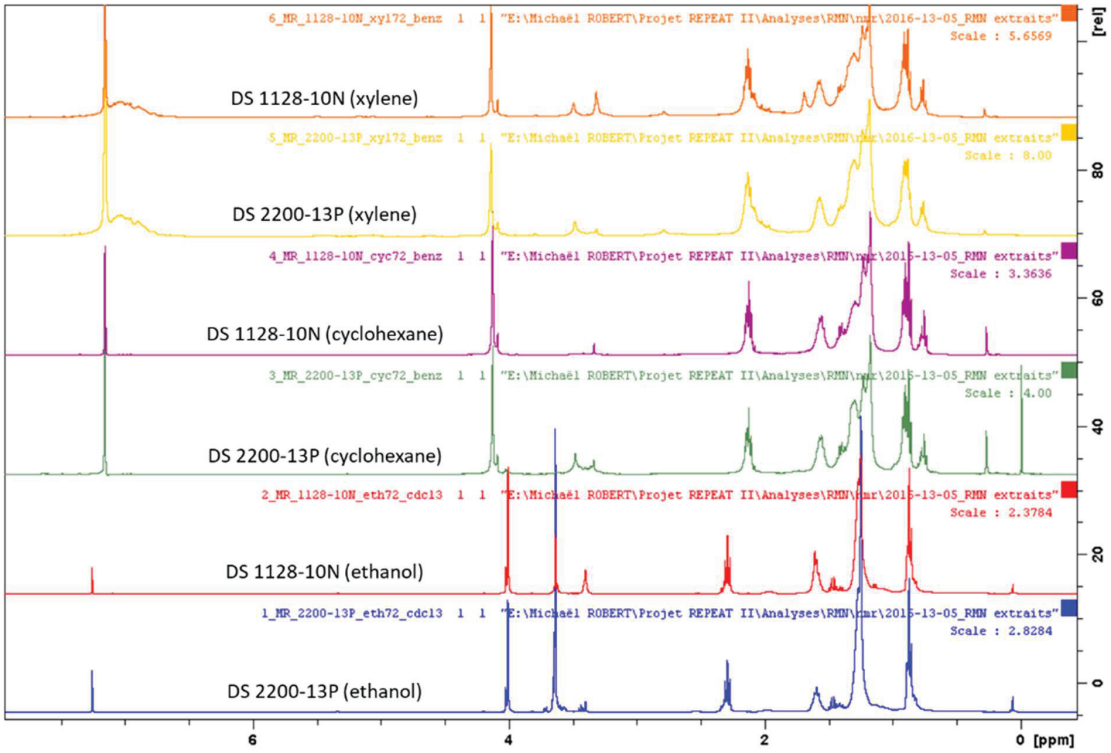

Figure 12. Spectra obtained from the ^{1}H NMR analysis of DS 2200-13P and DS 1128-10N glass fibre sizing extracts obtained by solid-liquid extraction using a Soxhlet extractor with different solvents (ethanol, cyclohexane and xylene)

3. Appendix C – Optimization of the extrusion process as part of the compatibilization of immiscible HDPE/PA6 blends using a C1608/T403 reactive system

3.1. Introduction

In this part of the study, a reactive system involving two functional oligomers as compatibilizer precursors was investigated in order to compatibilize HDPE/PA6 blends. The selected oligomers were Ceramer 1608 (C1608) and Jeffamine T-403 (T403), whose interactions with HDPE and PA6 were separately investigated in Chapter 5. The resulting blends were characterized in terms of morphology and mechanical properties in order to evaluate the compatibilization efficiency of the reactive C1608/T403 system. It should be noted that the present experimental work was focused on the interactions between the different constituents of the blends rather than on the optimization of the blend composition. Consequently, the blends investigated in this part of the study were all based on the same blend composition, while several variants of the extrusion process were considered.

3.2. Determination of the blend composition

The blends investigated in this part of the study were based on a 70/30 blend of HDPE and PA6. The weight fraction of PA6 was set at 30 wt% while the remaining 70 wt% consisted of HDPE and functional oligomers. Considering the difficulties associated with the injection of Jeffamine T-403 at very low flow rates, the weight fraction of Jeffamine T-403 was set at 1 wt%. The weight fraction of Ceramer 1608 was consequently set at 4 wt% to account for the amount of amine functional groups in the blend. The amounts of functional groups in the blend are given in Table 1.

Table 1. Calculation of the amounts of functional groups in the HDPE/PA6/C1608/T403 (65/30/4/1) blend

Component	Weight fraction (%)	Type of functional group	Functional group content (mmol/g)	Amount of functional groups in the blend (mmol/g)
HDPE	65	-	-	-
PA6	30	Carboxylic acid	0.032	0.0096
		Amine	0.033	0.0099
Ceramer 1608	4	Maleic anhydride	1.9	0.076
Jeffamine T-403	1	Amine	6.8	0.068

It is worth noting that the chemical interactions between PA6 and Jeffamine T-403 include two types of reactions, one of which involves the amide moieties of PA6 (transamidification) rather than the terminal carboxylic acid groups (amidification). However, the respective extents of amidification and transamidification would be difficult to determine and those reactions therefore not taken into account in the determination of the blend composition.

3.3. Optimization of the extrusion process

The blends were prepared using a co-rotating twin-screw extruder (L/D = 60) at a temperature of 240 °C and a flow rate of 3 kg/h, according to the protocol described in Chapter 2. In order to investigate the interactions between the different constituents of the blend and their impact on the compatibilization efficiency of the C1608/T403 system, several variants of the extrusion process were studied. The preparation of the HDPE/PA6/C1608/T403 blend via these different processing methods is detailed in the following paragraphs. They are illustrated by block diagrams in Figures 13-17.

3.3.1. Method n°1

In this method, all the constituents were blended in a single-step process. A dry blend of HDPE and Ceramer 1608 was fed through the main hopper into block n°1, while PA6 was introduced through a side feeder at block n°4 (L/D = 20) along with Jeffamine T-403 through an injection point.

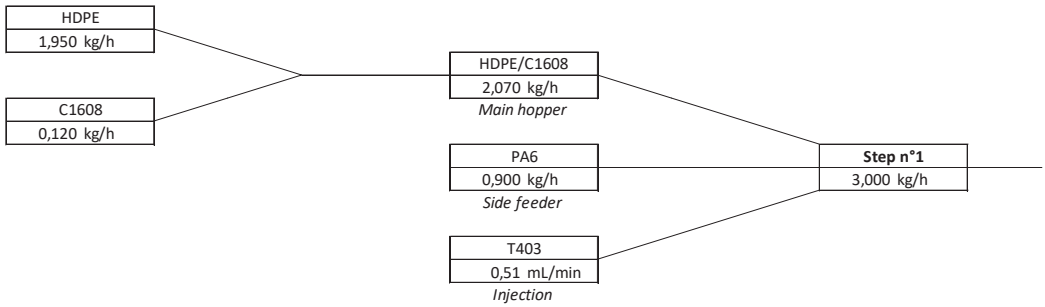

Figure 13. Block diagram illustrating method of extrusion n°1

3.3.2. Method n°2

In the second extrusion method, a premix consisting of HDPE, Ceramer 1608 and Jeffamine T-403 was prepared by extrusion. A dry blend of HDPE and Ceramer 1608 was fed through the main hopper into block n°1, while Jeffamine T-403 was injected at block n°4. In a second extrusion step, the HDPE/C1608/T403 premix was fed at block n°1 and PA6 was introduced at block n°4. This method was designed to favour the formation of the Ceramer/Jeffamine reactive system prior to the addition of PA6.

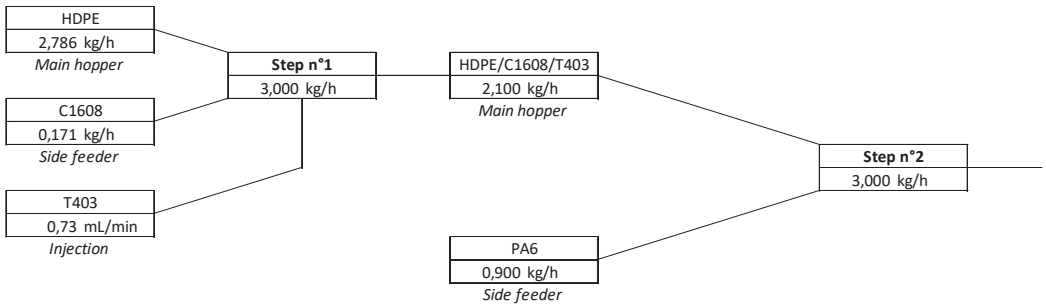

Figure 14. Block diagram illustrating method of extrusion n°2

3.3.3. Method n°3

In this third method, a premix consisting of PA6 and Ceramer 1608 was prepared by extrusion. Both constituents were fed into block n°1 in the form of a dry blend. In the second step, HDPE was fed at block n°1, while the PA6/C1608 premix was introduced at block n°4 along with Jeffamine T-403. This method was designed to favour the reaction between PA6 and Ceramer 1608 prior to the incorporation of Jeffamine T-403.

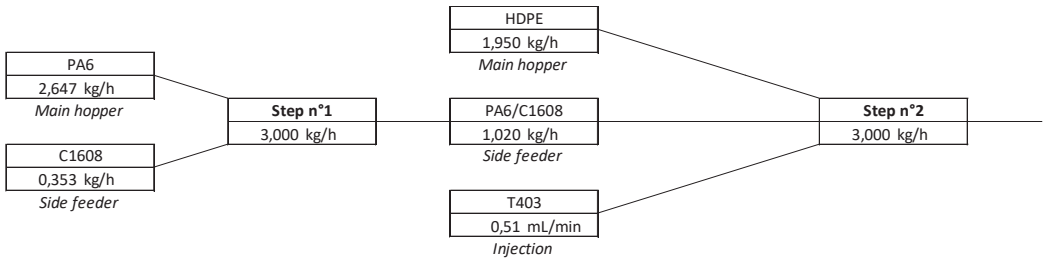

Figure 15. Block diagram illustrating method of extrusion n°3

3.3.4. Method n°4

In the fourth method, a premix consisting of PA6 and Jeffamine T-403 was prepared in a first extrusion step. PA6 was introduced at block n°1 and Jeffamine T-403 was injected at block n°4. In the second step, a dry blend of HDPE and Ceramer 1608 was fed into block n°1 while the PA6/T403 premix was introduced at block n°4. This method was designed to favour the viscosity reduction of the PA6 phase through the reaction with Jeffamine T-403 prior to blending with HDPE and Ceramer 1608.

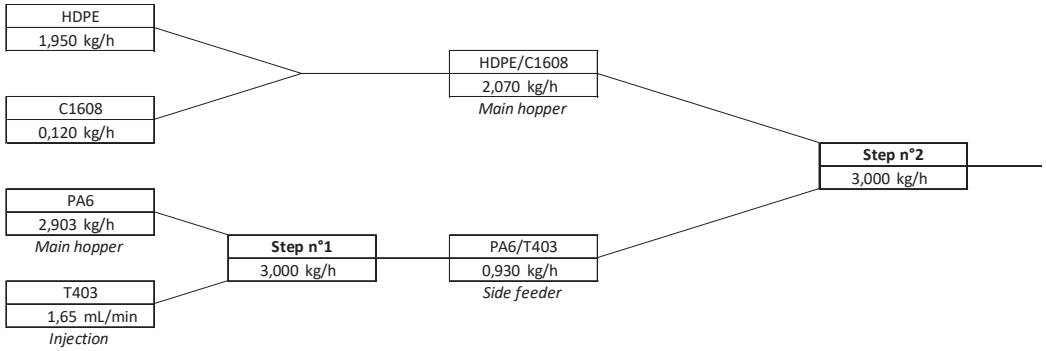

Figure 16. Block diagram illustrating method of extrusion n°4

3.3.5. Method n°5

The last method consisted in the preparation of a premix consisting of PA6, Ceramer 1608 and Jeffamine T-403. A dry blend of PA6 and Ceramer 1608 was fed into block n°1 and Jeffamine T-403 was injected at block n°4. In a second extrusion step, HDPE was fed at block n°1, while the PA6/C1608/T403 premix was introduced at block n°4. This method was designed to promote the reaction of PA6 with both functional oligomers prior to blending with HDPE.

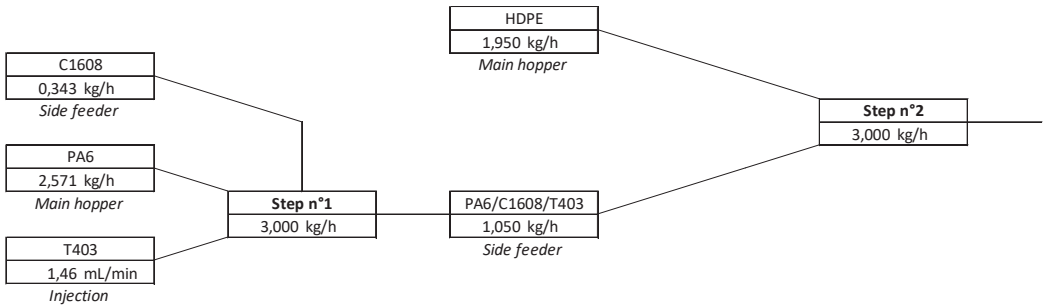

Figure 17. Block diagram illustrating method of extrusion n°5

3.3.6. Monitoring of the extrusion trials

The process variables recorded during the extrusion of HDPE/PA6/C1608/T403 blends are presented in Table 2. The process variables corresponding to the extrusion of the uncompatibilized HDPE/PA6 blend are also displayed in comparison.

Table 2. Process variables recorded during the extrusion of HDPE/PA6/C1608/T403 (65/30/4/1) blends

Blend	Mixing torque (%)	Pressure (bar)	Temperature (°C)
HDPE/PA6 (ref)	35	14	256
Method n°1	38	17	257
Method n°2	35	13	259
Method n°3	-	-	-
Method n°4	47	23	258
Method n°5	-	-	-

The extrusion of HDPE/PA6/C1608/T403 blends following methods n°1 and 2 presented no particular difficulty and the process variables were found to be similar to those recorded during the extrusion of the uncompatibilized HDPE/PA6 blend. The mixing torque and pressure recorded during the extrusion via method n°4 were slightly higher than with the other methods. This suggests an overall increase of the viscosity of the blend, despite the lower viscosity of the PA6/T403 premix compared to neat PA6.

The extrusion of premixes involving PA6 and Ceramer 1608 resulted in the blocking of the extruder due to the formation of a plug in the first block. Consequently, the blends could not be achieved through methods n° 3 and 5. Besides, extrusions involving Ceramer 1608 with Jeffamine T-403 and/or PA6 resulted in coarse foaming and irregular swelling of the extrudate. Additional extrusion trials involving only HDPE and C1608 at a similar temperature (240 °C) and oligomer concentration (12 wt%) as the PA6/C1608 premix did not result in foaming or swelling, indicating that foaming and swelling are most probably caused by the formation of water as a bi-product of the reaction between maleic anhydride and the amine functional groups of PA6 (rather than by the degradation of Ceramer 1608).

3.4. Properties and morphology of the blends

As previously mentioned, the extrusion of HDPE/PA6/C1608/T403 blends could not be achieved through methods n°3 and 5, hence the properties of those blends will not be discussed.

The morphologies of the HDPE/PA6/C1608/T403 blends prepared through methods n°1, 2 and 4 were determined by SEM and compared to the uncompatibilized HDPE/PA6 (70/30) blend. The corresponding SEM pictures are shown in Figure 18.

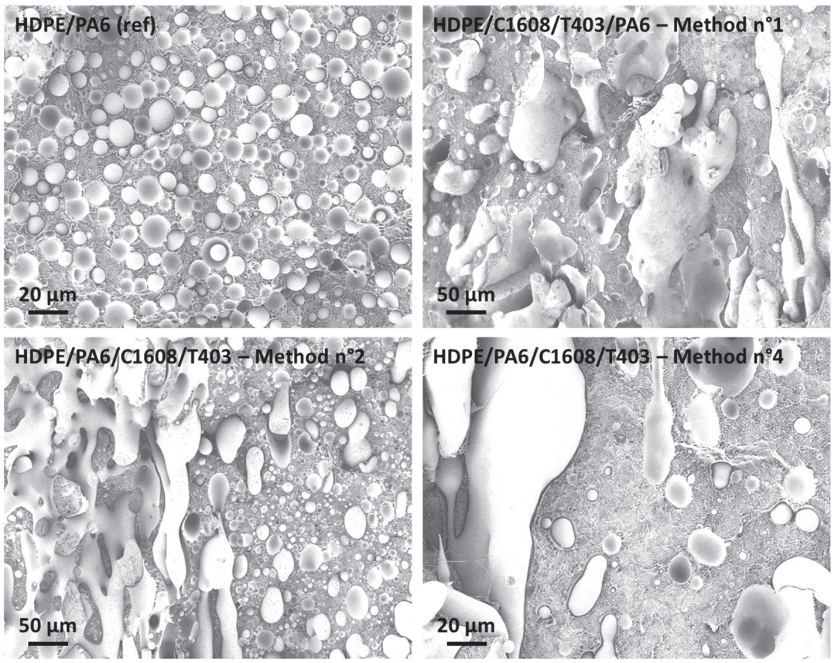

Figure 18. SEM pictures of HDPE/PA6 and HDPE/PA6/C1608/T403 blends prepared by different extrusion methods

The morphology of the uncompatibilized HDPE/PA6 blend was the same as described previously, with spherical PA6 domains dispersed in a continuous HDPE matrix, a typical domain size between 1 µm and 10 µm, and poor interfacial adhesion between the two phases.

The HDPE/PA6/C1608/T403 blends obtained through methods of extrusion n°1 and 4 also exhibited dispersed morphologies with spherical domains as well as large lumps with irregular shapes. The typical diameter of the spherical domains was measured between 1 µm and 10 µm while the larger lumps had by dimensions ranging from several micrometres to several millimetres.

The sample prepared via method n°2 was characterized by the coexistence of a dispersed morphology with regions of co-continuity between HDPE and PA6 phases. The dispersed domains were mostly spherical with a typical size of 1-10 µm, although some deformed domains with dimensions up to 50 µm were also observed. Additional SEM pictures of this sample are presented in Figure 19 to illustrate the coexistence of dispersed and co-continuous morphologies.

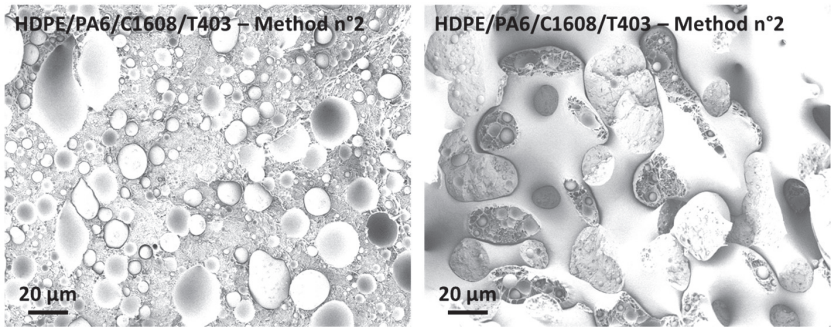

Figure 19. SEM pictures of the HDPE/PA6/C1608/T403 blend obtained through the extrusion method n°2, showing the two types of coexisting morphologies: dispersed (left) and co-continuous (right)

The different morphologies of the minor PA6 phase observed in HDPE/PA6/C1608/T403 samples once again suggest that low molar mass compatibilizer precursors favour droplet coalescence in the melt. The coexistence of well dispersed spherical domains with larger irregularly shaped objects also indicates that the selected oligomeric compatibilizer precursors fail to achieve a good control of the morphology in HDPE/PA6 blends, although the formation of the C1608/T403 compound within HDPE prior to blending with PA6 (method n°2) seems to promote phase co-continuity. Moreover, a poor interfacial adhesion between the two phases was observed in all samples, demonstrating the ineffective compatibilization of the HDPE/PA6 blend.

The mechanical properties of the blends were determined by tensile testing according to the protocol described in Chapter 2. Young's modulus (E), yield stress (σ_y) and strain at break (ε_b) measured by tensile testing are presented in Table 3.

Table 3. Mechanical properties of HDPE/PA6 and HDPE/PA6/C1608/T403 blends prepared by different extrusion methods

Blend	E (MPa)	σ_y (MPa)	ε_b (%)
HDPE/PA6 (ref)	1080 ± 70	25 ± 0	20 ± 0
Method n°1	660 ± 90	22 ± 0	10 ± 0
Method n°2	770 ± 220	23 ± 0	10 ± 0
Method n°4	1030 ± 70	21 ± 1	0 ± 0

A graphical representation of those values is provided in Figure 20.

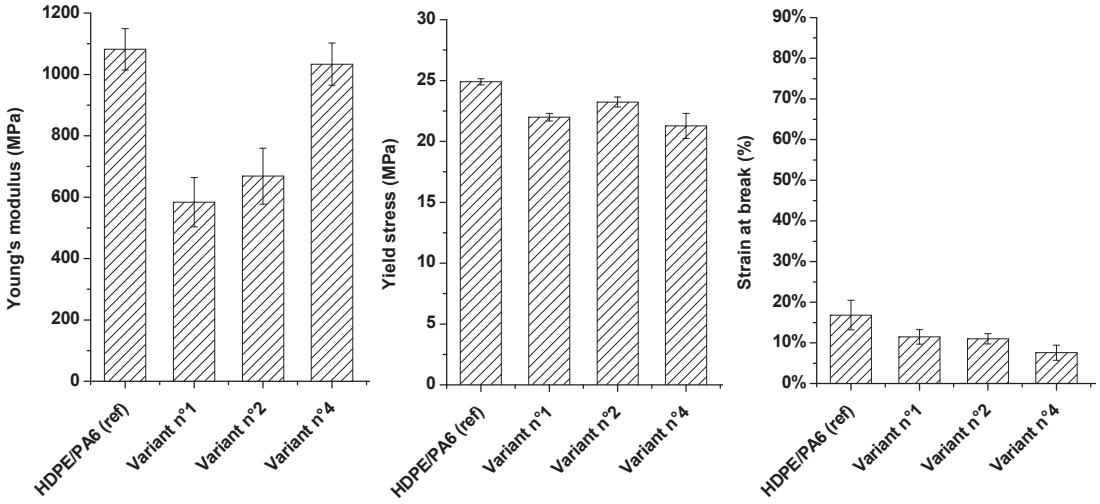

Figure 20. Mechanical properties of HDPE/PA6 and HDPE/PA6/C1608/T403 blends prepared by different extrusion methods

No significant variation of yield stress or strain at break was observed, regardless of the extrusion method used to prepare the HDPE/PA6/C1608/T403 blends. This is consistent with previous observations that all blends presented unstable morphologies and that interfacial adhesion between the two phases was not improved as a result of the poor compatibilization efficiency of the C1608/T403 system.

The blends obtained through methods of extrusion n°1 and 2 resulted in Young's moduli respectively reduced by 46 % and 38 % compared to that of the HDPE/PA6 blend, which indicates a loss of stiffness. Additionally, the measured Young's modulus values were similar to those typically encountered in the case of neat HDPE, suggesting that the elastic deformation behaviour of those blends is governed by the continuous HDPE phase.

3.5. Conclusions

The use of a reactive system based on Ceramer 1608 and Jeffamine T-403 functional oligomers to compatibilize HDPE/PA6 immiscible blends proved to be inefficient regardless of which chemical interaction was favoured by the design of the extrusion process, hence the extrusion protocol described in Section 3.1 of Chapter 4.